Role of keratoepithelin in inherited corneal dystrophies

Aikaterini Glavini

ProQuest LLC
789 East Eisenhower Parkway
P.O. Box 1346
Ann Arbor, MI 48106-1346

ABSTRACT

Corneal dystrophies are inherited bilateral diseases that compromise the transparency of the cornea. They are difficult to treat and re-occur in corneal transplants. A number of anterior stromal and Bowman's layer dystrophies have been linked to keratoepithelin. This is an extracellular matrix protein, synthesised and secreted by the epithelium and deposited in the accumulations found in the epithelial and stromal areas of the affected individuals. Keratoepithelin binds to different types of integrins on the cell surface and has been shown to regulate migration, proliferation adhesion and tumourgenicity. The gene encoding keratoepithelin, βig-h3, is induced by growth factor TGF-β and has been involved with growth, differentiation, development and wound healing. The aim of this study was to explore the effects the wild type and mutant forms of this gene and protein have on primary corneal cells.

βig-h3 cDNA was synthesised from fibroblast mRNA and in vitro mutagenesis was carried out to produce mutant constructs encountered in dystrophies Granular Groenouw Type I and Thiel Behnke, R555W and R555Q respectively. Replication deficient adenoviruses were constructed to achieve overexpression of the wild type and mutant βig-h3 genes in cultured cells. Native recombinant keratoepithelin protein was expressed and purified corresponding to the wild type and mutant cDNA sequences. Primary corneal epithelial cells and keratocytes were cultured in the presence of the recombinant constructs and the effects on adhesion, proliferation, migration and apoptosis were monitored.

Wild type recombinant keratoepithelin promoted significantly the adhesion of both epithelial cells and keratocytes ($p<0.001$). The mutant proteins had the same effect as the wild type on epithelial cell adhesion, but keratocytes showed a decreased adhesion ($p>0.05$). The corneal epithelial cells overexpressing wild type βig-h3 adhered significantly better ($p<0001$) than the control and the keratocytes showed higher adhesion ($p<0.001$) during overexpression of the mutant R555W βig-h3.

Epithelial proliferation was increased in response to the recombinant proteins (50.27 ±1.93% in the wild type compared to 35.59 ±6.26% in the control) and overexpression of βig-h3 genes ($p<0.001$), whereas the keratocyte proliferation was unaffected. R555W mutant protein was associated with slower migration rate of epithelial cells compared to wild type protein, whereas the keratocytes migration did not seem to be affected in any

case. Difficulties were encountered when using adenoviral constructs to assess the effects of overexpression of βig-h3 transgenes on cell migration and proliferation.

Annexin-V and propidium iodide staining suggested there may be an increase in the apoptosis of cells in the presence of the mutant recombinant proteins and adenoviruses. However, the apoptosis assay could only provide an indication of the effect of the recombinant constructs since the data could not be accurately quantified and analysed, due to a discrepancy on the setup of the FACS analyser.

These findings indicate the feasibility of using recombinant keratoepithelin proteins and βig-h3 overexpressing adenoviruses to assay their effects on primary corneal cells. The diversity of the behavioural responses of corneal cells to mutant and wild type keratoepithelin and βig-h3 gene can provide useful insight in the pathology of the anterior corneal dystrophies.

AKNOWLEDGEMENTS

During the work described in this thesis I was lucky to meet and know the following people who offered me plenty of intellectual, practical and emotional support.

I would like offer my never-ending gratitude to:

My supervisors, Professors Mike Boulton, Graeme Black and Maria Castro who gave me the opportunity to carry out this project

In detail, Maria and Tricia for teaching me the recombinant adenoviruses techniques, Graeme for his invaluable guidance and supervision, and Mike for his continuous encouragement, support and faith that led to the completion of this work.

Dr Julie Albon for her constant support and understanding and for taking me to Salsa,

Rahat, Niki and Pam for their valuable help and friendship when I was in Manchester,

Drs Louise Carrington and Jun Cai for enlighting me with their scientific wisdom in Cardiff,

Dr Ilyas Khan for answering my recombinant protein questions,

Dr Saeed Akhtar for his enthusiasm and help with image analysis,

Drs Gavin Wilkinson and Carole for their generous help with the recombinant adenoviruses,

Dr Chris Pepper for his kind assistance with the FACS analysis,

Katerina, Rania, Marina, Anna, Elina, Claudia, Veronique, Oksana, Jila, Tina, Andreas, Nikos, Georgia, Triada, Xrisa, Katherine, Kassiani and Steve for being amazing friends,

My relatives for not forgetting that I exist after being so many years away from Greece,

Rory for making every day sunny,

My parents Giorgos and Kanella and my brother Antonis for always being a source of inspiration

CONTENTS

LIST OF FIGURES

LIST OF TABLES

ABBREVIATIONS

A- adenine

Aa - amino acid

ACD - Avellino Corneal Dystrophy

Ad - adenovirus

Amp - Ampicillin

ATCC - American Type Culture Collection

ATP - Adenosine Triphosphate

βig-h3 - TGF-β induced gene-human clone 3

bp - base pair

C - Cytosine

CDB - Corneal Dystrophy of the Bowman's layer

CDGGI - Corneal Dystrophy Granular Groenoew type I

cDNA - complementary DNA

CDRB - Corneal Dystrophy Reis Bucklers Chl - chloramphenicol

CDTB - Conreal Dystrophy Thiel Behnke

CIAP-Calf Intestinal Alkaline Phosphatase

CNS - Central Nervous System

Contig - Group of clones representing overlapping regions of the genome

CPE - Cytopathic effect

DEPC - Diethylpyrocarbonate

DMEM - Dulbecco's Modified Eagles Medium

DMSO -Dimethylsulphoxide

DNA - Deoxyribonucleic acid

dNTP - deoxy trinucleotide triphosphate

ECM - Extracellular Matrix

E. coli - Escherichia coli

ES301 cells - DNA repair minus mutant strain of E.coli

EGF - Epidermal Growth Factor

FAK - Focal Adhesion Kinase

FCS - Fetal Calf Serum

G - Guanine

GCD - Granular Corneal Dystrophy

HUVEC - Human Umbilical Vein Endothelial Cells

IFN - Interferon

IL - Interleukin

IMS - Industrial Methylated Spirit

IPTG - Isopropyl-β-D-thiogalactopyranoside

JM109 cells - E.coli strain which is used for a host for transformation of plasmid vectors. Restriction of cloned DNA and recombination with host DNA are prevented and quality and yield of plasmid DNA are improved due to mutations on specific host genes.

Kan - Kanamycin

kb - kilobase

KU - Kilo Unit

LB -Luria Bertani

LCD - Lattice Corneal Dystrophy

L - Litre

μl - microliter

ml - milliliter

mM - millimolar

M - molarity (mol/l)

MDFD - Map Dot Fingerprint Dystrophy

MEM - Minimum Essential Medium

MOI - Multiplicity of infection

MWCO - Molecular Weight Cut-Off

OD - Optical Density

OSF - Osteoblast Specific Factor

ng - nanograms

PAGE - Polyacrylamide Gel Electrophoresis

PBS - Phosphate Buffer Saline

PCR - Polymerase Chain Reaction

PDGF - Platelet-derived Growth Factor

PES - Polyethanersfulfate

P_F - Forward primer

Pfu - plaque forming units

pmol - pico moles

P_R - Reverse primer

RB - Retinoblastoma

RBCD - Reis-Buckler's Corneal Dystrophy

RNA - Ribonucleic acid

rpm - revolutions per minute

RT - Reverse Transcription

SdH_2O - sterile distilled water

SDS - Sodium Dodecyl Sulfate

Sec - second

SPARC -Secreted Protein Acidic and Rich in Cystein

SSCP - Single Stranded Conformational Polymorphism

T - Thymine

TBE - Tris Borate EDTA

TGF - Transforming Growth Factor

TNF - Tumour Necrosis Factor

UV - Ultraviolet

X-gal - 5-Bromo-4-chloro-3-indolyl beta-D-galactopyranoside

YAC - Yeast Artificial Chromosome

1. CHAPTER ONE - General Introduction

1.1 CORNEA

The cornea is the most important ocular structure to come into contact with the environment. It is a transparent structure, convex on the outside and concave inside. It appears elliptical from the front and forms part of an organ which is almost a sphere. The average dimensions of the human cornea are 11.7mm horizontally wide and 10.6mm vertically, with a 0.52-0.67mm thickness (Kaufmann et al, 1998). A special characteristic of the structure of cornea is the lack of vascularisation, a property that makes it an ideal model for organ culture.

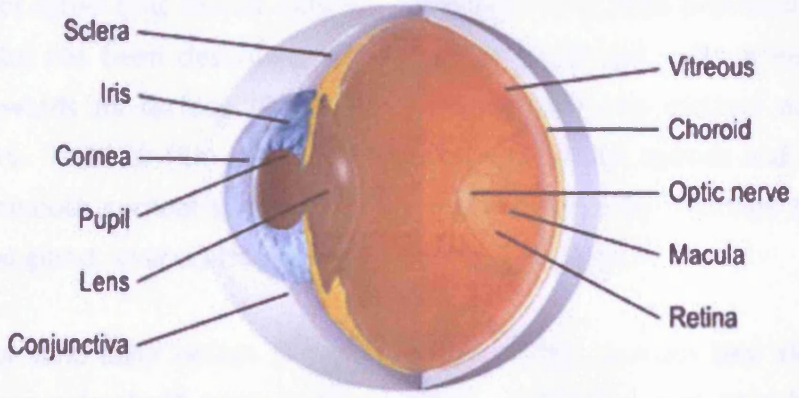

Figure 1.1: Ocular Tissues
Illustrated by Mark Erickson. (Source: http://www.stlukeseye.com/Anatomy.asp)

The position of the cornea assigns it a double protective role: The corneal epithelium and the overlying tear film form an effective barrier, which protects the eye from the outside environment. At the same time, due to its strong collagenous composition, the cornea resists the internal ocular pressure. Water from the aqueous humour is retained out of the cornea by the endothelium which separates these two different structures. In this relatively dehydrated state the corneal layers are maintained and both swelling and clouding are prevented.

The transparency of this organ is conferred by the organisation of collagen fibrils as well as their regular packaging (Maurice, 1957). Transparency is a prerequisite for the performance of its main function, which is the refraction of light into the eye. The cornea is the most important refractive structure of the eye due to its smooth surface and its regular curvature.

The cornea is composed mainly of water, which constitutes 78% of its total mass. 20% of the structure is occupied by proteins, 15% being constituted by collagen types I and VI. The remaining 5% comprises other proteins such as laminin, keratin, integrin, talin, vinculin etc. Glycosaminoglycans (keratan sulphate chondroitin/dermatan sulphate and hyaluronic acid) constitute 1% of the total mass and another 1% is contributed by salts (Muthiah et al, 1974, Muczar et al, 1973).

1.2 TEAR FILM

The preocular tear film is not part of the cornea, but lies in close contact with its anterior epithelial surface. The thickness of the tear film is still debated, but it is generally accepted that mucus extends more anteriorly than previously assumed. The tear film has been described as a hydrated mucin gel, with a viscosity that declines towards its surface (Dilly, 1994) rather than two distinct aqueous and mucin layers. The tear film is spread by the blinking of the eyelids and maintains a moist and smooth corneal surface. Tears leave the eye by drainage through the nasolacrimal gland, evaporation and conjuctival absorption.

The anterior lipid layer delays the evaporation of the aqueous tear film. It also protects from polar lipid contamination (Holly, 1978) and acts as a hydrophobic barrier to prevent the overflow of tears. It is secreted by meibomian glands and consists of esters, triacylglycerols, free sterols, sterol esters and fatty acids (Nicolaides et al, 1981).

The aqueous layer is produced by the lacrimal glands and contains salts, electrolytes, proteins, enzymes and other components. Metabolic products, such as oxygen and carbon dioxide are also present in this layer and are transported to and from the cornea. Tears contain several substances which protect against bacterial and viral infection and provide a route by which white blood cells may reach the eye. Lysozyme, lactoferrin and beta lysin are all antibacterial enzymes which have been identified in the tears (Fleming, 1922; Broekhuyse, 1974; Ford et al, 1978). All of the immunoglobulins have been found in tears, with IgA being present in a much higher concentration. Antibodies specific to several viruses (Vinogradova et al, 1979; Mull et al, 1970) have also been described, but their exact role remains uncertain.

The ocular surface is naturally wettable due to the presence of a surface glycocalyx, the fibrillar glycoprotein which coats the outer membranes of the microprojections of epithelial surface cells. The increased area on the epithelial cell surface formed by the microprojections and the glycocalyx help the adherence of mucoproteins, which form a hydrophilic coating (Nichols et al, 1985). A mucin gel, is also present in the intervening space and consists of mucoproteins, which are secreted by conjunctival goblet cells.

The main function of the cornea is the refraction of light. Projecting microvilli from the epithelial layer can potentially degrade the resulting image. The tear film forms a smooth surface and most of the refraction of light occurs in the tear/air interface.

1.3 CORNEAL STRUCTURE

The cornea consists of 5 distinct layers, which can be seen in a meridional section. These are, from top to bottom: Epithelium, Bowman's layer, stroma, Descemet's membrane and the endothelium.

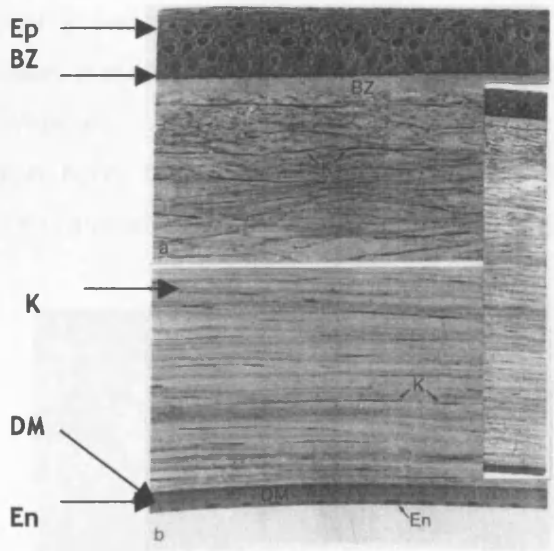

Figure 1.2: Meridian section of human cornea

(a) Epithelium and anterior stroma, (b) endothelium and anterior stroma Ep-Epithlium, BZ- Bowman's zone, K-keratocytes, DM-Descement's membrane, En-Endothelium. (Source: The Cornea, Smolin G and Thoft RA, 1994)

1.3.1 Epithelium

The corneal epithelium consists of 5-6 layers of cells and is stratified, squamous and non-keratinised. The thickness of the epithelium has been estimated to be around 50.7μm (Reinstein et al, 1994). The deepest layer of cells, the basal cells, are attached to the basal lamina. These cells, which are columnar with flat bases and rounded tops, constitute the germinative layer of the epithelium. The second layer of the epithelium consists of the wing or umbrella cells. These cells, like the next 2-3 layers, are polyhedral. The layers near the anterior surface of the cornea consist of progressively flatter cells. The top layer is comprised of cells with the maximum surface area, flattened nuclei and projecting microvilli.

The epithelial cells contain a cytoplasmic meshwork of intermediate filaments called tonofibrils (Sun and Vidrich, 1981) and composed of polymers of keratin subunits. These filaments are involved in a system that connects neighbouring cells to one another and to the extracellular matrix and provides great tensile strength. In vivo keratins are coexpressed and paired to form heterodimers consisting of a basic and an acidic molecule. The K12/K3 pair is found in the corneal epithelium of a variety of species and is important for the function of this layer. Meesmann's hereditary juvenile dystrophy is an autosomal dominant disorder that causes fragility of the anterior corneal epithelium and manifests with tiny epithelial vesicles. Missense mutations in K3 or K12 occurring in highly conserved keratin helix boundary motifs have been identified as the genetic defects in affected families.

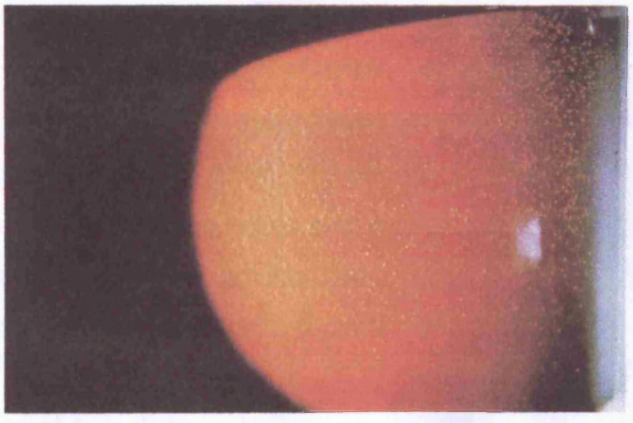

Figure 1.3: Meesmann's Dystrophy
(Courtesy of Prof. GCM Black)

Intercellular attachment of the basal cells is achieved by desmosomes (Fawcett, 1966) and hemidesmosomes attach these cells to their underlying basal lamina. Desmosomes keep the membrane of contiguous cells close together by interaction of protruding cadherin proteins, which are contributed by both cells. The transmembrane linker proteins in hemidesmosomes are integrins and they interact with proteins of the basal lamina. These anchoring junctions must be labile to allow migration of the proliferating basal cells to the surface of the epithelial sheet. Less desmosomal structures are found between wing cells, whereas adjacent epithelial cells at the surface are connected with tight/occluding junctions (Tonjum, 1974). These junctions make cells selectively impermeable by preventing diffusion of membrane proteins and leakage of water-soluble molecules between the cells. This facilitates the maintenance of an intact epithelial layer even in the presence of the overlying tear film.

The most superficial cells have projecting microvilli 0.5μm high and 0.3μm wide, which are thought to be important for the retention of the precorneal tear film. The older of these superficial cells are eventually shed (Hoffman, 1972) and replaced with cells from below. The germinative stem cells are not found at the basal epithelial layer of the central cornea, but at the limbus (Davanger and Evensen, 1971; Bron, 1973), an area which borders the periphery of the cornea. Limbal stem cells are slowly dividing and give rise to transiently amplifying cells, which then migrate towards the centre of the cornea. These cells undergo a series of divisions, which result in their differentiation and progressive movement to the surface of the layer before, ultimately being shed (Tseng, 1989).

The basal cells are responsible for the secretion of the components of the underlying basal lamina and the production of the hemidesmosomes (Kenyon, 1969). Hemidesmosomes consist of the cytoplasmic anchoring plaque, where integrins α_4 and β_6 traverse the cell membrane and associate with the basal lamina. This is an extremely strong attachment that protects the corneal epithelium from detachment (Khodadoust et al, 1968).

The lamina consists of two distinct layers, the lamina lucida and the lamina densa. The former is comprised of kalinen filaments associated with laminin. The lamina densa contains heparan sulphate proteoglycan (HPSG) and globular Type VII collagen. Anchoring fibrils consisting of helical collagen VII and glycoproteins arise

from the lamina densa and integrate into the Bowman's layer, where they firmly attach in anchoring plaques (globular VII collagen and laminin).

1.3.2 Bowman's layer

This is a structure which is largely restricted to the human cornea. While a similar structure can be found in some avian and reptile species as well as primates, it is not present in other mammals. Bowman's is an acellular layer, 8-14μm deep, consisting of fine collagen fibres (Type V) in a ground substance. The anterior side is in contact with the basal lamina of the epithelium. On the anterior side of the layer the fibrils become more ordered and extend into the substantia propria, where they merge with the stromal proteins.

Bowman's layer is resistant to both mechanical and infectious trauma, but if destroyed it is replaced by scar tissue (Duke-Elder and Wybar, 1960). In pathological cases such as corneal dystrophies and oedema or after death the epithelium detaches from Bowman's layer. In corneal dystrophies of the Bowman's layer (Reis Buckler's and honeycomb) this layer is partially or completely lost and replaced by granular deposits or honeycomb-shaped opacities (Okada et al, 1998).

1.3.3 Substantia propria (stroma)

This layer is 500μm deep and constitutes 90% of the corneal thickness. It is a transparent fibrous structure, which consists of compact lamellae of collagen fibres. The lamellae are embedded in a ground substance of proteoglycans, their arrangement being more regular towards the posterior surface. There is a low density cell population, the keratocytes, scattered throughout the lamellae. The sensory protection of the cornea is achieved by sensitive nerve endings, which do not compromise its transparency. The nerve axons and Schwann cells are present in the anterior and middle stroma.

Collagen fibrils are responsible for the special structural properties of the cornea, such as transparency and mechanical resistance to intraocular pressure (Newsome et al, 1980; Maurice, 1984). The bundles of polymerised collagen in the stroma run parallel to each other and to the corneal surface, from limbus to limbus and at varying angles and levels. The lamellae are surrounded by extracellular matrix, which is secreted by the keratocytes and maintains the distance between the fibrils (Kuwabara, 1978). Loss of the extracellular matrix (e.g. in oedema) results in

changes in the interfibrillar distance and results in loss of corneal transparency. Keratan and chondroitin sulphate are the major glycosaminoglycans of the matrix, with keratan sulphate being more concentrated in the central stroma and chondroitin sulphate in the peripheral cornea. The extracellular matrix interacts with individual collagen fibrils, but it is not known exactly how.

Keratocytes make up 3-5% of the stromal volume (Langham and Taylor, 1956). Their main function is to produce the collagen and extracellular matrix of the stroma during development and maintain it thereafter. Precursors of collagen and glycosaminoglycans can be seen in the area around keratocytes. The cell bodies of the keratocytes are thin, long and flat, running parallel to the collagen fibrils. Interactions between neighbouring keratocytes are believed to be important in the regulation of their cell function (Assoulline et al, 1992).

Keratocytes also have receptors for growth factors, which are important in response to wound healing. Repair of the stroma after injury results in keratocyte activation, migration and transformation into myofibroblasts. Scar tissue is formed which consists of collagen fibrils of larger diameter and reduced regularity (Schwarz, 1953b). Over time this tissue undergoes remodelling, which involves thinning and rearrangement of fibrils as well as increase in corneal transparency (Cintron and Kublin, 1977). In some pathologic situations, keratocytes produce large amounts of basal lamina and similar material that can result in opacification of the cornea (Kuwabara, 1978).

Other cell types sporadically found in normal human cornea are lymphocytes, macrophages and polymorphonuclear leucocytes.

1.3.4 Descemet's membrane

In contrast to Bowman's layer, which is a modified zone of the anterior stroma, Descemet's membrane is a thick basal lamina secreted by the corneal endothelium. It is a distinct structure found at the base of the stroma. Appearing at the fourth month of gestation, it is 3-4μm at birth and develops to 10-12μm in adult life. This basal lamina comprises two layers: the anterior banded and the posterior nonbanded layers. It is the anterior layer that appears first, before birth, the posterior developing later.

Attachment sites and short fibrils extending from the stroma into Descemet's membrane have been observed with the electron microscope (Binder et al, 1991). The anterior layer consists of a hexagonal array of collagen bundles. In cross section the bundles appear irregular and have intervals of 110nm. The major protein is collagen IV, but other basal laminar components, such as fibronectin have been identified (Newsome et al, 1981). The posterior part of the membrane comprises more recently produced fibrillogranular material and is attached to the endothelial cells by modified hemidesmosomes.

If endothelial cells are stimulated they produce excess amounts of basal lamina material and focal thickenings occur, called guttae. Peripheral guttae are known as Hassell-Henle warts and are common in ageing corneas (Lorenzetti et al, 1967). Central warts, however, are indicative of endothelial cell dysfunction. Central cornea guttata that spread peripherally, thickening and folding of the Descement's membrane and stromal oedema are all symptoms of Fuchs' endothelial dystrophy, an autosomal dominant disease. Eventually the endothelium is disrupted and epithelial oedema develops leading to epithelial bullae that may rupture.

Another difference of this layer from Bowman's layer is the healing process that takes place after injury (trauma or disease). Endothelial cells spread and produce new basal lamina identical to normal Descemet's layer.

1.3.5 Endothelium

This is a single layer of hexagonal cells, 4-6μm thick, which are generally considered amitotic. The surface that comes in contact with Descemet's membrane is uneven due to the interdigitation of adjacent cells. The posterior surface is thought to be coated with a viscous substance, in a similar way epithelium is coated with a mucin, which "adjusts" it in the wet environment (Wolf, 1968; Sperling et al, 1980).

The endothelium is essential for the maintenance of corneal structure and function. It serves as a barrier, protecting the cornea from oedema and allowing passage of salts and metabolites. Acting as a fluid pump it prevents excessive aqueous humour entering into the stroma.

Endothelial cells maintain tight physical contact with one another through the membranes of contiguous cells interdigitating one another and forming a marginal fold. Neighbouring cells are bound together by cell junctions (usually anchoring and seldom occluding), elaborate junctional complexes and gap junctions. ZO-1, a protein closely associated with the cytoslic surface of tight junctions, is distributed around the apical borders of endothelial cells (Barry et al, 1995), but the distribution of this protein around the cells is discontinuous with the largest gaps occurring between adjacent cells. All of the above result in a firmly sealed layer of cells that interconnect and convey chemical signals to each other.

Endothelial cells are very active metabolically in order to perform their substantial role. Whenever there is a demand for additional workload (e.g. during growth, ageing cell loss, intraocular surgery or trauma) they meet these requirements by enlarging. Therefore some degree of endothelial cell loss can be overcome by this process, but there is a limit below which the endothelium fails to maintain its integrity and decompensation occurs. Corneal oedema and visual loss follow. This minimum limit is 400cells/mm^2 contrasted with the normal average 2,000cells/mm^2.

1.4 CORNEAL DYSTROPHIES

Corneal dystrophies are primary, bilateral, inherited conditions that affect vision and can change the transparency and refraction of cornea (Bron, 2000). They are distinct from corneal degenerations, which are age-related changes of the cornea accompanied by other ocular diseases. Most of them are autosomal dominant with early or late onset and character variations (symptoms, clinical presentation, and progression) can be observed within the same and between different families.

The dystrophies have been extensively studied and characteristic histopathologic and immunological findings have been revealed by light and electron microscopy. The dystrophy can occur in any of the several layers of the cornea. According to the anatomic classification there are dystrophies of the epithelium, epithelial basement membrane, Bowman's layer, stroma and endothelium (Table 1.1). Corneal dystrophies have been classified in several different ways, but it seems that the best way to classify them is by defining the gene with the defect. It is not rare for patients who have similar clinical symptoms and/or histological findings to have different mutations and for patients suffering from different diseases to have

mutations in the same position of the same gene. Determination of the genetic cause can be helpful for understanding and distinguishing each dystrophy. Only the dystrophies which are known to involve mutations in the βig-h3 gene will be described in this chapter.

Corneal Location	Dystrophy
Epithelium	Recurrent Erosion
	Meesman's
	Stocker-Holt
	Rosette
	Map-Dot Fingerprint
Bowman's Layer	Anterior Crocodile Shagreen
	Grayson-Wilbrandt
	Thiel-Behnke
	Reis Buckler's
	Inherited Band
	Anterior Mosaic
	Familial Corneal Scarring
	Subepithelial Mucinous
Stroma	Granular (Groenouw type I)
	Avellino (Granular Type II)
	Macular (Types I, IA, II)
	Lattice (Types I, II, III, IIIA, IIIB, IV)
	Gelatinous Drop-Like
	Central Crystalline (Schnyder's)
	Marginal Crystalline (Bietti)
	Marginal Crystalline (Barraquer)
	Fleck
	Polymorphic Amyloid Degeneration
	Speckled
	Progressive
	Central Cloudy
	Congenital Hereditary
	Pre-Descement's
	Posterior Amorphous
Endothelium	Posterior Polymorphous
	Congenital Hereditary (Type I and II)
	Corneal Guttata
	Late hereditary Endothelial (Fuch's)

Table 1.1: Corneal Dystrophies of the different layers of the cornea
(Modified from Bron, 2000)

1.4.1 Keratoepithelin related corneal dystrophies

A number of anterior stromal dystrophies have been found to be associated with defective keratoepithelin. The following are the dystrophies, which have been reported to date to involve and be caused by defective βig-h3 gene. They all share the same inheritance pattern, which is autosomal dominant.

1.4.1.1 Granular Corneal Dystrophy (Groenouw type I)

This is one of the classically recognised autosomal inherited corneal dystrophies (Groenouw, 1933). It has an early onset in life but remains asymptomatic for years. Discrete, focal, milky, granular deposits in the anterior central stroma (and progressively with age in the deeper stroma) are defined from remaining clear areas. With progression, the stroma develops a ground-glass appearance. The lesions do not extend to the limbus but can protrude anteriorly through breaks in Bowman's layer.

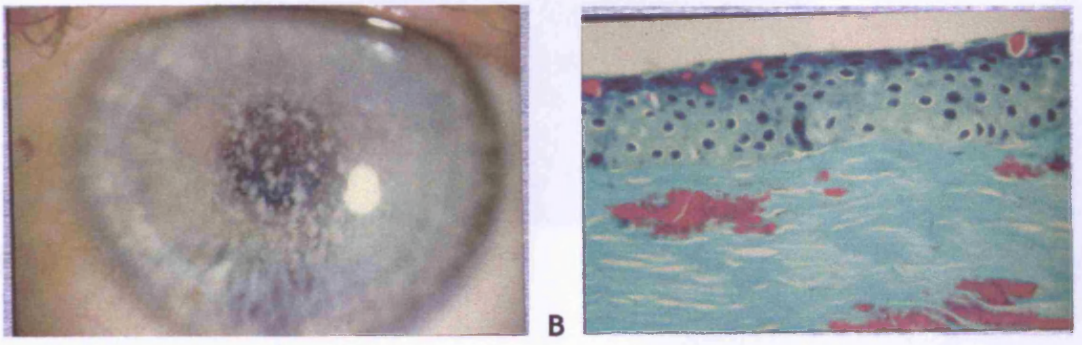

Figure 1.4: Granular corneal Dystrophy

A. Photograph from the cornea from a Granular dystrophy patient. B. Red Masson's staining (Courtesy of Prof. GCM Black)

Microscopically, the granular material is hyaline and stains bright red with Masson's trichrome stain.

An electron dense material made up of rod or trapezoidal shaped deposits immersed in an amorphous matrix is seen ultrastructurally (Akiya et al, 1970). Biochemical and immunohistochemical analysis reveals excess phospholipids and microfibrillar protein (Rodrigues et al, 1983). Stromal keratocytes appear normal or at various stages of degeneration.

The dystrophy is slowly progressive with vision rarely dropping below 20/200, therefore most patients do not require treatment initially. Recurrent erosions are rare. Lamellar keratoplasty is useful for alleviating the superficial symptoms. When visual acuity is affected penetrating keratoplasty is carried out. Recurrence in the graft anteriorly and centrally may occur with time (Santo et al, 1995, Inoue et al, 2002 and Ellies et al, 2003).

1.4.1.2 Avellino Corneal Dystrophy

This is a variant of granular dystrophy, which was described in a small number of families who trace their roots to Avellino, Italy. In spite of this, the mutations on the βig-h3 gene in families affected by this dystrophy have arisen independently and do not reflect a putative founder effect (Korvatska et al, 1998).

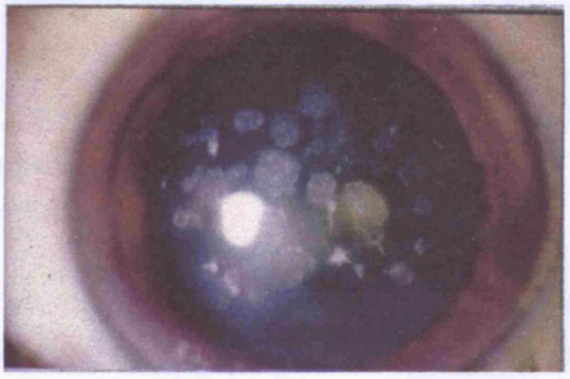

Figure 1.5: Avellino Dystrophy
(Courtesy of Prof GCM Black)

The affected patients have a granular as well as a lattice dystrophy both histologically and clinically (Ferry et al, 1997; Folberg et al, 1998). Discrete subepithelial granular deposits are seen in young affected individuals. Mid and posterior stromal refractile lines develop in the third decade, while the granular lesions progress. As the lattice phenotype is manifest later in life, a lot of the affected individuals are diagnosed as granular dystrophy patients (Stewart et al, 1999).

Older patients have anterior stromal haze between deposits, which reduces visual acuity (Holland et al, 1992). Recurrent erosions are more frequent than in granular dystrophy patients. Pathologically, both the hyaline deposits typical of granular dystrophy and the amyloid deposits of lattice dystrophy are seen. Granular deposits re-appear in corneal grafts (Ellies et al, 2002 and 2003).

1.4.1.3 Lattice Dystrophy

This disease has a variable expression. The corneal changes, those of classic branching lattice lines, vary significantly in different cases. Refractile lines, central and subepithelial ovoid white and diffuse anterior stromal haze appear. Initially, the white dots have a similar appearance to granular dystrophy. The stroma can take on a ground-glass appearance.

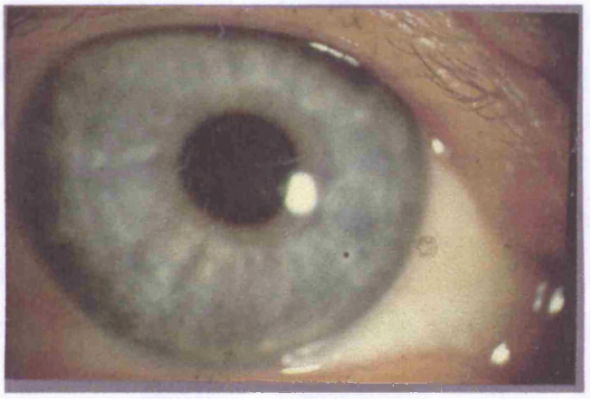

Figure 1.6: Lattice corneal dystrophy
(Courtesy of Prof. GCM Black)

This disorder is a primary localised corneal amyloidosis. The following three types of lattice dystrophy have been linked with keratoepithelin (apart from type III, which is recessive an the gene has not been mapped yet):

Type I (Biber-Haab-Dimmer)

This is a classic lattice dystrophy. Onset is in early childhood. Young patients are asymptomatic showing anterior refractile dots, filamentary lines and subepithelial white spots and corneal haze. Others might exhibit only recurrent erosions. In older patients the lines spread to involve the stroma and recurrent erosions result in irregularity of the epithelial surface and decreased visual acuity. Progressive clouding and scarring may result in opacities and in extreme cases vascularisation. Histopathologic examination reveals an irregular epithelium, with degenerating basal cells and thickened basement membrane. The basal lamina lacks hemidesmosomes and Bowman's layer is often fragmented. A thick layer composed of amyloid and collagen usually separates this layer from epithelial basement membrane. The stroma contains large and irregular deposits, which distort the regular lamellar pattern. Type AA amyloid has been identified in the cornea of several patients. The deposition of amyloid is observed in all levels of stroma,

especially in the anterior two thirds. There is no systemic amyloid deposition (Frayer et al, 1959).

Type III

This is a late onset dystrophy, arising in the fifth decade or later in life and has been reported in Asian patients (Hida et al, 1987). These deposits are midstromal and larger than the deposits in age-matched individuals with type I. The observed subepithelial and stromal opacities, deposits and haze are less prominent. Type III deposits are type AP amyloid in contrast to type AA in type I. The inheritance pattern is autosomal recessive and the gene has not been mapped yet. Recurrent erosion is uncommon in patients with this type of dystrophy.

Type IIIA

A variant described as type IIIA is similar to type III, except that recurrent erosions are common, inheritance is autosomal dominant and type IIIA is seen in white patients (Stock et al, 1991). The lattice lines in this case are deeper, ropy, branching and near to limbus.

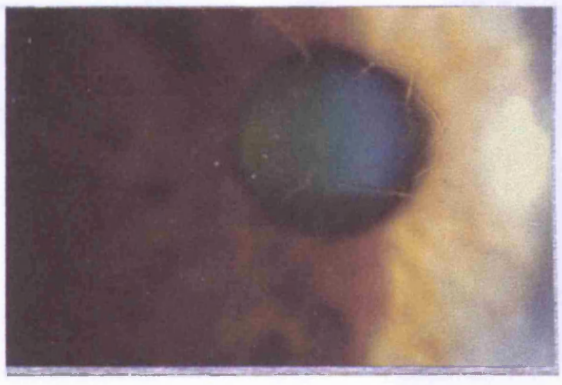

Figure 1.7: Lattice corneal dystrophy type IIIA
(Courtesy of Prof. GCM Black)

Amyloid stains rose to orange red with Congo red dye and metachromatically with crystal violet dye. Several cases with visual loss resulting from corneal dystrophy are treated with penetrating keratoplasty. Recurrence of the dystrophy in the cornea graft (usually in 2 to 12 years) occurs more frequently than granular or macular dystrophy (Stock et al, 1991).

1.4.1.4 Reis Buckler's Dystrophy (Corneal Dystrophy of Bowman's layer I)

This is a progressive dystrophy that appears in the first few years of life with recurrent attacks of photophobia and irritation. It is a severe disorder that results in anterior corneal opacification, irregular astigmatism, anterior stromal oedema and subsequent early loss of vision.

It mainly affects Bowman's layer, most of which is disrupted and replaced by granular deposits that correspond to confluent subepithelial opacities. The surface of the epithelium appears irregular and of varying thickness. The opacities are more dense in the central cornea, whereas there is a fine haze extending to the limbus (Paufique et al, 1966). Biomicroscopy reveals a superficial, gray-white reticular opacification. The epithelial cells show degenerative changes and a prominent subepithelial layer contains fragments of Bowman's layer, fibroblasts and fibrous tissue (Rice et al, 1968, Akiya et al, 1971 and Kuchle et al, 1995). The posterior cornea appears normal, but in advanced cases the anterior scarring can lead to surface irregularity. The fibrocellular deposits are stained red with Masson's trichrome and are arranged in a lamellar pattern.

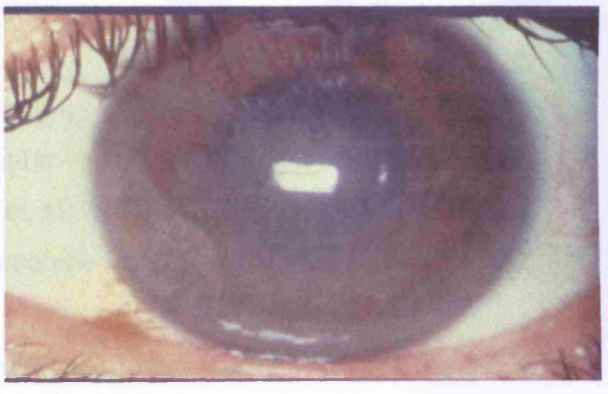

Figure 1.8: Reis Buckler's corneal dystrophy
(Courtesy of Prof. GCM Black)

Initial treatment is aimed at the recurrent erosions. Superficial keratectomy, lamellar keratoplasty, excimer excision, or rarely penetrating keratoplasty may be performed. Recurrence in the graft is common.

1.4.1.5 Honeycomb (Thiel and Behnke) Dystrophy

Also known as Corneal Dystrophy of Bowman Layer II, to distinguish from Corneal Dystrophy of Bowman's layer I (another name for Reis Buckler's Dystrophy).

Honeycomb dystrophy appears early in childhood and develops progressively with painful recurrent erosions and gradual moderate deterioration in vision (Weidle, 1999). Characteristics of this disorder are the subepithelial honeycomb-shaped, asymmetrical opacities, which are manifested in the second decade of life. In later stages the opacities affect mostly the central rather than the peripheral cornea at the level of Bowman's layer. The corneal surface is smooth and corneal sensation is not significantly decreased. Recurrence in the graft following keratoplasty is common.

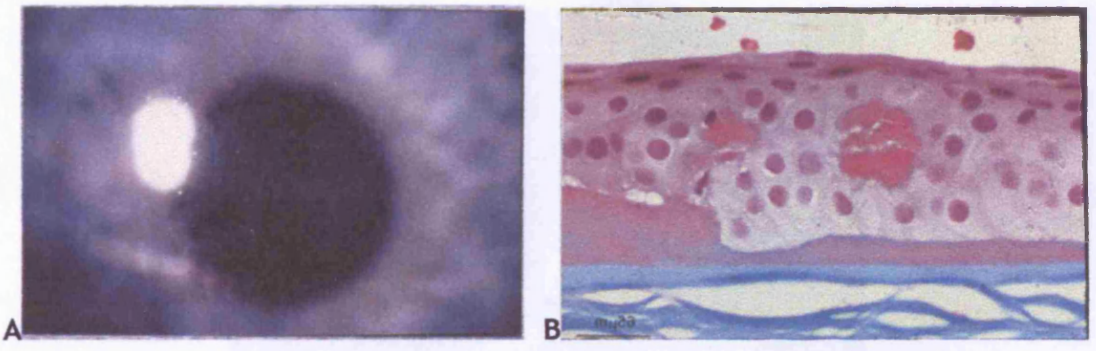

Figure 1.9: Honeycomb corneal dystrophy

A. Photograph of the cornea from a Thiel-Behnke patient. B. H&E staining (Courtesy of Prof. GCM Black)

Histopathological findings include thickened, split epithelial basement membrane and a fibrillogranular subepithelial layer with protrusions to the overlying epithelium (Okada et al, 1998). Deposits of curly fibers in the subepithelial region and superficial stroma are identifiable only by Electron Microscopy (Weidle, 1989).

1.4.1.6 Map-dot-fingerprint Dystrophy

This is a bilateral dystrophy of possibly dominant inheritance due to incomplete penetrance and lack of obvious inheritance patterns. It has not been attributed to mutations on the βig-h3 gene, but it is suspected to be linked and is currently under investigation. Symptoms vary from recurrent epithelial erosions to blurred vision. The dystrophy is characterised by three types of lesions which occur in the epithelium and the adjacent basement membrane:

i) Fingerprint lines. These are thin hairlike lines.

ii) Map lines. Same as the above, with the exception that they are thicker, more irregular and surrounded by a haze.

iii) Dots/microcysts. They are gray-white intraepithelial spaces with discrete edges. When these are prominent they are described as Cogan's microcystic dystrophy, (Cogan et al, 1964).

iv) Net and bleb patterns arise from thickenings of the basal lamina at the basal aspect of epithelial basal cells (Laibson et al, 1975).

Fingerprint and map lines comprise strips of epithelial basement membrane. Dots consist of the debris of epithelial cells that have collapsed before reaching the surface.

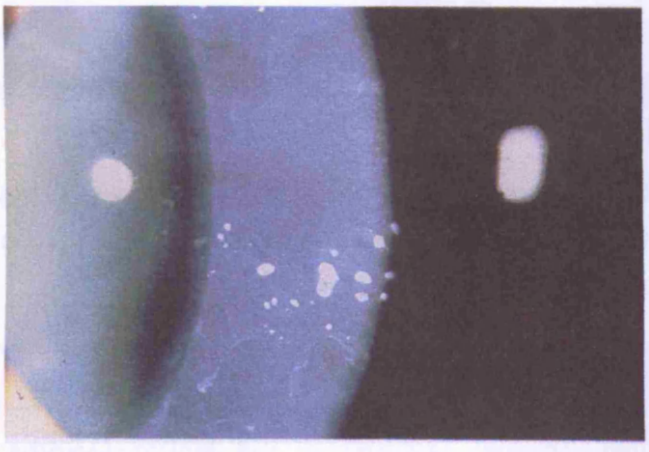

Figure.1.10: Map Dot Fingerprint dystrophy
(Courtesy of Prof. GCM Black)

Histopathologically there is thickening of the basement membrane with extension to the epithelium, abnormal epithelial cells with microcysts, fibrillar material between the basement membrane and Bowman's layer.

Treatment includes lubricating drops, epithelial scraping, anterior stromal puncture, removal of damaged epithelium (Laser).

1.5 KERATOEPITHELIN

1.5.1 Terminology

Both the gene and the protein have been described in the literature with various different names. To avoid confusion, in this report the gene will be termed βig-h3 and the resulting protein, keratoepithelin.

1.5.2 Gene and protein

The gene encoding for keratoepithelin, was first cloned and sequenced by Skonier et al, 1992, while trying to identify novel genes induced by Transforming Growth Factor-β (TGF-β). It was isolated from a cDNA library constructed from human adenocarcinoma cell line A549, which had been treated for 3 days with TGF-β. The gene was named after the clone it was derived from: TGF-β induced gene-human clone 3, i.e. βig-h3.

βig-h3 was mapped by in situ hybridisation on chromosome 5q31 (Skonier el al, 1994) and the nucleotide sequence was found to be 86% homologous with the murine equivalent, βig-m3, which is located on mouse chromosome 13 region B/C1.

DNA sequencing analysis revealed that βig-h3 encodes a 683 amino acid protein (Skonier et al, 1992). The protein has a 23 amino acid NH_2-terminal secretory sequence, which indicates that it is an extracellular protein. Dermal fibroblasts grown on a three-dimensional Vicryl scaffold secreted keratoepithelin into the extracellular matrix (LeBaron et al, 1995). An Arg-Gly-Asp (RGD) sequence is located in the carboxy-terminal but is possibly removed by post-translational processing since it is not present in secreted protein (Skonier et al, 1994). RGD sequence usually serves as a ligand recognition site for integrins (Ruoslahti et al, 1989).

Keratoepithelin has internal repeated domains, which have highly conserved sequences found in some secretory and membrane proteins of several species, like periostin/osteoblast-specific factor-2 (OSF2) (cross-species, like keratoepithelin), fasciclin-I (*Drosophila*) and MPB70 (*Mycobacterium tuberculosis*). *Drosophila*'s fasciclin-I, is found in nerve fibers (Zinn et al, 1988), associates with membranes and serves as a "homophilic adhesion molecule" (Elkins et al, 1990). The homologous domains of the above proteins have been designated fas-1, from fasciclin-I homologous domain. Keratoepithelin, like fasciclin-I and periostin, has 4 fas-1 domains whereas MPB70 has only one. Each fas-1 domain is characterised by two highly conserved sequences of about 10 amino acids, H1 and H2.

Repeat	Amino acids	Length
1	139-275	137
2	276-410	135
3	411-537	127
4	538-670	146

Table 1.2: Fas-1 repeat sequences (in amino acids) in keratoepithelin

Keratoepithelin is conserved between species and this has aided the identification of homologues in other species. The murine protein is 90.6% similar to human (Skonier et al, 1994) and the rabbit 92% (Rawe et al, 1997). A 66kD collagen fiber-associated protein (RGD-CAP) isolated from a fiber-rich fraction of pig cartilage was found to be 93% homologous with human and mouse keratoepithelin (Hashimoto et al, 1996). RGD-CAP is also homologous with OSF2 and fasciclin 1, like keratoepithelin. The bovine homologue MP78/70 has been extracted from fetal calf ligament and is thought to associate with microfibrils in ECM (Gibson et al, 1996).

Other characteristics of the keratoepithelin protein include no apparent predicted N-glycosylation sites, no disulfide-bonded dimer in solution and a heterologous charge: pI 6.2-6.71 (Escribano et al, 1994).

1.5.3 Tissue distribution

Since its discovery, several experimental procedures have been carried out to understand more about this gene and its expressed protein. One of the first steps (Escribano, 1994 and Skonier, 1994) was the identification of tissues where βig-h3 is expressed. βig-h3 transcripts were detected in the total RNA extracted from a variety of tissues: Heart, breast, testes, prostate, duodenum, epidermis, dermis, adrenal, ovary, liver, pancreas, parathyroid and spleen. Whereas, without any prior treatment several cell lines express βig-h3 the levels of the mRNA transcripts are usually low. Exception to this observation are human primary foreskin fibroblasts, which constitutively produce and secrete unusually high levels of keratoepithelin (LeBaron et al, 1995). In contrast, the brain and cerebellum showed consistently no βig-h3 expression.

Antibodies raised to synthetic human βig-h3 identified extracted MP78/70 and immunohistochemistry localised it in a variety of bovine tissues, including developing nuchal ligament, aorta, lung, kidney, mature cornea and foetal spleen (Gibson et al, 1997). The protein, the bovine homologue to keratoepithelin, was found in the region of interstitial collagen fibers and in association with some basement membranes. The staining pattern resembled collagen IV and double staining revealed localisation around collagen IV microfibrils, which are also found in association with the cell surface and attached to several basement membranes (Maier and Mayne, 1987; Rittig et al, 1990; Zhu et al, 1994).

Keratoepithelin is one of the molecules that have been identified in association with fibrillin-containing microfibrils in developing tissues. βig-h3 mRNA was found abundantly in both the extracellular matrix of human trabecular bone and in osteoblast cell culture (Kitahama et al, 2000).

The gene expression must be regulated by the cell shape and environment, since lung fibroblasts have a low level of keratoepithelin compared to the high level of expression in primary dermal fibroblasts. Keratoepithelin has been immunohistochemically localised in the human skin, where it is found in the papillary dermis, especially in the granular layer of epidermis (LeBaron et al, 1995).

βig-h3 is also expressed in the normal kidney. In diabetic rats, where there is an increased glucose concentration, TGF-β, collagen VI and βig-h3 transcription is increased 2-3 fold. Also in vivo, elevation in glucose levels leads to induction of TGF-β, which in turn causes overexpression of βig-h3 (Gilbert et al, 1998). The opposite happens in older rats, where the level of βig-h3 mRNA decreases in the kidney (Lane et al, 2001), possibly in response to the decreased amount of active TGF-β_1 available in these rats. βig-h3 has been used a marker for active TGF-β_1 in the kidney by Langham et al, 2001.

Immunohistochemistry of rat aortas localised keratoepithelin on endothelial cells, smooth muscle cells and in the matrix between elastic fibers (Ha, 2003). Diabetic aortas were more heavily stained. TGF-β_1 increased keratoepithelin levels in a dose-dependent manner in vascular smooth muscle cells. High glucose increases keratoepithelin and TGF-β_1 production. Conversely, neutralising antibodies to TGF-

β_1 block glucose induced keratoepithelin elevation, thus upregulation of keratoepithelin under high glucose concentration is mediated by TGF-β_1.

βig-h3 is transcribed almost exclusively in the corneal epithelium as shown by *in situ* hybridisation (Kublin and Cintron, 1996) and is preferentially expressed on the external surface of corneal epithelial cells (Escribano et al, 1994). It is a component of the stroma where it is found with collagen VI (Rawe et al, 1995; Hirano et al, 1996).

It is noteworthy that in the cornea, where the expression of keratoepithelin is high, TGF-β_1 and TGF-β_2 transcripts are low. Conversely in the lens where TGF-β_1 and TGF-β_2 levels are high there is little or no keratoepithelin. As in many pathologic cases (Genini et al, 1996, Kim et al, 2000, Hu et al, 2001), the βig-h3 expression is altered in lens as well. Lens epithelial cells express abundant keratoepithelin in anterior polar, but not in nuclear cataracts (Lee et al, 2000).

1.5.4 Function

Despite extensive work on the genetics of βig-h3, it is not clear yet what the exact role of this protein is. Assumptions and hypotheses have been made, based on the experimental findings. One of the areas it is implicated with is cellular proliferation, since it is induced by a growth factor. Transfection of Chinese Hamster Ovary (CHO) cells with expression vector carrying βig-h3 resulted in alterations in the shape, growth rate and tumourgenicity of these cells (Skonier et al, 1994).

Recombinant keratoepithelin promotes the adhesion and spreading of fibroblasts in a time and concentration-dependent fashion. This property is also exhibited by collagen VI, which is involved in several cellular and matrix interactions (Doane et al, 1992). Adhesion, spreading, migration and proliferation of vascular smooth muscle cells was mediated by immobilised keratoepithelin (Ha et al, 2003)

βig-h3 was first implicated in wound development and healing by O'Brien et al (1996) who were studying vascular lesions. TGF-β is overexpressed during coronary atherosclerosis and restenosis after balloon angioplasty. βig-h3 seems to be expressed in normal vascular tissue and overexpressed during the development of atherosclerosis and restenosis in human vascular lesions. Normal expression is seen

in epithelial cells, whereas in pathological lesions stellate-shaped smooth muscle cells (SMC), and in more severe conditions, macrophages also express this gene, the product of which is accumulated in ECM. Overexpression of both TGF-β and βig-h3 may cause excessive tissue repair and the formation of abundant scar tissue.

The mouse βig-h3 has been characterised extensively. Its structure and the number of exons are similar to human (Schorderet et al, 2000). To gain an insight into its physiological role, the embryonic expression was determined at different developmental stages. During embryogenesis βig-h3 is seen in tissues derived from mesoderm, like developing bones, cartilage, blood vessels, thymus, kidney, and peribronchial structure. It is highly expressed in developing heart and pancreas. In the fetal eye expression starts at the optic stalk and progresses towards the sclera and the choroid and finally reaches the cornea. Although the physiological role remains unknown it seems that βig-h3 is an important component of the mesenchyme and plays an important role in the development and maintenance of many organs.

Both native and recombinant form of the porcine homologue, RGD-CAP, bind to collagen. The triple-helical three-dimensional conformation of collagen seems to be crucial for this interaction, since RGD-CAP would not bind to collagen that had been boiled for 5 minutes (Hashimoto et al, 1997). The in vitro interaction between keratoepithelin and collagen VI is non-covalent (Hanseen et al, 2003). The keratoepithelin binding site is located close to the N-terminal end of triple helical region of collagen VI.

During the development and wound healing in the cornea, βig (rabbit gene) transcription is increased together with type VI and XII collagen and β-actin. This increase is observed during the first two weeks of wound healing and decreases during the following 4 weeks (El-Sabrawi et al, 1998). mRNA levels of βig are higher than type VI collagen in the early stages, which reflects differences in the deposition of these proteins in the extracellular matrix and the distinct roles they play in these processes.

The mRNA transcripts of βig, the rabbit homologue, are found to be located primarily in the corneal epithelium, but during development and healing they are found in the stroma as well (Rawe et al, 1997). The intensity of labelling changes

during development and healing, which suggests that the site, level and timing may vary at different stages.

βig-h3 mRNA is upregulated by TGF-β_1 but not by EGF in corneal epithelial cells in a cell density-dependent way. When these cells reach confluence the levels of βig-h3 drop, which indicates a decrease in the magnitude of TGF-β_1 induction (Wang, 2002). It is possible that βig-h3 expression is enhanced in response to TGF-β_1 at early stages of wound healing, but is later downregulated through a cell-cell contact inhibitionary autoregulatory mechanism, as happens with TGF-β_1 (Kaji et al, 2000) and a variety of other genes involved in the wound healing process.

Immobilised and soluble recombinant keratoepithelin, with and without the RGD sequence inhibits bone nodule formation in a dose-dependent manner, like fibronectin (Kim et al, 2000). The same observation was reported on the effects of exogenous keratoepithelin on periodontal ligament cells (Ohno et al, 2002). In addition downregulation of collagen I was inhibited, which collectively implicates keratoepithelin as a negative regulator of mineralisation and osteogenesis. In the periodontal ligament, keratoepithelin is expressed as a >200kDa product under non-denaturing and ~70kDa under reducing conditions, which suggests the presence of multimers in the native form (Ohno et al, 2002). The presence of cystein near the carboxy-terminus could be responsible for the multimerisation of the protein via the formation of disulfide bonds.

Staining for keratoepithelin varies during cartilage development of chick embryos (Ohno et al, 2002). Recombinant RGD-CAP in the presence of cyclohexamine, which inhibits synthesis of growth factors, promotes adhesion and spreading of mesenchymal stem cells and inhibits the mineralisation of hypertrophic chondrocytes. Therefore keratoepithelin plays an essential role in early cartilage development by enhancing adhesion and growth of pre-chondrogenic cells and acting as a negative regulator of mineralisation at the terminal stage of chondrogenic differentiation.

The effect of mechanical stimuli on the expression of keratoepithelin was investigated by Doi et al in 2003. βig-h3 mRNA and the corresponding protein were increased in periodontal ligament from orthodontic force and cells cultured under mechanical tensile force. This increase was abolished by neutralising antibodies

against TGF-β_1. Therefore βig-h3, induced by TGF-β_1 is upregulated in response to mechanical stimuli, possibly by contributing to remodelling and homeostasis of periodontal ligament tissue.

Although the brain is a tissue where βig-h3 expression was found to be non-existent under normal conditions (Skonier el al, 1994; Escribano et al, 1994; Aitkenhead, et al 2002), the pattern changes in response to injury. Astrocytes express significant amounts of βig-h3 at the site of a stab wound in the cerebral cortex of adult rats. Also cultured human and mouse astrocytes produce increased amounts of βig-h3 mRNA and protein in response to TGF-β_1 induction (Yun et al, 2002). Other cytokines including TGF-β_2, TNF-α, PDGF, IL-6 and IFN-γ had no effect on βig-h3 expression.

All the findings are suggestive that keratoepithelin is involved in growth, development, differentiation and wound healing. It is a component of the extracellular matrix, where it is associated (structurally/functionally) with collagen and cells. It probably binds to cell-surface components in conjunction with other ECM molecules and might be required for signal transduction or as a surface recognition/anchoring protein.

1.5.5 Integrins

Integrins are cell surface receptors composed of α and β-chain transmembrane heterocomplexes, which mediate interactions between the cell and the ECM proteins. The functional interaction between these receptors and ECM molecules is responsible for the transduction of bi-directional signals which ultimately regulate adhesion, differentiation, proliferation and tumour progression (Giancotti and Ruoslahti, 1999). Keratoepithelin is a component of the ECM and it is thought to interact with cells through various integrins, which seem to vary with the cell type.

Recombinant RGD-CAP (porcine keratoepithelin) promotes the spreading and attachment of a variety of chondrocytes and fibroblasts but not pulp-derived odontogenic cells and the reason for this was speculated to be different types of integrins expressed on the surface of the different cell types via which the attachment could be mediated (Ohno et al, 1999). Supportive of this speculation was the fact that spreading was inhibited by EDTA and required divalent cations, which is the case for integrins (Lallier et al, 1992; Garratt et al, 1995). Previously

keratoepithelin had been immunologically co-localised with integrin β_1, but it had been impossible to establish a cross-linking product (Escribano et al, 1994). Furthermore, neutralising antibodies against a variety of integrins demonstrated that α_1 and β_1 suppress the keratoepithelin mediated spreading. Therefore $\alpha_1\beta_1$ integrin is important for keratoepithelin, which is probably a ligand for it.

The same experiment as described above was repeated with human corneal epithelial (HCE) cells (Kim et al, 2000) and keratinocytes (Bae et al, 2001) and a different integrin-receptor was identified for these cells, $\alpha_3\beta_1$. Recombinant keratoepithelin does not only promote skin keratinocyte adhesion and spreading, but also enhances migration, which implicates it in wound healing.

Although both corneal epithelial cells and fibroblasts express $\alpha_3\beta_1$ and $\alpha_v\beta_5$ integrins, each one of them interacts through a different binding site in keratoepithelin mediated adhesion. HCE cells adhere through $\alpha_3\beta_1$ and fibroblasts through $\alpha_v\beta_5$ (Kim et al, 2002). This suggests that keratoepithelin may mediate various cell functions through multiple cell-adhesion motifs that interact with diverse integrins on different cell types.

Keratoepithelin mediates vascular smooth muscle cell adhesion via α_v integrin (Ha et al, 2003).

Immobilised keratoepithelin promotes adhesion of astrocytes and this interaction requires divalent cations and is blocked by RGD peptides, suggesting the implication of an integrin. The combined results from blocking monoclonal antibodies against integrin subunits and expression profile of integrins on the astrocyte cell surface indicate that keratoepithelin mediates adhesion on these cells through $\alpha_6\beta_4$ (Kim et al, 2003). For the first time keratoepithelin was associated with a signalling process: astrocyte interaction with keratoepithelin is dependent on signalling through the src kinase. Also focal adhesion kinase (FAK) and paxillin are Tyr phosphorylated upon this interaction and the phosphorylation is blocked by anti-β_4 integrin. Thus $\alpha_6\beta_4$ evokes keratoepithelin mediated cell changes through FAK activation. Since βig-h3 is upregulated in astrocytes after injury (Yun et al, 2002) its binding on $\alpha_6\beta_4$ may initiate cytoskeletal reorganisation of astrocytes during CNS repair.

Human umbilical cord endothelial cells (HUVEC) bind to keratoepithelin and each one of its fas-1 domains through integrin $\alpha_v\beta_3$ which is more predominant on HUVEC surface than $\alpha_v\beta_5$ (Nam, 2003). This binding takes place in a dose-dependent manner.

1.5.6 Identification of functional domains

It is interesting that $\alpha_1\beta_1$ integrin does not recognise the RGD sequence and therefore another sequence from keratoepithelin is responsible for ligation to $\alpha_1\beta_1$ (Ohno et al, 1999).

In order to identify the keratoepithelin motif responsible for integrin binding, different recombinant peptides were used to compare the adhesion of the HCE cells, each one corresponding to each fas-1 domain. The 2nd and 4th fas-1 domains mediated adhesion like the wild type protein and were also blocked by α_3 and β_1 antibodies (Kim et al, 2000). Therefore a sequence other than H1 and H2 must be responsible for the interaction with the integrin. Computer homology search among the fas-1 domains revealed aspartic acid and isoleucine, near H2, conserved in the 2nd and 4th domains. Mutant proteins for these two amino acids and synthetic peptides indicated that aspartic acid and isoleucine are essential for adhesion through $\alpha_3\beta_1$.

Different deletion mutants of the 4th fas-1 domain indicated that fibroblast adhesion was mediated by a sequence not yet identified. Two conserved amino acids, tyrosine (Y571) and histidine (H572) play an important role in $\alpha_v\beta_5$ adhesion, but also other flanking amino acids seem to be important for this interaction, such as isoleucine and leucine (Kim el al, 2002).

The above YH amino acids and the flanking isoleucine and leucine are also required for HUVEC adhesion on recombinant keratoepithelin (Nam, 2003). An 18 amino acid peptide including YH mediates endothelial and fibroblast adhesion and migration through interaction with $\alpha_v\beta_3$ and $\alpha_v\beta_5$ respectively. The same peptide inhibits angiogenesis in vitro and in vivo.

Integrins $\alpha_v\beta_3$ and $\alpha_v\beta_5$ share some ligands and both bind to RGD peptide. It is possible that both YH and RGD interact with both of these integrins in a similar

manner, but have different binding affinity for each or the affinity may depend on the activation state of the integrin (Nam et al, 2003).

1.5.7 Tumourigenesis

Throughout the last 8 years βig-h3 has been mentioned in various papers (sections 1.5.7.1 and 1.5.7.2 below) that examine the changes in gene expression of malignant cells. Further research on the protein itself and the way it interacts with cells defined a more specific role in tumourigenesis.

Downregulation	Upregulation
ERMS	ESCC
HeLa x fibroblast hybrid	Angiogenesis
Melorheostosis	Glioma
Non-senescent HUVEC	Lung cancer
Malignant bronchial cells	Pancreatic cancer

Table 1.3: Altered expression of βig-h3 in various tumour or growth associated conditions

1.5.7.1 Downregulated in tumour

The chromosomal position of βig-h3, 5q31, is also a region deleted in all leukaemias and some carcinomas and it has been suggested that this region may contain a tumour suppressor gene (Skonier et al, 1994).

Overexpression of βig-h3 in CHO cells resulted in alterations in their shape, growth rate and tumourgenicity (Skonier et al, 1994). This was the first time it was suggested that βig-h3 might be a non-DNA binding anti-oncogene that may exert its function by interacting with cell surface integrins and ECM molecules.

Purified protein was also found to inhibit the attachment of A549, HeLa and human lung fibroblast (WI-38) cells to plastic in serum-free media, presumably by causing cell-cell aggregation. Cell attachment and migration are important for tumour progression.

Embryonal rhabdomyosarcoma (eRMS) is a skeletal muscle malignancy, where p53 tumour-suppressor gene and *ras* oncogene are mutated (Stratton et al, 1990; Felix,

1992). βig-h3 is one of ECM proteins downregulated and consistently differentially expressed in RMS cells (Genini et al, 1996). The expression of βig-h3 by myoblasts and the loss of expression in the malignant cells suggests that βig-h3 plays a role in normal cell growth.

βig-h3 is also one of 17 genes differentially expressed in non-tumorigenic HeLa×fibroblast hybrids (Tsujimoto et al, 1999). Some of the other genes which have similar expression, e.g. collagen I α-2 chain, have also been associated with suppression of tumourgenicity.

Subtractive hybridisation of mRNA from early passage and senescent HUVEC demonstrated that βig-h3 is upregulated in senescent cells (Grilliari et al, 2000). Therefore increased expression of βig-h3 and some other ECM proteins, including PAI-1, fibronectin and IGFBP-3 may contribute in the growth arrest of senescent cells.

Melorheostosis is a rare condition characterised by hyperostosis of the cortex. βig-h3 is the most dramatically downregulated gene in melorheostosis skin fibroblasts (Kim et al, 2000). It has already been described that keratoepithelin is involved in early stage bone formation where it plays a negative role as regulator of osteoblastic differentiation (Ohno et al, 2002). Therefore reduced expression of βig-h3 may contribute to the excessive growth that characterises this disorder. Other adhesion proteins downregulated in this experiment include fibronectin, OSF-2 and osteonectin, which together with βig-h3 reflect the negative regulation they exhibit on the cell growth rate.

An asbestos-induced bronchial malignant cell line showed a 7-8 fold decrease in βig-h3 expression, which was accompanied by loss of half chromosome 5 (Zhao et al, 2002). βig-h3 overexpression in these cells resulted in limiting their ability of anchorage-dependent growth and tumourgenicity. 14 human tumour cell lines tested by these researchers demonstrated decreased βig-h3 expression, which suggests that loss of keratoepithelin contributes to the cancerous phenotype.

Loss and gain of specific integrins is involved with malignant transformation, tumour progression and metastasis (Mizejewski, 1999). Depending on the cell and

tumour type, integrins act either as promoters or inhibitors of carcinogenesis. It was found that $\alpha_5\beta_1$ is upregulated in the malignant bronchial cell line used above (Zhao et al, 2003), whereas βig-h3 is downregulated (Zhao et al, 2002). $\alpha_5\beta_1$ is actually upregulated in a variety of cancer cells and protects from apoptosis in vitro by inducing anti-apoptotic Bcl-2 (Zhang et al, 1995). Therefore βig-h3 may play a role in the regulation of expression of $\alpha_5\beta_1$ receptor.

The first report that attempted to provide an explanation for the anti-proliferative effect of βig-h3 was by Kim et al in 2003. The research was based on the fact that RGD peptides cause anoikis, a form of apoptotic response due to the absence of cell matrix interactions. RGD peptides are thought to block the integrin-ligand interactions and thus the signals for cell survival. Wild type keratoepithelin undergoes C-terminal cleavage after secretion and releases RGD peptides. Several cell lines that were transfected with wild type βig-h3 undergo apoptosis in contrast with the RGD peptide mutant transfectants, which grow normally. Therefore keratoepithelin may mediate its apoptotic effect by releasing soluble RGD peptides.

1.5.7.2 Upregulated in tumours

Even though all the above findings associate βig-h3 with an apoptotic character, a number of cancers have also been described where βig-h3 is significantly upregulated.

βig-h3 is one the 13 genes that were upregulated ≥2fold in 2 Esophageal Squamous Cell Carcinomas (ESCC). Normal esophageal epithelium expresses βig-h3, but in low amounts (Hu et al, 2001).

Angiogenesis plays an important role in a number of physiological and pathological processes including tumour formation (Yancopoulos et al, 2000). Aitkenhead et al in 2002, determined angiogenic genes from endothelial cells that form tubes in 3D collagen gels and βig-h3 was found to be 5.3 fold differentially upregulated. Aggressive tumours are associated with high angiogenesis (Tas et al, 2000). βig-h3 expression levels were consistently increased in a variety of tumour samples (from breast, uterus, colon, stomach and rectum), in some cases up to 70-fold. Antisense oligonucleotides to βig-h3 dramatically decreased tube formation in 3D, but had no

effect on 2D cultures. No significant correlation was made between βig-h3 and the angiogenic state due to broader expression of this gene (O'Brien et al, 1996).

Although the βig-h3 transcript is not detectable in normal adult brain, it is increased in brain tumours (Golembienski et al, 2002). cDNA array demonstrated that βig-h3 is switched on by SPARC (Secreted Protein Acidic and Rich in Cystein), which is also upregulated in human gliomas. βig-h3 increased expression is not reversed by removing the SPARC effect.

Another tissue where βig-h3 mRNA is elevated during tumour is the lung. It was examined whether βig-h3 could be used as a marker for advanced lung cancer but the correlation between expression levels and survival rates was not significant, although βig-h3 levels increased with the stage of cancer (Sasaki et al, 2002).

In normal pancreas the levels of βig-h3 mRNA are moderate compared with the high levels (32.4 fold elevation) observed in pancreatic cancer (Schneider et al, 2002). βig-h3 is induced in this tissue by TGF-βs, which exert their effects via divergent signalling pathways.

1.5.8 In the cornea

The first association of corneal dystrophies with chromosome 5q was made in 1994 by Stone et al. The pedigrees of eight families affected with three different types of corneal dystrophies (Lattice corneal dystrophy I, Granular dystrophy and Avellino) were studied. Chromosome linkage analysis with highly polymorphic markers mapped all three dystrophies to chromosome 5q. At that time Skonier et al had not published the results of their research, mapping βig-h3 on 5q31. Therefore the nature of the unknown gene was attempted to be explained from the scope of the clinical and histopathological findings associated with the above dystrophies. It was hypothesised that the abnormal protein was synthesised by epithelial cells or keratocytes and transported/diffused to the corneal stroma, where it deposited forming insoluble aggregates. These hypotheses were more or less confirmed by further research that was carried out on several types of corneal dystrophies. βig-h3 was extracted from normal human corneas (Klintworth et al, 1994), but more research was carried out before it was associated with the dystrophies.

Further fine chromosomal mapping refined the genetic localisation of corneal dystrophies between known markers (Eiberg et al, 1995; Gregory et al, 1995, Small et al, 1996 and Korvatska et al, 1996). A YAC contig of the linked region was generated (Munier et al, 1996) and cDNA selection identified a clone with 100% homology with the βig-h3 gene. This gene was considered as a good candidate, due to its chromosomal location and its preferential expression in both corneal epithelium and stromal keratocytes (Skonier et al, 1994; Escribano et al, 1994).

In 1997 Munier et al discovered that four distinct corneal dystrophies, Lattice type I (LCDI), Granular Groenouw type I (CDGGI), Reis Bucklers (CDRB) and Avellino (ACD) were caused by mutations in the βig-h3 gene. All of the mutations are amino acid substitutions which were hypothesised to result in distortion of the three-dimensional shape of the keratoepithelin molecule. LCD1 and ACD had a common amino acid substitution on codon 124. LCDI had a C to T transition at nucleotide position 417 (R124C) and Avellino had a G to A transition at nucleotide position 418 (R124H). Likewise, CDGG1 and CDRB had mutations on codon 555; CDGG1 exhibiting a C to T transition at nucleotide 1710 (R555W) and CDRB having a G to A transition at position 1711 (R555Q).

Screening of 10 additional families from different ethnic groups affected with the above four types of corneal dystrophies, confirmed these mutations and indicated that they occurred independently and were responsible for the phenotypic manifestations of these diseases (Korvatska et al, 1998). Therefore, it was concluded that CpG dinucleotides at amino acids R124 and R555 represent hot spots for mutations.

Another interesting observation is that both amyloid-related phenotypes, ACD and LCD1, were mutated in the R124 hotspot and that both non-amyloid phenotypes, CDGG1 and CDRB, were defective in R555. It could be possible that the position of the mutated amino acid determines the pathogenesis of the resulting dystrophy, depending on how it affects the three-dimensional conformation and function of the mutant protein. R555 is located in the predicted coiled-coil domain and a mutation could alter it by impairing binding to stromal proteins, such as collagen (Hirano et al, 1996). According to the same principle, R124 would remove a putative phosphorylation site and could modify the structure of the protein.

However mutations solely in R124 can result in variable phenotype, depending on the amino acid alteration that has taken place. Thereby R124C results in amyloid deposition, R124H has mixed amyloid and granular deposits, or in the case of many Japanese patients only granular deposits. R124S is associated with CDRB (Stewart et al, 1999) and has non-amyloid deposits. Therefore apart from the position of the protein that has been affected by the mutation another important factor in determining the dystrophic phenotype is the nature of the amino acid substitution.

Corneas with granular dystrophy have accumulations of keratoepithelin. Whereas the ratio of albumin/keratoepithelin is 3:1 in normal corneas, in corneas with granular dystrophy the ratio is 1:4 (Klintworth et al, 1998). The deposits in the stroma of the affected corneas reacted with anti-βig-h3 antibody, but the epithelium did not stain.

Corneal dystrophies have an autosomal dominant inheritance pattern, so even one copy of the mutated gene is enough to exhibit the diseased phenotype. It seems that the phenotype for the affected individuals who are homozygous is more severe than the heterozygous patients. This was demonstrated by Okada et al (1998) who studied a family affected with Granular Dystrophy Groenouw type I, where there was a consanguineous marriage. Mutation R555W was found by Single Stranded Conformational Polymorphism (SSCP) and the homozygous patient had a very early onset (6 years of age) and a severe placoid type of corneal dystrophy with early recurrence after surgery. The same author selected five patients from different families to study their genotype. All the patients were affected with a rare and severe form of granular corneal dystrophy characterised by juvenile onset and confluent superficial opacities. All were found to be homozygous for the same mutation in keratoepithelin: R124H. As mentioned above, this mutation is responsible for Avellino corneal dystrophy.

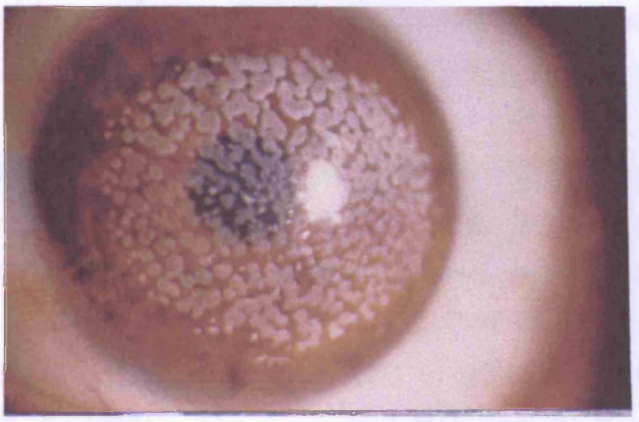

Figure 1.11: Avellino corneal dystrophy in a homozygous patient
(Courtesy of Prof. GCM Black)

Another illustration that the homozygous phenotype is more aggressive was provided by Inoue et al, in 2002. They showed that the recurrence-free interval after phototherapeutic keratectomy (PTK) in patients with R124H mutations was 9.5±3.1 months for homozygous and 38.4±6.2 months for heterozygous eyes. Also the clinical features and the intensity of the recurrence differed between the two groups.

Reis Buckler's Dystrophy has always been confused with Thiel-Behnke Dystrophy and patients diagnosed with the same dystrophy were frequently found to have different pattern of severity and opacification. The reason for this is the fact that the two dystrophies have very similar clinical appearance, but differ histologically and genetically (Weidle et al, 1995). Extensive light and microscopic examination of several corneas concluded that there are two distinct autosomal dominant dystrophies that affect the Bowman's layer (Kuchle et al, 1995). Further distinction between the two diseases came when their genotypes were established. Different mutations are responsible for each type of dystrophy, but both of the mutations are found on the mutation hotspots described previously (Korvatska et al, 1998). Reis Bucklers was caused by R124L mutation and Thiel-Behnke was related with R555Q. These mutations were again single nucleotide changes, resulting in single amino acid substitution. RBCD has been proposed to be the same as superficial GCD (sCGD) (Mashima et al, 2000).

Ethnic differences seem to play a role in the genotype-phenotype correlation of each dystrophy. The classic form of granular dystrophy in Japanese patients was reported to be R124H, which has been associated with Avellino Dystrophy in

Caucasians. 1 out of 10 Japanese patients diagnosed with granular dystrophy has R555W and 9 have R124H mutations (Konishi et al, 1998).

Similarly, Reis Buckler's dystrophy in two families with a common ancestor in Sardinia was found to be caused by a mutation other than R555W. Linkage and sequence analysis on the two families revealed a novel mutation on keratoepithelin responsible for the usual RB phenotype. A deletion of a single amino acid at position 540 (ΔF540) was the mutation found in all affected members of both families (Rozzo et al, 1998). The same mutation was diagnosed as LCDIIIA by Munier et al in 2002.

Keratoepithelin is mutated in positions other than the two hotspots R555 and R124. A mild form of deep stromal lattice corneal dystrophy was encountered in Japanese patients (Fujiki et al, 1998). The deposits varied in size and shape and amyloid was found in the corneal base between posterior stroma and Descemet's membrane. The genetic defect responsible for this disorder was a single amino acid change in keratoepithelin; L527R.

A case of an Asian patient suffering from typical granular dystrophy, with later onset than classical Groenouw Type I was reported by Stewart et al (1999). DNA analysis with SSCP defined the causative mutation on keratoepithelin hot spot, R124. A single nucleotide substitution (C417A) causes amino acid substitution R124S. It is interesting that different substitutions of the same amino acid, R124, result in quite distinct phenotypes (see table1.4).

Mutation analyses of as many members as possible from kindreds affected with corneal dystrophies, reveals more genotypes. LCDI, which has been linked almost exclusively with the R124C genotype, has recently been reported to have arisen from a different mutation in an American family. All the affected individuals are heterozygous for the point mutation L569R which affects βig-h3 exon 13 (Warren et al, 2003).

It may also be more efficient to classify the dystrophies according to their causative mutations, rather than the histological or clinical findings, which show significant variation. Mutation analysis of three kindreds with corneal dystrophy IIIA unveiled two new mutations in keratoepithelin (Stewart et al, 1999), N622H

and H626R. The same type of dystrophy (according to the conventional classification system) in Japanese patients was associated with keratoepithelin mutation P501T (Yamamoto et al, 1998). More recent mutations that attribute the LCDIIIA phenotype are: T538R, V627 (which is a frameshift mutation due to a nucleotide deletion) and A546T (Munier et al, 2002; Dighiero et al, 2000).

Mutation (nucleotide)	Mutation (amino acid)	Dystrophy	Reference
417 CGC → TGC	R124C P → UP	LCDI	Munier et al, 1997 Mashima et al, 1997
418 CGC → CAG	R124H P →PP	ACD GCD	Munier et al, 1997 Mashima et al, 1997
418 CGC → CTC	R124L P → NP	CDBI SGCD	Mashima et al, 1999 Stewart et al, 1999
417 CGC → AGC	R124S PP → UP	CDGG1	Stewart et al, 1999
1710 CGG → TGG	R555W P → NP	CDGG1	Munier et al, 1997 Yamamoto et al, 2000
1711 CGG → CAG	R555Q P → UP	CDBII	Munier et al, 1997 Okada et al, 1998
1618-1620 TTT → -	ΔF540 NP deleted	CDRB LCDIIIA	Rozzo et al, 1998 Munier et al, 2002
1627 CTG → CGG	L527R NP → P	LCD	Mashima et al, 2000
1548 CCA → ACA	P501T NP → UP	LCDIIIA	Yamamoto et al, 1998
1911 AAT → CAT	N622H UP → PP	LCDIIIA	Stewart et al, 1999
1924 CAT → CGT	H626R PP → P	LCDIIIA	Stewart et al, 1999 Chau et al, 2003
1926 GTC → TC	V627 NP	LCDIIIA	Munier et al, 2002
1600 CTG → CCG	L518P NP → NP	LCDI	Endo et al, 1999
1678 AAT → AGT	N544S UP → UP	LCDI	Mashima et al, 2000
1915 GGC → GAT	G623D NP → N	RBCD	Afshari et al, 2001
1683 GCC → ACC	A546T NP → UP	LCDIIIA	Dighiero et al, 2000
1939 GTT →GAT	V631D NP → N	CDL-deep	Munier et al, 2002
1661 ACA → AGA	T538R UP → P	CDLI/IIIA	Munier et al, 2002
414 GAC → CAC	D123H N → P	GCD (atypical)	Ha et al, 2003
1753 CTG → CGG	L569R NP → P	LCDI	Warren et al, 2003

Table1.4: Nucleotide and amino acid changes in βig-h3 related corneal dystrophies. PP-positive polar, UP- uncharged polar, NP- nonpolar, P- positively and N- negatively charged referring to amino acids

1.5.9 Insights into mutations

The role of keratoepithelin and the mechanism by which it results in the formation of a great variety of phenotypes in the cornea has been one of the main areas of interest. How do the mutations described in the table above give rise to amyloid or granular deposits? The approaches that were taken to answer this question include examination of corneas with dystrophies and application of recombinant DNA technology.

It has been suggested that keratoepithelin is expressed by the corneal epithelium and diffuses to the stroma where it covalently binds collagen VI (Bron, 2000). There is an anterior to posterior progression of CDs, as determined by the initial confinement of the recurrences after PTK. However, it has been demonstrated that both epithelium and corneal fibroblasts express keratoepithelin (Korvatska, 1999 and Escribano, 1994). Also the clinical and histopathological observations of recurrent LCDI were milder, comprising of anterior haze and subepithelial opacities, lacking lattice lines and amyloid in stroma. This may be because the keratocytes in the donor stroma produce wild type keratoepithelin (Snead et al, 2002). In the case of corneal transplant patients, the mutant keratoepithelin is derived from the patient limbus, which progressively provides the epithelium layer for the donor cornea. This layer expresses mutant keratoepithelin which could contribute to the recurrence of the milder subepithelial opacities.

The normal cornea, is characterised by diffuse staining for keratoepithelin in the Bowman's layer, stroma and less at Descemet's membrane (Streeten et al, 1999). In GCD cornea, keratoepithelin is a major component of the deposits but the question is if the deposits are comprised of the mutant or also wild type protein. The distribution of aggregates resembles the picture of normal corneas: Heaviest in Bowman's layer and between lamellar tissue.

Korvatska et al in 1999 used 2 different polyclonal antibodies, that were made against the N and C-terminal of keratoepithelin, to immunolocalise it in dystrophic corneas. Although both GCD and ACD reacted with both of the antibodies at the site of the deposits, in LCD corneas the N-terminal antibody gave no or weak staining. This is either because the N-terminal part of the protein is not accessible or due to presence of truncated mutant protein in amyloid deposits. Amyloid

diseases are characterised by extracellular deposition of abnormally folded protein precursors that form fibrils.

The normal cornea contains the following species of keratoepithelin: 68, 64, 57, 47 and 29 kDa (Korvatska et al, 2000). These species have the same sequence with N-terminal deletions, and therefore may be proteolysis products. 68kDa comprises the majority of keratoepithelin in the cornea. In mutated corneas there is an overall increase in keratoepithelin, especially at deposits, alteration in the amount of some species and accumulation of unusual sized fragments, possibly due to abnormal proteolysis (Hedegaard et al, 2003).

Light and electron microscopy of 22 amino acid synthetic peptides with R124 and C124 revealed fibrillar material of amyloid nature for C124, but not R124 (Schmitt-Bernard et al, 2000). Also C124 has more propensity to form amyloid. Cys is prone to disulfide bonding and may stabilise the peptide and play a role to its amyloid transformation.

Cells transfected with R124C and R555W mutant βih-h3 had a higher rate of cell death than wild type transfectants (Morand et al, 2003). It is thought that caspase -3 is more activated in the presence of mutant overexpression and that the 124 amino acid C-terminal keratoepithelin sequence is important for mediating apoptosis. However Kim et al in 2002 reported that the biochemical properties of wild type and mutant recombinant keratoepithelin are similar. No differences were observed during their interaction with other ECM molecules and the mediation of cell adhesion.

A very important finding was reported when the skin from an R124C patient was screened to check for amyloidosis. No deposits were found suggesting that another factor, possibly locally determined is responsible for the precipitation of deposits in the cornea (Schmitt-Bernard et al, 2000). This is supported by the fact that patients with corneal dystrophies do not appear to have any systemic abnormalities. There has already been described, another eye disease where the gene (REP-1) interacts with a retinal specific protein (Rab27) to produce the disease (Seabra et al, 1995).

1.5.10 Structure

Fasciclin-I, the protein which possesses the domain fas-1 found in many secreted and membrane-bound proteins, was crystallised (Clout et al, 2003). It was actually the 3rd and 4th fas-1 domains of this protein that were crystallised since previous attempts to determine the structure of the full-length protein had failed.

A novel domain fold is observed in fasciclin, consisting of the two globular fas-1 motifs (3rd and 4th) located on different poles. The two motifs are similar, with hydrogen bonds reinforcing the fold at key positions, but there are no stabilising disulfide bridges. Despite the determination of this novel fold it was not possible to predict how the homophilic adhesion is exerted by fasciclin-I. Fas-1 domains 1 and 2 may be required for resolving this.

Figure 1.12: Cartoon representation of Fasciclin-I
3rd and 4th domains structure (green and blue, respectively. (Source: Clout et al, 2003)

An alignment of the determined α-helixes and β-sheets with keratoepithelin fas-1 sequence was carried out in an attempt to predict the effect of mutations on keratoepithelin structure. Based on the fasciclin-I structure and the sequence alignment, the 4th fas-1 domain of keratoepithelin was modelled (Clout et al, 2003).

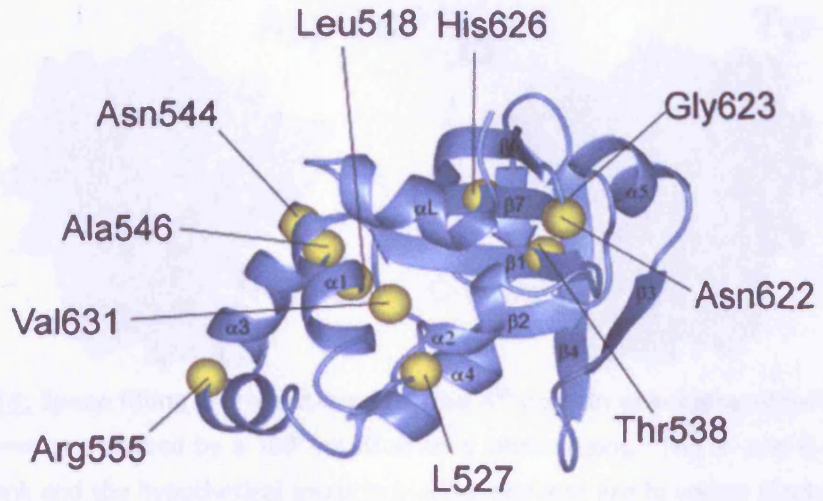

Figure 1.13: Cartoon representation of the model of 4th fas-1 keratoepithelin domain Location of missense mutations (yellow spheres). (Source: Clout et al, 2003)

It has therefore been feasible to determine the position of the corneal dystrophy mutations and the residues that have been implicated in integrin binding on this hypothetical 3-dimensional model of keratoepithelin. The most common mutation hotspots, R124[1] and R555, are located on the predicted surface of the keratoepithelin structure and therefore it is unlikely that a mutation in these hotspots would result in misfolding. However the altered protein solubility of the secreted mutant protein could result in extracellular aggregates. The binding properties of the mutant keratoepithelin could be changed or abolished, which would affect downstream protein-protein interactions.

The less common mutations, which are generally associated with the milder forms of corneal dystrophies, are found in the core of 4th fas-1 domain and are more likely to cause misfolding of the mutant protein.

[1] Predicted by sequence alignment, since R124 is located in the 1st fas-1 repeat of keratoepithelin

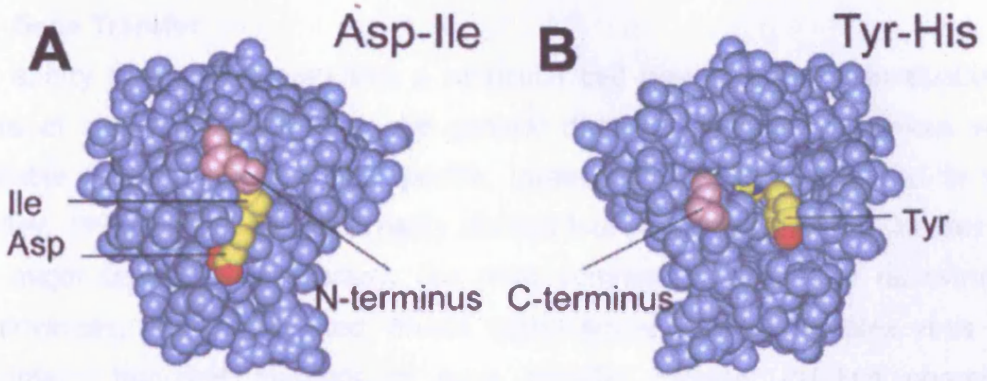

Figure. 1.14: Space filling representations of the 4th domain of keratoepithelin. The two views are related by a 180° rotation on a vertical axis. The N- and C-termini are coloured pink and the hypothetical integrin binding domains are in yellow (Carbon) and red (Oxygen). (Source: Clout et al, 2003)

The aspartic acid and isoleucine amino acids that have been described as essential for $\alpha_3\beta_1$ integrin binding (Kim, 2000) are located on the surface of the 4th fas-1 domain. It seems more possible that these amino acids interact with the 3rd domain rather than being involved with an integrin. Although on the surface, aspartic acid is structurally important due to a formation of a hydrogen bond between β_6 and α_5.

Tyrosine and histidine have also been implicated to have an important role in $\alpha_v\beta_5$ adhesion (Kim et al, 2002). Histidine is located in the fas-1 domain core and is tightly conserved, so it is unlikely to be involved with integrin binding. Tyrosine is more exposed but there are no additional surface features implying the existence of a protein-protein interface.

From the predicted structure of keratoepithelin it seems unlikely that real integrin-binding sites have been identified. The discrepancy in the results between the modelling and the cell-adhesion experiments can be due the peptides that were used for determination of the above amino acids. Cells adhered in the way that has been described with the primary structure of synthetic peptides, but it is possible that these interactions deviate from the ones that take place between the cells and the native, tertiary structured protein. Another feature that remains to be examined is the involvement of RGD with $\alpha_v\beta_5$ integrin.

1.6 Gene Transfer

The ability to transfer genes into a particular cell type of tissue is invaluable in terms of studying and treating the genetic disorders. There are various ways available to deliver genes into specific target cells, both in vitro and in vivo (Ledley, 1994). These can be broadly divided into viral and non-viral. Viruses are the major tool of gene therapy, the most common of which are retroviruses, adenoviruses, adeno-associated viruses (parvoviruses), herpes simplex virus and vaccinia. Non-viral methods of gene transfer include: calcium phosphate transfection, electroporation, ballistic DNA injection, microinjection, liposomes, peptides, cationic lipids, polymers, virosomes, proteosomes, hydrogel, ligand mediated.

1.7 ADENOVIRUSES

1.7.1 Structure

Adenoviruses are icosahedral particles 70-100nm in diameter, containing 13% DNA, 87% protein and trace carbohydrate. They comprise a protein outer shell, capsid, which encloses the DNA, a linear double-stranded molecule. The capsid is composed of 240 hexons and 12 pentons. Projecting fibres from the surface of the virion and associated with the pentons, determine the serotype of the virus. There are 47 human adenovirus serotypes and more in other mammals and birds. The serotypes used as vectors for gene transfer are based on human serotypes 2 and 5.

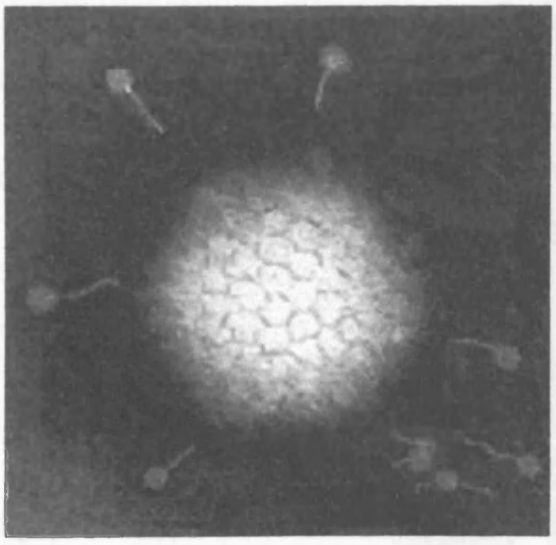

Figure 1.15: Electron micrograph of human Adenovirus

(Source: Linda Stannard, of the Department of Medical Microbiology, University of Cape Town)

Adenoviruses have a genome of about 36kb, for which the complete sequences of Ad5 and Ad2 are available. The viral DNA is associated with four polypeptides in the capsid. The DNA has inverted terminal repeat sequences that range from 100 to 140bp and enable single strands of DNA to circularise and replicate.

1.7.2 Genome organisation

The genomes from all serotypes of adenoviruses have the same general organisation. Thus there are specific positions where the genes encoding each specific protein are located. The adenoviral genetic material is a single linear DNA molecule containing two identical origins of replication, one in each terminal repeat. The chromosome carries five early transcription units (E1A, E1B, E2, E3 and E4) two delayed early units (IX and Iva2) and the major late unit, which generates five families of mRNA (L1-L5) transcripts. Adenoviruses operate a cascade system for replication. The first genes to be expressed following infection are in the E1 gene region. They are responsible for activating transcription of the early genes E2-E4, which in turn drive the expression of the delayed and late genes. (Shenk et al, 1995). Adenoviruses compensate for their small genomic size by using a complex system of post transcriptional processing. Each of the adenoviral genes transcribed by RNA polymerase II produces multiple mRNAs that are differentiated by alternative splicing and the use of different poly (A) sites. Proteins derived from the same transcription unit have some or even no sequence in common.

1.7.3 Replicative Cycle

The adenoviral cycle has been extensively studied, especially in serotypes 2 and 5. The cycle can be separated in two stages, early and late. The events that occur during infection are: entry in to the host cell, activation of early viral genes, activation of host cell to enter the S phase, DNA replication, activation of late viral genes, virus assembly and release from the cell.

1.7.3.1 Entry

Adenoviral infection is a highly complex process. It is initiated by the virus binding to the cellular receptor. The binding is a double process since it involves interaction of both the viral fiber protein with an unknown cellular receptor (Devaux et al, 1987) and the RGD sequence of the penton base protein with integrins (Wickham et al, 1993). Internalization occurs via receptor-mediated

endocytosis (Chardonnet et al, 1970). The overall process is not extremely efficient since 85% of the virus that binds on the surface of susceptible cells is internalized. Half of the absorbed virus moves to the endosomes and 90% of this reaches the cytosol within 5 minutes, and manages to escape it before a lysosome is formed (Mellman et al, 1992). After endosomal release, the virus particles travel across the cytoplasm to the nucleus, possibly by interaction of hexon with microtubules (Dales et al, 1973). The viral capsid undergoes disassembly as it migrates to the nuclear pore. Entry of the viral DNA into the nucleus is followed by capsid dissociation, and the viral DNA does not integrate into the host genome but remains in an episomal state. Once the viral genome has reached the host nucleus there are 3 goals to be scored:

1. Induction of the host cell to enter the S phase of cell replication (transformation)
2. Protection of the infected cell from antiviral defence
3. Synthesis of viral proteins essential for DNA replication

1.7.3.2 Early transcription

The next phase includes transcription of the early viral gene, E1A, which is controlled by a constitutive promoter. Transcription of E1A produces two phosphorylated proteins, 12S and 13S, known as trans-activators since they can activate other viral genes. These two proteins have the same 5' and 3' termini, but different internal sequences. Their ability to bind to a variety of cellular transcription factors and regulatory proteins results in alterations in the expression of cellular genes in order to promote transcription.

13S binds to TATA binding protein (TBP), which is part of the transcription factor TFIID, an important element for DNA replication. 13S also displaces tumor suppressor protein p53 from TBP. 12S binds to a transcription inhibitor (Dri) and prevents it from inactivating TBP.

E2F is a transcription factor that is inhibited by the binding of retinoblastoma tumor suppressor protein, pRB. pRB inhibits cell cycle progression by binding to E2F and blocking transcriptional activation. E1A proteins bind to pRB and therefore dissociate it from E2F. Liberated E2F can promote the cellular entrance to the S phase.

The second protein transcribed is E1B, which together with E1A and independently of other virus proteins are capable of transforming primary cells in vitro. E1A can immortalize primary cells in vitro, whereas E1B does not transform cells on its own, but "co-operates" with E1A to stably transform cells.

E1B targets p53, a protein which activates the genes that prevent entry to the S phase. The transforming effects of E1A proteins induce cellular proliferation, which can trigger p53 activation and apoptosis. E1B protein prevents apoptosis by binding to p53.

Ad12 E1A hinders class I MHC expression, possibly allowing proliferating cells to escape destruction by Cytotoxic T Lymphocytes.

Another early viral protein is E4, which binds to E2F and activates early and late adenoviral promoters.

1.7.3.3 DNA Replication

Adenovirus DNA replication has been studied extensively both in vivo, using mutant viruses and in vitro. The most important viral gene in DNA replication is E2. It produces at least 3 different proteins:

1. TP, a 55kD terminal protein, which acts as a primer for initiation of synthesis. It is active in the initiation of DNA replication and is found covalently attached to the 5' ends of the viral chromosome.
2. Ad DNA Pol, a 140 kD distinct DNA-dependent polymerase, which contains both a 5' to 3' polymerase activity and a 3' to 5' exonuclease proofreading activity.
3. Ad DBP, a 59kD DNA-binding, phosphorylated protein.

In addition, many cellular proteins in the nucleus also participate in replication of the genome (e.g. NFI, NFII, topoisomerase I).

When the E2 viral gene products accumulate viral replication starts. First the synthesis is initiated at either termini of one of the two DNA strands and results in a double stranded (consisting of a parental and a daughter strand) and a single stranded DNA molecule. The latter circularizes through its self-complementary termini and replicates.

1.7.3.4 Late Transcription

The late genes are transcribed from the major late promoter at the onset of DNA replication. The activity of this promoter is low in the early stages of infection, but increases by several hundredfold at late stages (Shaw et al, 1980). The late regions are transcribed into a single large primary transcript of about 29,000 nucleotides (Evans et al, 1977). Alternative splicing generates at least 18 distinct mRNAs, which have been classified into five families, L1 TO L5. L4 100kD protein stimulates viral translation (Adam et al, 1987) and is selectively activated during this stage.

A complex of two viral proteins, E1B 55kD and E4 34kD, inhibit accumulation of cellular mRNA and facilitate cytoplasmic accumulation of viral mRNA, where translation of viral proteins occurs.

1.7.3.5 Assembly and release from the cell

Assembly occurs in the nucleus, but it begins in the cytoplasm when individual monomers form into hexon and penton capsomers. Assembly is facilitated by the late protein L4 (100kD), which acts as a scaffold. Empty, immature capsids are assembled from these protomers in the nucleus, where the core is formed from genomic DNA and associated core proteins.

Several viral proteins make the assembly and packaging possible by their variable functions, but a lot of them remain unknown. L1 52-55kD protein assists the encapsidation process (Hasson et al, 1989) and is not found in mature virions. L3 codes a proteinase, which releases mature polypeptides and terminal proteins from the associated DNA (Tihanyi et al, 1993).

Although host cell macromolecular synthesis ceases earlier in the infection, infected cells can remain intact and do not lyse. Virus particles tend to accumulate in the nucleus and are visible in the microscope as eosinophilic crystals, inclusion bodies. Adenovirus can persist for years in a host, which appears normal. There are three adenoviral proteins, which antagonize the antiviral responses of the host. Viral infection results in the induction of interleukin 5, a protective cytokine. However this seems to activate viral E2 coded DNA binding protein, which in turn activates E1A and E3 promoters. E1A products inhibit cellular response to α and β

interferons. E3 proteins protect cells from cytotoxic T lymphocytes and tumor necrosis factor (Williams et al, 1990).

Viral proteinases, such as E1B 19 kD polypeptide, facilitate viral release from the cell. They disrupt intermediate filaments by acting on its components, e.g. vimentin and cytokeratin (D'Halluin et al, 1978). Cell lysis and release of the progeny virus ensue.

1.7.4 ADENOVIRUSES IN GENE THERAPY

While most of the viral genome is essential for virus growth, replication deficient recombinant adenovirus can be constructed with transgene insertion into E1, E3 or E4 regions. Replication-deficient adenovirus vectors can be constructed by deletions in the E1 region, but may carry additional deletions or mutations in the genome. These viruses are propagated in a helper cell line, which provides the deleted E1 gene, such as the 293 cell line. In normal mammalian cells the recombinant adenovirus is taken up and transported to the nucleus, but no progeny copies of the virus are produced due to the missing E1 region. The desired gene has been inserted into the virus under the control of constitutive promoters and therefore is expressed using the cellular transcription system.

Adenoviruses can be used to achieve high levels of transgene expression in a variety of cell types and tissues (Shering et al, 1997; Castro et al, 1997). The advantages of using adenoviruses are that the virus replication does not require the host cells to be dividing and also replication deficient adenoviruses can be constructed. The recombinant viruses can be grown to high titres (up to 10^{12} plaque forming units per ml). The expression of the transgene can be controlled by selecting and using the appropriate promoter. They do not give rise to mutations by random integration into the host genome. Target cells can be infected with more than one recombinant adenovirus, if necessary. However there are also some disadvantages of adenoviral vectors: expression is transient since the viral DNA does not integrate into the host and adenoviral proteins are expressed in the host following infection. Moreover, *in vivo* delivery may be hampered by prior host immune response since adenoviruses are common human pathogens.

1.7.5 CORNEAL GENE TRANSFER

Transfer of marker genes to several parts of the eye has been demonstrated by various investigators. Gene transfer to the anterior part of the mouse, rat, rabbit and human eye has been successful (Larkin et al, 1996; Malecaze et al, 1999; Budenz et al, 1995; Fehervani et al, 1996; Arancibia-Carcamo et al, 1998; Oral et al, 1997, Abraham et al, 1995, Seitz et al, 1998). Recently the cornea has been the subject of many studies, but the layer that is usually reported to be transfected following adenoviral transfection is the endothelium (Arancibia-Carcamo et al, 1998; Larkin et al, 1996; Budenz et al, 1995; Fehervani et al, 1996, Oral et al, 1997).

The experiments that have used pieces or whole organ cultured corneas for gene delivery suggest that it is more laborious to achieve transfer of genes to the corneal epithelial and stromal layer, but not impossible, as several researchers have shown (Tsubota et al, 1998; Abraham et al, 1995; Seitz et al, 1998). Epithelial layer transfection was accomplished both *in vitro* and *in vivo* by Abraham et al, 1995. A rabbit epithelial cell line was infected with a recombinant adenovirus in vitro. For the in vivo transfection the virus was administered with intracameral, intra-vitreal and subretinal injection. RNA extraction and RT-PCR analysis demonstrated that the corneal epithelium was transfected strongly with the intracameral and weakly with the intra-vitreal injection. Other ocular tissues transfected with this method were: iris, lens, retina, and corneal endothelium. Incubation of corneal epithelium *ex vivo* with recombinant adenovirus for 2 days resulted in gene transfer. The recombinant adenovirus carried the lac Z gene and staining with X-gal demonstrated efficient transfection (Tsubota et al, 1998). Transfection of stromal keratocytes, both on frozen sections and on cultured trephine sections of de-epithelialised corneas, was carried out with a retroviral vector (Seitz et al, 1998).

The distribution of integrins is associated with the efficiency of adenoviral infection. Adenoviruses infect the eyes and indeed are one of the causes of viral keratoconjuctivitis. Adenoviral entry into the cells involves two stages: one is the attachment of the virus via the fibril receptor (Bergelson et al, 1997) and the other is the internalisation via interaction between the RGD peptide sequence on α_v integrins and the penton base of the adenoviral coat protein. It has been demonstrated that expression of $\alpha_v\beta_5$ integrins is necessary for efficient

adenovirus-mediated gene transfer to the human airway (Goldman et al, 1995). Therefore the presence of α_v integrins might be important for the transfection of corneal tissue with adenoviruses.

Distribution of integrins $\alpha_v\beta_5$ and α_v in the normal human cornea has been studied (Rayner et al, 1998) and it was concluded that both the epithelial and the endothelial layers possess these integrins and should allow viral entry. However, the observed higher efficiency by which endothelial cells are transfected may be due to either of the following reasons:

- Endothelial cells are more active metabolically than epithelial cells.
- Epithelial cells proliferate (in contrast with the non-mitotic endothelial) and therefore stable transfection cannot be achieved.
- The epithelial layer is overlayed by a protective tear film and mucus layer, which are both physical and chemical barriers protecting the cornea from entry of foreign bodies.
- The epithelial superficial cells are susceptible to desquamation

Epithelial stem cells, in contrast, can provide a more stable means of transfection with adenoviruses, which do not integrate with the cellular genome.

An alternative method to transferring transgenes to the cornea is by the use of lipoadenofection. This is delivery of the gene to the target cells by using a combination of liposomes, adenovirus and a plasmid vector carrying the transgene. It has been observed that lipoadenofection is an efficient method to deliver reporter genes to the cornea and that use of adenovirus and plasmid DNA alone is less efficient (Arancibia-Carcamo et al, 1998). Although overall a highly effective method, transgene expression was restricted to corneal endothelium. Exception to this is the case reported by Abraham et al (1995), where the recombinant adenovirus carrying the transgene was mixed with liposomes and injected directly to the intracameral space. The corneal epithelium was positive for transgene expression after this application.

Gene transfer to the cornea has not only been achieved by adenoviruses, but with other vectors as well. Retroviral vector transfected the stromal keratocytes and keratocyte cell culture (Seitz et al, 1998). Nonviral systems have also been designed. A system based on synthetic peptides containing an integrin-binding segment for cellular targeting and a polylysine segment for DNA binding was used

to transfect corneal endothelial cells (Shrewing et al, 1997). Activated polyamidoamine dendrimers comprise another nonviral vector system. They are synthetic spherical macromolecules with radiating branches, which terminate at charged and uncharged amino groups and bind to negatively charged DNA to form a complex. Corneal endothelium has received reporter genes with this system (Hudde et al, 1999). Injection of plasmid DNA to the anterior chamber in conjunction with electric pulse resulted in transfection of corneal endothelial cells only (Oshima et al, 1998; Sakamoto et al, 1999).

1.8 SUMMARY OF INTRODUCTION

The cornea is a vital part of the outer eye whose critical functions include transparency, refraction and protection. The inherited corneal dystrophies compromise its function. Treatment is mediated by corneal transplantation, but it is common for the dystrophies to re-appear in the corneal graft. Understanding the underlying defects allow an analysis of molecules critical to corneal integrity. Recent definition of the gene βig-h3 underlying a number of dystrophies has demonstrated a protein, keratoepithelin whose function appears to be important in epithelial attachment, wound healing and repair. Adenoviruses have been extensively studied in the laboratory and used as tools for gene transfer. Some of the ocular tissues, including corneal epithelium can be transfected with recombinant adenoviruses. The study of this protein with the aid of adenoviruses and recombinant proteins will improve our understanding of its function and implication in corneal dystrophies. This might even lead to the treatment/prevention of these diseases at the genomic level, using tools of gene therapy.

1.9 Aims of the study

The aim of this study was to examine the role of keratoepithelin in corneal dystrophies. Hence the thesis was divided in 5 chapters which are intended to investigate and develop the following:

1. Cloning the wild type βig-h3 cDNA and synthesising the equivalent corneal dystrophy mutants
2. Constructing recombinant adenovirus expressing wild type and mutant βig-h3
3. Producing recombinant wild type and mutant keratoepithelin protein
4. Assessing the effects of overexpression wild type and mutant βig-h3
5. Assessing the effects of recombinant protein on corneal cells

2. CHAPTER TWO

βig-h3 cDNA synthesis, cloning sequencing and in vitro mutagenesis

2.1 INTRODUCTION

A number of corneal dystrophies (Granular, Lattice, Bowman's layer) are caused by mutations in the βig-h3 gene on chromosome 5q31 (Munier et al, 1997). The gene, which is comprised of 17 exons, encodes keratoepithelin, a 683 amino acid protein. This protein is an extracellular matrix molecule, which is ubiquitously expressed. However its function in the cornea - in particular in the corneal epithelium - remains uncertain although it is known to influence cell adhesion, migration and also would healing.

Therefore one of the primary aims of the project is to study the role of keratoepithelin in vitro, comparing the effects of mutant and wild-type forms of the protein both in primary and immortalised cell culture as well as developing a method for studying the effects of the protein of epithelial cell behaviour in ex-vivo corneal organ culture.

Total RNA was extracted from fibroblasts and was converted to cDNA by reverse transcription polymerase chain reaction (RT-PCR). The coding nucleotide sequence of βig-h3 was published by Skonier et al in 1992. Based on this sequence we created primers for PCR amplification of cDNA sequence and this fragment was used for cloning into prokaryotic vectors, transformation into competent *Escherichia coli* cells and plasmid preparation. DNA sequencing, using external and internal primers, confirmed that the correct nucleotide sequence had been amplified. Finally in vitro mutagenesis enabled us to give rise to two mutant versions of the βig-h3 cDNA, R555W and R555Q, which have been associated with granular and Thiel-Behnke corneal dystrophies, respectively.

2.2 METHODS

2.2.1 DEPC treatment

RNAse is very resistant to heat inactivation and is therefore removed with DEPC. DEPC reacts with an active-site histidine residue on RNase, forming a carbamate and liberating a molecule of carbon dioxide and ethanol. After treatment solutions have to be incubated at 120^{0}C to destroy DEPC and evaporate ethanol.

2.2.1.1 Water and solutions

DEPC was added to water to a final concentration of 0.1%. This was done in a fume cupboard. The water was shaken well and was allowed to stand overnight. The following day it was autoclaved. The same procedure is also used for solutions, apart from Tris containing, which are prepared by DEPC treated and autoclaved water in RNA se free glassware.

2.2.1.2 Glassware

Glassware was either treated at 200°C overnight or according to the following if delicate: Rinse with 95% IMS, soak in 3% aqueous hydrogen peroxide for 10 minutes, rinse in DEPC treated water and dry.

2.2.2 RNA EXTRACTION

The frozen cell pellets of primary human fibroblast and lymphoblast cells were obtained from the Immunogenetics Department, St Mary's Hospital, Manchester. The approximate content per pellet was 10^7 cells. TRIzol™ Reagent (Gibco BRL) was used for total RNA extraction, i.e. isolation of a variety of RNA species of large and small molecular size (Chomczynski and Sacchi 1987). All plastic and glassware as well as H_2O were DEPC treated to ensure RNAse elimination. The entire procedure was performed on ice to minimise the rate of RNA degradation.

2.2.2.1 Homogenisation

The cells were rapidly thawed at 37°C and briefly vortexed. Cell lysis followed with addition of 1ml TRIzol™ Reagent, repetitive pipetting and subsequent vortexing.

2.2.2.2 Phase Separation

The samples were then incubated at room temperature for 5-10 minutes in order to dissociate protein complexes. 0.2ml chloroform was added to precipitate protein and the tubes were capped, wrapped with cling film and shaken for 15 seconds. This was followed by 5-10 minutes incubation on ice. The tubes were vortexed and their contents transferred to 2ml centrifuge tubes and spun at 12,000 × g for 50 minutes at 4°C in a Micro 24-48R Hettich Centrifuge. After the centrifugation 3 separate layers should be seen: Lower red (phenol/chloroform phase), an interphase and a colourless upper aqueous phase, where RNA is found.

2.2.2.3 RNA Precipitation

The aqueous phase was transferred to a fresh 1.5ml tube, 0.5ml isopropanol was added, the tube was vortexed and RNA was precipitated at -80°C for at least ½ hour or overnight. The samples were centrifuged at 12,000 × g for 45 minutes at 4°C. RNA can be seen as a gel-like pellet on the side/bottom of the tube.

2.2.2.4 RNA Wash

The supernatant was removed and 1ml 75% ethanol was added. The tube was vortexed for 2 minutes and centrifuged at 7,500 × g for 40 minutes at 4°C.

2.2.2.5 Redissolving the RNA

As much ethanol as possible was removed and the pellet was air-dried for approximately 15 minutes. RNA was treated with DNase before it was redissolved in 20μl RNAse-free H_2O by passing through the pipette tip a few times. The samples were subsequently incubated at 55-60°C in a water bath, vortex-mixed and stored at -80°C. The quality of RNA was determined spectrophotometrically at 260 and 280nm and calculating the A_{260}/A_{280}. A260 is frequently used to measure DNA/RNA concentration and A280 is used to measure protein concentration. A ratio of A260/A280 > 1.8 suggests little protein contamination in a DNA/RNA sample.

2.2.3 Reverse Transcription

The conversion of RNA to single-stranded cDNA was achieved with AMV Reverse Transcription System (Promega). The reverse transcription reaction was carried out according to the supplier's instructions and the newly synthesised cDNA was stored at -20°C.

2.2.4 Design of βig-h3 PCR primers

The design of the PCR primers was based on the online sequence of βig-h3 cDNA from the NCBI Nucleotide Database (NM 000358) (Fig. 3.1). 9 forward and reverse oligonucleotides were selected from the online sequence of βig-h3 cDNA to serve as PCR primers. The primers were carefully selected so that they did no show any complementary regions with other primers that were going to be paired with or with self. The GC content was preferably not more than 50%. All primers were ordered for synthesis from MWG-Biotech AG and were delivered in freeze-dried form. Addition of the appropriate volume of sterile distilled water and resuspension by vortexing provided a stock of 100pmol/μl (100μM), which was

stored at -20°C. The primers synthesised for PCR amplification of βig-h3 are summarised on the following table together with the number indicating their nucleotide position on the cDNA.

```
   1 gcttgcccgt cggtcgctag ctcgctcggt gcgcgtcgtc ccgctccatg gcgctcttcg
  61 tgcggctgct ggctctcgcc ctggctctgg ccctgggccc cgccgcgacc ctggcgggtc
 121 ccgccaagtc gccctaccag ctggtgctgc agcacagcag gctccggggc cgccagcacg
 181 gccccaacgt gtgtgctgtg cagaaggtta ttggcactaa taggaagtac ttcaccaact
 241 gcaagcagtg gtaccaaagg aaaatctgtg gcaaatcaac agtcatcagc tacgagtgct
 301 gtcctggata tgaaaaggtc cctggggaga agggctgtcc agcagcccta ccactctcaa
 361 acctttacga gaccctggga gtcgttggat ccaccaccac tcagctgtac acggaccgca
 421 cggagaagct gaggcctgag atggaggggc ccggcagctt caccatcttc gcccctagca
 481 acgaggcctg ggcctccttg ccagctgaag tgctggactc cctggtcagc aatgtcaaca
 541 ttgagctgct caatgccctc cgctaccata tggtgggcag gcgagtcctg actgatgagc
 601 tgaaacacgg catgaccctc acctctatgt accagaattc caacatccag atccaccact
 661 atcctaatgg gattgtaact gtgaactgtg cccggctcct gaaagccgac caccatgcaa
 721 ccaacggggt ggtgcacctc atcgataagg tcatctccac catcaccaac aacatccagc
 781 agatcattga gatcgaggac acctttgaga cccttcgggc tgctgtggct gcatcagggc
 841 tcaacacgat gcttgaaggt aacggccagt acacgctttt ggccccgacc aatgaggcct
 901 tcgagaagat ccctagtgag actttgaacc gtatcctggg cgacccagaa gccctgagag
 961 acctgctgaa caaccacatc ttgaagtcag ctatgtgtgc tgaagccatc gttgcggggc
1021 tgtctgtaga gaccctggag ggcacgacac tggaggtggg ctgcagcggg gacatgctca
1081 ctatcaacgg gaaggcgatc atctccaata aagacatcct agccaccaac ggggtgatcc
1141 actacattga tgagctactc atcccagact cagccaagac actatttgaa ttggctgcag
1201 agtctgatgt gtccacagcc attgaccttt tcagacaagc cggcctcggc aatcatctct
1261 ctggaagtga gcggttgacc ctcctggctc ccctgaattc tgtattcaaa gatggaaccc
1321 ctccaattga tgcccataca aggaatttgc ttcggaacca cataattaaa gaccagctgg
1381 cctctaagta tctgtaccat ggacagaccc tggaaactct gggcggcaaa aaactgagag
1441 tttttgttta tcgtaatagc ctctgcattg agaacagctg catcgcggcc cacgacaaga
1501 gggggaggta cgggaccctg ttcacgatgg accgggtgct gacccccca atggggactg
1561 tcatggatgt cctgaaggga gacaatcgct ttagcatgct ggtagctgcc atccagtctg
1621 caggactgac ggagaccctc aaccgggaag gagtctacac agtctttgct cccacaaatg
1681 aagccttccg agccctgcca ccaagagaac ggagcagact cttgggagat gccaaggaac
1741 ttgccaacat cctgaaatac cacattggtg atgaaatcct ggttagcgga ggcatcgggg
1801 ccctggtgcg gctaaagtct ctccaaggtg acaagctgga agtcagcttg aaaaacaatg
1861 tggtgagtgt caacaaggag cctgttgccg agcctgacat catggccaca aatggcgtgg
1921 tccatgtcat caccaatgtt ctgcagcctc cagccaacag acctcaggaa agaggggatg
1981 aacttgcaga ctctgcgctt gagatcttca aacaagcatc agcgttttcc agggcttccc
2041 agaggtctgt gcgactagcc cctgtctatc aaaagttatt agagaggatg aagcattagc
2101 ttgaagcact acaggaggaa tgcaccacgg cagctctccg ccaatttctc tcagatttcc
2161 acagagactg tttgaatgtt ttcaaaacca agtatcacac tttaatgtac atgggccgca
2221 ccataatgag atgtgagcct tgtgcatgtg ggggaggagg gagagagatg tacttttaa
2281 atcatgttcc ccctaaacat ggctgttaac ccactgcatg cagaaacttg gatgtcactg
2341 cctgacattc acttccagag aggacctatc ccaaatgtgg aattgactgc ctatgccaag
2401 tccctggaaa aggagcttca gtattgtggg gctcataaaa catgaatcaa gcaatccagc
2461 ctcatgggaa gtcctggcac agtttttgta aagcccttgc acagctggag aaatggcatc
2521 attataagct atgagttgaa atgttctgtc aaatgtgtct cacatctaca cgtggcttgg
2581 aggcttttat ggggccctgt ccaggtagaa aagaaatggt atgtagagct tagatttccc
2641 tattgtgaca gagccatggt gtgtttgtaa taataaaacc aaagaaacat a
```

Figure 2.1: βig-h3 cDNA sequence (NM 000358)

Highlighted sequences correspond to primers on table 2.1

PRIMER	FORWARD OR REVERSE	POSITION (BP)
Prom 1	Forward	9-28
Seq 6	Forward	340-358
Seq1	Forward	543-562
Seq7	Forward	851-869
Seq2	Forward	1022-1042
Seq2R	Reverse	1022-1042
Seq8	Forward	1339-1361
Seq3	Forward	1518-1539
Seq3R	Reverse	1518-1539
Seq9	Forward	1887-1907
3primer	Reverse	2131-2150

Table 2.1: List of primers for βig-h3
(Highlighted on Figure 2.1)

2.2.5 Polymerase Chain Reaction (PCR)

Amplification of DNA cDNA was performed with PCR (Saiki *et al.*, 1985 and 1988) on a thermal cycler. Several PCR systems and reaction conditions were tested in order to obtain the optimum reaction product.

Each system comprised a different DNA polymerase, dNTP mix and reaction buffer (RB). Premix (Advanced Biotechnologies) and MegaMix (Helena Biosciences) are ready-to-use PCR mixes containing Taq, dNTPs, buffer and stabiliser. Extensor Long PCR (Advanced Biotechnologies) is a system that allows amplification of long DNA sequences by the use of a combination of DNA polymerases (Enzyme mix). Two buffers are supplied with the system, Buffer 1 & 2, for PCR products shorter and longer than 12kb respectively. PFU Taq is a proofreading polymerase with an exonuclease activity. It was used with either PFU reaction buffer or with Anglian Buffer. The following table summarises the main PCR reactions carried out.

	PREMIX	MEGAMIX	EXTENSOR LONG PCR	PFU TAQ	COMBINED
DNA	25-100ng	25-100ng	25-100ng	25-100ng	25-100ng
20mM dNTPs	-	-	3.5μl	3μl	3.5μl
10 x RB	-	-	2μl Buffer 1	2μl A / PFU	2μl Buffer 1
10μM P_F	2μl	2μl	1.5μl	2μl	1.5μl
10μM P_R	2μl	2μl	1.5μl	2μl	1.5μl
Enzyme	10μl mix	13μl mix	1μl enzyme mix	0.1μl PFU Taq	0.1μl PFU Taq
DH_2O	Up to 20μl	Up to 20μl	Up to 50μl	Up to 20μl	Up to 50μl

Table 2.2: List of PCR reactions

The size of the PCR products depended on the primer pair that was used and varied from 500 to 2150bp (for list of βig-h3 primers see materials). Two standard cycling conditions were used: 1, for products 1000bp or larger and 2, for less than 1000bp.

	1		2	
Initial Denaturation	95°C for 5mins		95°C for 5mins	
Denaturation	94°C for 1min		94°C for 1min	
Annealing	56°C for 2mins	35×	56°C for 1min	28-30x
Extension	72°C for 5mins		72°C for 1min	
Final Extension	72°C for 10mins		72°C for 10mins	

2.2.6 Agarose gel electrophoresis

One way of visualising and displaying PCR products and generally DNA is agarose gel electrophoresis. Electrophoresis grade agarose was mixed with 1×TBE buffer and microwaved on low power for 2½ minutes. The resulting gel had 0.8-1.5% agarose depending on the size of the DNA fragments that were to be checked. 9μl 10mg/ml Ethidium Bromide was added to the gel before it was set and it was poured in a tray with a comb to form wells. After the gel had set, the comb was removed and the gel was immersed into a tank containing 1×TBE buffer. 6-10μl DNA sample mixed with 2μl 5×Glycerol Loading Dye were loaded in each well. 2.5μl of a 0.5μg/μl 100bp or 1000bp DNA ladder (Gene Ruler™ - MBI Fermentas)

was also loaded on the gel as a size reference. Mass Ruler™ High Range DNA ladder (MBI Fermentas) was used for quantitative analyses. The gel was electrophoresed at 100-120V until adequate separation of DNA bands. The gel was visualised on an ultraviolet transilluminator, where DNA fluoresced due to the intercalated ethidium bromide. A picture was captured by a camera and previewed from the connected monitor. The photograph was printed by a video copy processor (Mitsubishi).

2.2.7 PCR purification

After a PCR the reaction tube contains: Amplified DNA, leftover dNTPs and primers, DNA polymerase. In rare cases even after the optimisation of the conditions more than one size of DNA product (multiple bands) appears on the gel. In such cases it is important to purify the desirable PCR product from everything else present in the tube, before proceeding to more sensitive applications such as cloning and sequencing. Three systems were used for such purposes according to the protocols described in the operating manual: Centricon Concentrators (Amicon Inc), QIAGEN PCR Purification kit (QIAGEN) and QIAquick Gel Extraction Kit (QIAGEN).

2.2.8 Cloning

2.2.8.1 Bacterial Culture And Storage

All bacterial work was carried out in a Biosafety Level 1 Laminar Flow Microbiological cabinet and all plastic, glassware and media were sterile.

2.2.8.2 Bacterial growth

All liquid cultures were grown at 37°C on a mechanical shaker at 225rpm. All plates were incubated inverted overnight at 37°C. Liquid cultures were grown in Luria Bertani (LB) medium and plates were made with LB agar. The appropriate antibiotic was added to the media when necessary according to the following (final) concentrations:

Ampicillin 100μg/ml

Chloramphenicol 20μg/ml

Kanamycin 25μg/ml

2.2.8.3 Storage of bacterial cells

For long term storage of bacterial cells at low temperatures glycerol stocks were made by mixing 1.3ml of overnight culture with 200μl sterile glycerol. Glycerol stocks were stored at -80°C.

2.2.8.4 TOPO™ TA Cloning

Direct cloning of PCR products into a plasmid vector was achieved with TOPO™ TA Cloning Kit (Invitrogen).

Taq polymerase amplified PCR products have incorporated single deoxyadenosine (A) residues on their 3' ends due to the nontemplate-dependent terminal transferase activity of this enzyme. TOPO™ TA Cloning provides a linear plasmid, with single 3' deoxythymidine (T) bases and a Topoisomerase I molecule covalently attached to each end of the plasmid.

A 5-minute incubation of the following at 25-30°C in a water-bath:

Purified PCR product	3μl (20ng)
Sterile H_2O	1μl
pCR®2.1-TOPO vector	1μl (10ng)

results in ligation of the PCR product with the pCR®2.1-TOPO vector and release of Topoisomerase I. The PCR product is inserted in the lacZ gene of the vector, which allows blue/white colony selection on agar plates.

TOPO TOP10F' One Shot™ competent cells were retrieved from -80°C and were placed on ice to thaw slowly. 2μl 0.5M β-mercaptoethanol was added to the competent cells and mixed gently with the pipette tip. 2μl of the ligation reaction was also mixed with the cells, which were kept on ice for 30 minutes. Transformation of the cells with the plasmid was carried out by heat-shock at 42°C, in a water-bath, for 30 seconds. The cells were then transferred on ice for 2 minutes, 250μl of SOC medium was added to them and incubation followed at 37°C in an orbital shaker at 225rpm for 1 hour. In the meantime 20μl 250mg/ml IPTG and 40μl 40mg/ml Xgal were spread on LB-kanamycin plates. The plates were left to dry for 15 minutes in the laminar flow cabinet and were then placed in the 37°C oven for 30-60 minutes to allow solutions to diffuse. 60μl of the shaken cells were

spread on 4 large (150mm) LB-kanamycin plates and were allowed to grow at 37°C overnight. The plates were examined the following day for white colonies.

2.2.8.5 Restriction Digestion

Another way of cloning a DNA fragment into a vector is by cutting the two DNA species with Restriction Endonucleases, which produce complementary cohesive ends and ligating them with T4 DNA ligase. Two main restriction digestions were performed for the purposes of cloning:

Reaction components	RE1: SpeI RE2: XbaI	RE1: MluI RE2: XhoI
DNA	5μg	5μg
NEB 10× Buffer	5μl Buffer 2	5μl Buffer 3
10mg/ml BSA	0.5μl	0.5μl
40mM spermidine	1μl	1μl
10U/μl RE1	3μl	3μl
20U/μl RE2	1.5μl	1.5μl
dH_2O	Up to 50μl	Up to 50μl

Table 2.3: Restriction Digestions

Complete digestion took place at 37°C, in a water bath, for 2 hours and was verified by agarose gel electrophoresis.
The reaction was heated at 65°C for 30 minutes to inactivate the restriction enzymes.

2.2.8.6 Dephosphorylation of digested plasmid DNA

If the plasmid vector is digested with a single enzyme or with two different enzymes that produce the same cohesive ends, it will tend to recircularise during ligation. Therefore it must be dephosphorylated with an enzyme such as Calf Intestinal Alkaline Phosphatase (CIAP), which removes the 5' phosphate groups from cohesive termini and renders self-ligation impossible. The standard dephosphorylation reaction is:

Components	Volume (μl)
Linearised plasmid DNA	(I pmol of ends)*
10× CIAP Buffer	4
1U/μl CIAP	1
dH_2O	Up to 40

Table 2.4: Dephosphorylation Reaction

*1 pmol of ends = (μg/kb) × 3.08 × N
where N is number of restrictions per plasmid

Dephosphorylation is carried out at 37°C, in a water bath, for 30 minutes. Following this, a heat-inactivation step takes place at 65°C for 15 minutes.

2.2.8.7 DNA Clean-up

Before digested DNA is used in a ligation reaction it must be cleaned from

a. restriction digestion reagents (buffers, enzymes)
b. other DNA fragments products of the restriction digestion which are not wanted for ligation.

Depending on which category the digested DNA belongs to, the appropriate clean-up step is carried out. For simple removal of enzymes and salts either the Wizard ® DNA Clean up System (Promega) or the QIAquick PCR Purification Kit (QIAGEN) was used according to the instructions of the manufacturer's protocol. For purification of a digestion fragment from the rest of the reaction products, the whole of the restriction digest was run on an agarose gel and the band corresponding to the desired fragment was excised from the gel and recovered with QIAquick Gel Extraction kit (QIAGEN).
In both of the cases purified DNA was resuspended in dH_2O which has been pre-warmed at 65°C. This increases the yield of recovered DNA.

2.2.8.8 DNA Ligation

When performing a ligation between a DNA fragment and a plasmid vector it is important to find the molar ratio insert:vector that gives optimal results. Therefore the following insert:vector molar ratios were used for every ligation that

was carried out; 1:3, 3:1, 1:1. The formula which describes the conversion of molar ratios to mass ratios is

Molar ratio insert/vector = ng of insert × kb size of vector/ng of vector × kb size of insert

A typical ligation reaction was made up with the appropriate volumes of vector and insert DNA, mixed with 4μl 5× Ligation Buffer and 1μl 1U/μlT4 DNA Ligase (Gibco BRL). H_2O was added to 20μl. The reaction was incubated at either 23-26°C for 3 hours or at 16-4°C overnight. A heat inactivation step was carried out at 65°C for 15 minutes before proceeding to transformation.

2.2.8.9 Preparation of competent cells

Two protocols were used for generating chemically competent *E. coli* cells which will serve as hosts for the plasmid DNA cloning.

2.2.8.9.1 Modified Calcium Chloride method

This protocol, a variation of the method described by Cohen et al (1972), generates competent cells with transformation efficiencies 5×10^6-2×10^7 cfu/μg of supercoiled DNA (Maniatis et al, 1984).

Cells were streaked on a LB agar plate and incubated overnight at 37°C. A single colony was inoculated into 100ml LB medium in a 1Lt flask and shaken at 160rpm at 37°C for 2.5 hours. Culture was poured into two chilled 50ml tubes and was centrifuged at 4,500 x g for 10 minutes at 4°C in a Sorvall Centrifuge. Supernatant was discarded and cells of each tube were resuspended in 10ml ice-cold 0.1M $CaCl_2$. Centrifugation was carried out under the same conditions as before, supernatant was removed and cells were resuspended in 2ml 0.1M $CaCl_2$. Cells were combined and left on ice until use or overnight at 4°C to increase competency.

2.2.8.9.2 Modified Rubidium Chloride Method

This protocol, which is an adaptation of the method described by Carswell et al (1989) gives rise to competent cells with better transformation efficiencies.

Cells were streaked on LB agar plates and incubated overnight at 37°C. A single colony was inoculated in 2.5ml LB broth in a 20ml sterile universal tube and incubated overnight at 37°C with shaking at 225rpm. 250ml LB medium containing 20mM $MgSO_4$ was inoculated with the 2.5ml overnight culture in a 1Lt flask. Cells were grown at 37°C shaker for 3-5 hours, until OD_{600nm} = 0.4-0.6. The culture was transferred to two GSA pots and centrifuged at 4,500 × g for 5 minutes at 4°C. The supernatant was discarded and the cells of each pot were resuspended in 50ml ice-cold TFB1 Buffer. The cells were combined and incubated on ice for 5 minutes. Centrifugation was repeated as before, supernatant was discarded and cells were resuspended 10ml ice-cold TFB2 Buffer. Cells were left on ice for 15-60 minutes and then 100μl aliquots were made in 1ml cryogenic tubes, quick frozen in liquid nitrogen and stored at -80°C. Competent cells prepared by this method are stable 3-6 months (ES1301) to 1 year (JM109).

2.2.8.10 Transformation of competent cells

Chemically competent cells were heat-transformed with the ligated DNA as described on the following protocol.

Sterile 17×100mm polypropylene tubes were placed on ice. Competent cells were removed from -80°C and were placed on ice to thaw. The tube was flicked to mix and 100μl competent cells were transferred to each polypropylene tube. Ligated DNA was added* and mixed by stirring gently with the pipette tip. Tubes were kept on ice for 10-30 minutes (depending on bacterial strain and transformation efficiency). Up-take of DNA was facilitated by heat-shocking the cells at 42°C for 1 minute. The tubes were replaced on ice for 2 minutes and 900μl SOC medium or LB was added to each transformation reaction and they were incubated at 37°C for 60 minutes by shaking at 225rpm. 100μl of each reaction was spreaded in duplicate on a 150mm plate containing the appropriate antibiotic and incubated at 37°C overnight.

*The following volumes of each ligation reaction were used to transform competent cells: 5μl, 10μl, 5μl and 10μl of 1:50 dilution.

2.2.8.11 Streaking positive clones on a gridded plate

After the overnight incubation the plates were checked for colonies of transformed cells. If plasmid allows blue/white screening then the white colonies were

selected. Otherwise single colonies (approximately 10 per transformation) were streaked on a 150mm gridded plate containing LB agar and the appropriate antibiotic. Grids were numbered, in order to refer to specific clones.

2.2.8.12 Subculturing of bacterial clones

Gridded clones were streaked on fresh antibiotic containing plates and incubated overnight to get individual colonies.

2.2.8.13 Plasmid preparation

This method was used to extract plasmid DNA from the subcultured clones. The QIAGEN Plasmid Mini Purification Kit enables separation of plasmid from genomic DNA and other cellular components and it was used according to the following protocol.

A single colony was transferred to a sterile 20ml universal tube containing 5ml LB and the appropriate antibiotic. The bacterial culture was grown overnight at 37°C until OD_{600nm} = 1-1.5. 1.5ml of the overnight culture was transferred to 2 1.5ml tubes and centrifuged at 10,000 x g for 5 minutes at 4°C in a Micro 24-48R Hettich Centrifuge. Supernatant was discarded and both pellets were thoroughly resuspended in 0.5ml Resuspension Buffer P1 and pooled in the same centrifuge tube. 0.5ml Lysis Buffer P2 was added and tube was inverted gently 4-6 times and incubated at room temperature for 5 minutes. 0.5ml chilled Buffer P3 was also added, the tube was inverted several times and placed on ice for 5 minutes. Centrifugation followed at 10,000 x g for 10 minutes at 4°C. In the meanwhile a QIAGEN tip-20 column was shaken and equilibrated with 1ml Equilibration Buffer QBT. The supernatant was transferred to a clean 1.5ml tube and was centrifuged as before. The new supernatant was applied to the column and allowed to enter the resin by gravity flow. The column was washed 4 times with 1ml Wash Buffer QC and allowed to drain. QIAGEN tip-20 was transferred to a clean 1.5ml tube where DNA was eluted by applying 0.8ml Elution Buffer QF prewarmed at 65°C. 0.7 volumes room temperature isopropanol was added to DNA and the sample was centrifuged at 10,000 x g for 30 minutes. The supernatant was carefully decanted and DNA pellet was washed with 1ml 70% ice-cold ethanol and then with 1ml 70% room temperature ethanol. Ethanol was removed and the pellet was allowed to air-dry at room temperature for no longer than 5 minutes. Plasmid was resuspended in 25μl sterile dH_2O by stirring with the pipette tip. If necessary

sample was warmed to 50°C for 10-15 minutes to ensure complete resuspension. 1μl of the plasmid preparation was electrophoresed on an agarose gel against a Mass Ruler for determining concentration. The rest of the preparation was stored at -20°C.

2.2.9 In Vitro Mutagenesis

Site directed mutagenesis (Hutchinson et al, 1978) involves alteration of a specific part of the sequence of a cloned gene by hybridising it with mismatch-containing synthetic oligonucleotides.

Altered Sites ®II Mammalian Mutagenesis System (Promega) was used to perform in vitro mutagenesis. This system makes use of pALTER-MAX, a plasmid vector with two antibiotic resistance genes: chloramphenicol and ampicillin. Of these two genes, ampicillin is inactivated by a point mutation. The DNA to be mutated was inserted into the multiple cloning site of the vector with restriction digestion of both the insert and the vector DNA followed by T4 DNA ligation.

The mutagenesis reaction takes place by hybridising two mismatch oligonucleotides with pALTER-MAX containing the cloned DNA insert. One oligonucleotide produces the desired mutation on the cloned gene (mutagenic oligo) and the other repairs the inactivated ampicillin gene (repair oligo). A mutagenic strand is formed by T4 DNA polymerase, with two (or more if more than one point mutations are induced) mismatches. DNA ligase seals the nicks and the double stranded product transforms a suitable E.coli host. Ampicillin selection serves as a screening method for the mutant plasmids. The mutagenic oligonucleotide was synthesised by MWG-Biotech AG, whilst the Repair oligonucleotide was provided by the system's manufacturer.

2.2.9.1 Cloning into the mutagenesis vector

Plasmid pCR®2.1-TOPO containing βig-h3 cDNA was subjected to restriction digestion with enzymes SpeI and XbaI. This double digestion produces two fragments: one 2.2kb, which is the βig-h3 cDNA and a 3.9kb, which is the pCR®2.1-TOPO vector. Agarose gel electrophoresis resolved these two fragments and βig-h3 was retrieved with QIAquick Gel Extraction Kit (QIAGEN). Furthermore, plasmid pALTER-MAX was linearised by digesting with enzyme SpeI, dephosphorylated with CIAP and cleaned with QIAGEN PCR Purification kit (QIAGEN).

βig-h3 cDNA was inserted into pALTER-MAX vector with the enzymatic action of T4 DNA Ligase and the produced plasmids transformed into competent JM109 cells. The plasmid from the resulting clones was extracted with QIAGEN plasmid mini purification kit and it underwent restriction digestion to check for presence of desired insert.

2.2.9.2 Design and phosphorylation of mutagenic oligonucleotides

For mutations involving one mismatch the ideal oligonucleotide length is 17-20 bases, with 8-10 nucleotides flanking either side of the mismatch. Also the sequence of the mutagenic oligonucleotide must be complementary to the same strand of the plasmid construct.

The sequence of the mutagenic oligonucleotides was derived from the online cDNA sequence of βig-h3 cDNA (Table 2.1). The oligonucleotides synthesised were 19 bases long with the mismatch occurring on the 10th base. The following table summarises the three mutagenic oligonucleotides that were synthesised for performing the in vitro mutagenesis. The base in pink indicates the point of base change and mismatch.

AA mutation	Nucleotide mutation	Corneal Dystrophy	Sequence (19mer)
R124C	C417T	LCDI	5'...TACACGGACTGCACGGAGA...3'
R555W	C1710T	CDGGI	5'...CCAAGAGAATGGAGCAGAC...3'
R555Q	G1711A	CDTB	5'...CAAGAGAACAGAGCAGACT...3'

Table 2.5: βig-h3 mutagenic oligonucleotides

In order to assist nick sealing by DNA ligase after the polymerisation of the mutant strand, the mutagenic oligonucleotides were phosphorylated. This way they can provide a 5' phosphate group for the formation of the phosphodiester bond:

Oligonucleotide	100pmol
Kinase 10× Buffer	2.5μl
T4 polynucleotide kinase	5U
10mM ATP	2.5μl
sd H_2O	up to 25μl

pmol of oligonucleotide were calculated based on the formula

$$\text{ng of oligonucleotide} = \text{pmol of oligonucleotide} \times 0.33 \times N$$

where N is the length of the oligonucleotide in bases

The phosphorylation reaction was allowed to proceed at 37°C in a water bath, for 30 minutes. Subsequent inactivation of the enzyme took place by heating the reaction at 70°C for 10 minutes. Oligonucleotides were stored at -20°C until further use.

2.2.9.3 Alkali denaturation of plasmid DNA

The plasmid DNA must be alkali denatured just before starting the mutagenesis reaction. Heat denaturation is not sufficient since DNA reanneals too quickly. The following reaction was set up in a 0.5ml tube:

Ds DNA template	0.5pmol
2M NaOH, 2mM EDTA	2μl
sdH_2O	up to 20μl

pmol of dsDNA were calculated based on the formula

$$\text{ng of dsDNA} = \text{pmol of dsDNA} \times 0.66 \times N$$

where N is the length of dsDNA in bases

Incubation took place at room temperature for 5 minutes. 2μl 2M ammonium acetate pH4.6 and 75μl 100% ice-cold ethanol were mixed with the reaction. DNA was precipitated at -80°C for 30 minutes and pelleted by centrifugation at 10,000 x g for 20 minutes at 4°C. The pellet was washed with 200μl 70% ice-cold ethanol and re-centrifuged as before. It was allowed to air dry at room temperature and was redissolved in 100μl sdH_2O. A 10μl fraction was analysed by quantifying agarose gel electrophoresis.

2.2.9.4 Annealing reaction

During this step the mutagenic and antibiotic oligonucleotides anneal to the plasmid DNA. For this reason the oligonucleotides are used in excess according to the following molar ratios; oligonucleotide:template 5:1 for the antibiotic and 25:1 for the mutagenic oligonucleotide.

The annealing reaction was set up in a sterile 0.5ml tube along side a control reaction:

Mutagenic reaction	
Template DNA	~10μl (0.05pmol)
Ampicillin repair oligo	1μl (0.25pmol)
Mutagenic oligo	1.25pmol
Annealing 10× Buffer	2μl
SdH_2O	up to 20μl

Control reaction	
pALTER-MAX	10μl (0.05pmol)
Antibiotic repair oligo	1μl (0.25pmol)
Antibiotic knockout oligo	1μl (0.25pmol)
Annealing 10× Buffer	2μl
SdH_2O	up to 20μl

These reactions were transferred to a thermal cycler and annealed at 75°C for 5 minutes. Temperature was dropped by 1°C per minute until 45°C was reached. Then by 2°C per minute to 22°C, minimising the nonspecific annealing of the oligonucleotides.

The synthesis of the mutagenic strand took place at 37°C for 90 minutes by mixing the following in the following order:

Annealing reaction	20μl
SdH_2O	5μl
Synthesis 10× buffer	3μl
T4 DNA polymerase	1μl (5-10U)
T4 DNA ligase	1μl (1-3U)

2.2.9.5 Transformation of ES1301 mutS competent cells

After the synthesis of the mutant strand the plasmids are used to transform strain ES301, which is a repair minus strain of E. coli and does not select against the mismatched DNA.

17×100mm polypropylene tubes were chilled on ice and competent ES301 cells were transferred on ice to thaw. The cells were mixed gently by flicking the tubes and 100μl was transferred to each polypropylene tube. 1.5-3μl of the mutagenesis/control reaction was added to each tube and the cells were kept on ice for 10 minutes. Uptake of plasmid DNA was facilitated by heat-shock treatment at 42°C for 50-60 minutes. Then the cells were returned to ice for two minutes. 900μl LB was added to each transformation and the cells were incubated at 37°C by shaking at 225 rpm for 30 minutes. Overnight cultures were set up by adding 500μl of each transformation to 4.5ml LB containing the appropriate antibiotic, i.e. ampicillin. Incubation continued at 37°C and 225 rpm for 24 hours.

2.2.9.6 Plasmid purification

The above 24-hour cultures were harvested to purify the mutagenic plasmids. QIAGEN mini plasmid purification kit was used for this purpose.

2.2.9.7 Transformation of JM109 competent cells

The mutagenic plasmids purified from the overnight ES301 cultures are used to transform competent JM109 cells. Transformed cells were spread on LB-amp plates and incubated overnight. For transformation procedure see section 2.2.8.10.

2.2.9.8 Analysis of transformants

The clones that grow on the LB-amp plates stand 50-90% possibility to have the desired mutation. Single colonies are transferred to overnight cultures and their plasmids are extracted. Sequencing analysis reveals whether the mutation is present or not.

2.2.10 DNA SEQUENCING

The DNA samples to be sequenced were either PCR products or Plasmid Preparations. Sequencing is a sensitive application and therefore requires DNA of maximum purity. Plasmid preparations are generally pure DNA samples, as

determined by A_{260}/A_{280}, but PCR products must be cleaned before being used in the Sequencing reaction.

2.2.10.1 SHRIMP-cleaning of PCR products

2μl 1U/μl Shrimp Alkaline Phosphatase and 0.4μl 10U/μl Exonuclease I were used per 20 μl PCR product to be cleaned. The above were mixed, overlayed with one drop of mineral oil and transferred to a thermal cycler, where they were incubated at 37°C for 30 minutes and then heated to 85°C for 15 minutes.

2.2.10.2 Cycle Sequencing reaction (Thermo Sequenance II)

This sequencing reaction was carried out with Thermo Sequenance II dye terminator cycle sequencing Kit (Amersham Pharmacia Biotech Inc.), used for the ABI 373A DNA Sequencer.

The following were added in a sterile 0.2μl tube in the order described:

Components	Volume (μl)
dH_2O	3.5
DNA	4
5μM Primer	0.5
Sequenance II Premix	2

Table 2.6: Sequenance II Sequencing reaction

PCR product volume was varied depending on concentration assessed by agarose gel electrophoresis; H_2O was adjusted to a final volume of 10μl.

The reaction tube was placed in a thermal cycler, where single strand amplification took place under the following conditions:

Initial Denaturation	96°C for 1min	
Denaturation	96°C for 30secs	30 ×
Annealing	50°C for 15 secs	
Extension	60°C for 1min	

2.2.10.3 Precipitation of Sequencing DNA

The sequencing reaction was transferred to a sterile 0.5ml tube containing 1.0μl 1.5M Sodium acetate/250mM EDTA (pH>8) and 30μl 100% room temperature

ethanol. The tube was vortexed and left at room temperature for no more than 15 minutes. The sequencing reaction was centrifuged at 10,000 x g for 40 minutes at 4°C in a Micro 24-48R Hettich Centrifuge. The supernatant was removed and 20μl 70% room temperature ethanol was added. Centrifugation was repeated as before, supernatant was removed and DNA pellet was air dried at room temperature. DNA sequencing pellets were stored at -20°C until loading on the sequencing gel.

Before loading, the pellet was resuspended in 1μl fuschin loading dye, vortexed, briefly spun, denatured on a thermal cycler at 85°C for 5 minutes and placed on ice.

2.2.10.4 Preparation of Denaturing Sequencing Gel

The glass plates, spacers and comb were soaked in Alconox (Alconox Inc.). The surface of the plates was rinsed with warm tap water and then with dH_2O. The plates were air dried and then assembled, clamped and placed on a flat base surface. A 6% polyacrylamide gel was made by mixing 40ml Sequa-Gel-6 acrylamide (National Diagnostics), 10ml Sequagel complete buffer and 0.4ml fresh 10% ammonium persulphate. The mix was poured between the two plates, the comb was inserted and it was allowed to polymerise. The gel was assembled into the 373A DNA Sequencer according to the manufacturer's instructions (Perkin Elmer Applied Biosystems). A plate-check and a pre-electrophoresis run were carried out. The wells were washed with 1×TBE buffer and the samples were loaded. The gel was run at 2500 Volts for 12 hours.

2.2.10.5 Data Analysis

The sequencing results were collected with ABI Prism 373 software and analysed with DNA Sequencing Analysis Software, version 3.3 (Applied Biosystem Division).

2.2.10.6 Cycle sequencing Reaction (BigDye)

This reaction is carried out with BigDye Terminator Mix and was used for DNA processed on the 377 DNA Sequencer.

The following reaction took place in a sterile 0.2ml tube:

Components	Volume (μl)
dH_2O	2
DNA	1
2μM Primer	2.5
DMSO	0.5
BigDye Mix	4

Table 2.7: BigDye Sequencing Reaction

The cycling conditions of the reactions were:

Initial Denaturation	96°C for 4mins	
Denaturation	98°C for 30secs	30 ×
Annealing	50°C for 15secs	
Extension	60°C for 4mins	

2.2.10.7 Precipitation of Cycle sequenced products (BigDye)

The following were mixed in a sterile 0.5ml tube: 10μl sequencing reaction, 90μl sterile H_2O, 300μl 95% room temperature ethanol and 5μl 3M sodium acetate pH 5.2. The tube was incubated for 15-20 minutes at room temperature and centrifuged at 10,000 x g for 20 minutes. The supernatant was removed and the pellet was suspended in 100μl 70% room temperature ethanol and was left to stand for a minimum of 15 minutes. The sample was centrifuged as before, but only for 5 minutes. The supernatant was removed and the tubes were left at room temperature for 5 minutes before removing all traces of supernatant and excess dye terminators. The pellets were air dried for at least 20 minutes.

DNA sequencing and data analysis were performed at the Biochemistry Department of the University of Manchester.

2.3 RESULTS

2.3.1 Overview

In order to obtain βig-h3 cDNA, RNA was extracted from fibroblasts and reverse transcribed into cDNA. PCR allowed the amplification of βig-h3 cDNA, 2150kb fragment. This was cloned initially into pCR®2.1-TOPO plasmid vector and sequenced to check for any mutations or polymorphisms. In Vitro Mutagenesis was performed, in order to produce the mutant constructs of βig-h3. Before this step was carried out βig-h3 cDNA was inserted into plasmid pALTER-MAX, a mammalian expression vector.

2.3.2 Generation of cDNA

RNA was extracted from both fibroblast and lymphoblast control cell lines using the Trizol Reagent (Gibco BRL). A_{260}/A_{280} was determined to be within the acceptable range 1.9-2.1. The RNA was stored at -80°C. Figure 2.2 represents electrophoresis of the extracted RNA where the two bands are visible.

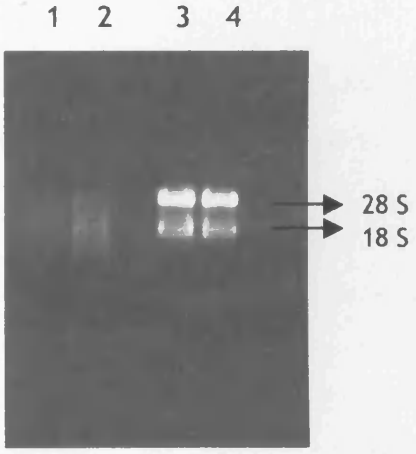

Figure 2.2: Agarose gel electrophoresis of RNA samples.

Lane 1 - 1μl Fibroblast, Lane 2 - 1.5μl Fibroblast, Lane 3 - 1μl Lymphoblast, Lane 4 - 1.5μl Lymphoblast. The characteristic 18S and 28S ribosomal bands appear intact which suggests RNA integrity has not been compromised

A portion of the two RNA samples was transcribed to cDNA with AMV Reverse Transcription System. The stock cDNA was serially diluted 1:10, 1:20 and 1:50 in sterile distilled water and dilutions were stored at -20°C.

A control PCR was carried out with all serial dilutions as template DNA to assess quality of the cDNA samples. The primers used for this reaction, 4AB forward and

reverse, were from exons 8-12 of versican (CSPG2) mRNA sequence. The result was amplification of an approximately 250bp part of the versican cDNA (figure 2.3). Fibroblast cDNA was amplified better than lymphoblast, which may be because the versican gene is expressed at higher levels in fibroblasts when compared to lymphoblasts (Perveen et al, 1999).

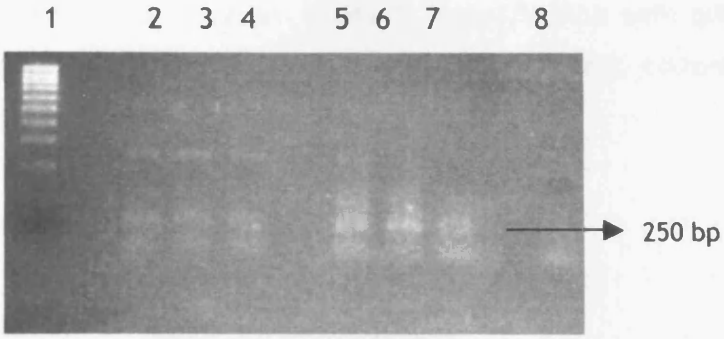

Figure 2.3: Control PCR of cDNA.
Lane 1 - 100bp DNA ladder. Lanes 2-4 - Lymphoblast cDNA (1:10, 1:20 and 1:50). Lanes 5-7 - Fibroblast cDNA (1:10, 1:20 and 1:50). Lane 8 - negative control

2.3.3 PCR optimisation

The whole βig-h3 cDNA is 2150bp long, which is a relatively quite large fragment for a PCR product. Before the whole βig-h3 cDNA sequence was amplified, internal primers were used for optimisation of conditions, such as cycling temperatures, amount of template required per reaction, selection of PCR system which seemed to be offering best results, selection of appropriate buffers. The system that made the amplification of the whole 2150bp possible (Figure 2.4) was the Extensor PCR System (ABgene). The DNA used for this reaction was 2-3μl from 1:10 fibroblast-derived cDNA dilution. The optimum PCR conditions of the reaction are listed in section 2.2.5.

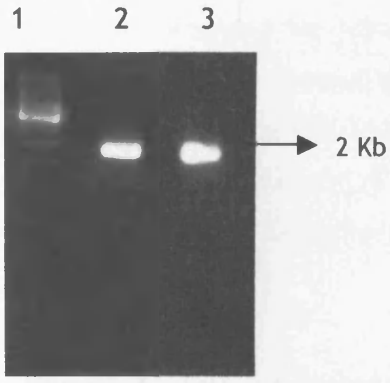

Figure 2.4: PCR amplification of βig-h3 cDNA (2.1kb) from fibroblast with the Extensor Long PCR system (Abgene) Lane 1 - 1kb DNA ladder, Lane 2 - with buffer 2, Lane 3 - with buffer 1

It became apparent from the first few PCRs that cDNA derived from fibroblast cell line gave better results than lymphoblast-derived cDNA. PCRs using lymphoblast cDNA as template did not produce the expected size of DNA fragment. Specifically, amplification with primer pair Seq2-3prime gave two fragments corresponding to approximately 1000 and 370bp (figure 2.5). The expected PCR product for this primer pair is 1100bp. Similarly, amplification with primer pair Prom1-3prime resulted in a band corresponding to about 1200bp, compared with the 2150bp expected.

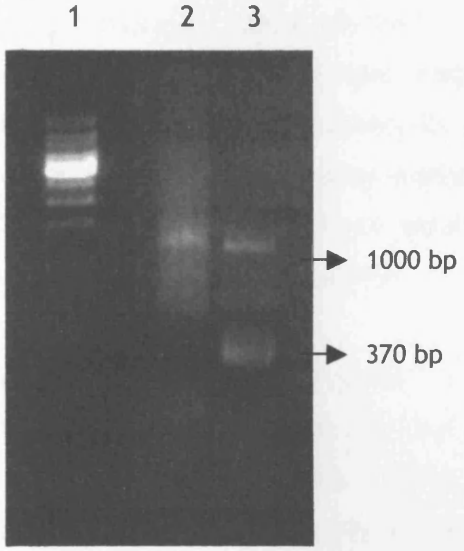

Figure 2.5: PCR amplification of lymphoblast cDNA with Prom1-3prime (Lane 2) and Seq2-3prime (Lane 3) primers. Lane 1 - 1kb DNA ladder

In order to check whether these PCR products were indicators of alternative splicing, which could be taking place in different types of cells, the above fragments were cloned into the pCR®2.1-TOPO vector, the cloned plasmids purified and the insert sequence amplified with the same primers used for the original PCR reaction. The resulting sequences were compared for homology with the βig-h3 sequence. The comparison showed that there was no relation between βig-h3 and the produced sequence. A BLAST search found some EST sequences of MHC-related genes. Alternative splicing was excluded. The failure of lymphoblast cells to amplify βig-h3 cDNA may reflect the low levels of this gene expression in this cell type.

The 2150bp PCR product from fibroblast cDNA was cloned in a pCR®2.1-TOPO vector and the vector was purified. PCR using external and internal primers was

carried out on the recovered plasmid to confirm the presence of the correct insert. Sequencing was carried out with several primers in order to obtain the whole sequence. The resulting cloned βig-h3 cDNA was found to have two already reported (Tsujikawa, 1998) polymorphisms and several single base substitutions, which in some cases resulted in amino acid substitutions in the corresponding protein sequence. These base changes were found in random positions in the cDNA, were not associated with any of the known mutations and differed between different clones. Therefore it was concluded that the changes were resulting from failure of the Enzyme Mix in the Extensor Long PCR system to provide a proofreading, high fidelity Taq polymerase. Since the amino acid substitutions could affect the structure/function of the protein in later stages of the project, e.g. while expressing it in the cornea and trying to assess its pathophysiological effects, it was necessary to reclone the gene using other methods. The problem was that proofreading PFU Taq polymerase (Stratagene) would not amplify the 2150bp βig-h3 cDNA neither with PFU nor with Anglian Buffer.

The buffers provided by the Extensor Long PCR System were used for the amplification of long PCR products using proofreading PFU Taq polymerase. This combined PCR provided a 2150 product, which after cloning, purification and complete sequencing was found to be identical with the normal βig-h3 cDNA and have no unwanted nucleotide changes.

2.3.4 In vitro mutagenesis

The next step after the βig-h3 cDNA had been cloned into a plasmid vector was to produce mutant constructs of this gene which would be related with the mutations encountered in patients with corneal dystrophies. In addition to the normal gene the following mutant versions were selected for construction:

Mutant name	Mutation	Corneal Dystrophy
W	R555W	Granular type I
C	R124C	Lattice type I
Q	R555Q	Thiel-Behnke
C/W	R124C & R555W	Lattice & Granular

Table 2.8: **In vitro mutagenesis products**

It was thought that the above dystrophies exhibit characteristic histological and ultrastructural findings that could be used as ideal models for studying the role of keratoepithelin.

The system that was used to perform the mutations on the cloned, wild type βig-h3 cDNA, was the Altered Sites II Mammalian Mutagenesis System. This system utilises a plasmid, which can be expressed both in bacterial cells, (e.g. *E. coli*) and mammalian cells. Therefore this system is useful for the generation of mutants, as well as for their subsequent transfer into mammalian cells and cell lines.

2.3.4.1 Cloning into pALTER-MAX

Before the in vitro mutagenesis system was put into practice, βig-h3 cDNA was excised from the pCR®2.1-TOPO vector using restriction enzymes. Double digestion with *XbaI* and *SpeI* cut on either side of the inserted cDNA gave rise to two fragments of different size: a 2.237 bp βig-h3 cDNA containing fragment and a remaining 3.813bp, which is the pCR®2.1-TOPO plasmid. The whole of the reaction was loaded onto an agarose gel and fractionated by electrophoresis (figure 2.6). The lower band corresponding to the 2.2kb cDNA to be cloned was excised and DNA was recovered using the QIAquick Gel Extraction kit.

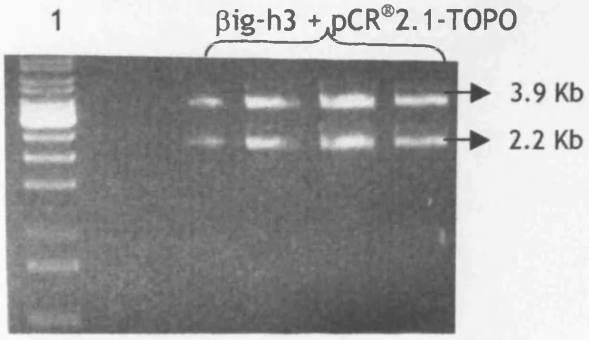

Figure 2.6: Restriction digestion of pCR®2.1-TOPO clones with XbaI and SpeI.
Top band is the vector (3.9kb) and lower band the cloned βig-h3 cDNA (2.2kb)

The recipient plasmid, pALTER-MAX was linearised by restriction digestion with enzyme XbaI (figure 2.7), for which it has only one restriction site. XbaI and SpeI recognise different palindromes, but produce complementary overhangs:

XbaI 5'...TCTAGA...3' → 5'...T-^{OH} ^{P}-CTAGA...3'
3'...AGATCT ...5' 3'...AGATC-^{P} ^{OH}-T...5'

SpeI 5'...ACTAGT...3' → 5'...A-^{OH} ^{P}-CTAGT...3'

3'...TGATCA ...5' 3'...TGATC-^{P} ^{OH}-A...5'

Therefore it is the same principle as using a single restriction enzyme.

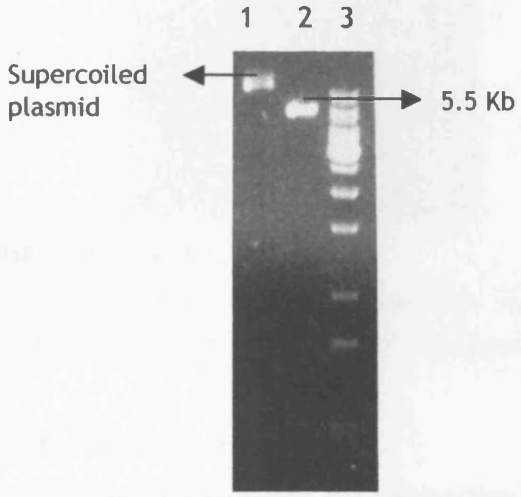

Figure 2.7: XbaI restriction digestion of pALTER-MAX.

Lane 1 - Non-digested plasmid. Lane 2 - digested plasmid. Lane 3 - 1kb DNA ladder

The presence of any pALTER-MAX plasmid that has not been linearised is unwanted, since the circular vectors of the minimum size will be favoured for entry in the competent cells. This increases the difficulty in finding clones that have been transformed with plasmid containing the gene of interest.

In order to maintain a high efficiency of ligation and at the same time ensure complete digestion of the plasmid and abolish the chance of self-ligation, the vector was digested in the presence of spermidine and was subsequently dephosphorylated with CIAP.

Ligation and transformation was carried out as described in sections 2.2.8.8 and 2.2.8.10. The plasmids of the positive clones were purified and digested with a single cutting enzyme, for determination of the total size and with double cutting enzyme(s), for separation of the plasmid and vector DNA (figure 2.8).

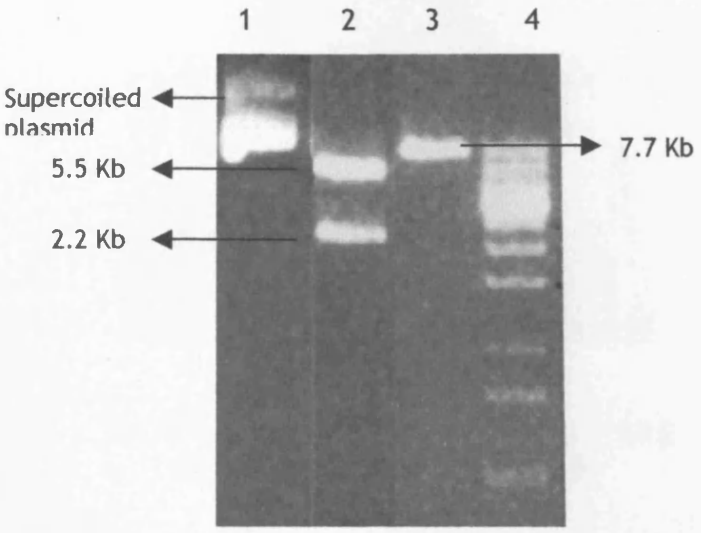

Figure 2.8: pALTER-MAX carrying the βig-h3 cDNA.

Lane 1 - non-digested. Lane 2 - Digested with XhoI and MluI. (5.5kb pALTER-MAX and 2.2kb βig-h3). Lane 3 - Digested with XhoI (7.7kb). Lane 4 - 1kb DNA ladder

2.3.4.2 Generation of mutant βig-h3

The protocol of the In Vitro Mutagenesis procedure was followed (section 2.2.9) and selected clones were screened by direct sequencing. Figure 2.9 illustrates wild type versus mutant sequence.

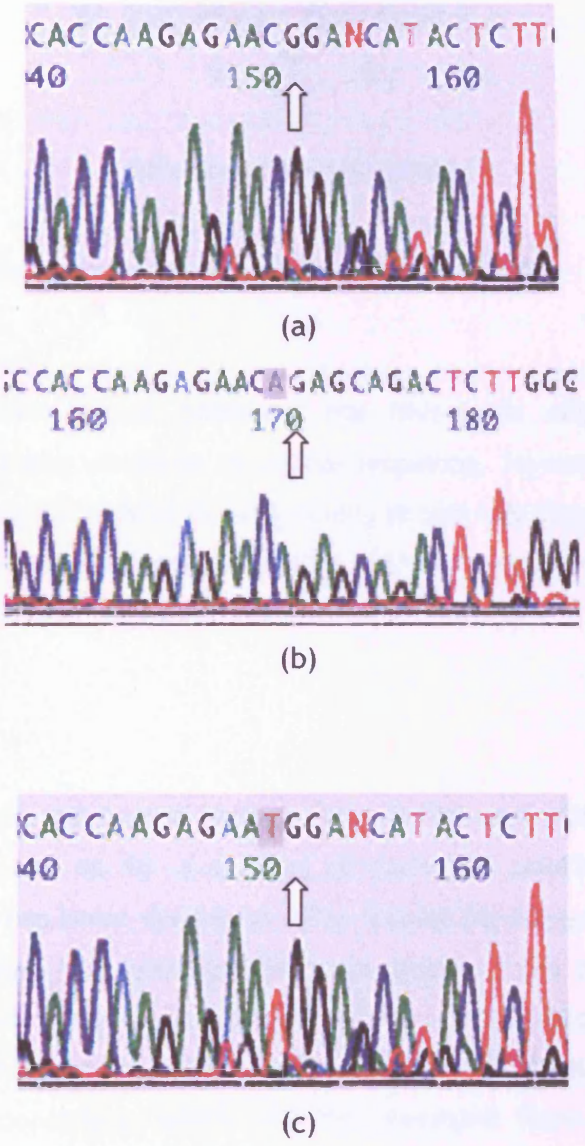

Figure 2.9: Wild type versus mutant sequences

(a) Wild type R555 (CGG). (b) Mutant R555Q (CAG). (c) Mutant R555W (TGG)

R555w and R555Q mutant versions of βig-h3 cDNA have been produced by the described method of In Vitro Mutagenesis. The difficulty in producing R124C mutant may have been the sequence of the mutagenic oligonucleotide, which included a 6 nucleotide-long repeat (Figure 2.10).

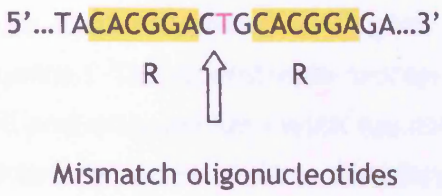

Figure 2.10: Schematic diagram showing mutagenic oligo R124C
R - repeat sequence

In order to overcome these problems the mutagenic oligonucleotides were redesigned, so that there would be no repeat sequence. However, it was again not possible to create any successful mutant clone, maybe this time due to the shifting of the mutagenic nucleotide from the centre of the sequence, which is the optimal position.

2.15 DISCUSSION

Human fibroblast cells were used to derive βig-h3 RNA and cDNA. The full human sequence is known and so far a number of mutations relating to the inherited corneal dystrophies has been described. The human βig-h3 gene has been studied more extensively than the corresponding homologues from other species. The human keratoepithelin has been compared with mouse (Skonier, 1994), rabbit (Rawe, 1997), pig (Hashimoto, 1996) and bovine (Gibson, 1996) homologues. The viral and nonviral constructs which will be developed from the wild type and mutant cDNA described in this chapter will be used on cultured: human epithelial cell line and human/bovine primary epithelial cells and keratocytes.

RNA was extracted from both human fibroblast and lymphoblast cells, but only the fibroblast RNA could adequately amplify the βig-h3 sequence. This might be a reflection of the variable expression profile of βig-h3 between different cell types. Fibroblasts have been reported to express high levels of keratoepithelin (LeBaron, 1995) and in spite of the fact that a variety of tissues and cells have been screened for keratoepithelin expression, no data is available for lymphoblast cells. It is possible that lymphoblasts do not transcribe βig-h3.

Most of the corneal dystrophy mutations have a common characteristic: they are point mutations of a single nucleotide base, which gives rise to an altered amino acid on the protein sequence. The downstream process that takes place on the mutant protein in the cell and extracellular matrix has not been deciphered, but it is obvious from the dominant character of these disorders that a single amino acid change is enough for the emergence of the aberrant phenotype, at the clinical, histological, ultrastructural and molecular level. Moreover, new mutations are still being reported, which are associated with already known disease phenotypes. Thus it is imperative that there are no nucleotide alterations in the PCR amplified sequence.

The PCR amplification of βig-h3 cDNA was followed by DNA sequencing to detect and eliminate unwanted nucleotide changes. Published polymorphisms (Dota, 1998, Tsujikawa, 1998, Schmitt-Bernard, 2000, Kim 2001) and silent mutations were taken into account. Several PCR systems were tried but the one that gave the most reliable sequence was the combination of proofreading PFU Taq polymerase with the buffer 1 set from the Extensor Long PCR system.

During examination of the effects of keratoepithelin overexpression in cultured cells and corneas, it is important to compare our findings with the effects of the dystrophy-related mutants. In vitro mutagenesis, by Altered sites II Mammalian Mutagenesis System was carried out based on the PCR amplified wild type βig-h3 cDNA. Four mutant versions of βig-h3 were attempted: R124C, R555W, R555Q and R124C&R555W. The above mutations correspond to the two most common dystrophies, lattice and granular and Thiel-Behnke. These three dystrophies differ phenotypically. In granular dystrophy rod shaped bodies corresponding to aggregates of the mutant protein are found within the epithelium while in lattice dystrophy abnormal amyloid deposits are also found amongst epithelial cells. Finally in Thiel-Behnke dystrophy there is an extremely early tendency to epithelial recurrent erosions, which may reflect a significant reduction in epithelial cell attachment.

The amino acid positions of these mutations have been described as hotspots, due to the number of different substitutions that have been reported in them (Table 1.3).

Mutants R555W and R555Q have been successfully synthesised, however it has been impossible to give rise to the R124C mutant and the double mutant R124C&R555W. The position 124 on the keratoepithelin protein sequence could be laborious to mutate, possibly due to the presence of flanking repeat sequences (Figure 2.10). Different oligonucleotides sequences were designed and the conditions of the mutagenesis protocol were varied, but all the resulting clones were resistant to the nucleotide substitution TGC of the wild type sequence CGC. The two mutant versions of βig-h3 cDNA, which both lie at mutation hotspot R555, enable us to compare their effects with those of the wild type constructs and distinguish any differences that may reflect their dystrophic phenotype. It was therefore decided to progress with the R555W and R555Q mutants at this stage.

3. CHAPTER THREE

Construction of recombinant adenovirus carrying the βig-h3 gene

3. 1 INTRODUCTION

One of the strategies that was followed to reveal the role of βig-h3 was overexpression of this gene and monitoring its effect on cell behaviour. Recombinant adenoviruses were constructed to carry the wild type and mutant βig-h3 gene and facilitate their transport and overexpression in corneal cells.

Recombinant adenoviruses have been used to achieve high levels of transgene expression within a variety of cell types and tissues (Shering et al, 1997, Brown et al, 1997, Castro et al, 1997). Compared with non-viral gene transfer methods adenoviruses are more efficient in delivering the transgenes to the target cells. This is especially important when using primary cell cultures, which are more difficult to transfect than immortalised cell lines. However, transfection with adenoviruses is transient since the viral DNA does not integrate in the host genome therefore repetitive administration of the virus is essential, especially in dividing cells. Integration in the host DNA might result in unwanted changes of the target cells since this insertion is random and could affect the expression of vital host genes.

The method that was used in this study for the generation of adenoviruses was homologous recombination of adenoviral genomic DNA between two plasmids (pJM17 and pΔE1-cl) in the presence of the helper adeno-transformed embryonic kidney cell line, 293. pJM17 carries the entire genome of type 5 adenovirus, Ad5d1309, with a deletion on the viral E3 gene and an insertion into the E1 region. When co-transfected with the left end shuttle plasmid, such as pΔE1-cl, infectious viral vectors arise by in vivo recombination. The E1 region is replaced eventually with the transgene cassette (Lowenstein et al, 1996) and the resulting recombinant adenoviruses are replication deficient.

The wild type and mutant βig-h3 transgenes were inserted downstream of the major immediate early human cytomegalovirus promoter (hCMV-MIE), a strong constitutive promoter, to facilitate their overexpression upon infection. The analysis of the effects of overexpression on corneal cells may elucidate the role of βig-h3 gene as well as the pathogenesis of corneal dystrophies.

3.2 METHODS

All steps were conducted in a Laminar Flow Cabinet Safety level 2 under sterile conditions and with all the decontamination procedures administered.

3.2.1 The helper 293 cell line

Recombinant adenoviruses derived from vectors with deletion of the E1 gene were grown on cells which express this gene. The cell line used for this purpose was 293, which is derived from embryonic kidney cells transformed with sheared human adenovirus type 5 DNA. These cells are sensitive to human adenoviruses and adenovirus DNA can be used to isolate transformation-defective host range mutants of human adenovirus type 5 and for titrating human adenoviruses.

3.2.1.1 293 cell culture

A cryovial of liquid nitrogen frozen 293 cells was thawed rapidly at 37°C, in a water bath. The cells were added to a sterile 15ml Falcon tube containing 9ml 293 medium warmed to 37°C and centrifuged at 160 x g in a Hettich Universal centrifuge for 5 minutes in order to remove DMSO from the freezing medium. Supernatant was discarded and cells were resuspended in 2ml 293 medium (see Materials) and transferred to a 25cm^2 flask containing 6ml 293 medium. The flask was incubated at 37°C in a 5% CO_2 humidified incubator. 24 hours later the cells were examined microscopically for adhesion to the base of the flask. Incubation continued until cells were 80-90% confluent.

3.2.1.2 Splitting 293 cells

The medium from the 25cm^2 flask containing 80-90% confluent cells was aspirated and cells were washed briefly in prewarmed sterile Dulbecco's PBS. 1ml Trypsin-EDTA solution warmed to 37°C was added to the base of the flask ensuring even coating. The flask was warmed in the palm of the hand for 1-2 minutes and then was tapped repeatedly onto the bench to suspend the cells. 7ml prewarmed 293 medium was added and cells were pipetted to wash them off the flask base and triturate them. 2ml of the resuspended cells were added to each of 4 25cm^2 flasks containing 6ml fresh 293 medium. Flasks were returned to the incubator.

3.2.1.3 Production of 293 stocks

A 25cm^2 flask containing 293 cells of 80-90% confluency was trypsinised. 9ml 293 medium was added and the cells were triturated and transferred to a sterile 15ml Falcon tube. They were then centrifuged at 200 x g for 10 minutes. Supernatant was discarded and

cells were resuspended in 1ml freezing medium and transferred to a 1ml cryo vial. The vial was wrapped in cotton and placed in a polystyrene container, which was kept at -80°C overnight. The following day the vial was stored in liquid nitrogen.

3.2.1.4 Transferring cultures to larger flasks

In order to scale up the replication-deficient adenovirus 293 cells must be infected in larger culture volumes. Therefore 293 cells must be cultured on 175cm^2 flasks.

Starting from a 80-90% confluent 25cm^2 flask, the cells were trypsinised and resuspended in 7ml 293 medium. They were then transferred to a 75cm^2 flask containing 8ml fresh 293 medium and incubated until 80-90% confluent. Following the same procedure the cells were subcultured to a 175cm^2 flask and then passaged twice in a 1:3 ratio ($1 \rightarrow 3 \rightarrow 9$). 8 of the 9 175cm^2 flasks were split into 20 flasks by pooling together the cells of 4 flasks and splitting them in 10 flasks. The ninth 175cm^2 flask was subcultured in 1:3 ratio to maintain an ongoing culture of 293 cells.

3.2.2 Generation of recombinant adenoviruses

3.2.2.1 Cloning

Wild type and R555W and R555Q mutants βig-h3 cDNA were cloned into the pΔE1-cl plasmid vector. The ligated clones were transformed in competent JM109 cells, which were cultured in large volumes and plasmids were extracted with QIAGEN Plasmid MAXI Purification Kit. (See section 2.2.8 for cloning and transformation methods)

3.2.2.2 Plasmid preparation

Plasmid DNA was extracted from the subcultured clones with QIAGEN Plasmid MAXI Purification Kit according to the following protocol.

A single colony was transferred to a sterile 20ml universal tube containing 5ml LB and the appropriate antibiotic. The bacterial culture was incubated at 37°C in an orbital shaker at 250rpm for 8 hours. The starter culture was diluted 1/1000 to inoculate 500ml LB medium and was allowed to grow at 37°C for 12-16hours in an orbital shaker at 250rpm. The bacterial cells were harvested by centrifugation at 6,000 x g for 15 minutes at 4°C in a Beckman JA-10 rotor. The supernatant was discarded and the pellet was resuspended in 10ml buffer P1. After the mixture was homogeneous, 10ml of buffer P2 was added to lyse the cells and the contents were mixed by inverting the tube 4-6 times. The lysate was incubated at room temperature for 5 minutes. 10ml of chilled buffer P3 was added, the

tube was inverted 4-6 times and incubated on ice for 20 minutes to allow precipitation of genomic DNA, protein, cell debris and SDS to take place. Following this the sample was mixed again and centrifuged at 20,000 x g in a Beckman JA-17 rotor for 30 minutes at 4°C. The supernatant containing the plasmid DNA was removed, placed in a clean 50ml polypropylene tube and centrifuged at 20,000 x g for 15 minutes at 4°C. In the meanwhile a QIAGEN-tip 500 was equilibrated by applying 10ml buffer QBT and allowing it to flow through the column by gravity. The supernatant from the last centrifugation step was loaded onto the column and after it had emptied the column was washed with 2x30ml with buffer QC. Finally the DNA was eluted with 15ml of buffer QF and collected in a clean 50ml tube. The DNA was precipitated by adding 10.5ml (0.7 volumes) room-temperature isopropanol and centrifuging at 5,000 x g for 60 minutes at 4°C. The supernatant was carefully removed by pipetting and the pellet was washed with 5ml room-temperature 70% ethanol and centrifuged at 5,000 x g for 60 minutes at 4°C. The ethanol was removed and the pellet was allowed to air dry for 10 minutes. Plasmid DNA was redissolved in 2ml TE buffer pH 8.0 and was stored at -20°C.

3.2.2.3 Co-transfection in 293 cells

(Modified from Lowenstein et al, 1996)

293 cells were split the day before co-transfection so that the next day they are 50% confluent. 25cm^2 flasks were used. The next day medium was aspirated and 5ml of prewarmed 293 medium was added to the cells immediately before transfection. 200μl low TE buffer was added to a 15ml tube. An equal volume of the two plasmids, pJM17 and pΔE1-cl was added in the same tube, as well as 30μl of 2M $CaCl_2$. The tube was centrifuged ensuring that the mixture was at the bottom. 240μl 2xHBS buffer pH 7.2 was added to a second tube. Whilst bubbling air through the HBS, using a Pasteur pipette, the DNA mix was added dropwise. The precipitate was allowed to form for 30 minutes and it was then added to the flask containing the 293 cells. The fine precipitate that formed on the cells was viewed at high magnification. The cells were incubated at 37°C in a 5% CO_2 humidified incubator for 4-16 hours. The medium was aspirated and the cells were washed once with PBS and once with 293 medium. 6-10ml of fresh medium was added to the cells and it was replaced every 3 days or when it turned acidic.

When the co-transfection was successful plaques appeared after 6-8 days, which indicate assembled viral entities which can infected the 293 helper cell line. The medium was not changed after the first plaque appeared and cells were incubated until 100% cytopathic

effect (CPE) occurred. CPE is observed by detachment of the cell layer from the bottom of the flask, cells appear rounded and the medium colour might turn yellowish.

3.2.2.4 X-gal assay

This assay was carried out to determine the number of cultured mammalian cells in a $25cm^2$ flask expressing β-galactosidase upon transfection with control plasmid pMV12.

3-4 days post transfection the medium was aspirated from the cells and they were washed with prewarmed PBS. 5ml 4% paraformaldehyde solution was added to fix the cells for 15 minutes. Following this the cells were washed twice with PBS for 5 minutes. 2ml 0.1% Triton X-100 in PBS was used to permeabilise the cells for 5 minutes. The cells were washed again twice with PBS for 5 minutes each wash. 10ml of staining solution containing X-gal was applied to allow development of blue colour for 1-3 hours. The wash with PBS was repeated and the flask was allowed to air dry.

3.2.2.5 Arclone extraction of adenovirus

The contents of the $25cm^2$ flask were transferred to a 15ml tube and centrifuged at 160 x g for 15 minutes. The supernatant was discarded and the cells were resuspended in 100-200μl PBS. An equal volume of Arclone P™ (ICI) was added to the cells and they were mixed thoroughly. Following a 30-minute centrifugation at 370 x g the mixture was separated in three layers, the top layer containing the recombinant adenovirus in PBS, the middle layer of cell debris and the bottom layer of Arclone P™. The top layer was removed carefully and it was quick-frozen in liquid nitrogen and stored at -80°C.

3.2.2.6 Plaque Purification technique

36 wells of a 96-well plate were inoculated with $8x10^3$ 293 cells per well. 24 hours post inoculation the cells were infected with appropriate serial dilutions of the virus in 100μl of fresh prewarmed 293 medium. Starting at a dilution 10^{-2} to 10^{-11}, each dilution was carried out in triplicate. The virus was circulated every 15 minutes for 90 minutes to ensure even distribution over the monolayer. 24 hours later a further 100μl of fresh prewarmed medium was added to each well and the medium was changed every 3 days or before if necessary.

The cells were monitored daily for evidence of plaque formation. After approximately 8 days the end point well was found, i.e. the last well in the serial dilution with the formation of a single plaque. The cells in the end-point wells were harvested by

resuspending in the media in the wells and were placed in cryovials. The cryovials were frozen and thawed three times to break the cells open and release the virus. The virus from this plaque purification round was used to carry out the second round of purification and the virus from the second round was used to carry out a third round of plaque purification. The virus from the third round was used for scaling up and production of viral stocks.

This technique was carried out three times to ensure that the virus was derived from a single entity before being expanded to produce a virus stock.

The virus from all three fractions was stored at -80°C. Storage of adenoviruses in optimal buffer (e.g. Buffer B, see Materials) containing 10% glycerol or in MEM culture medium supplemented with serum is stable for 1-2 years at -80°C.

3.2.2.7 Extraction of DNA from adenovirus-infected cells

293 cells were seeded in 25cm^2 flasks the day before the infection. 20µl of the virus from the third round of plaque purification was added to the cells with 5ml of fresh prewarmed 293 medium. The medium was changed the next day and the cells were incubated at 37°C in a 5% CO_2 humidified incubator until they appeared rounded. The contents of the flask were collected and centrifuged at 300 x g for 5 minutes. The cells were rinsed with 2ml of PBS and were centrifuged for a further 5 minutes at 300 x g. The pellet was resuspended in 700µl 1xTris-EDTA, pH 8.0, 25µl 10% SDS, 8µl 0.5M EDTA, 8µl 20mg/ml proteinase K and was incubated at 37°C for 2 hours. After the addition of 100µl 5M NaCl the mixture was kept on ice (4°C) for 3-16 hours. The mixture was then centrifuged at 15,000 x g for 1 hour at 4°C and the supernatant was thoroughly harvested. An equal volume of phenol: chloroform: isoamyl alcohol (25:24:1) was added to extract the DNA and the mixture was centrifuged for 5 minutes at 15,000 x g. The DNA was precipitated once with 2 volumes of alcohol and centrifuged for 10 minutes at 15,000 x g. The pellet was washed with 70% ethanol and resuspended in 50µl dH_2O containing 0.1mg/ml RNase.

3.2.2.8 Scaling up adenovirus stocks

A 25cm^2 flask of 70% confluent 293 cells was inoculated with 20µl of end point virus from the final round of plaque purification with fresh medium. The next day the medium was replaced and the cells were maintained at 37°C in a 5% CO_2 humidifed incubator until 100% cytopathic effect was observed. The cells were then harvested and centrifuged at 500 x g for 5 minutes. The supernatant was discarded and the pellet was resuspended in 500µl

Dulbecco's PBS. The cells were frozen and thawed three times to open them and the cell debris was pelleted by centrifuging for 5 minutes at 160 x g. This virus stock was used to infect the 20 175cm^2 flasks for the Arclone purification step and it was stored at -80°C.

3.2.2.9 Arclone purification of adenovirus

20 70-80% confluent 175cm^2 flasks of 293 cells were aspirated, and 18ml of fresh 293 medium was transferred to each flask. 20μl of the virus up-scaled with the above protocol or 3 MOI of titrated adenovirus were used to infect each flask. Flasks were incubated until a total cytopathic effect occurred.

When the 100% cytopathic effect is observed, the 20 175cm^2 flasks were harvested by transferring the flask contents in 50ml sterile polypropylene tubes and centrifuging them at 500 x g for 15 minutes. The supernatant was discarded and the cells were resuspended in 10ml PBS. An equal volume of Arclone P™ (ICI) was added and mixed with the cells. Centrifugation at 370 x g for 20 minutes produced three distinct layers: the top layer containing PBS and virus, the middle layer the cell debris and the bottom layer consisting of the Arclone. The top layer was removed carefully and transferred to a sterile 15ml falcon tube. The virus was quick frozen in liquid nitrogen and stored at -80°C.

3.2.2.10 Caesium Chloride Gradient purification of Adenoviruses

This protocol was used to purify and concentrate the Arclone preparation of the adenovirus. It is a modification of the procedure described in Virology: A practical approach (Mahy, 1991).

Two different concentrations of caesium chloride were prepared by dissolving CsCl in 5mM Trizma Hydrochloride, 1mM EDTA pH 7.8; 1.33g/ml and 1.45g/ml. Solutions were sterilised by passing through a 0.2μm filter.

2.5ml 1.33g/ml CsCl was pipetted in a 14ml Beckman centrifuge tube. Using a wide bore syringe 1.5ml 1.45g/ml CsCl was pipetted slowly on the bottom of the tube to form the gradient. Approximately 4ml of Arclone virus solution was applied on the gradient and mineral oil was layered to the top of the tube. Tubes were balanced to an identical weight (up to two decimal points) and placed in the rotor and sealed prior leaving the Safety cabinet. Velocity density gradient centrifugation took place in a Beckman ultracentrifuge at 90,000 × g (22,500rpm for the SW40 rotor) for 2 hours at 4°C (Accel=1, Decel=7). The tubes were opened in the safety cabinet and the following three bands (top

to bottom) could be observed: Debris, defective virus, "functional" virus. The "functional" virus was removed with a wide bore syringe, which was inserted in the side, wall of the tube approximately 1cm below the band.

The retrieved virus was diluted in half a volume of sterile TE buffer pH7.8. A second CsCl gradient was prepared as before, but this time with 1ml of 1.45g/ml CsCl and 1.5ml 1.33g/ml CsCl. The gradient was layered with the diluted virus, topped with mineral oil, balanced and centrifuged at 100,000 × g (23,800prm for the SW40 rotor) for 18 hours at 4°C. The viral band was recovered as before and transferred to 10cm treated dialysis tubing, which was clipped at both ends. The virus was dialysed twice against 1L Buffer A for 1 hour and once against Buffer B (see Materials section) for 2 hours. 10μl aliquots were transferred into sterile 0.5ml tubes and the purified virus was stored at -80°C.

3.2.2.11 Preparation of Dialysis Tubing

The dialysis membrane was cut into 10cm long pieces and boiled in 500ml 2% Sodium bicarbonate and 1mM EDTA for 10 minutes. The tubing was rinsed thoroughly in distilled water and boiled in 500ml 1mM EDTA for 10 minutes. It was allowed to cool in the EDTA containing beaker, covered with foil and stored at 4°C ensuring it was always submerged. Before use the membrane was removed from the storage buffer in the laminar flow safety cabinet and washed thoroughly in distilled water.

3.2.2.12 Adenovirus Titration

A 96-well plate was inoculated with 5-10,000 cells per well in 100μl 293 medium and incubated for 24 hrs. The following day 22 serial dilutions of the virus were made from 10^{-2} down to 7.63×10^{-12} in a 24-well plate. 100μl of each dilution was added to 4 well from the 96-well plate that was inoculated the previous day.

After one day's (16-24hrs) incubation, 100μl fresh pre warmed medium was added to each well. Medium was aspirated after 3-4 days and replaced with 100μl fresh medium. 6 days after infection the wells were monitored for plaque formation. Results were recorded for CPE, plaques, single plaque, uncertain and none. 8 days after infection the well with the single plaque should be identified. This is the end point of the titration and determines the pfu/ml of the virus, according to the following table.

Well	Dilution	Pfu/ml
1	10^{-2}	1×10^{3}
2	10^{-3}	1×10^{4}
3	10^{-4}	1×10^{5}
4	10^{-5}	1×10^{6}
5	10^{-6}	1×10^{7}
6	5×10^{-7}	2×10^{7}
7	2.5×10^{-7}	4×10^{7}
8	1.25×10^{-7}	8×10^{7}
9	6.25×10^{-8}	1.6×10^{8}
10	3.12×10^{-8}	3.2×10^{8}
11	1.56×10^{-8}	6.4×10^{8}
12	7.81×10^{-9}	1.28×10^{9}
13	3.91×10^{-9}	2.56×10^{9}
14	1.95×10^{-9}	5.12×10^{9}
15	9.77×10^{-10}	1.02×10^{10}
16	4.88×10^{-10}	2.05×10^{10}
17	2.44×10^{-10}	4.1×10^{10}
18	1.22×10^{-10}	8.19×10^{10}
19	6.1×10^{-11}	1.64×10^{11}
20	3.05×10^{-11}	3.28×10^{11}
21	1.53×10^{-11}	6.55×10^{11}
22	7.63×10^{-12}	1.31×10^{12}

Table 3.1: Titration table of diluting factors and respective pfu/ml

3.2.2.13 Supernatant Rescue Assay

The viruses used in all the applications above are replication deficient and although they can express the transgenes they carry they cannot replicate themselves. However propagation of these viruses takes place in 293 cells, which contain stably integrated E1 viral genes. Therefore it is not impossible for wild type, replication efficient virus to appear as a result of homologous recombination with the genes that are provided by 293 cells. Any viral preparations which contain replication-efficient virus should be decontaminated and discarded.

One way to detect the presence of the wild type virus is PCR amplification using primers that hybridise with the deleted E1 sequences. An alternative and more sensitive detection system is the supernatant rescue assay (Dion et al, 1996) according to which the wild type can be rescued from the supernatant of cells exposed to high MOIs of recombinant virus containing very limited numbers of wild type virus.

3×10^6 HeLa cells were plated on tissue culture dishes (primary plates). A $25cm^2$ flask was seeded with HeLa cells and incubated in parallel. The following day one of the tissue culture plates was apirated, washed with PBS and trypsinised with 1.5ml trypsin and cells were resuspended in 8.5 ml RCA medium. Cells were counted on a haemocytometer and based on the determined concentration the tissue culture dishes were infected with an MOI of 30. An appropriate number of dishes were infected by the virus, so that a total 10^9 pfus were tested in total.

6 hours later 4ml of RCA medium was added to each dish and incubation continued. The next day the $25cm^2$ flask with the HeLa cells was split (1:3) into a $75cm^2$ flask. These cells were cultured with grow-all medium. The following day these cells were used to inoculate the wells of a 24-well plate with 0.5ml 4×10^4cells/ml (secondary plate). After overnight incubation the wells were aspirated and washed with PBS. Meanwhile the supernatants of the primary plates were centrifuged at 160 x g for 5 minutes. 300μl supernatant of each was transferred to three wells of the secondary plate, which was then incubated for 6 hours. The supernatant was then replaced by maintenance medium and incubation continued. 3 days later plates were examined for the presence of plaques or CPE. The medium was changed and incubation was carried on for three more days when wells were finally evaluated.

3.3 RESULTS

3.3.1 DEVELOPMENT OF ADENOVIRAL VECTOR

Plasmid pΔE1-cI is a product of ligation between two BamHI -BglII digested plasmids, pΔE1sp1A (Microbix) and pCI-neo (Promega) (see Materials). It contains adenoviral sequences 22 -5790 bp (0-16 mu) with a deletion of E1 sequences 342-3528 bp (1-9.8 mu). Both wild type and mutant βig-h3 cDNA were cloned into plasmid pΔE1-cI.

3.3.1.1 Cloning into pΔE1-cI

The main strategy that was followed for the cloning of βig-h3 into the pALTER-MAX vector was applied in this case. βig-h3 cDNA (wild type or mutant) was cut off pALTER-MAX with double digestion using the enzymes XhoI and MluI. pΔE1-cI was digested with the same enzymes, which give rise to different overhangs and allow positional cloning. This eliminates the need for dephosphorylating the plasmid vector, since self-ligation is impossible. The restriction sequences of the above enzymes are shown below:

XhoI

5'...CTCGAG...3' → 5'...C-^{OH} ^{P}-TCGAG...3'

3'...GAGCTC...5' 3'...GAGCT-^{P} ^{OH}-C...5'

MluI

5'...ACGCGT...3' → 5'...A-^{OH} ^{P}-CGCGT...3'

3'...TGCGCA ...5' 3'...TGCGC-^{P} ^{OH}-A...5'

The standard ligation and transformation procedures were carried out and positive clones were confirmed by restriction analysis with a single and double digestion, as illustrated in figure 3.1, below.

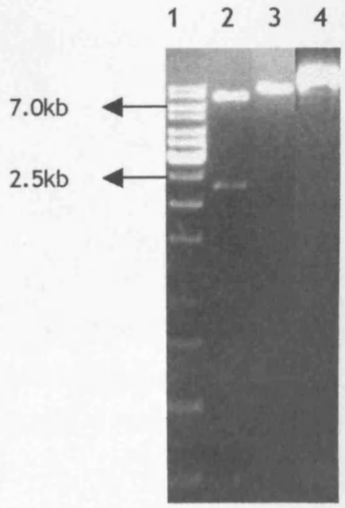

Figure 3.1: pΔE1-cI containing βig-h3

Lane 1 - 1kb DNA ladder. Lane 2 - XhoI & MluI digestion produces 7.7kb plasmid and 2.2kb insert. Lane 3 - XhoI digestion linearises the 9.9kb vector. Lane 4 - uncut vector

3.3.1.2 Scaling up of pJM17

pJM17 carries the entire Ad5d1309 genome (3.7-100 mu). It can be used to construct replication defective AD5 vectors with inserts in the early region 1 (E1) and deletion in the E3 region. The plasmid itself is noninfectious since it contains an insertion at 1339bp (3.7 m.u.) in Ad5 sequences which makes the resulting viral genome too large to package. pJM17 must be cotransfected with a left end shuttle plasmid, such as pΔE1-cl, to generate infectious vectors of a packable size by in vitro recombination. The inserts in E1 region, derived from the shuttle vector, can be up to 5.2kb.

To produce a stock, the plasmid was cloned into DH5α cells and plasmid preparations were carried out using the QIAGEN plasmid MAXI prep kit. Due to its large size (40kb), it was prepared with a method that eliminates the chances of recombination. After transformation of competent cells, a single colony was transferred to a 5ml liquid culture, which after 8 hours was used to subculture (1:100) the overnight culture to be used for the MAXI preparation.

Despite this, approximately 50% of the plasmid preparations of this large vector had recombined as demonstrated by restriction digestion with HindIII (Gibco BRL) (Figure 3.2). Only those preparations that gave the expected restriction pattern were retained for further use.

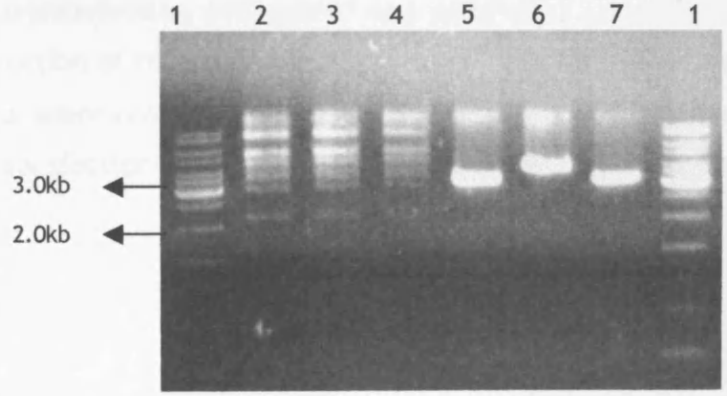

Figure 3.2: HindIII digestion of various pJM17 maxi preps

Lane 1 - 1kb DNA ladder. Lanes 2-4 - normal pJM17. Lanes 5-7 - recombined pJM17

3.3.1.3 Optimising cotransfection

In order to determine the amount of plasmid DNA required to achieve efficient transfection of 293 cells, the cotransfection protocol was carried out initially with different amounts of a single plasmid, pMV12. This is a 13.0 Kb plasmid vector which carries the *LacZ* gene and encodes the enzyme β-galactosidase. Expression of this reporter

gene can be monitored by production of blue colour following the reaction with the substrate X-gal (5-bromo-4-chloro-3-indolyl-b-D-galactoside).

50% confluent 293 cells cultured in 25cm^2 flasks were transfected with 2, 5 and 8μg of plasmid DNA pMV12 which had been prepared with the QIAGEN Plasmid MAXI Purification Kit. After carrying out the X-gal assay all the cells were stained blue with the intensity of the staining increasing in proportion with the amount of pMV12 plasmid that was used for the transfection (figure 3.3). Since all of the cells appeared blue with the 5μg of pMV12, this amount of plasmid was used for the following experiments.

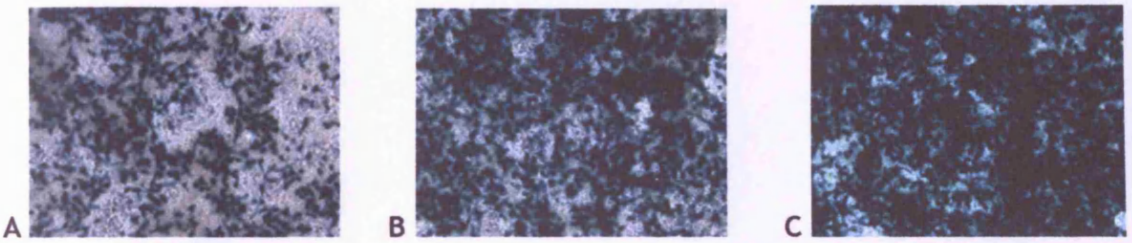

Figure 3.3: Control co-transfection with pMV12

Cells were stained with X-gal for blue colour detection of *Lac*Z expression. A. 2μg of plasmid, B. 5μg and C. 8μg

3.3.1.4 Co-transfection with pJM17 and pΔE1-cl

The construction of the recombinant adenovirus is a result of recombination between the homologous adenoviral genome sequences on plasmids pJM17 and pΔE1-cl. The principle of the co-transfection technique is demonstrated on the following diagram (figure 3.4).

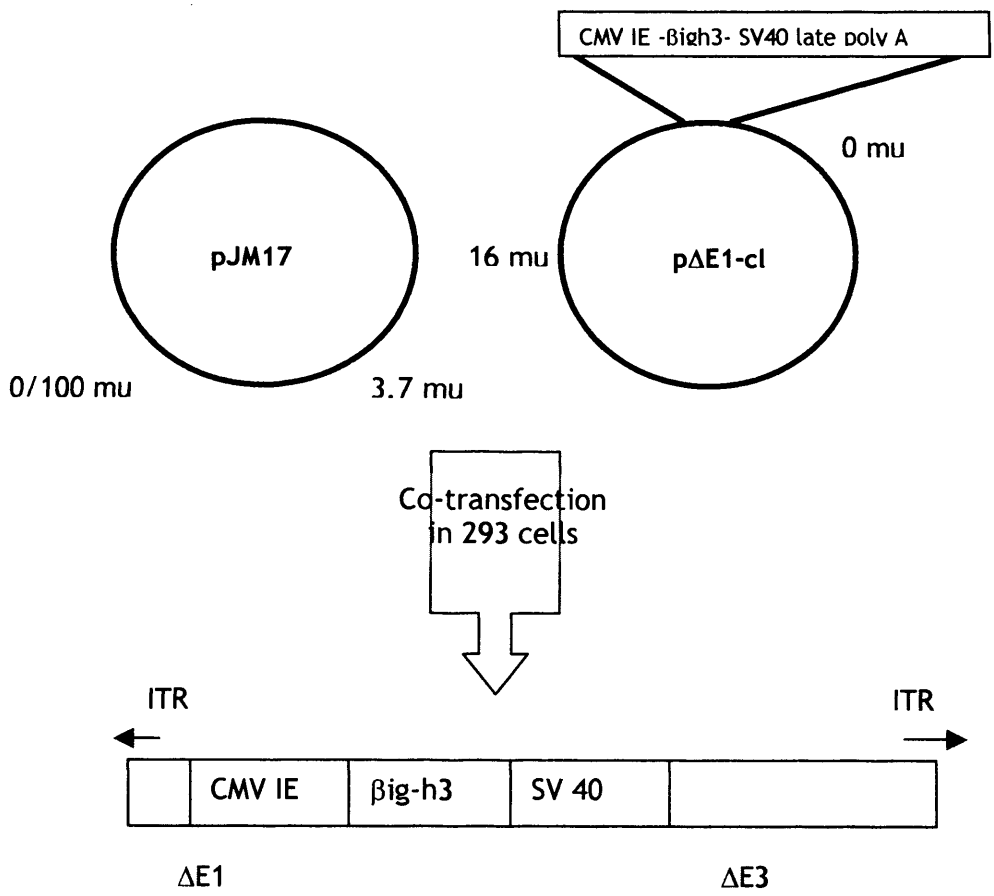

Figure 3.4: Mechanism of homologous recombination of pJM17 and pΔE1-cl during co-transfection

8 25cm^2 flasks of 293 cells were co-transfected with 5μg of pJM17 and 5μg of pΔE1-cl carrying the wild type and mutant R555W βig-h3 cDNA. 9 days after transfection the first plaques appeared and three days later 7 out of the 8 flasks had rounded cells and many plaques. The co-transfections with pJM17 and pΔE1-cl carrying the R555Q mutant cDNA did not yield any plaques although the experiment was repeated three times.

The recombinant adenoviruses from the co-transfection flasks were extracted with Arclone P™ and stored at -80°C. One virus with each transgene was used for the three rounds of plaque purification technique.

3.3.1.5 Nomenclature

The product of recombination between pJM17 pΔE1-cl carrying the wild type βig-h3 cDNA will be referred to as Radβigh3. The product of recombination between pJM17 and pΔE1-cl carrying the mutant R555W βig-h3 cDNA will be named RadR555W.

3.3.2 Characterisation of the adenovirus

Vector systems are designed so that the vast majority generate of the product is virus with the appropriate insert. However, occasionally inappropriate recombination can take place and result in aberrant viral construct. The recombinant adenoviral genome was extracted and was analysed with the following methods to confirm the presence of the insert.

3.3.2.2 PCR amplification

Six different viral constructs were tested for Radβigh3 and five for RadR555W. The viral DNA was extracted according to the method in section 3.2.2.7. The DNA of each viral construct was diluted 1:10 and was read spectrophotometrically at A_{260}. The concentrations varied between 1.375 and 2.2μg/μl.

The presence of the transgenes, were confirmed with PCR amplification of the βigh3 cDNA sequence (figure 3.5) with two different sets of primers: prom1-3prime, which amplify the whole 2.150kb cDNA sequence, and seq1-seq2R, which amplify a 500kb internal part of the cDNA sequence (543-1042bp) (see table 2.1).

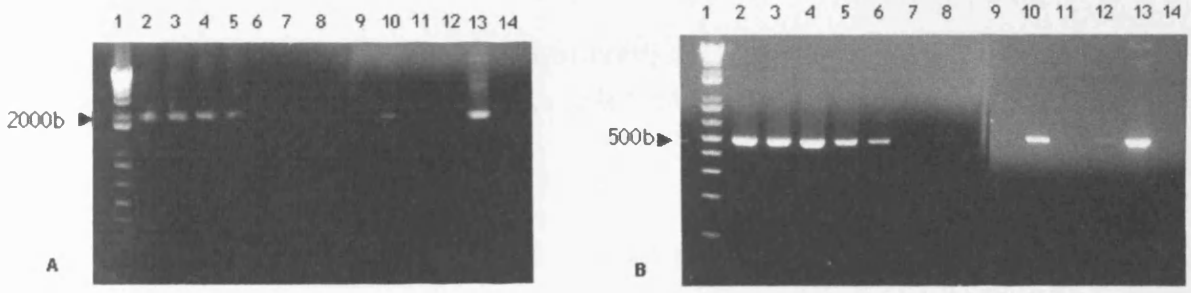

Figure 3.5: **Confirmation of the presence of βig-h3 transgenes with PCR amplification.** Gel A - amplification of the whole 2150bp insert sequence. Gel B - Amplification of a 500bp fragment with internal primers. Lane 1 - Molecular weight standard. Lane 2 - RadR555WF6. Lane 3 - RadR555WE6. Lane 4 - RadR555WD6. Lane 5 - Radβigh3F6. Lane 6 - Radβigh3C6. Lane 7 - Radβigh3D7. Lane 8 - Radβigh3F7. Lane 9 - Radβigh3C9. Lane 10 - Radβigh3D7. Lane 11 - RadR555WE8. Lane 12 - RadR555WC7. Lane 13 - positive βig-h3 amplification control. Lane 14 - negative control (no DNA)

From the PCR products on the above gels it appears that 6 out of the 11 screened viral constructs amplify the expected size of βig-h3 sequence: RadR555WF6, RadR555WE6, RadR555WD6, Radβigh3F6, Radβigh3C6, Radβigh3D7. These constructs will be used for further experiments. The rest of the constructs are either the products of inappropriate recombination or correspond to DNA which is not of good quality. Four of the five viral DNA samples which did not give the expected PCR product were extracted in a separate round of DNA extraction. During the spectrophotometric analysis they appeared to contain high levels of protein (5-8mg/ml), which could potentially inhibit efficient PCR.

3.3.2.3 DNA sequencing

The extracted recombinant adenoviral genome was also subjected to DNA sequencing to confirm the correct sequence as well as that the in vitro mutagenesis sites have been maintained. The sequencing took place using the BigDye Terminator Mix as described in section 2.2.10.6, with the primers described on table 2.1. The resulting sequence had not been changed form the original cloned cDNA βig-h3 sequence and the R555W mutation was also confirmed (Figure 3.6).

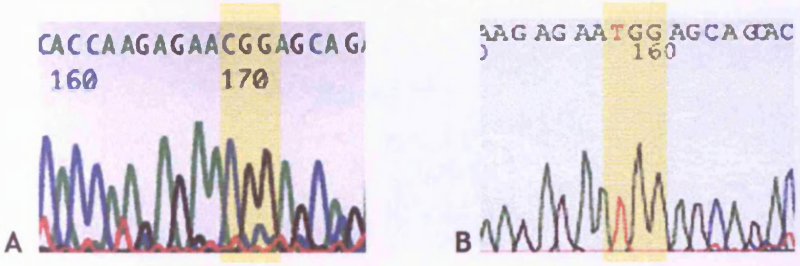

Figure 3.6: DNA sequencing confirming the mutation R555W

A. Radβigh3 with the wild type codon CGG. B. RadR555W with the mutated codon TGG

3.3.3 Recombinant adenovirus stocks

After the characterisation of the correct adenoviral constructs, one of each recombinant, Radβigh3 and RadR555W, were selected for up-scaling and experimental use. These adenoviruses were used to infect 20 175cm^2 flasks and were then extracted with Arclone and purified with $CsCl_2$ gradient centrifugation. The titres of the purified viruses was determined with end point dilution to be 1.64×10^{11} and 3.28×10^{11} pfu/ml for Radβigh3 and RadR555W respectively.

Propagation of replication deficient adenovirus in 293 cells, which provide the deleted adenoviral genes can sometimes result in stocks which contain wild type recombinants.

These are replication competent and infectious and therefore should not be used. Supernatant rescue assay was carried out to detect such recombinant by incubating HeLa cells with the supernatant from HeLa cells exposed to high MOI of the recombinant stock. No wild type recombined virus was detected in the preparation.

3.3.4 Confirmation of expression of adenoviral transgene

The integration of the βig-h3 cDNA sequence in the recombinant adenoviral genome was confirmed as described in section 3.3.2. However it was important to ensure that this transgene was efficiently expressed when the adenovirus infected cultured cells, thereby mediating overexpression.

The purified adenoviruses were used to infect cultured cells, primary keratocytes and epithelial cells at an MOI of 100. 72 hours post infection the RNA was extracted and RT-PCR was carried out as described in sections 2.2.2 and 2.2.3. The 2150bp fragment of the βig-h3 cDNA was amplified using the Prom1-3prime primers (table 2.1).

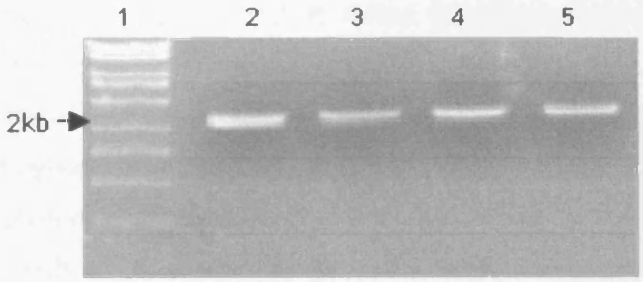

Figure 3.7: PCR amplified βig-h3 fragment from RNA extracted from adenovirus infected cells
Lane 1 - Molecular Weight standard. Lane 2 - Epithelial cells infected with Radβigh3. Lane 3 - Keratocytes infected with Radβigh3. Lane 3 - Epithelial cells infected with RadR555W. Lane 4 - Keratocyte infected with RadR555W.

3.3.5 Control recombinant adenoviruses

In addition to the above recombinant adenoviruses which carry the wild type and mutant βig-h3 inserts, two control adenoviruses were also up-scaled, Rad35 and Rad332. Rad35, (kindly provided by M.G. Castro), carries the *LacZ* gene and Rad332 (kindly provided by G.W.G Wilkinson) has been constructed to express the Green Fluorescent Protein (GFP). These strains were required in order to test the feasibility of transfection of corneal epithelial cells in different systems. These were i) transformed cell lines ii) primary epithelial cell culture iii) ex vivo rat corneal organ culture.

A small sample from each of these viruses was used to infect 20 175cm^2 flasks at an MOI (Multiplicity Of Infection) = 3. They were subsequently extracted with Arclone and purified according to the described protocol. The titre of the purified viruses, Rad35 and Rad332 were determined with end point dilution to be 1.64×10^{11} pfu/ml and 2×10^{8} respectively. Supernatant rescue assay demonstrated the absence of replication competent virus in the preparation.

3.4 DISCUSSION

Radβigh3 and RadR555W were synthesised with homologous recombination of adenoviral genome containing plasmids, pJM17 and pΔE1-cl, which also carried the βig-h3 cDNA. The co-transfection took place in the helper cell line 293.

It was originally intended to construct a third virus, which would express keratoepithelin with the R555Q mutation. Although the co-transfection experiment was carried out several times after the optimisation of the protocol with the control plasmid pMV12, it resulted repeatedly in no plaques and CPE. The sequence corresponding to the R555Q mutant cDNA of βig-h3 is cloned on plasmid pΔE1-cl, but it failed to successfully recombine with the pJM17 plasmid to give rise to recombinant adenoviral constructs. In order to ensure that the plasmid preparations are suitable for transfection of mammalian cell culture, the plasmids were prepared again using the EndoFree™ Plasmid Maxi purification Kit (Qiagen), which eliminates the presence of endotoxins from bacterial lysates and gives rise to ultrapure plasmid DNA with improved efficiency of transfection. However this did not improve the efficiency of co-transfection of the R555Q plasmid either.

The integrity of the recombinant viral DNA and the presence of the transgene were determined with restriction digestion, PCR amplification of the cloned βig-h3 insert and DNA sequencing. Expression of the insert was demonstrated by RNA extraction from cells infected with the adenovirus and subsequent RT-PCR amplification of the βig-h3 cDNA.

Construction of the recombinant adenoviruses carrying the wild type and mutant βig-h3 gene is a powerful tool to help our understanding of the mechanisms behind the Corneal Dystrophies. They enable the overexpression of βig-h3 gene constructs in ocular tissues which would override the corneal expression levels. This is a novel approach to the study of these inherited ocular diseases, since no other reports have been published to date of recombinant viral vectors with this transgene.

4. CHAPTER FOUR

Production of native recombinant keratoepithelin

4.1 Introduction

The pathologic phenotype observed in corneal dystrophies is due to the accumulation of aggregates in the anterior cornea and corneal stroma, which compromise the transparency of this tissue. Although not completely understood, these aggregates contain high amounts of the keratoepithelin protein. There is evidence that keratoepithelin is accumulated in the affected human cornea in greater amounts than in control (Klintworth et al, 1998) by comparing the albumin:keratoepithelin ratio. This was also demonstrated by histological staining where the deposits in affected corneas stain intensely for keratoepithelin compared with the diffuse stain in normal corneal stromal tissue (Streeten et al, 1999).

The function of this protein remains unclear, although it seems to play a role in growth (Skonier et al, 1994, Wang et al 2002), differentiation (Ohno et 2002), development (Schorderet et al, 2000, Ohno et al, 2002), wound healing (O'Brien et al, 1996, El-Sabrawi et al, 1998) and tumourgenicity (Skonier et al, 1994). Keratoepithelin seems to exert its biological effects by interacting with the transmembrane proteins on the cell surface, integrins (Kim et al, 2000, Bae et al, 2001).

Little is understood about the manner by which the changed amino acids on the mutant protein lead to the formation of deposits. Missense mutations alter protein folding and the affinities of subunit interactions. Protein folding, especially in the case of secretory and plasma membrane proteins, involves interaction with molecular chaperones and enzymes (Swallow and Edwards, 1997). Mutations which disrupt these interactions result in protein instability and loss of function. However, mutations in critical regions may not affect normal synthesis and stability, but disrupt normal function, e.g. mutations in binding sites for enzymes, ligands or other proteins. Many missense mutations lead to abnormal protein folding. In certain instances the effect is the excessive accumulation of abnormal protein, e.g. amyloid plaques in Alzheimer's brain disease, which are composed of insoluble forms of lysozyme (Booth et al 1997 and Perutz 1997).

To further explore the role of the intriguing keratoepithelin molecule, a recombinant form was produced, corresponding to the wild type and mutant cDNA clones obtained with the cloning and in vitro mutagenesis. Native protein is difficult to extract from tissue and it

usually involves harsh methods, like denaturation, which affect the protein integrity. Also the quantity of the extracted protein from tissue is usually low.

Recombinant protein can be a useful tool for the study and sometimes pharmaceutical intervention in inherited disorders. *Escherichia coli* is a common host for recombinant protein production, although other methods are available which involve mammalian cells, such as yeast, insect or even plant cells. The advantages for using the prokaryotic host *Escherichia coli*, are that it provides a simple, inexpensive, fast and efficient alternative to recombinant protein, its genetics are well understood and there is a large number of compatible tools available.

Recombinant keratoepithelin has been expressed and reported by other researchers (Billings et al, 2002, Yuan et al, 2004, Bae et al, 2002, Kim et al, 2002). In all the above cases a prokaryotic system was used for the expression of the recombinant protein, which was isolated from inclusion bodies, in an insoluble form. The formation of insoluble aggregates (inclusion bodies) is a common event in *Escherichia coli*, resulting from overexpression and accumulation of high concentration of recombinant protein into the cytoplasm or inefficient processing of the polypeptide. The protein in the inclusion bodies is usually misfolded and biologically inactive (Villaverde et al, 2003). It is possible to refold protein which has been extracted from inclusion bodies, but this a time consuming process which requires optimisation of the refolding conditions and usually the recovery yield is poor. Moreover there is the possibility that re-solubilisation can affect the integrity of refolded protein.

The culture conditions and cloning options of the protein expression protocol can be manipulated in different ways in order to improve the chances of solubility of the recombinant protein and extract it in its native form. The way this was carried out is described in the methods below. Therefore recombinant protein was expressed in *Escherichia coli* and extracted in the insoluble, native conformation and this was used to study its effect on corneal cells.

4.2 METHODS

The expression system used for the recombinant protein production was the pET by Novagen. This system provides a variety of plasmid vectors, where the DNA of interest can be cloned in a variety of host cells where the expression of the cloned proteins takes place.

The host used was the bacterial strain BL21(DE3)pLysS. DE3 is a lysogen of λDE3 and carries a copy of T7 RNA polymerase under the control of the *lac*UV5 promoter (Studier et al, 1986). The plasmid pLysS encodes T7 lysozyme, which inhibits T7 RNA polymerase. The only promoter known to direct transcription of the T7 RNA polymerase gene is the *lac*UV5, which is inducible by IPTG. This bacterial strain is used to suppress the basal expression of T7 RNA polymerase prior IPTG induction and therefore stabilises recombinants that express recombinant protein which affects cell growth and viability.

Another way to control basal expression is to use vectors with the T7*lac* promoter (Dubendorff et al, 1991). These plasmids contain the *lac* operator sequence just downstream of the T7 promoter. They also carry the *lac* repressor, *lac*I, which acts on the *lac* operator. When this type of plasmid is used with the DE3 lysogens, the lac repressor acts both on the *lac*UV5 promoter in the host chromosome to prevent RNA polymerase transcription and the T7*lac* promoter to block transcription of the inserted gene. When using T7lac promoter the expression in pLysS host can be reduced.

E. coli codon usage is different from mammalian cells, especially codons Arg, Ile, Leu, Gly and Pro are rarely used and heterologous target proteins can be difficult to express correctly. To compensate for this, pLysS expresses the rare codon tRNA's on the same backbone as T7 lysozyme.

To enhance the solubility and folding of the recombinant protein BL21(DE3)pLysS transformed cells were not cultured overnight. Alternatively culture periods were not more than 5 hours long and the temperature of up-scale growth and induction was 30°C. Also BugBuster reagent in combination with rLysozyme were used, which can increase solubilisation of the extracted proteins.

The antibiotic ampicillin was replaced with carbenicillin, which can be used to select for plasmids containing ampicillin resistance. The reason for this is because ampicillin selection tends to be lost in cultures because secreted β-lactamase and the drop in pH that accompanies bacterial fermentation both degrade the antibiotic. For the same reasons extended periods of culture were avoided. Increased degradation of ampicillin results in increase of the number of cells in culture which do not have resistance and therefore lack the desired recombinant plasmid.

4.2.1 Cloning

The βig-h3 cDNA was PCR-amplified with appropriate primers to give rise to a fragment, where restriction endonuclease sites were inserted at either ends. Both this PCR product and the chosen plasmid vector underwent restriction digestion with the same restriction enzyme(s). Following this the digested fragments were ligated. All these steps were carried out as described in section 2.2.8 with the modifications mentioned in 4.3 section below.

4.2.2 Mini preparation of protein with Ni-NTA resin

A fresh colony of transformed BL21(DE3)pLysS competent cells was inoculated in 5ml of LB medium containing 50μg/ml carbenicillin and 34μg/ml chloramphenicol. The cells were incubated at 37°C orbital shaker at 250 rpm until OD_{600} = 0.5-0.7. A 500μl sample was taken for uninduced control, the cells were pelleted at 15,000 x g for 1 minute, resuspended in 50μl 1x SDS sample buffer and frozen until SDS-PAGE was carried out. The rest of the culture was induced with 1mM IPTG and was incubated at 30°C for 4 hours. The culture (3ml) was centrifuged at 15,000 x g for 1 minute to harvest the cells. The supernatant was discarded and the pellet was frozen at -20°C for 10-20 minutes. The cells were then thawed and resuspended in 100μl 1x Ni-NTA Bind buffer. 5KU rLysozyme were added to the cells and incubated at 30°C for 15 minutes. The cells were lysed by vortexing and 2.5U Benzonase nuclease were added and the contents of the tube were mixed. Separation of the insoluble and soluble fractions of the cells took place by centrifugation at 15,000 x g for 10 minutes. The supernatant, soluble part, was transferred to a fresh tube and the pellet was retained. 20μl of the 50% slurry of Ni-NTA His-Bind resin was added to each tube and proteins were mixed with the resin by shaking at 150 rpm 4°C for 30 minutes. The tubes were then centrifuged for 10 seconds at 15,000 x g to pellet the resin. 10μl supernatant was kept on ice and the rest was discarded. The resin was washed twice with 100μl 1x Ni-NTA Wash buffer and centrifuged at 15,000 x g. 10μl of each wash supernatant was kept on ice. The recombinant protein was eluted three times with 20μl of 1x Ni-NTA Elute buffer. At each elution step the sample was centrifuged at 15,000 x g for 10 seconds and the supernatant was removed to a fresh tube.

4.2.3 Large scale protein production

4.2.3.1 IPTG Induction

A fresh colony of transformed BL21(DE3)pLysS competent cells was inoculated in 3ml of LB medium containing 50μg/ml carbenicillin and 34μg/ml chloramphenicol. The culture was

grown at 37°C in an orbital shaker until OD_{600} = 0.5. This culture was used to inoculate 100 ml LB medium with the above antibiotic concentration. The cells were incubated at 30°C shaker until OD_{600} = 0.5 - 1.0. The cells were split in two 50ml cultures and one of them was induced with 0.6mM IPTG and the other culture was the uninduced control. Incubation took place at 30°C shaking at 250rpm for 4 hours.

4.2.3.2 Total cell protein (TCP)

Prior to harvesting cells, 1ml of each culture was transferred to 1.5ml centrifuge tube and spun at 10,000 x g for 1 minute. The supernatant was discarded and the pellet was allowed to dry by inversion. Excess liquid was tapped on a paper towel. The pellet was resuspended in 100μl PBS and 100μl 4x SDS buffer was added and the sample was passed through a 27 gauge needle several times to reduce viscosity. Heating took place for 3 minutes at 85°C to denature the proteins and the total cell protein fraction was stored at -20°C until analysed with SDS-PAGE.

4.2.3.3 Soluble cytoplasmic fraction

The cells from the two 50ml cultures were harvested by centrifugation at 10,000 x g at 4°C for 10 minutes. The supernatant was discarded and the pellet was allowed to drain by inverting the centrifuge tube. The cells were resuspended in 5ml room temperature BugBuster protein extraction reagent (Novagen) by gently pipetting with a Pasteur pipette. 5KU rLysozyme, 125U Benzonase Nuclease and 250μl protease inhibitor coctail set III were added and the lysate was incubated for 20 minutes at room temperature on a roller. The insoluble cell debris was removed by centrifugation at 16,000 x g 4°C for 20 minutes. The supernatant was transferred to a fresh tube and the pellet was kept to extract the insoluble fraction. A sample of the supernatant was used for analysis by mixing with an equal volume of 4x SDS buffer, heating at 85°C for 3 minutes and storing at -20°C. The rest of the cytoplasmic fraction was retained for further purification.

4.2.3.4 Insoluble cytoplasmic fraction

The pellet from the previous step was resuspended in 5ml BugBuster reagent by pipetting repeatedly with a Pasteur pipette. 5KU rLysozyme were added and the sample was mixed by vortexing. It was then incubated for 5 minutes at room temperature. 6 volumes of 1:10 diluted BugBuster (in dH_2O) were added and the mixture was mixed on a vortex for 1 minute. The inclusion bodies were collected with centrifugation at 5,000 x g 4°C for 15 minutes. The supernatant was discarded and the pellet was resuspended in half the original volume of the diluted 1:10 BugBuster, vortexed and centrifuged as before. The

supernatant was removed and this resuspension and step was repeated. This time the insoluble fraction was centrifuged at 16,000 x g 4°C for 15 minutes. The supernatant was discarded and the inclusion bodies present in the pellet were:

i) For SDS-PAGE: resuspended in 1.5ml 1% SDS sample buffer with heating and vigorous mixing. 100µl were removed and combined with 100µl 4x SDS sample buffer, heated at 85°C for 3 minutes and stored at -20°C.

ii) For purification: resuspended in 10ml 1x Binding Buffer with 6M urea. The solution was incubated on ice for 1 hour to dissolve the protein and centrifuged at 16,000 x g 4°C for 30 minutes. The supernatant was passed through a 0.45µ membrane.

4.2.4 Protein purification

The recombinant protein was constructed to carry a His-Tag sequence which enabled the purification with the following methods.

4.2.4.1 His-Bind column chromatography

After removing the His-Bind column cap, the storage buffer and the lower Luer plug were removed. The column was equilibrated with 10ml of 1x Binding buffer. After the Binding buffer was allowed to drain the column was loaded with the cell extract. This was allowed to flow through and the column was washed with 10ml of 1x Binding buffer and then with 10ml of 1x Wash buffer. The protein was eluted with 5ml of 1x Elution or Strip buffer. The eluate may be captured in fractions.

4.2.4.2 Ni-NTA His-Bind batch purification under native conditions

1ml of Ni-NTA His-bind slurry was mixed with 4ml 1x Ni-NTA Bind buffer. The resin was allowed to settle by gravity and the 4ml of supernatant were removed carefully with a pipette. 4ml of lysate was added to the His-Bind slurry and mixed by shaking at 200 rpm at 4°C for 1 hour. The mixture was loaded to a column with the bottom outlet capped. The cap was removed and the flowthrough was collected. The protein was washed twice with 4ml 1x Ni-NTA wash buffer and the fraction was collected. Finally the protein was eluted from the resin with 2ml 1x Ni-NTA elution buffer and the eluate was collected in a clean tube.

4.2.5 Buffer exchange with Vivaspin 20

After being purified from the Ni-NTA resin the recombinant protein was in the Elution buffer, which has a high concentration of imidazole (250mM). The protein must be suspended in an appropriate buffer, which will not alter its conformation and solubility.

For this buffer exchange the Vivaspin 20 concentrator tubes were used. These are tubes which comprise of a removable upper chamber and a lower chamber, separated by a membrane, in this case a 10,000 MWCO PES membrane. The initial solution is applied to the upper chamber and after centrifugation the salts, contaminants and solid particles flow with the buffer to the lower chamber. The macromolecules are collected in an impermeable concentrate pocket integrally moulded below the membrane surface, thereby eliminating the risk of dryness. After a three wash cycle with the desired buffer 99% of the initial salt content is removed. The buffer was exchanged according to the following protocol.

All the steps were carried out in a Laminar Flow Cabinet to ensure sterility of the protein. The upper chamber was filled with sterile dH_2O and centrifuged at 6,000 x g for 4 minutes. The dH_2O was decanted from the lower chamber. The protein sample was placed in the top chamber and centrifuged at 3,000 x g for 5 minutes. The flowthrough was discarded and the chamber was filled with 15ml of the final buffer, centrifuged at 6,000 x g for 10-20 minutes. This step was repeated twice and the purified recombinant protein was recovered from the bottom of the concentrate pocket and stored at the appropriate conditions (See method development).

4.2.5 SDS-Polyacrylamide Gel Electrophoresis (PAGE)

4.2.5.1 Assembly of the gel casting apparatus

The glass plates were cleaned with ethanol and dried with a paper towel to ensure even surface for the new gel. Two glass plates of different height (usually the shorter being non-transparent white) were assembled with the appropriate thickness spacers matching the thickness of the comb, which is determined by the sample volume to be loaded on the gel. The assembly was placed in a cassette, taller glass plate facing out, to hold it together while the gel was poured.

4.2.5.2 Preparation of the gels

The discontinuous system was used, where a non-restrictive large pore gel (stacking) was layered on a separation gel (resolving). Each gel was made with a different buffer and the resolution obtained was much greater than using a single separating gel.

A 10% resolving gel was prepared (see materials) and poured in the set of plates up to 1.5 cm from the top of the shorter plate. The gel was overlaid with ethanol to ensure a flat surface and exclude air bubbles. Setting time was determined from a remaining sample of

gel mixture in a universal tube. The stacking gel was prepared (see Materials), the ethanol was removed and the stacking gel was poured. The comb was inserted to form the sample wells and the gel was allowed to set for 10 minutes.

4.2.5.3 Preparation of the protein sample

Laemmli Sample buffer (Biorad) containing 5% β-mercaptoethanol was used to mix with the protein sample in a 2:1 ratio. The SDS in this buffer denatures proteins by wrapping around the polypeptide backbone and the β-mercaptoethanol reduces disulfide bridges. The sample mixed with the Laemmli buffer was denatured by heat at 95°C for 5 minutes and loaded onto the gel.

4.2.5.4 Assembly of the electrophoresis apparatus

The plates containing the gel were removed from the gel casting cassette and were clamped on the electrophoresis tank. The area behind the gel was filled with Running buffer (1x Tris/glycine/SDS, BioRad) and the assembly was checked for leakage. The electrophoresis tray was half-filled with the same buffer. The comb was removed from the gel and 5μl of the denatured protein samples were loaded onto the wells. The tank was covered and the electrodes were connected to the power pack and run at 35 mA (for two gels) until the sample buffer blue dye runs off the gel.

4.2.5.5 Coomasie blue staining

The gel was removed from the glass plates and placed in a plastic tray where it was stained with Coomassie Brilliant Blue R-250 Stain by shaking for ½ - 2 hours. The gel was de-stained with Coomassie Brilliant Blue R-250 Destain by agitating overnight.

4.2.5.6 Image capture

The gel was photographed with either a digital camera or scanned with an EPSON Expression 1680 Pro series scanner. Captured images were analysed with the image acquisition and analysis software, Labworks.

4.2.6 Western Blotting

The separated proteins after SDS-PAGE can be transferred to a solid membrane for Western Blotting analysis, which is detection of specific proteins by antibody-antigen interaction.

4.2.6.1 Protein transfer

1 nitrocellulose membrane and 5 filter papers (Biorad) per gel were cut at 8.4x6 cm and they were soaked in Transfer Buffer (1x IEF cathode buffer, BioRad) for 5 minutes. The gel was removed from the glass and it was put briefly in Transfer buffer. Three filter papers were placed on the transfer surface of the Biometra electro-transfer machine, the membrane was placed on top of them and then the gel and the remaining two filter papers. The proteins were transferred to the membrane under electric current 120 mA for 30 minutes.

The proteins on the membrane can be visualised by staining with Ponceau S solution for 2 minutes and the stain can be effectively removed by rinsing with water.

4.2.6.2 Blocking

Before the antibody was allowed to interact with the protein, all sites which did not contain blotted protein from the gel were non-specifically blocked with non-fat dry milk (Santa Cruz Biotechnologies). This eliminated the non-specific binding of the antibody.

The membrane was placed in a 50ml centrifuge tube, with that side which came in contact with the gel during the transfer facing the inside of the tube. The membrane was blocked with 10% milk in PBS containing 50mM NaF and 0.05% Tween 20 for 30 minutes on a roller at room temperature.

4.2.6.3 Antibody binding

To detect the antigen blotted on the membrane a primary antibody was added at the appropriate dilution. The dilution was made with PBS 50mM NaF and 0.05% Tween 20 5% milk. 5ml of the primary antibody dilution was incubated with the membrane on a roller for 2 hours. The mouse monoclonal anti - polyhistidine antibody (anti-His-Tag) was used for the detection of the recombinant protein at a 1:2000 dilution. This antibody is prepared by conjugation of horseradish peroxidase and therefore eliminates the need for secondary antibody.

4.2.6.4 Washing

The excess antibody was washed away with PBS 50mM NaF and 0.05% Tween 20. The membrane was washed 5-6 times with 20ml of this buffer and excess buffer was blotted on paper towel by inverting the tube.

4.2.6.5 Chemiluminescence

After washing, Western Blotting Luminol Reagent (Santa Cruz Biotechnology) was used for chemiluminescent detection of the peroxidase conjugate on the anti-His-Tag antibody, which was bound on the recombinant protein. An equal volume of Reagent A and B was mixed and incubated with the membrane for 1 minute.

4.2.6.6 X-ray film exposure and development

The membrane was covered with cling film, ensuring that there are no trapped air bubbles and was secured with tape on one side of the exposure cassette. X-ray film was inserted in the cassette and exposed to the light given off by the chemiluminescent membrane for 30 minutes.

The X-ray film was then removed from the cassette and incubated with Kodak Developer and Repleniser (Sigma) according to the intensity of the forming bands, washed in water and fixed with Kodak Fixer and Replenisher (Sigma) for 5 minutes.

4.3 METHOD DEVELOPMENT AND RESULTS

4.3.1 Cloning

Initially the vector pET-23c was chosen for cloning with the wild type and mutant βig-h3 cDNA. This is a 3.7 kb plasmid which carries the T7 promoter. It adds a 6-His-tag repeat downstream of the insert DNA. The recipient plasmid and DNA insert were ligated following XhoI and HindIII restriction digestion.

4.3.1.1 Preparation of insert DNA

The following primers were designed for the amplification of mutant and wild type βig-h3 to insert these restriction sites at the termini.

HindIII

Forward primer: 5' GTCCAAGCTTCATGGCGCTCTTCGTG 3'

Reverse primer: 5' CTTCCTCGAGATGCTTCATCCTCTC 3'

XhoI

The glycerol stocks of clones pALTER-MAX βig-h3, pALTER-MAX R555Q1 and pALTER-MAX R555W31 were subcultured on LB agar plates containing 20μg/ml chloramphenicol.

Plasmids were extracted according to the method in section 2.2.9.6. PCR amplification took place with the above primers using the Extensor Long PCR kit, as described in section 2.6. The annealing temperature was increased to 60°C to reduce background, which appeared with the use of a different thermal cycler (Figure 4.1).

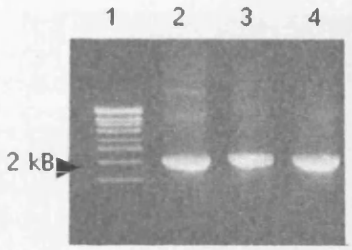

Figure 4.1: PCR amplification at 60°C annealing

Lane 1 - Molecular weight marker. Lane 2 - Wild type βig-h3. Lane 3 - R555Q mutant βig-h3. Lane 4 - R555W mutant βig-h3

The PCR products were purified with the Qiagen PCR purification kit and subjected to dual restriction digestion at the newly incorporated HindIII and XhoI sites (see section 2.2.8.5).

4.3.1.2 Preparation pf pET vector

1μg of plasmid pET-23c was used to transform JM109 competent cells and a glycerol stock was made. A culture was set up and a plasmid preparation was extracted with the QIAGEN plasmid mini purification kit (2.2.9.6).

The extracted pET-23c was digested with HindIII and XhoI and subsequently cleaned with the PCR purification kit.

4.3.1.3 Ligation

The two DNA fragments were ligated at a 1:1 ratio at room temperature for 2 hours and were subsequently used to transform JM109 competent cells. The transformed cells were incubated on LB agar plates containing 50μg/ml ampicillin. 6 colonies were selected from each plate and these were cultured overnight and the corresponding plasmids were extracted.

4.3.1.4 Characterisation of the clones

The extracted plasmids were subjected to restriction digestion with XhoI and HindIII to confirm the presence of the insert, βig-h3 cDNA, 2.1kb (Figure 4.2).

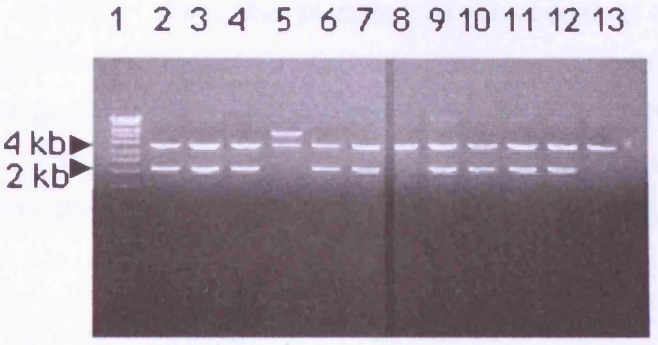

Figure 4.2: Endonuclease restriction digestion

Lane 1 - Molecular weight marker. Lane 2 - Wild type clone 1. Lane 3 - Wild type clone 2. Lane 4 - Wild type clone 3. Lane 5 - Wild type clone 4. Lane 6 - Wild type clone 5. Lane 7 - Wild type clone 6. Lane 8 - R555Q clone 1. Lane 9 - R555Q clone 2. Lane 10 - R555Q clone 3. Lane 11 - R555Q clone 4. Lane 12 - R555Q clone 5. Lane 13- R555Q clone 6.

From Figure 4.2, the clones that appear to have the correct restriction pattern were: Wild type clones 1, 2, 3, 5 and 6 and R555Q mutant clones 2, 3, 4 and 5.

These clones were sequenced in the upstream region with the T7 promoter primer (Novagen) to confirm correct incorporation into the plasmid genome. The sequences were amplified with the BigDye Terminator Mix and and sequenced in a 377 DNA sequencer according to the method in section 2.11.6.

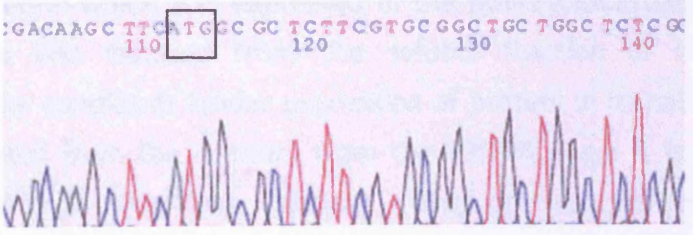

Figure 4.3: DNA sequencing with T7 promoter. The start codon ATG is present and the integrity of the following βig-h3 sequence was confirmed

4.3.1.5 Protein expression and analysis

One of each clone with pET-23c vector carrying the wild type, R555Q and R555W mutant βig-h3 cDNA was used to transform 20μl of competent BL21(DE3) cells. The cells were plated on LB agar containing 50μg/ml ampicillin and 34μg/ml chloramphenicol and incubated overnight at 37°C. Then the protein was expressed as described in section 4.2.3, but only the soluble fraction of the culture was extracted to determine expression of native recombinant protein. This fraction was purified using the His-Bind Columns and Buffer kit (Novagen). The eluted proteins were separated with SDS-PAGE and they were allowed to interact with the anti-His-tag antibody during western blot analysis (Figure 4.4).

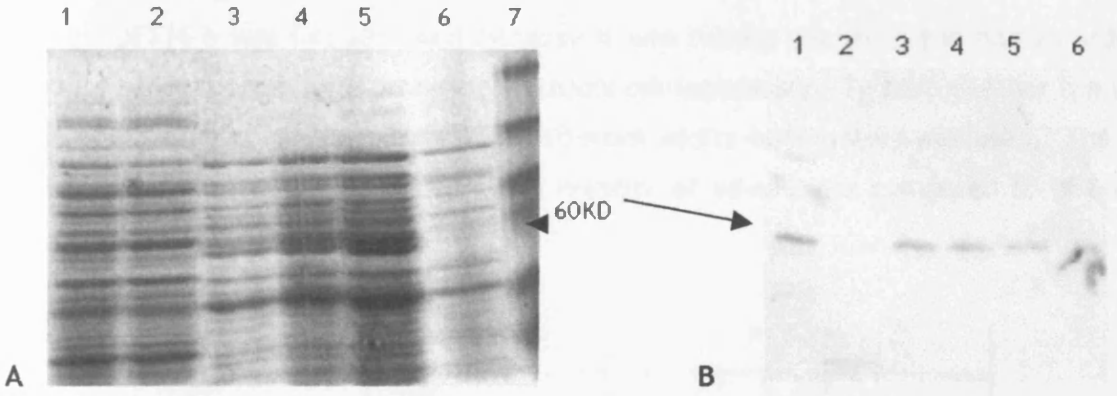

Figure 4.4: **Protein expression and purification. A.** SDS PAGE and **B.** Western Blotting. Lane 1 - Supernatant, soluble extract. Lane 2 - Flowthrough. Lane 3 - Eluate fraction 1. Lane 4 - Eluate fraction 2. Lane 5 - Eluate fraction 3. Lane 6 - Eluate fraction 4. Lane 7 - Protein ladder

4.3.1.6 Results

The recombinant protein which was expressed in the pET-23c-BL21(DE3)pLysS vector-host combination system was isolated from the soluble fraction of the culture. This demonstrates that the conditions favour expression of protein in its native form. Although this protein was eluted from the column, from the SDS-PAGE gel it is evident that other proteins were present in this final fraction. Only one species from these proteins interacted with the anti His-Tag antibody and therefore contained the His-tag repeat sequence.

It is unknown what the other proteins could be. The possibility of these proteins being the products of proteolytic degradation is small, because in this case, at least some of them would react with the anti His-Tag antibody. Moreover protease inhibitors were used during

the extraction of the protein from the culture. The basis of purification was the affinity of the His-Tag sequence on the recombinant proteins with the column. However none of these proteins interact with the anti-His tag antibody, which suggests that they react non-specifically with the column or that they are proteins associated and co-purified with the recombinant protein.

It was attempted to wash protein bound to the column under more strigent conditions and the imidazole concentration was increased from 60mM to 100mM, but this did not eliminate the presence of the multiple bands in the eluted fractions.

4.3.2 Cloning

Plasmid pET16-b was initially used because it was readily available and had already been used for other recombinant protein constructs our laboratory. To test whether the protein yield and quality could be improved, a different vector-host system was used. The vector pET-16b was chosen because it offers a number of advantages compared to pET-23c, as shown on the following table.

pET-23c	PET-16b
3.7Kb	5.7Kb
T7 promoter	T7*lac* promoter
COOH-terminal His-Tag	NH_2-terminal His-Tag
6-repeat His	10-repeat His
No protease cleavage	Factor Xa
Transcription vector	Translation vector

Table 4.1: Comparison between the two prokaryotic expression vectors

The expression vector incorporates the His-Tag sequence at the N-terminal end of the recombinant which is thought to be less critical in terms of function and folding than the C-terminus. This vector also carries the protease cleavage site, Factor Xa sequence, where the added his-Tag repeat can be removed after protein purification. PET-16b is a translation vector and thus contains a highly efficient ribosome binding site for the expression of target genes without prokaryotic ribosomal binding site.

4.3.2.1 Preparation of insert DNA

The following primers were designed for the amplification of mutant and wild type βig-h3 to insert a single restriction site, XhoI, at either termini.

XhoI

Forward primer: 5' TTACTCGAGCTGGGCCCCGCCGCGACCCTG 3'

Reverse primer: 5' ATTCTCGAGCTAATGCTTCATCCTCTCTAA 3'

XhoI

These primers amplify the βig-h3 cDNA from nucleotide 93 to 2096 and remove the 23 amino acid long NH_2-terminal secretory sequence. The resulting protein can therefore be extracted from the harvested cells and minimise the export to the cytoplasm.

PCR amplification took place with the above primers using the Extensor Long PCR kit, as described in section 2.6. A variety of annealing temperatures were attempted ranging form 60°C to 75°C to reduce the background smear, which suggests non-specific DNA amplification (Figure 4.5). Also the cycling conditions were changed; the number of cycles was reduced from 33 to 30 and the extension time from 5 to 3 minutes (Figure 4.5, Lanes 7-21).

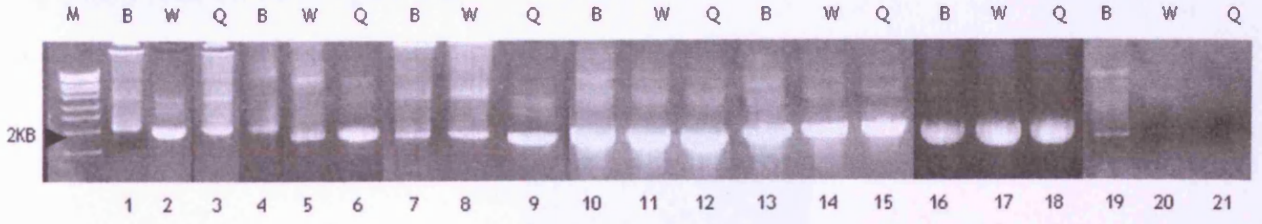

Figure 4.5: Effect of increased annealing temperatures on PCR product

M - Molecular weight marker. B - Wild type βig-h3 cDNA. W - R555W mutant βig-h3 cDNA. Q - R555Q mutant cDNA. Lanes 1 - 3: 60°C. Lanes 4 - 6: 63°C. Lanes 7 - 9: 60.6°C. Lanes 10 - 12: 62°C. Lanes 13 - 15: 66°C. Lanes 16 - 18: 70°C. Lanes 19 - 21: 75°C.

From the above figure the temperature which seems to result in optimum PCR products is 70°C. The fragments which were amplified at this temperature were used for cloning with

the expression vector. Therefore they were digested with XhoI and cleaned with the PCR purification kit.

4.3.2.2 Preparation pf pET vector

100ng of pET-16b (Novagen) were digested with XhoI and the vector was subjected dephosphorylation with CIAP (see section 2.2.8.6), in order to eliminate the possibility of self ligation and selection for clones which lack the insert βig-h3 cDNA. The enzymes and different buffers were removed from the dephosphorylated plasmid with the QIAGEN PCR purification kit.

4.3.2.3 Ligation

Insert and vector were ligated at a 3:1 molar ratio at room temperature for 2 hours and were subsequently used to transform JM109 competent cells. The transformed cells were incubated overnight at 37°C on LB agar plates containing 50μg/ml ampicillin. The number of the resulting colonies was low, especially the plate corresponding to clones with wild type βig-h3 had only one colony. The available colonies were cultured and the recombinant plasmids were extracted.

4.3.2.4 Characterisation of the clones

The extracted plasmids were subjected restriction digestion with XhoI to confirm presence of the insert DNA and dual digestion with XhoI and BamHI to check the orientation of the insert. BamHI cuts the βig-h3 sequence 340bp downstream the XhoI ligaton site and the double digestion with XhoI and BamHI should result in 3 fragments of 5.7Kb (vector), 1.7Kb and 340bp (insert), as in figure 4.6.

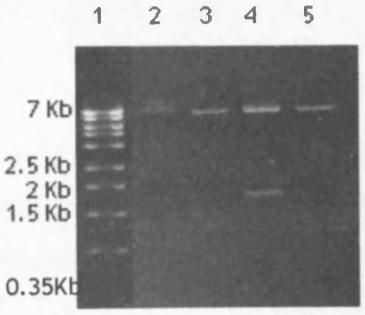

Figure 4.6: Restriction digestion of cloned DNA

Lane 1 - Molecular Weight marker. Lane 2 - Wild type cDNA cloned to pET-16b. Lanes 3 and 5 - mutant cloned cDNA. Lane 4 - Mutant cloned cDNA with the correct restriction pattern. Note: the lower 340bp band was present in the gel, but cannot be visualised on the captured picture.

From the above gels it can be deduced that although the ligation of pET-16b with the mutant βig-h3 cDNAs was successful, no positive clones were produced with the wild type insert. The ligation between the wild type βig-h3 and pET-16b was repeated with varying the insert : molar ratios and extending the incubation time to 4½ hours. None of these changes resulted in any colonies when the transformed cells were cultured on agar plates. It is possible that something in the DNA preparation of βig-h3 could hinder the ligation reaction. Therefore fresh preparations of both insert and vector were made.

A variety of high fidelity PCR systems were used for the amplification of wild type βig-h3 cDNA under a gradient of temperatures (50-65): Gene amp XL PCR Kit (Perkin Elmer), Long Extensor PCR buffers and Pfx polymerase (Invitrogen), Platinum Pfx DNA polymerase kit (Invitrogen). The first two systems failed to produce any bands, whereas the Platinum Pfx kit gave rise to many non-specific bands, even at high temperatures.

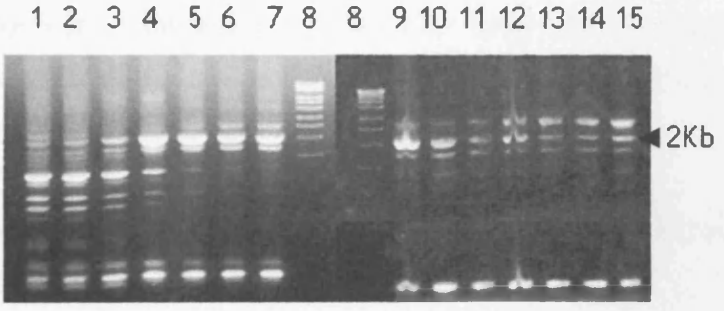

Figure 4.7: Gradient amplification with Platinum Pfx DNA polymerase

Each lane represents annealing at a different temperature. Lane 1 - 50°C. Lane 2 - 51°C. Lane 3 - 54°C. Lane 4 - 59°C. Lane 5 - 62°C. Lane 6 - 64°C. Lane 7 - 65°C. Lane 8 - Molecular Weight Marker. Lane 9 - 65°C. Lane 10 - 66°C. Lane 11 - 68°C. Lane 12 - 71°C. Lane 13 - 73°C. Lane 14 - 74°C. Lane 15 - 75°C.

The Platinum Pfx PCR system was further optimised with the addition of 0.5x Enhancer solution, which enables primers to anneal to problematic DNA sequences. The addition of this reagent reduced the multiple bands and resulted in the amplification of a single fragment of 2Kb at 65°C.

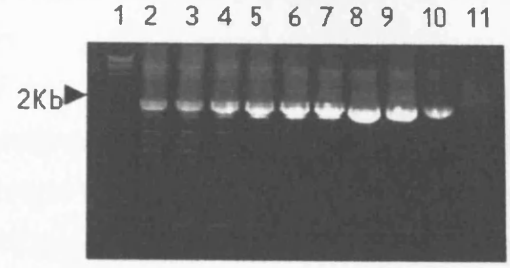

Figure 4.8: Optimised Platinum Pfx amplification of βig-h3

Each lane represents annealing at a different temperature. Lane 1 - Molecular Weight Marker. Lane 2 - 50°C. Lane 3 - 51°C. Lane 4 - 54°C. Lane 5 - 57°C. Lane 6 - 59°C. Lane 7 - 61°C. Lane 8 - 63°C. Lane 9 - 64°C. Lane 10 - 65°C. Lane 11 - negative control (no DNA)

Therefore wild type βig-h3 was amplified at 65°C with the forward and reverse primers which employ the XhoI restriction sites at both termini. After being digested and purified as described previously (sections 4.3.2.1 - 4.3.2.2), the pET-16b vector and insert DNA were ligated at 1:1, 3:1 and 3:1 molar ratios respectively at 4°C overnight. Each ligation was used to transform 50μl competent JM109 cells. After overnight incubation on LB agar plates it was observed that the majority of the colonies corresponded to the 3:1 insert:vector molar ratio.

8 colonies were randomly selected for plasmid extraction and characterisation of the DNA with restriction digestion.

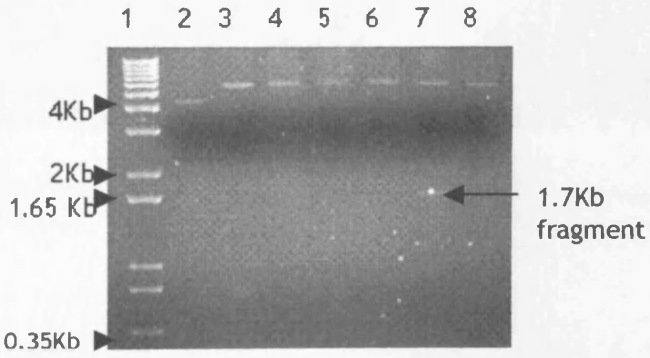

Figure 4.9: XhoI and BamHI restriction digestion of pET-16b-βig-h3 clones

Lane 1 - Molecular Weight Marker. Lane 2 - Clone 1. Lane 3 - Clone 2. Lane 4 - Clone 3. Lane 5 - Clone 4. Lane 6 - Clone 5. Lane 7 - Clone 6. Note: the lower 340bp band was present in the gel, but cannot be visualised on the captured picture. Lane 8 - Clone 7.

The above gel (Figure 4.9) shows that clone 6 (lane 7) has the correct restriction pattern, result of successful ligation.

The positive clones were sequenced in the upstream region with the T7 promoter primer (Novagen) to confirm correct incorporation into the plasmid genome and with βig-h3 primer Seq 3 (see table 2.1) to check the sequence at the mutagenic codon 555.

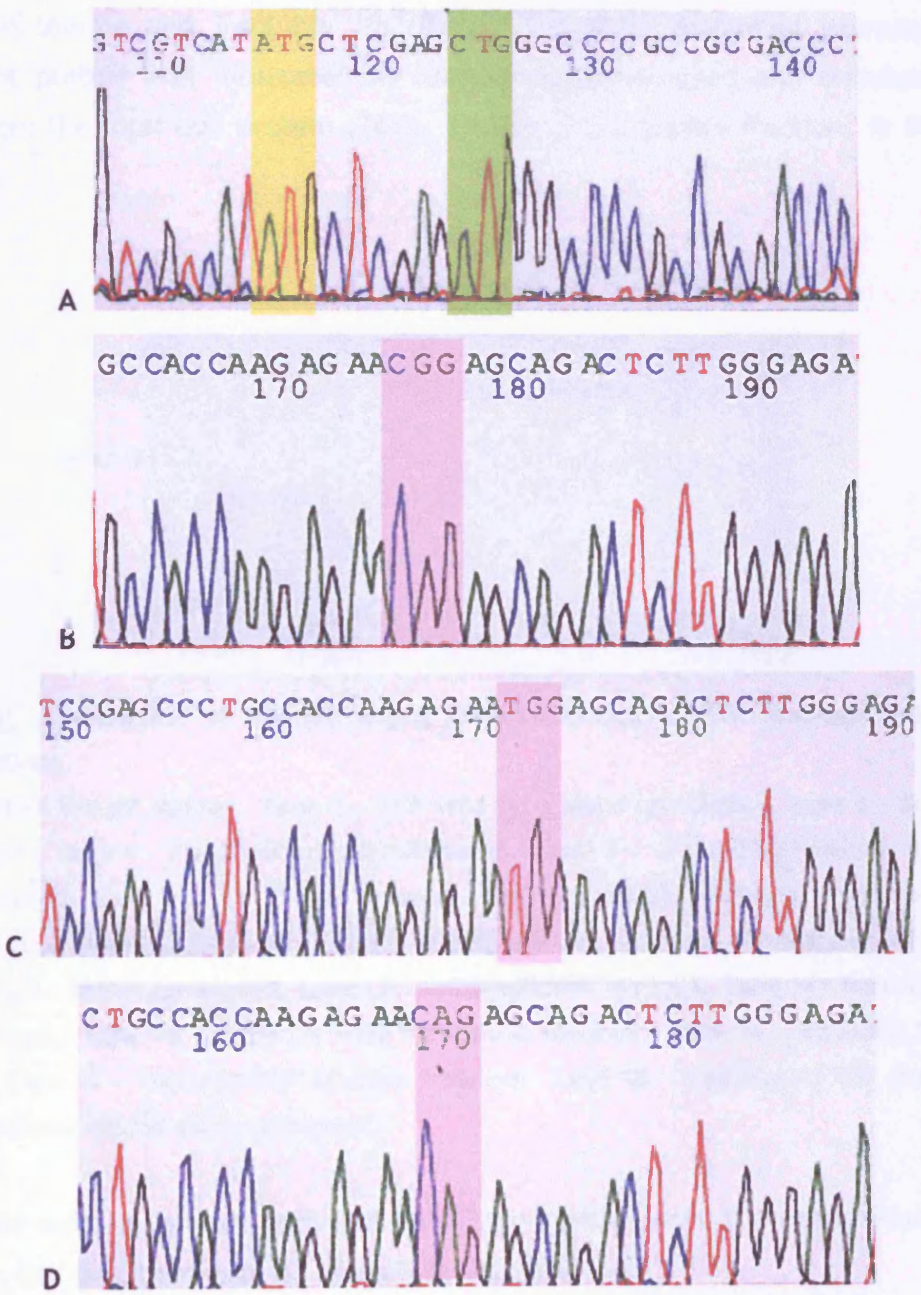

Figure 4.10: DNA sequencing with T7 and βig-h3 Seq3 primers

A. Sequencing with T7 primer. Note the ATG codon (yellow band) provided by the plasmid is in frame with the first codon of βig-h3 DNA, CTG (green band). R555 codons are highlighted by the pink bands B. Wild type 555 codon (CGG). C. R555W mutant codon (TGG). D. R555Q mutant codon (CAG)

4.3.2.5 Protein expression and analysis

One of each clone of pET-16b vector carrying the wild type, R555Q and R555W mutant βig-h3 cDNA was used to transform BL21(DE3) cells and recombinant protein was induced as described in section 4.2.3. The soluble and insoluble fractions were extracted and the soluble part was purified with the His-Bind pre-charged columns and buffer kit. Western blotting with the His-Tag antibody demonstrated that the recombinant protein was present in both the soluble and insoluble fractions. The IPTG controlled expression of the recombinant protein was illustrated by comparing the induced and uninduced culture extracts from the total cell protein (TCP), soluble and insoluble fractions in the Western Blot below.

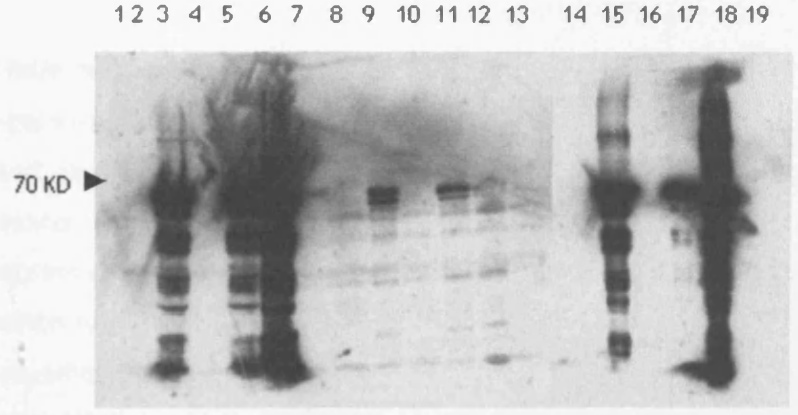

Figure 4.11: Comparison of the extracted proteins between IPTG induced and uninduced culture fractions

Lane 1 - Protein Weight Marker. Lane 2 - TCP wild type clone uninduced. Lane 3 - TCP wild type clone induced . Lane 4 - TCP R555Q clone uninduced. Lane 5 - TCP R555Q induced. Lane 6 - TCP R555W uninduced. Lane 7 - TCP R555W induced. Lane 8 - Soluble wild type uninduced. Lane 9 - Soluble wild type induced. Lane 10 - Soluble R555Q uninduced. Lane 11 - Soluble R555Q induced. Lane 12 - Soluble R555W uninduced. Lane 13 - Soluble R555W induced. Lane 14 - Insoluble wild type clone uninduced. Lane 15 - Insoluble wild type clone induced. Lane 16 - Insoluble R555Q clone uninduced. Lane 17 - Insoluble R555Q clone induced. Lane 18 - Insoluble R555W clone induced. Lane 19 - Insoluble R555W clone uninduced.

The proteins were separated with SDS-PAGE and stained with Coomassie Blue, where it became obvious that there was no protein in the eluate.

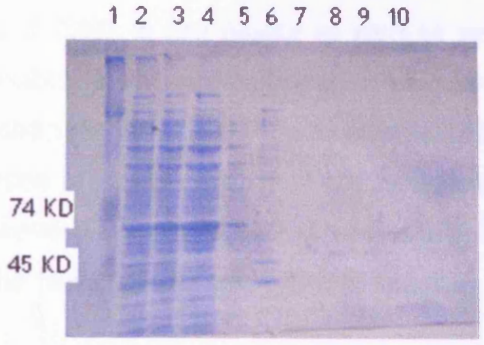

Figure 4.12: SDS-PAGE of purified recombinant protein

Lane 1 - Protein Weight Marker. Lane 2 - Soluble extract. Lane 3 - Soluble extract filtered with 0.45μ filter. Lane 4 - Flowthrough. Lane 5 - Wash 1. Lane 6 - Wash 2. Lane 7 - Eluate 1. Lane 8 - Eluate 2. Lane 9 - Eluate 3. Lane 10 - Eluate 4.

4.3.3 Protein mini prep with Ni-NTA His-Bind resin

Since the pre-packed columns failed to recover the recombinant protein, a different method was used for the purification of His-tagged protein. The Ni-NTA His bind resin, which allows extraction and purification from small samples of culture and therefore simplifies the optimisation of the recombinant protein production. The protocol for mini protein preparation was carried out (see section 4.2.2) and the Ni-NTA His-Bind resin was used to purify recombinant protein from both the soluble and the insoluble fraction (under non-denaturing conditions) (figure 4.13).

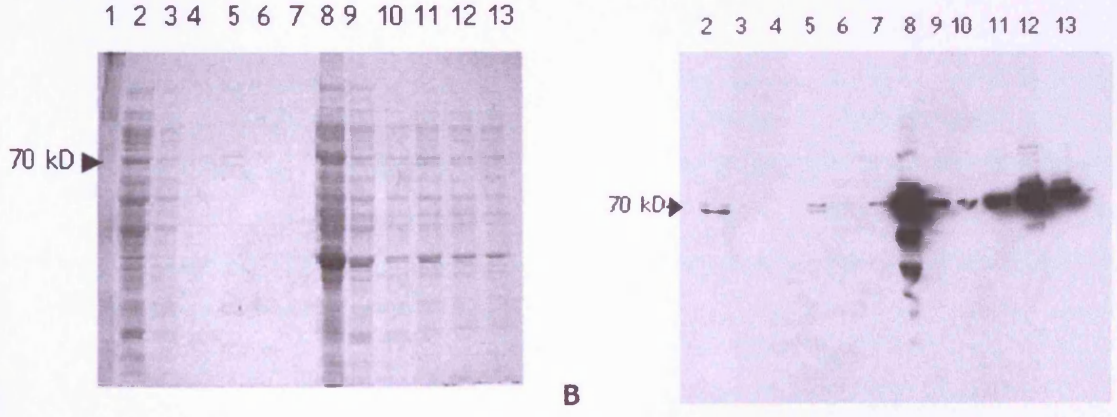

Figure 4.13: Proteins extracted with Ni-NTA His-Bind resin mini prep

A. SDS-PAGE and B. Western Blot. Lane 1 - Protein marker. Lane 2 - Soluble Flowthrough. Lane 3 - Soluble Wash 1. Lane 4 - Soluble Wash 2. Lane 5 - Soluble Eluate 1. Lane 6 - Soluble Eluate 2. Lane 7 - Soluble Eluate 3. Lane 8 - Insoluble Flowthrough. Lane 9 - Insoluble Wash 1. Lane 10 - Insoluble Wash 2. Lane 11 - Insoluble Eluate 1. Lane 12 - Insoluble Eluate 2. Lane 13 - Insoluble Eluate 3.

SDS-PAGE and Coomasie Blue staining of the protein samples demonstrated that there is a double protein species around 70KD in the eluate as well as some lower molecular weight bands (Figure 4.13). A double keratoepithelin species has been reported previously (Skonier et al, 1994 and Hashimoto et al, 1997) and corresponds to 66 and 69kD. Western Blotting of the electrophoresed proteins confirmed the isolation of recombinant His-Tagged protein in the eluate. However, some of the native protein failed to stay bound to the resin and was detected in the flowthrough and wash samples.

Apart from the soluble fraction, considerable amounts of the protein were present in the insoluble fraction of the cell culture. Since the protein in the soluble fraction was enough for extraction and *in vitro* experimental use, the insoluble fraction was not harvested in the following Maxi preparations.

4.3.4 Large Scale recombinant protein production

The three recombinant proteins were expressed according to the protocol described in section 4.2.3 and purified with the Ni-NTA His-Bind resin (see 4.2.4). SDS-PAGE and Western blotting demonstrated the efficiency of recombinant protein purification in figure 4.14.

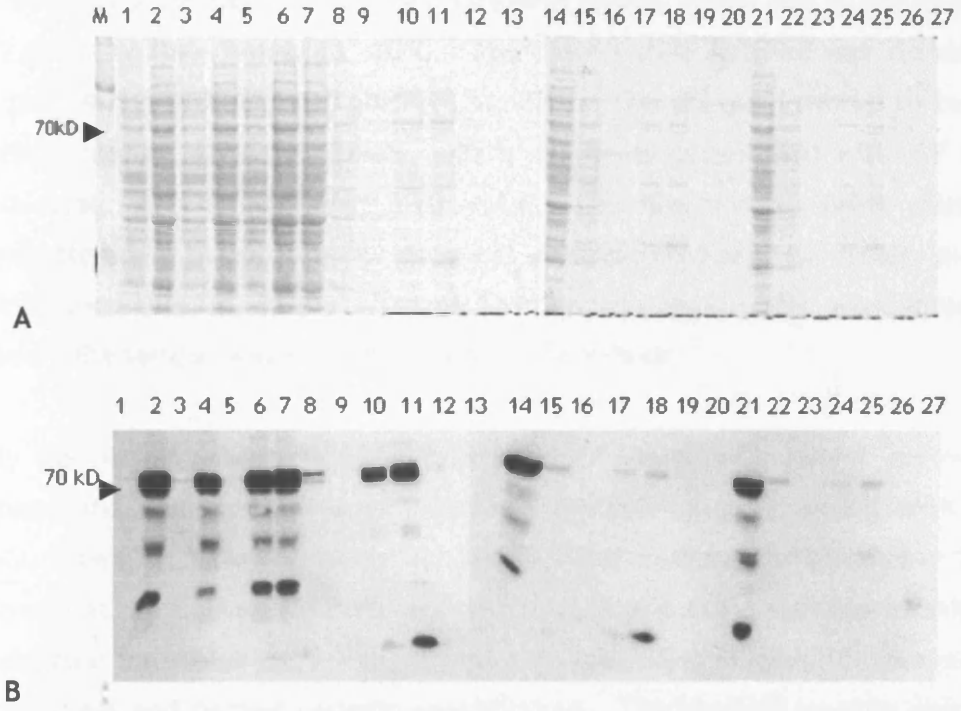

Figure 4.14:Large scale recombinant protein purification

A. SDS-PAGE, B. Western Blot. Lane 1 - Lysate Wild type uninduced. Lane 2 - Lysate Wild type induced. Lane 3 - Lysate R555W uninduced. Lane 4 - Lysate R555W induced. Lane 5 - Lysate R555Q uninduced. Lane 6 - Lysate R555Q induced. Lane 7 - Wild type flowthrough. Lane 8 - Wild type wash 1. Lane 9 - Wild type wash2. Lane 10 - Wild type eluate 1. Lane 11 - Wild type eluate 2. Lane 12 - Wild type eluate 3. Lane 13 - Wild type eluate 4. Lane 14 - R555W flowthrough. Lane 15 - R555W wash 1. Lane 16 - R555W wash 2. Lane 17 - R555W eluate 1. Lane 18 - R555W eluate 2. Lane 19 - R555W eluate 3. Lane 20 - R555W eluate 4. Lane 21 - R555Q flowthrough. Lane 22 - R555Q wash 1. Lane 23 - R555Q wash 2. Lane 24 - R555Q eluate 1. Lane 25 - R555Q eluate 2. Lane 26 - R555Q eluate 3. Lane 27 - R555Q eluate 4.

4.3.5 Optimisation of recombinant protein processing after purification

After the protein was eluted from the Ni-NTA His-Bind column, it was essential to change the buffer to avoid protein precipitation and potential loss of function. It was empirically determined that the purified protein should be processed straight after coming off the

column. Storage of the eluate at -20°C and subsequent thawing resulted in precipitation of the protein.

The buffer was changed using the Vivaspin 20 concentrators (see section 4.2.5). The buffer originally used for the resuspension of the recombinant proteins was chosen from previous references of recombinant keratoepithelin preparation. Kim et al, reported in 2000 the isolation of keratoepithelin from inclusion bodies, which was stored in 20mM Tris-HCl, pH 7.8, 50mM NaCl buffer at -20°C. Therefore native purified was stored in 10mM Tris-HCl, pH 7.4, 50mM NaCl, 10% glycerol at -20°C. The pH was lowered to be closer to the protein's natural isoelectric point, which has been determined with IEF to be 6.0 (Srivastava et al, 1999) and between 6.20 and 6.71 (Escribano et al, 1994). Although this protein was stored in 0.5ml aliquots to avoid multiple freeze-thaw cycles, precipitates were visible upon thawing of the aliquots for the first time. The precipitates did not dissolve when the sample was incubated at 37°C for ½ hour.

Eventually the buffer which enabled the storage of these recombinant proteins in low temperatures and eliminated precipitation was the following: 10mM Tris-HCl pH 7.4, 50mM NaCl, 1mM DTT, 50% (v/v) glycerol. The high concentration of glycerol in this buffer allows storage at -80°C where the protein can remain stable and reduces freezing extend and freeze-thaw intervals. DTT can reduce the formation of disulfide bonds between protein molecules and further prevent precipitation. The purified protein concentration after buffer exchange was determined with the BCA assay to be 0.6-0.7 mg/ml.

4.4 DISCUSSION

Although not initially straightforward, the recombinant keratoepithelin was successfully produced from the prokaryotic *E. coli* strain BL21(DE3)pLysS. The prokaryotic expression system was used because of the ease and efficiency it brings to the process of constructing a recombinant protein. The difference in codon usage was compensated with the presence of pLysS plasmid, which encodes rare prokaryotic aminoacids.

Cloning of the protein coding sequence to expression vector pET-16b resulted in better yield of recombinant protein and in fewer multiple bands in the final eluted protein. The 10-His repeat which was added at the NH_2-terminal end of the recombinant protein to aid detection and purification can be removed with proteolytic digestion with Factor Xa.

The presence of T7*lac* promoter on pET-16b in combination with the *lac*UV5 promoter in BL21(DE3)pLysS ensure a tight regulation of recombinant protein expression. This was demonstrated during electrophoresis of the proteins extracted form induced cultures, compared to those derived from cultures grown in the absence of IPTG.

Recombinant keratoepithelin was present in the cell culture both in the insoluble and soluble form after IPTG induction. The levels of the protein in the soluble fraction were sufficient to carry out extraction and purification. Therefore denaturing and refolding of insoluble protein was avoided.

Despite the amino acid (555) difference between the three recombinant proteins the pattern during protein expression, extraction and purification was the same in all variants. It has already been reported that mutations found in the 5q31 corneal dystrophies do not significantly affect the molecular properties of keratoepithelin (Kim et al, 2002).

The potential native recombinant keratoepithelin brings into the study of corneal dystrophies is can be immense. It can be a useful tool for carrying out a number of biological assays on cultured cells and comparing between the effects of the wild type and mutant proteins. It can serve for a variety of biochemical analyses, such as solution scattering, which can provide information about the three dimensional shape the protein assumes in solution, and BIACORE, which can demonstrate the way it interacts with other proteins.

5. CHAPTER FIVE

Effects of recombinant keratoepithelin on cell behaviour

5.1 INTRODUCTION

Cell culture offers possibilities to screen for effects of compounds and macromolecules in a controlled way and under a wide variety of conditions. Culture systems have been developed to allow the study of single cellular functions under controlled environmental conditions. In vitro systems exclude the influence of other organs and the circulatory and immune system, thus providing the possibility to study direct effects on a cell population. However the absence of these organ-related influences prevent the cell culture model from being an identical reflection of the in vivo cells. In this chapter corneal cell culture systems were used in combination with the recombinant keratoepithelin proteins to enhance our understanding of the cellular effects of these proteins.

Various transformed immortalised corneal keratocytes (Stuart et al, 1997, Zorn-Kruppa et al, 2004) and epithelial cells (Chiambaretta et al, 2002, Gao et al, 2002) have been described by different researchers. However, the transformation, which confers the cells with the proliferative capacity, may lead to changes in the genetic expression profile and therefore behaviour of these cells. For the purpose of minimising the genotypic and phenotypic alterations of the corneal cells primary cell cultures were preferentially used.

Recombinant keratoepithelin has been employed in cell culture experiments previously, but the effects seem to vary and depend on the cell type used. Its anti-adhesion effect on A459, HeLa and W1-38 cells (Skonier et al, 1994) seems to contradict the cell-adhesive effect it exerts on human astrocytoma cells (Kim et al, 2003) and HUVEC (Nam et al, 2003). This differential effect has been attributed to the ability of this protein to interact with different integrins on the surface of different cells to mediate the same effect. For example, migration is mediated through $\alpha_v\beta_3$ integrin in human umbilical cord endothelial cells (Nam et al, 2003), whereas in skin keratinocytes through $\alpha_3\beta_1$ interacting motifs (Bae et al, 2002).

Keratoepithelin seems to be derived from the corneal epithelium (Escribano et al, 1994, Akhtar et al, 1999, Ridgway et al, 2000), therefore epithelial cells are of particular interest. The accumulations of granular and amyloid deposits in anterior dystrophies have been localised in the epithelium (Akhtar et al, 1999), Bowman's layer (Ridgway at al,

2000), extracellular stoma (Klintworth et al, 1998) and intracellular in keratocytes (Akhtar et al, 1999). The corneal keratocytes are not only affected in corneal dystrophies but may also contribute to the deposition of stromal keratoepithelin.

The effects of wild type and mutant keratoepithelin were studied in cultured primary corneal epithelial cells and keratocytes. Four different areas were examined: migration, adhesion, proliferation and apoptosis. The results of these assays may indicate the way this protein interacts with the corneal cells to maintain tissue integrity in normal corneas and abolish it in the case of dystrophies.

5.2 METHODS

5.2.1 Coating of culture dishes with collagen Type I

Flasks and multiwell plates that were going to be used for culturing corneal epithelial cells were previously coated with collagen Type I. 10μg of collagen were used per cm^2 of culture area. 0.1% calf skin collagen Type I (Sigma) was diluted 1:10 with 0.1M acetic acid and was incubated with the culture flask for 2-5 hours at 37°C. The collagen solution was then aspirated and the dishes were air dried in a laminar flow safety cabinet. Coated surfaces were rinsed twice with PBS before using for cell culture.

5.2.2 Primary Cell Culture

Human corneal epithelial cells and keratocytes were isolated form human corneas but the large number of cells needed for the assays could not be generated from the rarely available human corneas. Primary epithelial cells and keratocytes were predominantly isolated from bovine corneas, although the same methods were used to process both human and bovine corneas.

Freshly enucleated bovine eyes were obtained from a local abattoir and transported to the laboratory on ice. Extraneous muscle and other tissue were dissociated from the globe and the eyes were submerged in 2% v/v Betadine solution in PBS for 2 minutes and rinsed briefly in sterile PBS.

5.2.2.1 Epithelial cells

A primary corneal epithelial cell culture involves the removal of the epithelial sheet from the anterior corneal surface and its attachment on the bottom of a culture dish. To do this corneal trephine sections were removed (using a 1mm diameter sterile trephine) from the corneo-limbal area and were placed on the surface of a well of a 6-well plate, epithelial side facing the bottom of the dish. The surface of the well had previously been scraped with a sterile blade to ensure firmer attachment of the explant and prevent it from floating after application of the culture medium. Approximately 5 explants were placed per well of a 6-well plate and they were incubated at 37°C for 20 minutes to dry the excess liquid and allow them to attach to the dish. One drop of Keratinocyte serum-free supplemented medium (Invitrogen) (see Materials) was applied on each explant and incubation was carried out overnight at 37°C in a 5% CO_2 humidified incubator. The next day 1ml prewarmed Keratinocyte Serum-free medium was added to each well and incubation was continued until the epithelial cells were observed to migrate out of the explant on to the culture surface, usually 1-2 weeks. The explant was then removed and

the medium was replaced with fresh and primary cells were incubated until confluent. The same explant was placed on to a new well for culturing cells from the deeper layers of the epithelium, where less differentiated epithelial cells, closer to the limbal area, are normally residing.

Cell cultures that reached confluence were aspirated, washed once with PBS and were detached with fresh prewarmed 0.05% trypsin & 0.53mM EDTA (Invitrogen) by incubating at 37°C for no more than 5 minutes. The trypsin was neutralised with the addition of PBS containing 10% FCS and cells were centrifuged at 300 x g for 5 minutes. The pellet was resuspended in fresh Keratinocyte serum-free supplemented medium and cells were dispensed onto collagen I coated flasks. Medium was renewed every 3 days and cells were subcultured before reaching confluence with this method in a 1:3 ratio.

5.2.2.2 Keratocytes

For the extraction of keratocytes from the intact cornea the epithelium was scraped off using a sterile scarpel. The cornea near the limbal area was removed from the rest of the eye by cutting approximately 1mm inside the limbal margin. 5 corneas were placed in a sterile 50ml pot and were incubated with 10ml of 4mg/ml collagenase in Minimal Essential Medium (MEM) at 37°C overnight. The cell suspensions were centrifuged at 100g for 5 minutes and the pellet was resuspended in 1ml MEM. The number of cells was calculated using a haematocytometer and cells were seeded in 25cm^2 culture flasks at 7x10^5 cells/flask in 10ml DMEM/F10 medium (see Materials).

Cell cultures were allowed to grow at 37°C in a 5% CO_2 humidified incubator. When confluency was reached the medium was aspirated and the cells were rinsed in PBS. 0.05% trypsin & 0.53mM EDTA was used to dissociate the cells form the culture surface by incubating at 37°C for approximately 5 minutes. The cells were then resuspended in fresh DMEM/F10 medium and were subcultured in a 1:3 ratio.

5.2.3 Confirmation of culture purity

Cell cultures were observed for their morphologic characteristics and immunostained for confirmation of purity. Cultures were fixed with 4% paraformaldehyde for 20 minutes and washed twice with PBS for 5 minutes. They were then incubated with 0.2% Triton X-100 (v/v in PBS) for 20 minutes at room temperature and washed twice with PBS. Cells were immunohistochemically stained with cytokeratin, which is an epithelial cell marker. Epithelial cells should stain positive for cytokeratin whereas keratocytes should stain

negative. The cytokeratin polyclonal mouse primary antibody (Sigma) and the goat anti-mouse FITC conjugated IgG (Sigma) secondary were used at 1/150 dilution.

5.2.4 Adhesion Assay

(Modified from Vaughan-Thomas et al, 2001)

Multiwell plates were coated with recombinant proteins diluted in PBS at 37°C for 2 hours. The plates were rinsed twice with PBS and uncoated surfaces were blocked with PBS containing 2% heat-inactivated BSA for 1 hour at 37°C. The plates were rinsed again and were used for the adhesion assay. 10^5 cells were seeded per cells per well of 24 well plate or $2x10^4$ cells per well of 96-multiwell plate. The cells were allowed to attach on the wells by incubation at 37°C for 40 minutes. Unattached cells were removed by washing twice with PBS. The attached cells were quantified with the hexosaminidase assay (Landegren U, 1984).

5.2.4.1 Hexosaminidase assay

This assay allows estimation of cell numbers by using a chromogenic substrate (p-nitrophenyl-N-acetyl-β-D-glucosaminide) for a ubiquitous lysosomal enzyme, hexosamindase. The attached cells were incubated for 1 hour at 37°C in 50mM citrate buffer pH 5.0 containing 3.75mM p-nitrophenyl-N-acetyl-β-D-glucosaminide and 0.25% Triton X-100. The reaction was stopped and colour was developed by addition of 50mM glycine buffer pH 10.4 containing 5mM EDTA. The absorbance was measured at 405 nm in a Dynex MRX Revelation microplate reader (Dynex Technologies).

5.2.5 Proliferation Assay

Cells were seeded at a 10^4 cells/well density in 24 well plates the day before the start of the assay. After overnight incubation the medium was aspirated and replaced with fresh medium containing the recombinant proteins. The cells were viewed under an Olympus IX70 inverted light microscope at x4 objective. Pictures of the cultured cells were captured with the SPOT Advanced software equivalent to a 2220x2960μm area. Pictures were taken at 0, 24, 48 and 72 hours after the replacement of the medium from the same area of the multi-well plate. Cell numbers per captured image were quantified using the AnalySIS software.

5.2.6 Migration Assay

Cells were seeded onto a 24-well plate at a density 10^5 cells/well and were allowed to attach overnight. The next day a straight scrape wound was made across the monolayer of

each well with a sterile yellow pipette tip. The medium then aspirated to remove any floating cells and replaced with fresh prewarmed, containing the appropriate concentration of recombinant protein. The cells were viewed under an Olympus 1X70 inverted light microscope at x4 objective. Pictures of the cultured cells and the scrape wound were captured with the SPOT Advanced software equivalent to a 2220x2960μm area. Pictures were taken at 0, 8, 16 and 24 hours post wounding and the average distance between the separated cells was measured along the same 220μm region using the Image Pro Plus software.

5.2.7 Apoptosis Assay

Cell apoptosis was detected with the TACS™ Annexin V-FITC kit (R&D Systems). The principle of this assay is that in early apoptotic cells phosphatidylserine, which is usually in the intracellular part of cytoplasmic membrane, gets exposed to the outer surface of the membrane. This event is thought to be important in the macrophage recognition of these cells. Annexin V binds to phosphatidylserine and allows colourimetric detection of the apoptotic cells with the FITC conjugate. DNA-binding dye Propidium Iodide can be used in conjunction to differentiate late apoptotic cells, which should have lost membrane integrity and stain for both this and Annexin V (Martin et al, 1995). Therefore early apoptotic cells should stain only with Annexin VI (interacting with phosphatidylserine on cell membrane), whereas the ones that are at the later stages of apoptosis and would stain both with Annexin VI and Propidium Iodide (interacting with DNA).

Cells were seeded at a density 10^5 cells/well, in a 24-well format, cultured overnight and the medium was aspirated. Fresh medium was added containing the recombinant proteins and a positive apoptosis control was included: 50mM etoposide (Sigma). Cells were harvested and processed with the TACS™ Annexin V-FITC detection kit at the following time points: 0, 24, 48 and 72 hours after addition of the proteins.

100μl Annexin V Incubation reagent was prepared for each sample of 10^5 cells containing 10μl 10x Binding Buffer, 10μl Propidium Iodide, 1μl Annexin V-FITC and 79μl dH_2O and the mixture was kept in the dark on ice. Cells were aspirated and trypsinised with 100μl 0.25% Trypsin-EDTA (Invitrogen) for 2-5 minutes. The action of trypsin was stopped with addition of 900μl PBS 10% FCS (for epithelial cells) or DMEM/F10 medium (for keratocytes). Cells were centrifuged at 500 x g for 5-10 minutes at room temperature. The pellet was washed by resuspension with ice-cold PBS and centrifuged again as above. The PBS was removed and cells were gently resuspended in 100μl of the Annexin V Incubation reagent and were

kept in the dark at room temperature for 15 minutes. 200μl 1x Binding buffer was added to each sample and samples were analysed in a BD Facscalibur Flow Cytometer. Results were analysed in WinMDI 2.8 software.

5.2.8 Experimental design

Two different recombinant protein concentrations were used for all assays, 50ng/ml and 500ng/ml. The control was 50ng/ml BSA diluted in the same buffer which was used for the recombinant proteins. The flasks cultured with primary and immortalised epithelial cells were always coated with collgen I, apart from the case of the adhesion assay.

5.2.9 Data analysis

All assays were carried out at least twice in triplicate unless otherwise stated. Data were analysed for Gaussian distribution, for analysis of variance (ANOVA) with Dunnett test to compare control with experimental values using Prism software. T test was used when needed to compare the difference between two sets of results.

5.3 RESULTS

5.3.1 Primary corneal cell culture

The method described in section 5.2.2 was the optimum for the culture and growth of corneal epithelial cells. Lack of scraping the culture surface resulted in floating of the corneal explants after addition of the culture medium. Use of keratinocyte serum-free medium minimised the proliferation of corneal keratocytes which may have come out of the explant. The combination of serum-free medium and low calcium concentration has been described previously for the impeding effect they have on cell differentiation (Martin et al, 1991) and have been optimised for the culture of corneal epithelial cells (Hackworth et al, 1990). Often the epithelial cells derived from the first time an explant was laid on a culture surface appeared to be resistant to trypsinisation, where long periods of exposure to the enzyme failed to lift the cells of the surface. Cells that were dissociated from the culture surface by a cell scraper failed to assume viability when subcultured. Interestingly, epithelial cells derived from the second and third rounds of explant usage did not exhibit any difficulties in detachment during trypsin treatment.

Primary epithelial cell cultures were characterised by staining for cytokeratin 3 and 12 (Figure 5.1.C). A human corneal epithelial cell line, CRL11516 (ATCC) was used as positive control for the interaction with the cytokeratin marker (Figure 5.1.D). This cell line was propagated following the same method (5.2.2) used for primary epithelial cells.

Primary keratocytes were easier than epithelial cells to culture. The cell turnover using the collagenase method was greater and faster than that of epithelial cells. A 75cm^2 flask would contain 6x10^6 keratocyte cells compared with 7x10^5 epithelial cells. Part of this diversity is due to the difference in cell size between the two cell types (Figure 5.1).

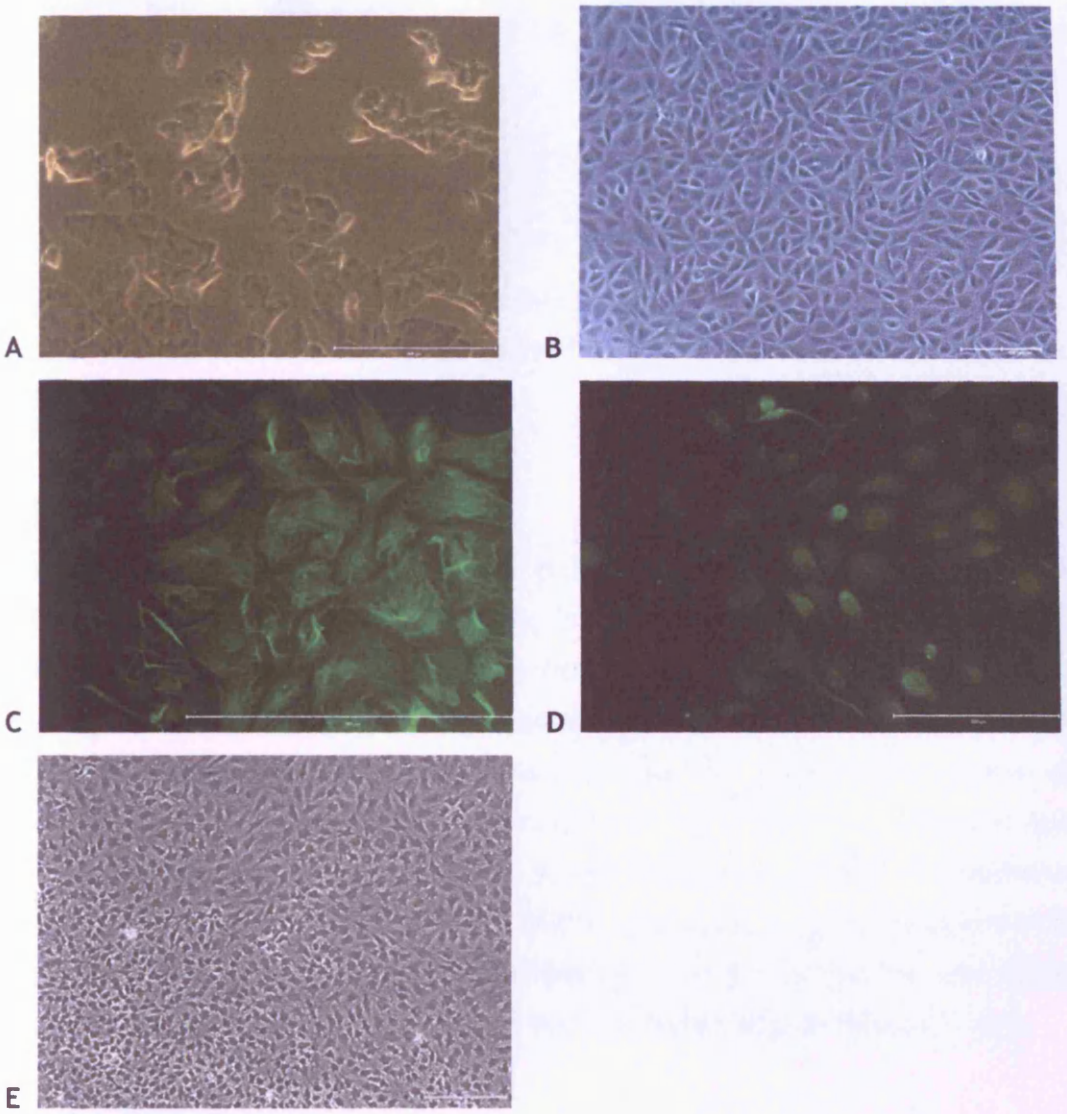

Figure 5.1: Corneal cells

A. Epithelial sheet derived from bovine corneal explant. B. Confluent primary epithelial monolayer C. Cytokeratin staining of primary bovine epithelial cells. D. Cytokeratin staining of human corneal epithelial cell line. E. Primary bovine keratocytes (White line on the bottom right side corresponds to 200 microns)

5.3.2 Summary of the assay results

The following table summarises the results from the assays that were carried out to determine the effects of wild type and mutant recombinant proteins on primary epithelial and keratocyte cell culture.

Protein	Cell type	Adhesion	Proliferation	Migration	Apoptosis
WT	Epithelia	+	+	o	o
	Keratocytes	+	o	o	o
R555Q	Epithelia	+	o	o	+
	Keratocytes	o	o	o	+
R555W	Epithelia	+	+	o	+
	Keratocytes	o	o	o	+

Table 5.1: Summary of the results of recombinant keratoepithelin

Symbols: + more effect than the control cells, - less effect than the control cells, o similar to the control

5.3.3 Adhesion Assay

Although no standard curves were drawn to correlate the A_{405} readings of the hexosaminidase assay to cell numbers, Landegren U. demonstrated in 1984 the linear relationship of cell populations ranging from $8x10^2$ to 10^5 cells and the corresponding A_{405} readings for 5 different cell types (Hepatocytes; CTLL-2, a T cell growth dependent mouse cell line; Jurkat, a human T leukaemia cell line; Raji, a Burkitt lymphoma cell line and peripheral blood lymphocytes). The number of cells used in the adhesion assay is within this range and believed to correspond proportionally to the 405nm absorbance readings. The corresponding A_{405} readings to the above cell populations varied between 0.05 and 20, which is also within the ranges of the readings obtained during the cell adhesion assays. This assumes similar hexosaminidase content between cells of different type.

5.3.3.1 Epithelial cells

Both wild type and mutant keratoepithelin recombinant proteins seem to promote epithelial cell adhesion better than the control ($p<0.001$) (Figure 5.2). There is no significant difference between the two concentrations of the same protein or between the mutant and wild type proteins (Figure 5.2.A). The highest value of absorbance of the attached cells was 4.53 ±0.33 in the presence of 50 ng wild type protein compared to 2.97 ±0.71 in the control.

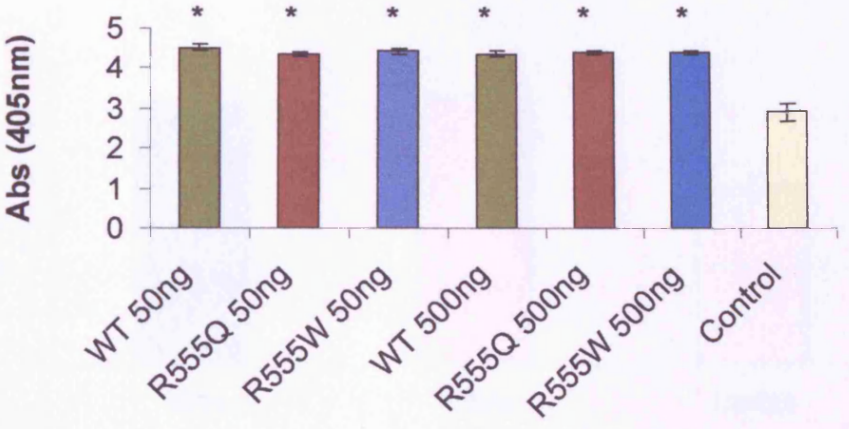
Abs (405nm)
5
4
3
2
1
0
*
*
*
*
*
*
WT 50ng
R555Q 50ng
R555W 50ng
WT 500ng
R555Q 500ng
R555W 500ng
Control

(A)

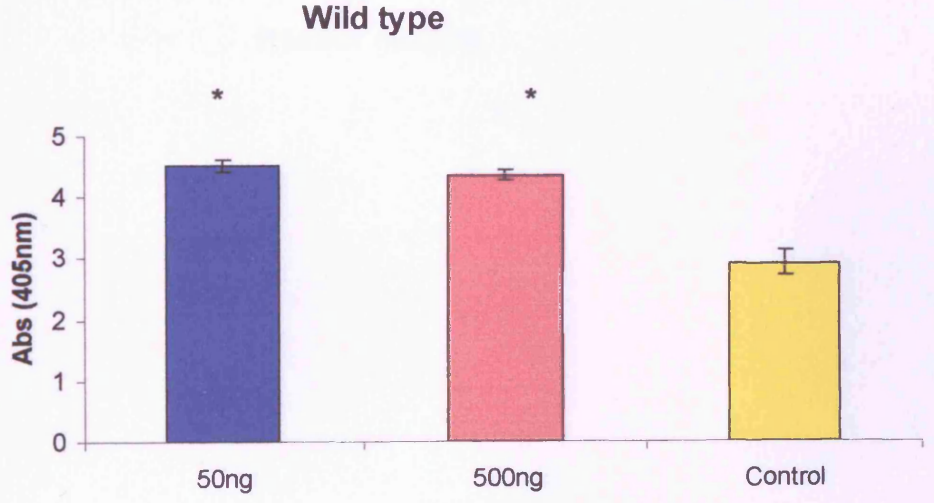
Wild type
Abs (405nm)
5
4
3
2
1
0
*
*
50ng
500ng
Control

(B)

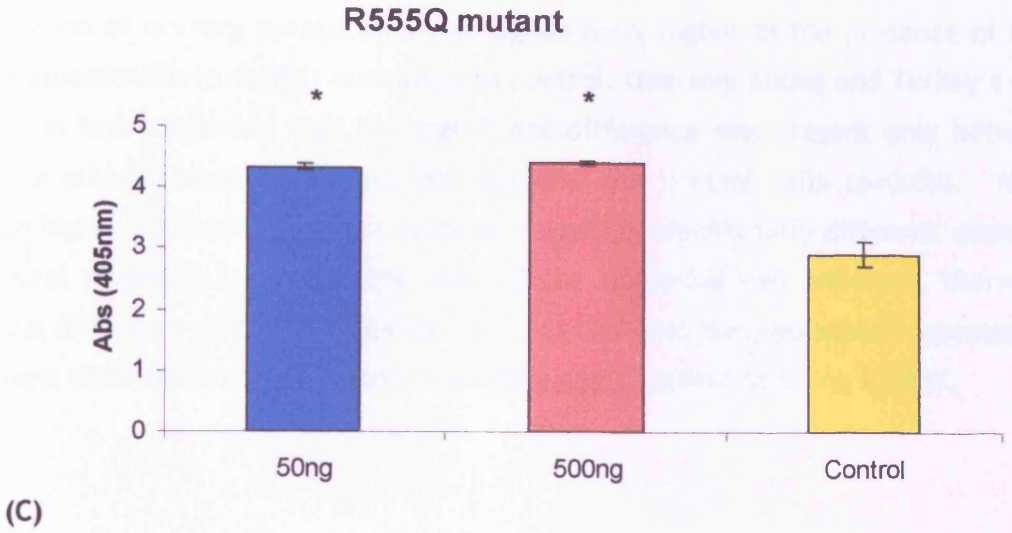

(C)

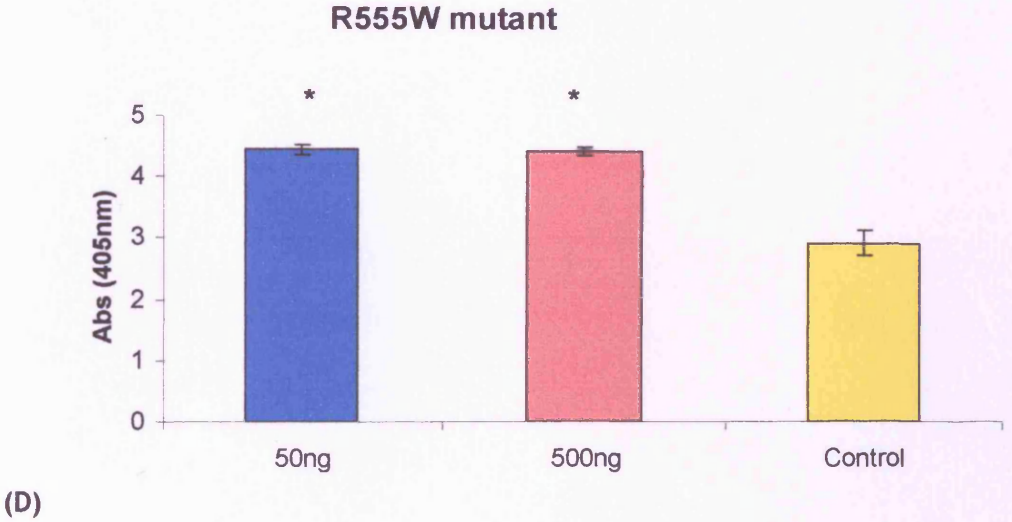

(D)

Figure 5.2: Epithelial cell adhesion on recombinant protein

A. Effect of wild type (WT) and mutant recombinant keratoepithelin. B. Effect of wild type keratoepithelin. C. Effect of R555Q mutant recombinant protein. D. Effect of R555W mutant recombinant protein. Columns represent mean values of the repeated experiments and error bars are ±SEM. * $p<0.001$

5.3.3.2 Keratocytes

The adhesion of primary keratocytes was significantly higher in the presence of the wild type keratoepithelin ($p<0.001$) compared to control. One-way Anova and Turkey's multiple comparison test confirmed that the significant difference was present only between the wild type protein treated (50 and 500 ng) and the control cells ($p<0.05$). However, although higher adhesion to mutant proteins it was not significantly different compared to the control (Figure 5.3). As in the case of the epithelial cell adhesion, there was no statistical difference of the absorbance readings between the two protein concentrations. The lowest absorbance corresponded to keratocytes attached to 500ng R555W.

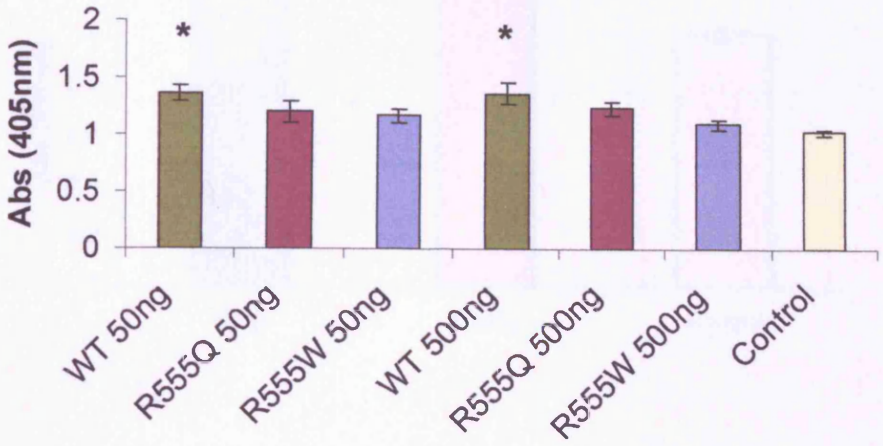
Abs (405nm)
2
1.5
1
0.5
0
*
*
WT 50ng
R555Q 50ng
R555W 50ng
WT 500ng
R555Q 500ng
R555W 500ng
Control

(A)

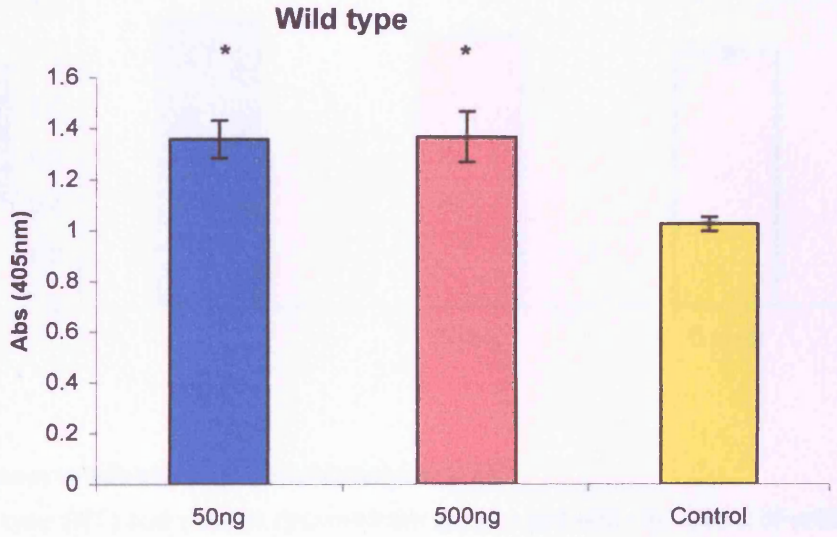
Wild type
Abs (405nm)
1.6
1.4
1.2
1
0.8
0.6
0.4
0.2
0
*
*
50ng
500ng
Control

(B)

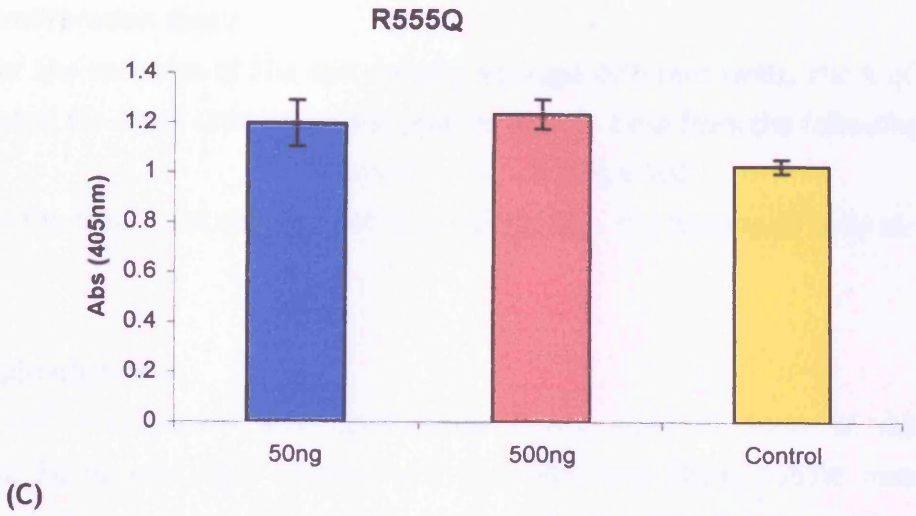

(C)

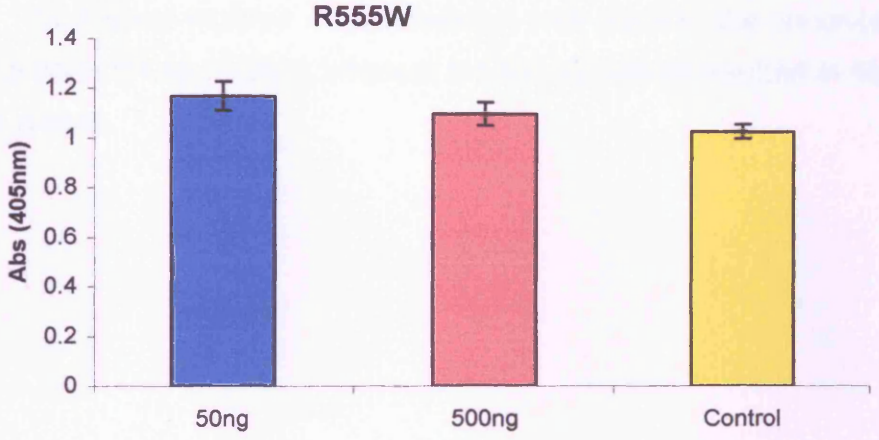

(D)

Figure 5.3: Keratocyte adhesion on recombinant protein

A. Effect of wild type (WT) and mutant recombinant keratoepithelin. B. Effect of wild type keratoepithelin. C. Effect of R555Q mutant recombinant protein. D. Effect of R555W mutant recombinant protein. Columns represent mean values of the repeated experiments and error bars are ±SEM. * $p<0.001$

5.3.4 Proliferation assay

To allow for the variation of the cell density amongst different wells, the % of cell growth was calculated for every time point and plotted against time from the following equation:

$$\% \text{ cell growth} = (N_t - N_0)/N_t \times 100$$

where N_t = the number of cells for this time point, N_0 = the number of cells at time point 0 hours.

5.3.4.1 Epithelial cells

Epithelial cell proliferation was significantly higher after 72 hours of culture in the presence of 50 ng wild type recombinant ($p<0.001$) and 500ng R555W mutant proteins ($p<0.01$) according to the results of the one-way ANOVA with the Dunnett's post test. T test with Welch's correction also shows significant difference between the control and 500 ng of wild type ($p=0.0027$) and 50ng of R555Q ($p=0.0319$). The mean cell growth increase in the presence of wild type keratoepithelin was 50.27 ±1.93% compared to 35.59 ±6.26% in the control. The highest increase of proliferation took place in the presence of 500 ng R555W mutant protein (54.68 ±6.26%), whereas the R555Q protein resulted in 46.97 ±8.79% increase of cell growth.

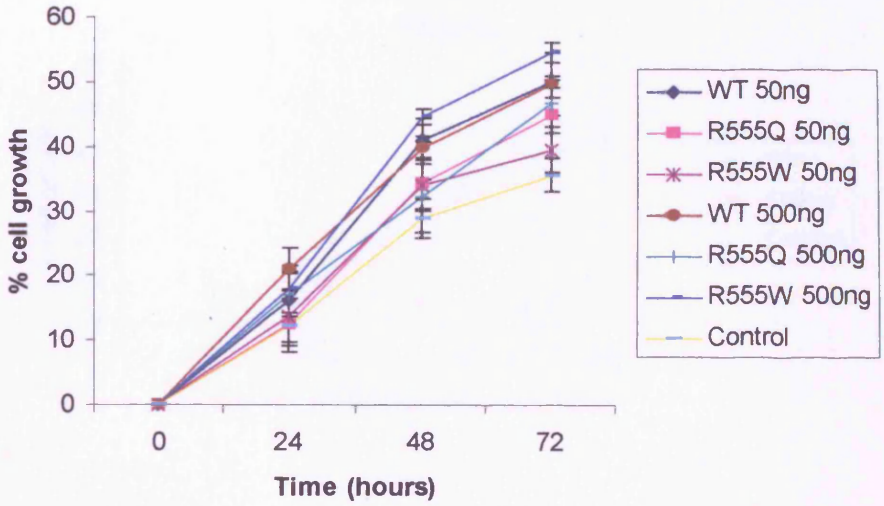
60
50
40
30
20
10
0
% cell growth
0
24
48
72
Time (hours)
WT 50ng
R555Q 50ng
R555W 50ng
WT 500ng
R555Q 500ng
R555W 500ng
Control

(A)

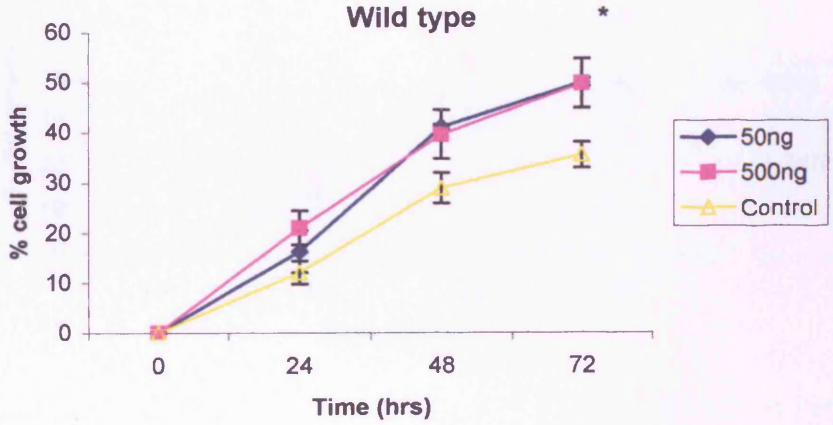
Wild type
*
60
50
40
30
20
10
0
% cell growth
0
24
48
72
Time (hrs)
50ng
500ng
Control

(B)

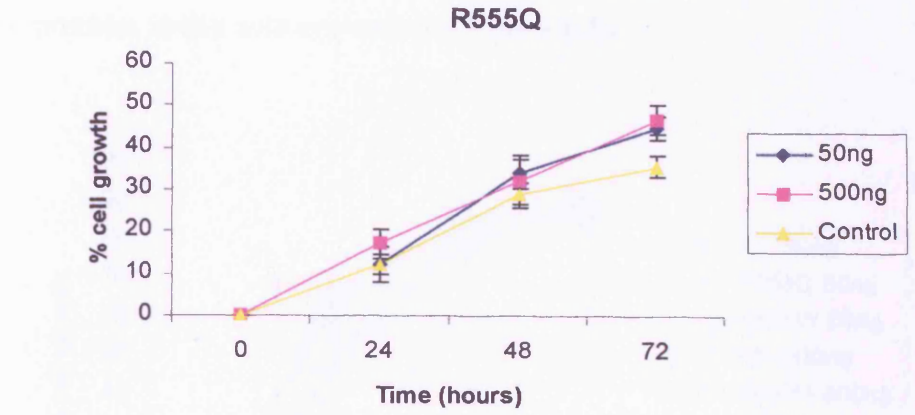

(C)

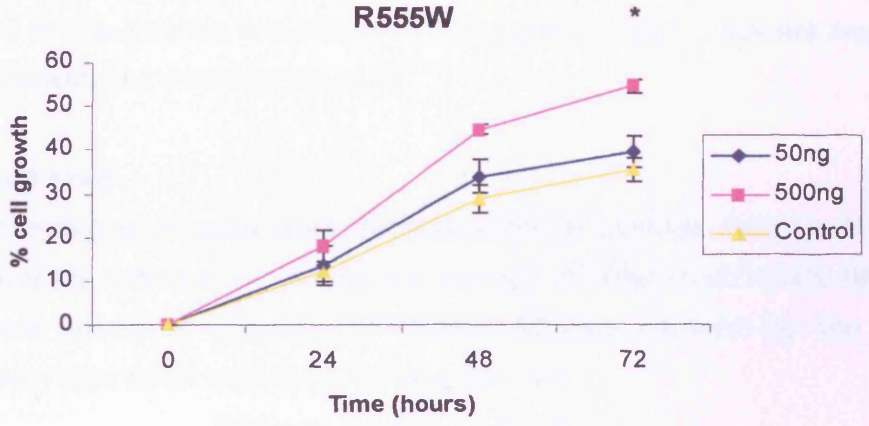

(D)

Figure 5.4: Epithelial cell proliferation

A. Effect of wild type (WT) and mutant recombinant keratoepithelin. B. Effect of wild type keratoepithelin. C. Effect of R555Q mutant recombinant protein. D. Effect of R555W mutant recombinant protein. Points represent mean values of the repeated experiments and error bars are ±SEM. * $p<0.001$

5.3.4.2 Keratocytes

The proliferation of keratocytes did not seem to be altered in the presence of the recombinant proteins in the culture medium (Figure 5.5).

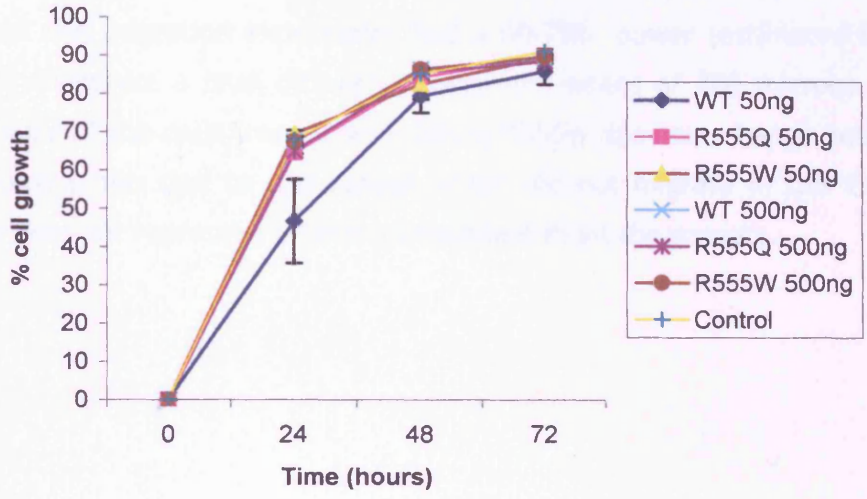

Figure 5.5: Keratocyte proliferation

Effect of wild type (WT) and mutant recombinant keratoepithelin. Points represent mean values of the repeated experiments and error bars are ±SEM.

5.3.5 Migration assay

The data from the migration assay were derived from the average distance between the cultured cells after the introduction of a scrape wound. In order to eliminate the variation between different widths of wound, the actual distance covered by the cells was estimated for every time point with the following formula:

$$\text{Distance migrated} = D_0 - D_t$$

Where D_0 is the distance (width of wound) measured at 0 hours (at the moment the wound was induced and after the protein was added) and D_t is the distance measured at the particular time point.

5.3.5.1 Epithelial cells

The corneal epithelial cells treated with wild type and mutant keratoepithelin did not exhibit any significant changes in their migration pattern (Figure 5.6) compared with the control cells. However, there was a significant difference between the migration mediated by the wild type and mutant proteins. Cells cultured with wild type keratoepithelin migrated the furthest distance: 521 ±64.58 microns whereas the 500ng of mutant proteins resulted in the least distances migrated: 348.3 ±14.9 and 393 ±54.19

microns for R555W and R555Q respectively. The difference between the wild type and each of these two means is significant ($p<0.05$) as determined with the t test. In the 2 hour time point there seems to be a difference in the distance migrated between the two different concentrations of the recombinant protein, especially in the case of R555W mutant. However, this difference could not be determined statistically. It is noteworthy to mention that this migration experiment had a 60-75% power (estimated by GraphPad StatMate 2.00) to detect a true difference between means of 200 microns. The mean migration distance of the cells treated with 500ng R555W does not change between the 16 and 24 hour time points due to one repeat which did not migrate in this time interval. Therefore this does not represent a finding consistent in all the repeats.

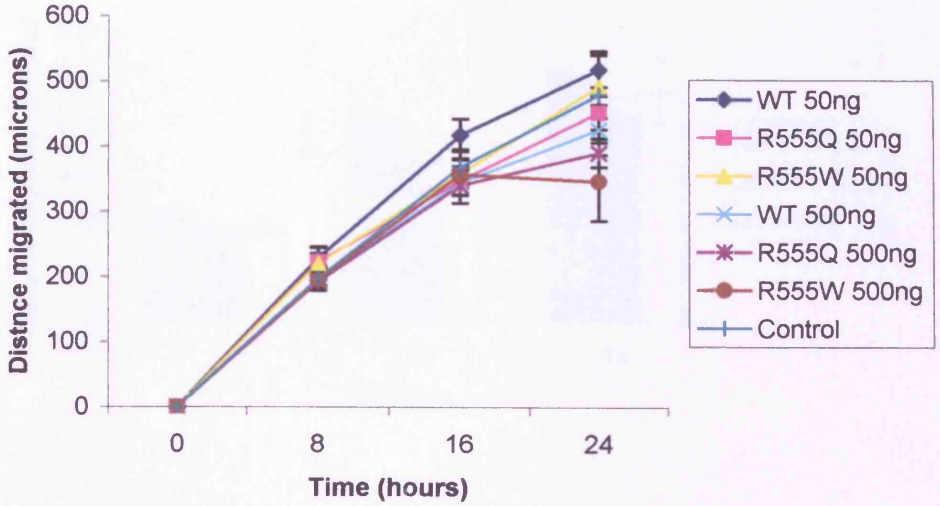
600
500
400
300
200
100
0
Distnce migrated (microns)
0
8
16
24
Time (hours)
WT 50ng
R555Q 50ng
R555W 50ng
WT 500ng
R555Q 500ng
R555W 500ng
Control

(A)

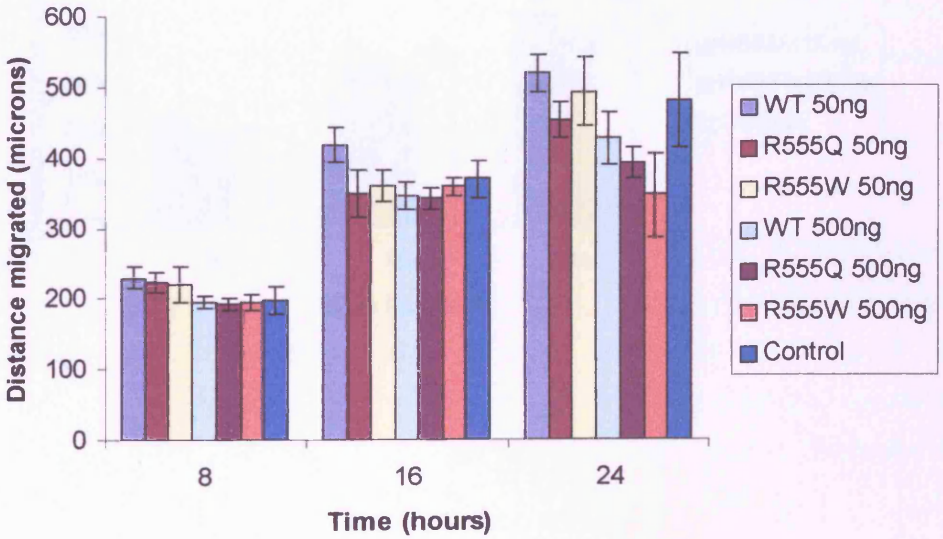
600
500
400
300
200
100
0
Distance migrated (microns)
8
16
24
Time (hours)
WT 50ng
R555Q 50ng
R555W 50ng
WT 500ng
R555Q 500ng
R555W 500ng
Control

(B)

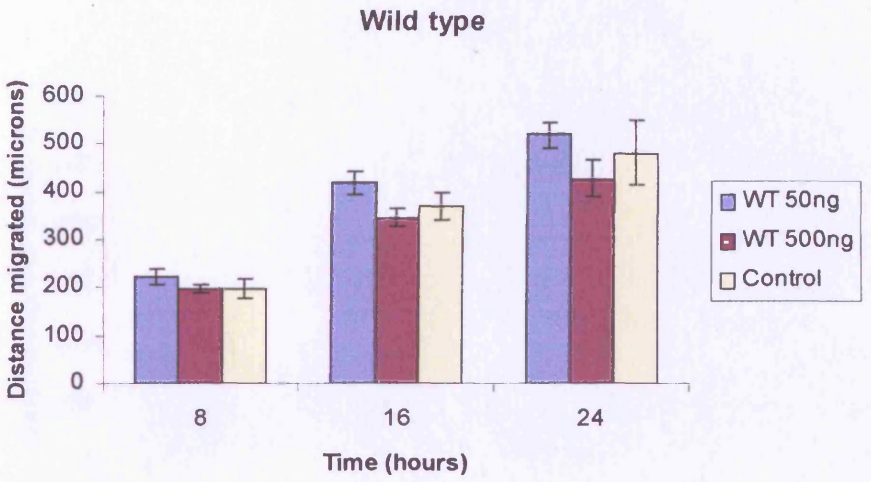
Wild type
Distance migrated (microns)
600
500
400
300
200
100
0
8
16
24
Time (hours)
WT 50ng
WT 500ng
Control

(C)

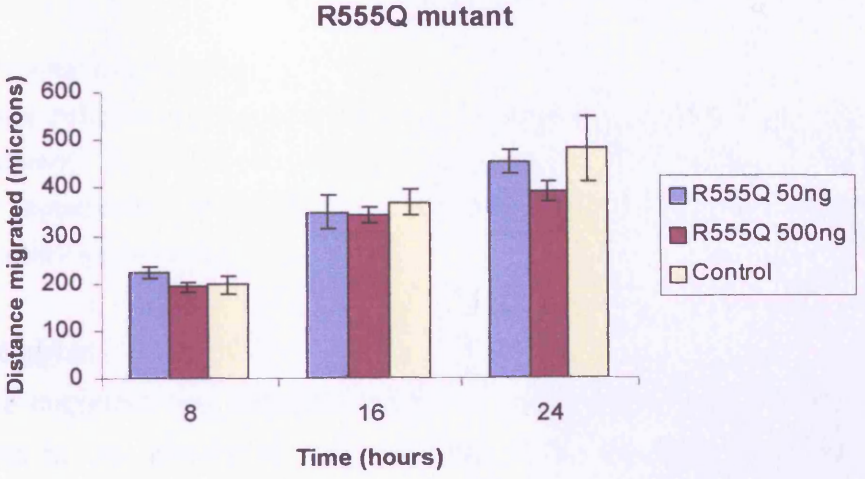
R555Q mutant
Distance migrated (microns)
600
500
400
300
200
100
0
8
16
24
Time (hours)
R555Q 50ng
R555Q 500ng
Control

(D)

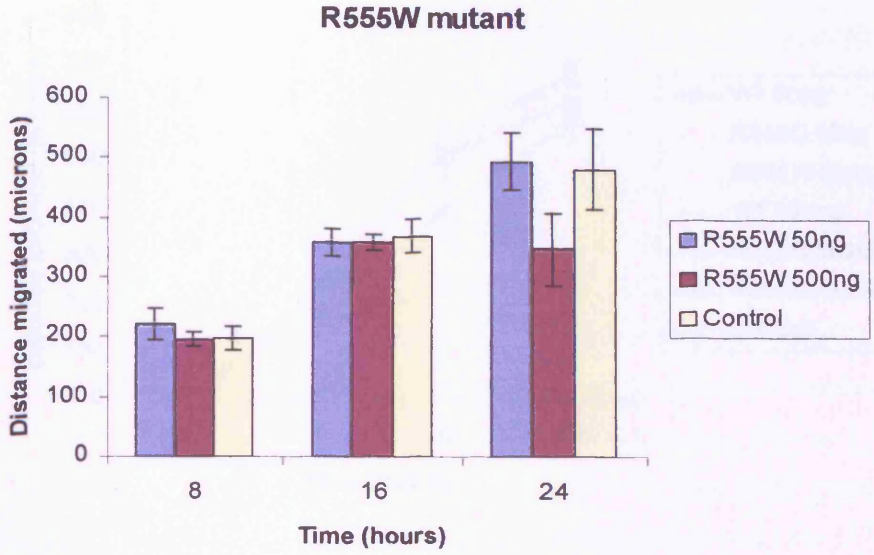

(E)

Figure 5.6: **Epithelial cell migration**

Effect of wild type (WT) and mutant recombinant keratoepithelin. A. Line chart. B. Column chart of all the treatments. C. Treatment with wild type protein. D. Treatment with R555Q mutant protein. E. Treatment with R555W protein. Points and columns represent mean values of the repeated experiments and error bars are ±SEM.

5.3.5.2 Keratocytes

The keratocyte migration was not affected by the presence of the recombinant proteins and in contrast to the picture of the epithelial cells, no significant differences exist between different protein treatments. However the minimum distance migrated corresponds to the cells cultured with 500ng R555W mutant protein, consistent with epithelial cells. Therefore the measurements of the migrated distance from the repeated experiments were as indicated in figure 5.7.

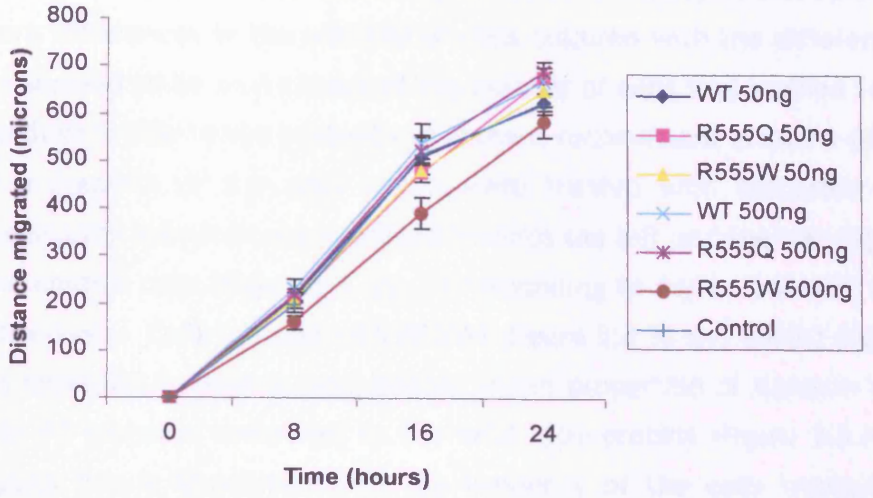

(A)

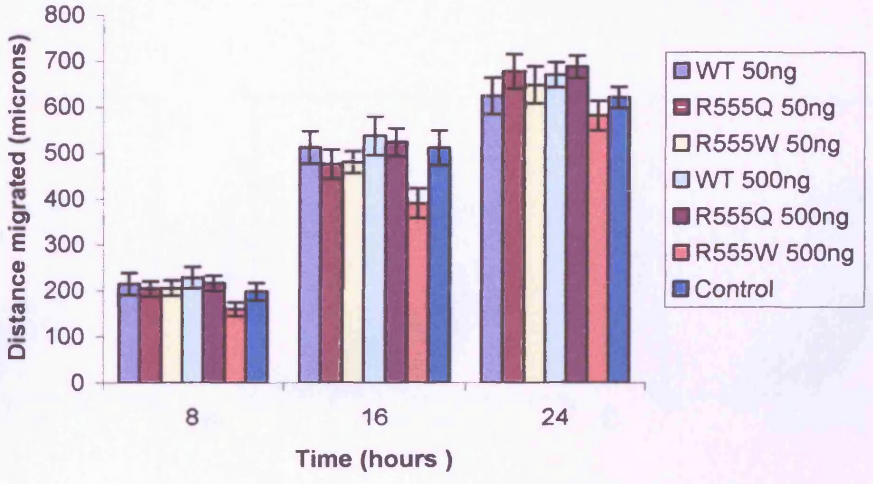

(B)

Figure 5.7: Keratocyte migration

Effect of wild type (WT) and mutant recombinant keratoepithelin. A. Line chart. B. Column chart. Points and columns represent mean values of the repeated experiments and error bars are ±SEM.

5.3.6 Apoptosis assay

Flow cytometry provided two types of information about the viability of the cells that have been processed. One is based on the fluorescence, which corresponds to the number of the cells that take up the Annexin V-FITC and Propidium Iodide stains. The other, more basic information is based on the forward and side scatter, which correspond to the size and granularity of the cells. Generally apoptotic cells decrease in size and increase in granularity.

The Annexin V- Propidium Iodide apoptosis assay of corneal keratocytes and epithelial cells indicated that are differences in the viability of cells cultured with the different types of proteins. There seemed to be an increase of the number of cells that stained for Annexin V-FITC and Propidium Iodide in the presence of mutant recombinant proteins (figure 5.8). The fluorescence dotplots of the cells which were treated with etoposide and were therefore predominantly apoptotic were shifted towards the left and the top (figure 5.8.E) compared to the control cells (figure 5.8.D), corresponding to higher Annexin V-FITC and Propidium Iodide counts. Cells treated with R555W (figure 5.8.B) and R555Q (figure 5.8.C) mutant proteins appeared to have a considerably higher proportion of Annexin V-FITC and Propidium Iodide PE emission compared to the wild type protein (figure 5.8.A). In the following dot plots this is illustrated with the tendency of the cells treated with the mutant proteins and etoposide to accumulate more left on the Annexin V-FITC axis and higher on the Propidium iodide axis.

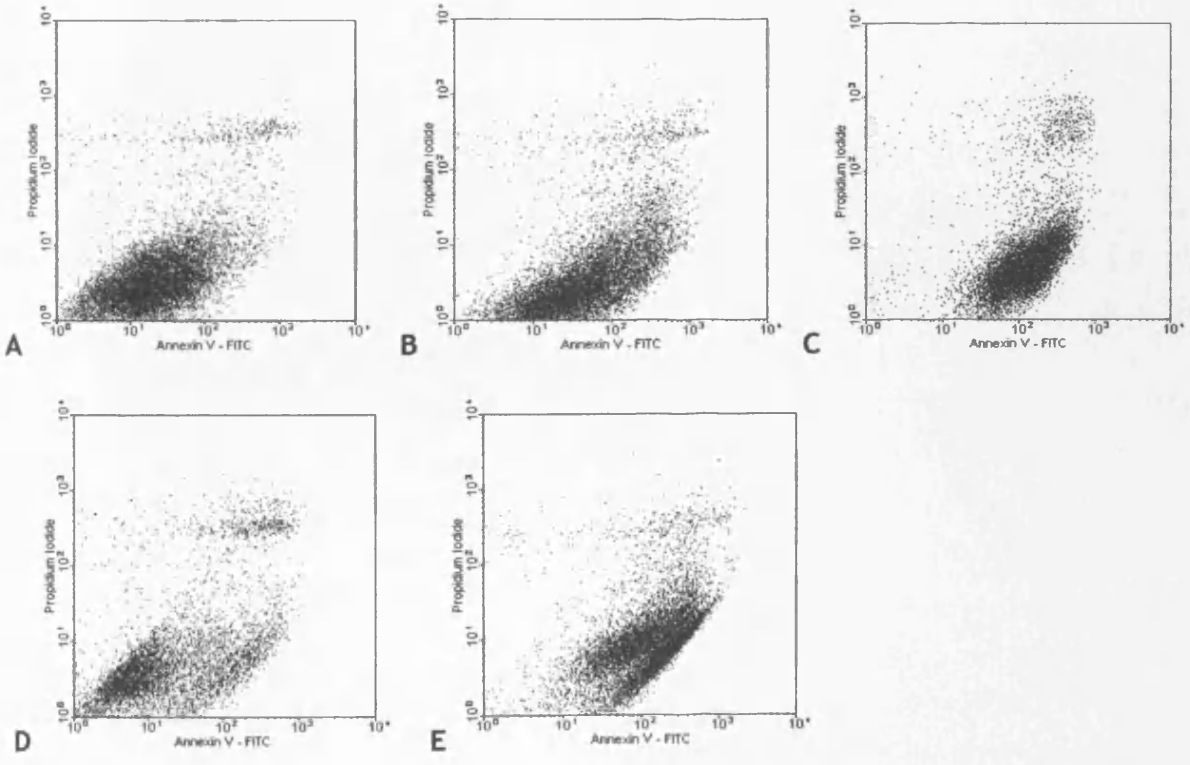

Figure 5.8: Keratocytes apoptosis assay

Keratocytes were cultured for 72 hours. A. Cells with wild type keratoepithelin. B. Cells with R555W mutant recombinant protein. C. Cells with R555Q mutant recombinant protein. D. Control cells. E. Etoposide treated cells

However these differences could not be quantified due to failure of the processed cells to distribute on the forward-side scatter and the Annexin V-Propidium Iodide graphs as distinct populations. The reason for this is unknown especially since the cytometer was calibrated according to the parameters of the corneal cells before the assay was carried out. Therefore the apoptosis assay needs to be repeated to include further optimisation and correction for any residual overlap of fluorescent spectra through the cytometer optical filters.

5.4 Discussion

The results that were presented in this chapter demonstrated the feasibility of the use of the recombinant proteins in cell culture experiments in order to extract information about the effects they exert on cells. These proteins seem to modulate the behaviour of primary corneal epithelial cells and keratocytes. These two cell types are in close proximity to the aggregates in corneal dystrophies and are affected as it has been shown ultrastructurally (Akhtar et al, 1999, Ridgway et al, 2000) during the accumulation of the deposits.

Wild type recombinant keratoepithelin promoted the adhesion of both epithelial cells and keratocytes. This is not surprising since keratoepithelin has been described as a cell-adhesive molecule (Kim et al, 2003) due to its ability to promote adhesion for many different cell types, including dermal fibroblasts (LeBaron et al, 1995, chondrocytes (Ohno et al, 1999), keratinocytes (Bae et al, 2002), human astrocytoma cells (Kim et al, 2003), periodontal ligament cells (Doi et al, 2003) and HUVEC (Nam et al, 2003). Corneal cells have also been tested previously for adhesion to recombinant wild type and mutant keratoepithelin (Kim at al, 2002) and they are thought to interact with keratoepithelin through the $\alpha_3\beta_1$ integrins (Kim et al 2000). However the effects between mutant and wild type recombinant proteins on human corneal epithelial cell adhesion reported by the above researchers were similar. Keratoepithelin-facilitated keratocyte adhesion was also described by Yang et al, 2004. The reduced adhesion of keratocytes to the mutant proteins may reflect the effect of the R555 mutations on the protein's interaction with specific integrins on the surface of keratocytes.

The epithelial cell proliferation was increased in response to mutant and wild type keratoepithelin, whereas keratocyte proliferation was not affected by the recombinant proteins. Other cells have responded to wild type keratoepithelin by increased proliferation, such as skin keratinocytes (Bae et al, 2002) and renal proximal tubular epithelial cells (Park et al, 2004). These cells also migrate more effectively in the presence of keratoepithelin, something was which not demonstrated with the epithelial cells and keratocytes in this chapter. However there is a significant difference between the migration effect of wild type and R555W mutant protein, which has been consistently associated with retarded cell migration (figures 5.6 and 5.7).

The staining of epithelial cells and keratocytes differs in the presence of wild type and mutant recombinant protein and it suggests that there may be an increase in apoptosis facilitated by the mutant proteins. Morand et al (2003) demonstrated with Annexin V

staining and fluorescence microscopy that transfection of corneal epithelial and HeLa cells with mutant βig-h3 constructs results in apoptosis. Also wild type βig-h3 may be important for the regulation of cell apoptosis by providing soluble RGD peptides (Kim et al, 2003).

The recombinant proteins did not have the same effects on epithelial cells and keratocytes. It is possible that these proteins interact via different types of integrins on the cell surface of these cells and facilitate different effects. Since keratoepithelin is an extracellular matrix protein it is possible it mediates extracellular environmental signals to the cells, especially keratocytes, which co localise in the stroma. The fact that these signals may affect the gene expression profile of the cells is supported by the increasing number of references, which implicate βig-h3 gene with the regulation of cell cycle (Genini et al, 1996; Tsujimoto et al, 1999; Zhao et al, 2002; Golembineski et al, 2002; Schneider et al, 2002).

Throughout all of the assays it was not possible to establish a concentration-dependent effect of the recombinant proteins on the corneal cells. This could be due to the concentration of recombinant proteins that were used in the assays (50-500ng/ml). Some researchers use much higher concentrations (10-50μg/ml) (Yuang et al, 2004). Although cell number availability prevented the use of a variety of protein concentrations, it would be beneficial to attempt a greater range of concentrations, such as 10ng-100μg/ml.

The recombinant proteins carry an NH_2-terminal Histidine repeat, which facilitated their purification. Although insertion of this exogenous sequence to the NH_2-terminal part of the recombinant protein is less likely to interfere with the biological activity, it is unknown how it may affect the conformation of the recombinant protein. This sequence can be removed by proteolytic digestion with Factor Xa to test whether the recombinant protein effects on corneal cells alter.

6. CHAPTER SIX

The effects of recombinant adenoviruses carrying the βig-h3 gene on cell behaviour

6.1 INTRODUCTION

The expression of the βig-h3 gene in the cornea seems to take place in the corneal epithelium (Escribano et al, 1994, Akhtar et al, 1999, Ridgway et al, 2000), but the possibility of keratocytes expressing this gene has not been ruled out, especially after the observation of the presence of aggregated deposits in the keratocyte cytoplasm (Akhtar et al, 1999). Overexpression of the wild type and mutant βig-h3 in cultured cells would be a useful indicator of the way that corneal cell behaviour is modulated by these genes.

Adenoviruses can be used to achieve high levels of transgene expression in a variety of cell types and tissues (Shering et al, 1997; Brown et al, 1997; Castro et al, 1997). Corneal adenoviral gene transfer has taken place repeatedly before, but the majority of the references report transfection of the endothelium (George et al, 2000), which has been easier to target than the epithelium. However, the feasibility of gene transfer to the corneal epithelial cells in culture was demonstrated by Tsubota et al, (1998). Corneal epithelial and conjunctival cell lines were transfected with adenovirus concentrations as low as $3.2x10^{-5}$ MOI. The optimum transfection was achieved with 50 MOI of replication deficient recombinant adenovirus. Abraham et al, (1995) also achieved rabbit epithelial cell line transfection with a recombinant adenovirus in vitro and in vivo transfection of the epithelium amongst other ocular tissues by viral intracameral and vitreal injection. Adenoviral transfection of corneal stromal keratocytes was achieved by intrastromal injection of adenoviral packaged DNA constructs carrying the E-GFP reporter gene (Carlson EC et al, 2004).

Adenoviruses were therefore used for the transfer of βig-h3 constructs in corneal cells in order to establish the effects of the overexpression of the wild type and the dystrophy-causing R555W mutant gene and whether there are any differences between them.

6.2 METHODS

The methods that were used in this chapter were described in section 5.2 of Chapter 4. Instead of recombinant proteins the replication deficient recombinant adenoviruses were added to the cells to be assayed: Radβigh3, RadR555W and control adenovirus Rad35. The cells were infected at an MOI[1] of 50.

The following modifications were made to the methods described in section 5.2:

6.2.1 Adhesion assay

The cells that were going to be tested for their adhesion were first cultured in a density of 10^5 cells per well in a 24 multiwell plate and incubated overnight at 37°C in a 5% CO_2 humidified incubator. The next day the medium was aspirated and the cells were infected with the respective recombinant adenoviruses. The adenoviruses were added to fresh medium and applied on the cultured cells. The cells were incubated overnight and the next day their medium was aspirated and replaced with fresh prewarmed medium. The following day the cells were treated with trypsin and were tested for their ability to adhere to the surface of multiwell plates by following the method described in section 5.2.4.

6.2.2 Proliferation assay

Cells were seeded at a 10^4 cells/well density in 24 well plates the day before the start of the assay. After overnight incubation the medium was aspirated and replaced with fresh containing the recombinant adenoviruses. Pictures were taken immediately after this for the 0 hours time point. The following day the medium was replaced with fresh and pictures were taken at 24, 48 and 72 hours. Determination of cell number and image analysis took place as described n section 5.2.5

6.2.3 Migration assay

Cells were seeded onto a 24-well plate at a density 10^5 cells/well and were allowed to attach overnight. The next day the medium was changed and replaced with fresh containing the recombinant adenoviruses. The cells were incubated for 24 hours with the viruses and then a straight scrape wound was made across the monolayer with a sterile 200 μl pipette tip. The medium was replaced to remove the virions and any floating cells and the migration of cells was monitored and analysed as described in section 5.2.6

[1] MOI = Number of virions per target cell

6.2.4 Apoptosis assay

Cells were seeded at a density 10^5 cells/well, in 24-well format, cultured overnight and the medium was aspirated. Fresh medium was added containing the recombinant adenoviruses. Cells were harvested and processed with the TACS™ Annexin V-FITC detection kit at the following time points: 0, 24, 48 and 72 hours after addition of the adenoviruses, according to the method in section 5.2.7.

6.2.5 Data analysis

All assays were carried out at least twice in triplicate unless otherwise stated. Data were analysed for Gaussian distribution, for analysis of variance (ANOVA) with Dunnett test to compare control with experimental values using Prism software. T test was used when needed to compare the difference between two sets of results.

6.3 RESULTS

6.3.1 Confirming the feasibility of gene transfer using the recombinant adenoviruses

The recombinant adenoviruses were used as vehicles to transport the genes of interest inside the cultured cells. In order to confirm the ability of these adenoviruses to transfer and express the transgenes in foreign cells, the Rad35 control adenovirus was used to infect corneal epithelial cells at MOI of 10 and 100. 48 hours post infection the cells were fixed and stained according to the X-gal assay (section 3.2.2.4). The feasibility of adenoviral gene transfer was demonstrated in figure 6.1, where the control adenovirus successfully transferred the Lac Z gene to the cells and expressed β-galactosidase. This enzyme was assayed by addition of X-gal, which when cleaved by β-galactosidase produces the blue stain observed in the pictures (Figure 6.1).

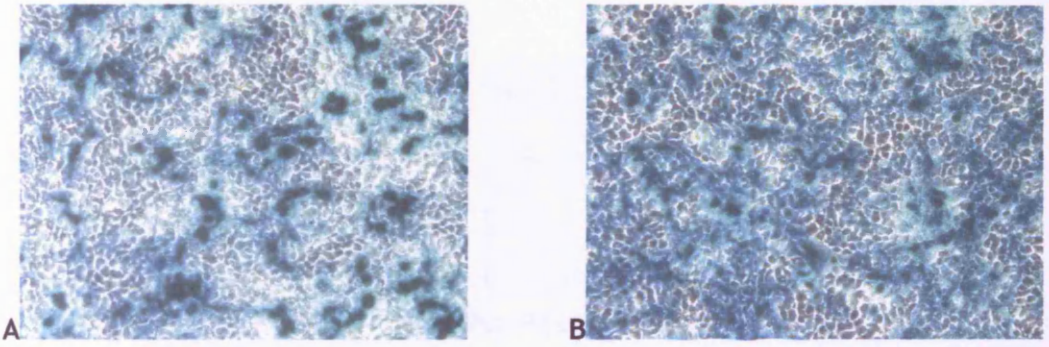

Figure 6.1: Gene transfer with recombinant adenoviruses

X-gal assay of Rad35 infected cells. A. 10 MOI B. 100 MOI

6.3.2 Summary of the assay results

The following table summarises the results from the assays that were carried out to determine the effect of wild type and R555W mutant transgenes overexpression in primary epithelial and keratocyte cells.

Transgene	Cell Type	Adhesion	Proliferation	Migration	Apoptosis
WT	Epithelia	+	o		o
	Keratocytes	o	o		o
R555W	Epithelia	o	+		+
	Keratocytes	+	o		+

Table 6.1: Summary of the results of βig-h3 overexpression

Symbols: + more effect than the control cells, - less effect than the control cells, o similar to the control

6.3.3 Adhesion assay

6.3.3.1 Epithelial cells

The epithelial cells that were transfected with Radβigh3, which carries the wild type βig-h3 gene adhered better to plastic wells than the cells that were transfected with the control adenovirus Rad35 ($p<0.001$) (Figure 6.2). Epithelial cells transfected with the recombinant adenovirus carrying the mutant βigh-h3 gene, RadR555W, attached to plastic less efficiently (Mean A_{405} = 0.94 ±0.24) than cells transfected with Radβigh3 (Mean A_{405} = 1.26 ±0.51)(figure 6.2).

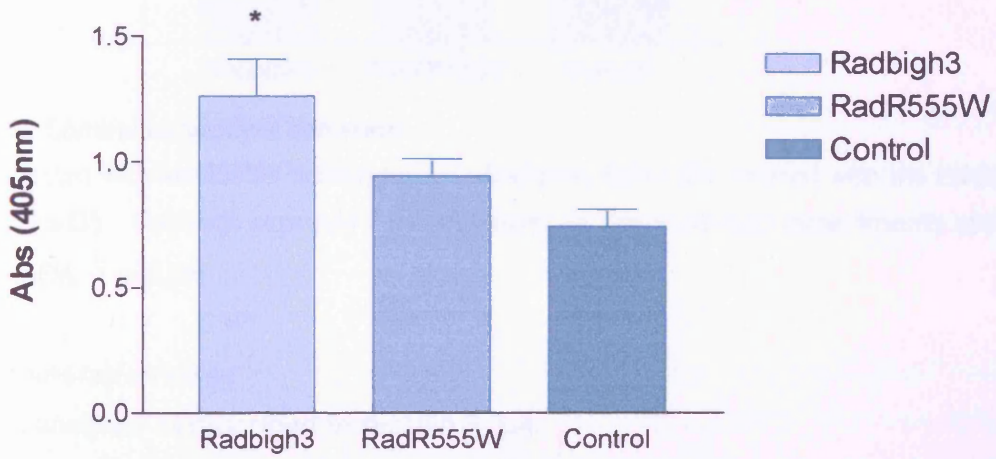

Figure 6.2: Corneal epithelial cell adhesion

Cells transfected with Radβigh3 adhered more efficiently than cells treated with the control adenovirus Rad35. Columns represent mean values of the repeated experiments and error bars are ±SEM. * $p<0.001$

6.3.3.2 Keratocytes

The opposite response was observed with keratocytes which were allowed to adhere to plastic wells after transfection with the recombinant adenoviruses (Figure 6.3). The cells transfected with the mutant adenovirus, RadR555W adhered better ($p<0.001$) than the cells transfected with the control virus. However the wild type βigh3 did not promote or inhibit the adhesion of keratocytes compared to the control cells ($p>0.05$).

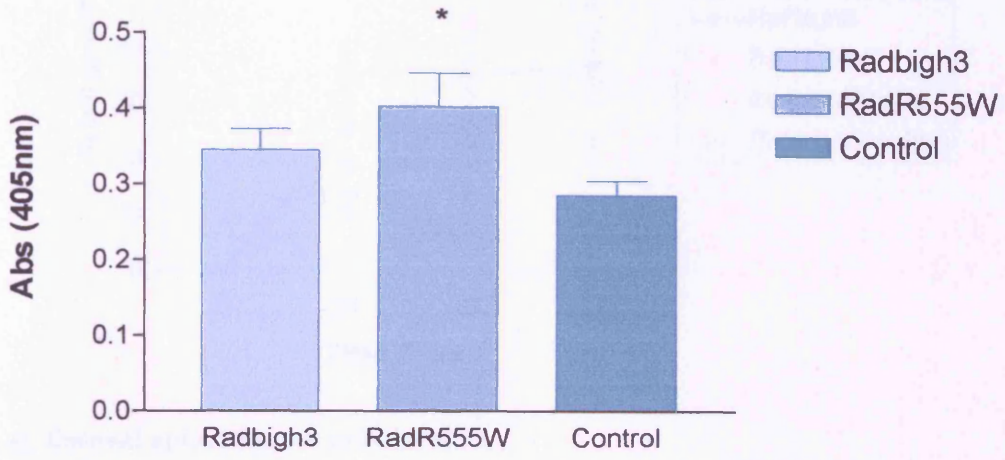

Figure 6.3: Corneal keratocyte adhesion

Cells transfected with RadR555W adhered more efficiently than cells treated with the control adenovirus Rad35. Columns represent mean values of the repeated experiments and error bars are ±SEM. * $p<0.001$

6.3.4 Proliferation assay

Data were analysed as described in section 5.3.4

6.3.4.1 Epithelial cells

The differences in the proliferation pattern of epithelial cells were significant at the 72 hours time point. The proliferation of epithelial cells overexpressing the mutant βig-h3 was higher than the cells transfected with the control adenovirus ($p<0.001$). The percentage of cell increase of the epithelial cells transfected with Radβigh3 was also higher ($p<0.05$) than the Rad35 infected cells. However it is evident from figure 6.4 that the rate of proliferation of the cells transfected with the control adenovirus decreases after the 48-hours time point. This might imdicate that the epithelial cell proliferation is compromised in the presence of the adenovirus, which is a phenomenon already described for other epithelial cells, such as lung (Teramoto et al, 1995). In this case the question why the recombinant adenoviruses carrying the wild type and mutant βig-h3 genes do not have the same effect on the cells remains. For this purpose the non-viral control cell measurements were included in the graph in figure 6.4, which do not appear to be significant different from the virally treated cells.

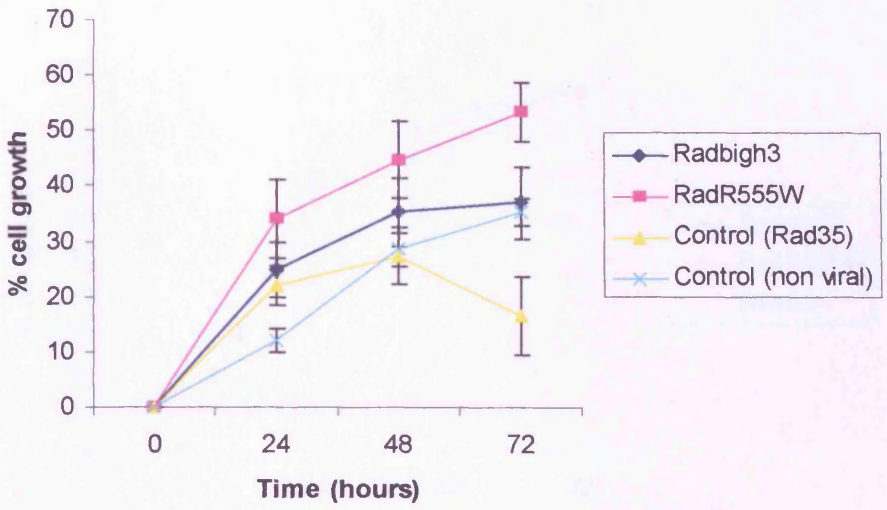

Figure 6.4: Corneal epithelial cell proliferation

Cells transfected with the two recombinant adenoviruses carrying the βigh3 gene proliferate better than the Rad35 transfected cells. Points represent mean values of the repeated experiments and error bars are ±SEM.

6.3.4.2 Keratocytes

The proliferation of keratocytes was not different for the different transfection with adenoviruses (figure 6.5). The same pattern which was observed with the recombinant proteins effect on these cells. It is noteworthy that the viability of the keratocytes, unlike the epithelial cells, was not affected by the adenoviruses.

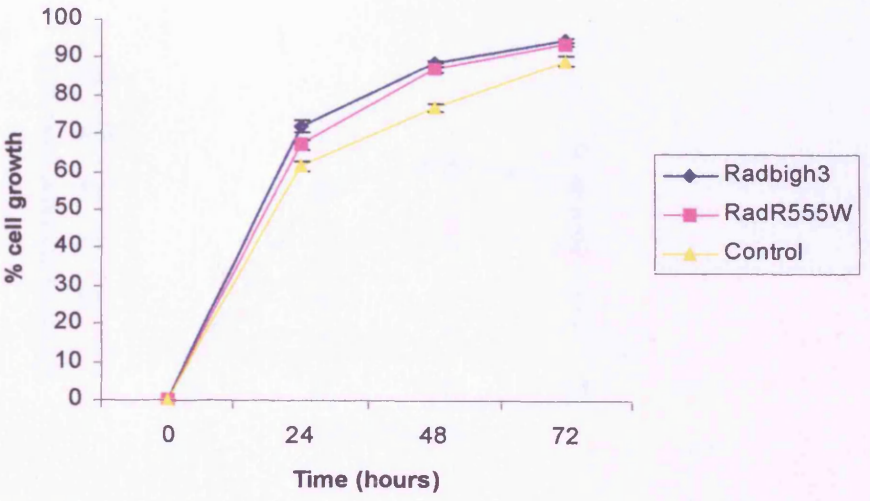

Figure 6.5: Corneal keratocyte proliferation

There is no difference between the different adenoviral treatments. Points represent mean values of the repeated experiments and error bars are ±SEM.

6.3.5 Migration assay

The migration assay was carried out four times in triplicate, but it was difficult to draw any conclusions about the efficiency of these cells to migrate. Two problems were encountered which made assaying the migration problematic. First, there were many wells in which the cells did not migrate after the introduction of the wound. Secondly, the wound caused some of the cells to go further apart, thereby creating a gap in the area, which was photographed for the estimation of the migration rate. These problems appeared equally in the cells transfected with the adenoviruses carrying the βig-h3 genes and the control Rad35 adenovirus and therefore were more likely to be attributed to the effect of the recombinant adenoviruses on the cells rather than the effect of the βig-h3 transgenes. The following graphs represent the migration of cells where the scrape wound was possible to measure for each time point. Data were analysed as described in section 5.3.5.

6.3.5.1 Epithelial cells

Due to the great variation among the wells of each treatment (figure 6.6) the data were not significantly different for any time point and the graph represents the general trend of the transfected cells.

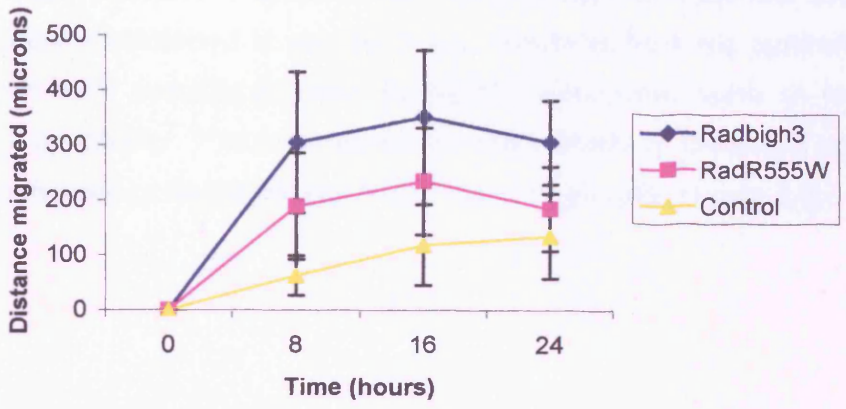

Figure 6.6: Corneal epithelial cell migration

There is no significant difference between the migration of cells with different adenoviral treatments. Points represent mean values of the repeated experiments and error bars are ±SEM.

6.3.5.2 Keratocytes

The proportion of keratocytes, which formed "gaps" in the area where the wound was introduced, was higher than that of epithelial cells. Therefore it was possible to retrieve even less measurements, which makes the data even less meaningful.

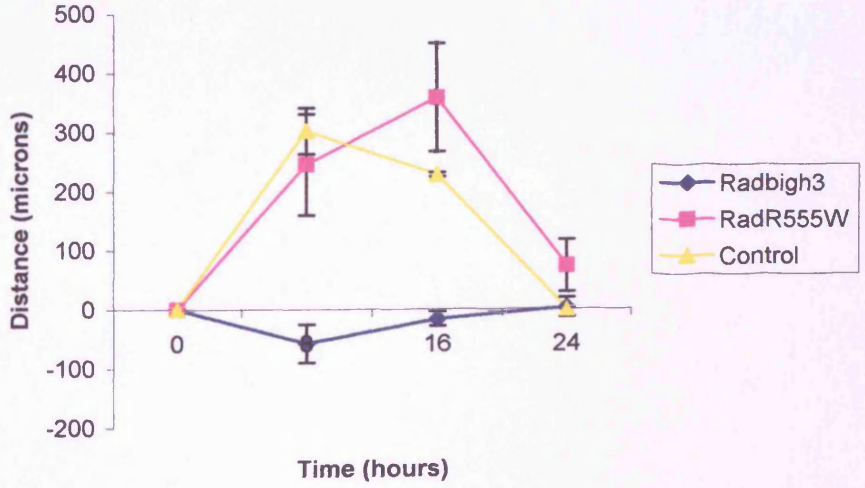

Figure 6.7: Corneal keratocyte migration

Measurements were too variable to compare or draw any conclusions

Points represent mean values of the repeated experiments and error bars are ±SEM.

6.3.6 Apoptosis assay

The limitations that were encountered whilst carrying out the apoptosis assay with the flow cytometry were summarised in section 5.3.6. However both the epithelial cells and keratocytes which were transfected with RadR555W adenovirus seem to have a larger population that is apoptotic. This corresponds to higher levels of Annexin V and Propidium Iodide staining compared to Radβigh3 and Rad35 transfected cells (figure 6.8).

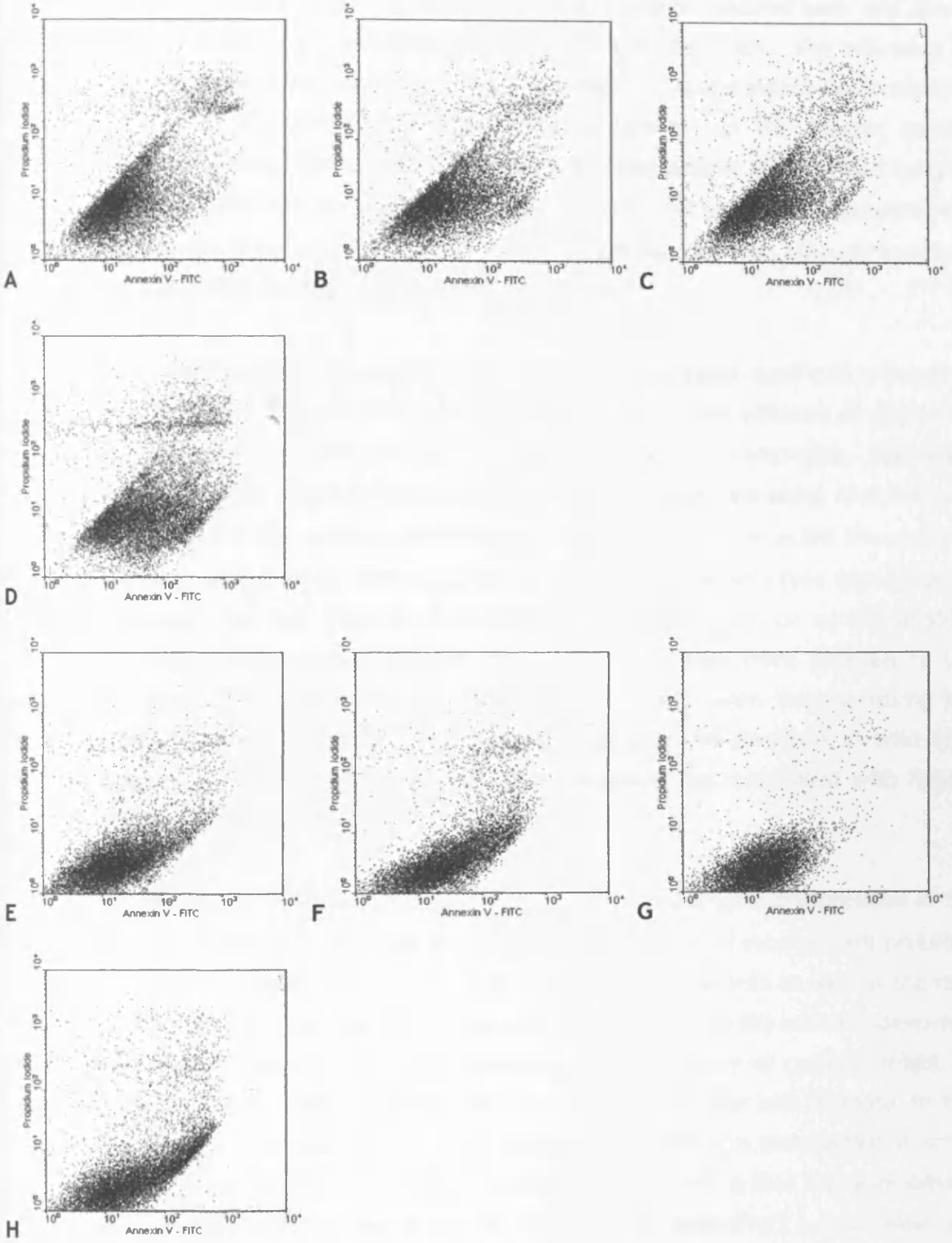

Figure 6.8: Apoptosis assay

Dot plots of the Annexin V-Propidium Iodide staining of adenovirally treated cells. A-D. Epithelial cells. E-H. Keratocytes. A&E. Radβigh3. B&F. RadR555W. C&G. Rad35. D&H: Etoposide

6.4 DISCUSSION

Recombinant adenoviruses allow transfer of cloned genes into cultured cells and strong expression with the aid of a constitutive promoter, in this case CMV. The efficiency of transfection is high even with low titres of the virus (figure 6.1) and allows examination of the effect the gene of interest has on the cells in culture. In this chapter corneal epithelial cells and keratocytes were transfected with recombinant adenoviruses carrying the wild type and R555W mutant βig-h3 genes, as well as a control adenovirus carrying the Lac Z reporter gene. These results gave us valuable information about the way the βigh3 gene may interact with the cells whilst expressed by them.

The corneal epithelial cells overexpressing wild type βig-h3 adhered significantly better to culture dishes than cells treated with the control adenovirus. The adhesion of cells when the mutant gene was overexpressed was decreased compare to the wild type. This might be associated with morphological/functional changes that could take place in these cells due to the presence of the mutant βig-h3 gene. The keratocytes reflected the opposite picture, where the adhesion was decreased in the presence of the wild type βigh-h3 gene. This could suggest that this increase is associated with the expression of the R5555W mutant gene. It is also interesting that when the keratocytes were exposed to the recombinant proteins they exhibited the reverse picture than when overexpressing the respective genes. Keratocytes adhered more efficiently in the presence of wild type protein, whereas in adenoviral transfection better adhesion was associated with R555W mutant transgene overexpression.

The proliferation patterns of epithelial cells and keratocytes during overexpression of the βigh3 genes were similar with the ones observed with the effects of recombinant proteins. The use of recombinant adenoviruses affected the viability of the cells as well as the rate of proliferation. The fact that the epithelial cells transfected with the control adenovirus showed a decrease in their growth rate, especially after 48 hours of culture, might be attributed to the virus itself. Decrease in the proliferation rate and increase in the apoptosis have been associated with control recombinant adenovirus transfection in some cell types (Teramoto et al, 1999 and 1995). However it is interesting that the recombinant adenoviruses carrying the βig-h3 transgene did not have the same effect on epithelial cell proliferation. βigh3, like TGF-β_1 which induces it, is thought to regulate the proliferation of different cell types in varying ways to achieve homeostasis (Doi et al, 2003, Grilliari et al, 2000, Skonier et al, 1994). Therefore expression of the βigh3 gene could contribute to the increasing rate of epithelial cell proliferation.

The migration assays did not provide much information about the ability of the transfected cells to migrate. Too many cells failed to migrate and in many cases started lifting off from the area where the scrape wound was created. Since this was a phenomenon which affected all cells irrespective of the virus that was used to transfect them and was absent when the cells were treated with the recombinant proteins, it could be associated with the characteristics the cells assume after infection with the adenoviruses.

The preliminary data from the Annexin V-Propidium Iodide assay suggested an increase of apoptosis in both cell types when the mutant R555W transgene was overexpressed (Figure 6.7). The cells with the wild type βig-h3 gene did not appear to have the same extent of apoptotic stained cells. Human corneal epithelial cell apoptosis was monitored by Morand et al, (2003) when the cells were transfected with mammalian expression plasmids carrying the R555W and R124C, but not with the wild type βig-h3 gene. The epithelial cells transfected with the control adenovirus appeared in some case to have a similar extent of apoptosis with the R555W mutant βig-h3 overexpressing cells (figure 6.8.C). This could further support the observation of decreased epithelial cell proliferation as an adenovirally-related effect. Non-virally treated negative control cells should be included upon repetition of the apoptosis assay for the quantification of the effects of the mutant and wild type transgenes.

7. CHAPTER SEVEN - GENERAL DISCUSSION

The stromal corneal dystrophies are a group of bilateral, autosomal dominant disorders. In most of the conditions there are signs at an early age on corneal examination. This is often well before symptoms develop. Some of them can be difficult to treat, since they keep re-appearing, even after corneal transplantation.

Accumulation of amyloid or hyaline material is a common finding in dystrophic corneas, however, the gene that appears to be mutated in a variety of superficial stromal dystrophies is βig-h3. Both this gene and its protein were discovered not long before they were associated with corneal dystrophies.

The role of keratoepithelin is still largely undefined in the normal cornea - as well as in other tissues where it is known to be expressed and act upon other cellular components. It also remains unknown how the normal role of keratoepithelin is affected by the mutations, occurring on hotspots on the gene. The association between keratoepithelin and subepithelial and stromal deposits has been shown with immunohistochemistry (Klintworth et al, 1998, Korvatska et al 1999 and 2000) in the corneas of affected individuals.

There is strong evidence that βig-h3 is important in the epithelium as observed by light and electron microscopy (Ridgway et al, 2000). The histological and ultrastructural findings indicate accumulation of deposits in the epithelial cell layer. Immunofluoresence has located the site of expression of βig-h3 in the ocular tissues. Keratoepithelin was found to be expressed in the corneal epithelium (Escribano et al, 1994), but also by corneal keratocytes (Korvatska et al, 1999).

The epithelial origin of the dystrophies can explain the recurrence of the disease in grafts from healthy donors. The epithelium on the donor cornea is renewed and derived from the recipient limbal stem cells. Therefore in the grafted cornea only the cells of the epithelial layer will carry the mutation for βig-h3, which seems to be enough for the recurrence of the characteristic accumulations in the epithelial/anterior stromal area.

In order to study the role of keratoepithelin in corneal dystrophies, the βig-h3 cDNA was manipulated with the tools of recombinant DNA technology and molecular biology. The βig-h3 cDNA was synthesised with RT-PCR from total RNA extracted from human skin fibroblasts. It was subsequently cloned to a variety of plasmid vectors for the appropriate

manipulations. In vitro mutagenesis gave rise to two mutant versions one with each mutation corresponding to the corneal dystrophies Thiel Behnke and Granular, R555Q (Okada et al, 1998) and R555W (Munier et al, 1997) respectively. Based on these cloned constructs three native recombinant proteins were synthesised as well as two replication deficient recombinant adenoviruses, expressing the wild type and R555W mutant βig-h3 genes. The recombinant normal and mutant genes were expressed in bovine corneal epithelial and keratocyte cell culture and the effects of recombinant mutant and wild type proteins were also examined. The species difference (human cDNA versus bovine cell culture) is not thought to pose an obstacle since keratoepithelin is highly conserved between species (90-93%) (Gibson et al, 1996, Hashimoto et al, 1996 and Skonier et al, 1994). Moreover the human constructs can be used in future eclectic experiments on human cell and organ culture. The following tables (7.1 and 7.2) summarise the effects of the recombinant proteins and synthetic adenoviruses on corneal cell adhesion, migration, proliferation and apoptosis and highlight the similarities and differences between them.

Before drawing any conclusions about the cellular responses to wild type and mutant recombinant protein and transgenes delivered to the cells with the recombinant adenoviruses it is essential to establish the difference between the way these different constructs mediate their effects. The recombinant proteins remain in the extracellular space and may interact with the surface of the cells, possibly via integrins, to affect cell behaviour. The recombinant adenoviruses transport the recombinant βig-h3 gene in the cell cytoplasm where it is expressed with the constitutive CMV-IE promoter. Therefore the effects of the recombinant adenovirus transfection correspond to the overexpression of the wild type and mutant βig-h3 in corneal epithelial cell and keratocytes.

Construct	Assays	Epithelial cells	Keratocytes
Recombinant proteins	Adhesion	Promoted almost equally with all proteins*	Promoted with WT and less with the mutants. Significant difference between WT and R555W
	Proliferation	Upregulated with all proteins, especially WT* and R555W*	No effect
	Migration	Fastest with WT protein slowest with R555W. Significant difference between WT and R555W	No effect
	Apoptosis	Suspected apoptosis with the two mutants	Suspected apoptosis with the two mutants
Recombinant adenoviruses	Adhesion	Promoted with Radβigh3* and less efficiently with RadR555W	Promoted with RadR555W* and less efficiently with Radβigh3
	Proliferation	Upregulated with RadR555W and less efficiently with Radβigh3. Significant difference between RadR555W and Rad35	No effect
	Migration	No conclusion	No conclusion
	Apoptosis	Suspected apoptosis with the mutant	Suspected apoptosis with the mutant

Table 7.1: Summary of the effects of recombinant keratoepithelin and βg-h3 gene overexpression.

WT - Wild type. * Significant difference with the control cells

	Epithelial cells	Keratocytes
Similarities	Adhesion increases with wild type protein and virus	No effect on proliferation by either protein or virus
	Proliferation increases with R555W mutant protein and virus	Apoptosis possibly increases with mutant proteins and viruses
	Apoptosis possibly increases with mutant proteins and viruses	
Differences	Adhesion increases with mutant protein but not virus	Adhesion increases with wild type protein but not virus
	Proliferation increases with wild type virus but not protein	Adhesion increases with mutant virus but not protein

Table 7.2: Comparison of the effects of recombinant protein and transgene overexpression (virus). Table summarises the main similarities and differences between the effects of recombinant protein and adenoviral transgene overexpression.

It is important to link the observations summarised in tables 7.1 and 7.2 with the physiology of the normal cornea and the clinical presentation of corneal dystrophies. In the case of extracellular protein-induced effects it is essential to remember that these observations were derived from cultured cells in the absence of other corneal-specific factors and aggregated deposits, which would accompany the dystrophies.

Epithelial cell adhesion does not seem to change in response to extracellular effect between normal and mutant protein. Similarly, no difference was exhibited in the migration and proliferation of corneal keratocytes in the presence of recombinant proteins. The keratocyte adhesion does not change significantly between wild type and mutant recombinant proteins but seems to be inversely proportional to R555W mutant concentration. This may suggest a putative alteration in the keratocyte response to mutant keratoepithelin in the Granular dystrophy affected corneal stroma.

Epithelial cell proliferation does not appear different between wild type and R555W mutant proteins, but it decreases in the presence of R555Q protein. This protein may also induce epithelial cell apoptosis as was suggested from the Annexin V assay. These two effects could be related to the erosions, which are associated with Thiel Behnke dystrophy, as well as the irregular and degenerate epithelium with vacuolated cells,

aggregates of cytokeratin filaments and areas of poor attachment to the substratum (Ridgway et al, 2000). The superficial layers of the epithelial cells have weak inter-connections and seem ready to detach from the rest of the epithelium in this dystrophy.

The epithelial cells seem to migrate slower in the presence of R555W mutant protein than the wild type, this could potentially affect the centripetal migration (Shapiro et al, 1981) of epithelial cells and the renewal rate of the corneal epithelium in Granular dystrophy. The suggestion that epithelial cells and keratocytes have increased apoptosis both when cultured with the recombinant proteins and when transfected with the recombinant adenoviruses could explain the generation of keratocytes and epithelial cells which were observed ultrastructurally in patients with primary and recurrent Granular dystrophy (Akhtar et al, 1999). Apoptosis is a complex process which involves numerous pathways. Keratoepithelin may induce apotosis by interacting with surrounding cells, directly, by binding to cellular receptors or through other members of the extracellular matrix. It has been suggested that mutated keratoepithelin could induce apoptosis through an integrin-related pathway.

Overexpression of mutant R555W gene results in increase of the proliferation of corneal epithelial cells. The levels of keratoepithelin in patients with Granular dystrophy are more plentiful than in unaffected individuals (Klintworth et al, 1998) and this has been suggested to take place due to polymerisation of the protein into insoluble fibrils. Could it be possible that if epithelial cell proliferation is increased in vivo in response to the mutant gene, that this would result in higher expression, and therefore extracellular accumulation of keratoepithelin?

Purified keratoepithelin can bind to collagen I & IV, fibronectin, fibrillin, laminin (Billings et al, 2002, Kim et al, 2002) and it has been found to co-localise with the deposits in the dystrophic stroma (Korvatska et al, 1999). The abnormal proteoglycans and disorganisation of collagen fibrils observed in electron microscope pictures (Akhtar et al, 1999) could result from the deposits and abnormal interaction with the mutant protein. However different R124 and R555 mutant recombinant proteins did not appear to exhibit different biochemical and molecular properties than the wild type protein (Kim et al, 2002).

Keratoepithelin is one of the major proteins in the normal cornea, where it is present in the full size as well as in a variety of proteolysis products. Although the reason for this is not known, it is interesting that in both amyloid and non-amyloid dystrophies the pattern

of the different isoforms changes, maybe due to abnormal proteolysis (Korvatska et al, 1999). However, fibroblasts extracted from the affected corneas did not produce any aberrant isoforms of keratoepithelin in culture.

The fact that the formation of the deposits in the corneal dystrophies is tissue specific was supported by the Schmitt-Bernard et al (2002) when they demonstrated that amyloid deposits where absent in the skin of Lattice dystrophy patients. Adult skin is one of the tissues where βig-h3 is transcribed and secreted by dermal fibroblasts (LeBaron et al, 1995). The deposits could be a result of cornea specific protein-protein interactions as happens in the case of choroideremia, another ocular disease where the mutated protein interacts with a retinal specific Rab27 protein in order to produce the disease (Seabra et al, 1995). Alternatively, abnormal protein processing by corneal specific proteases could be responsible for the deposits.

The results that were presented in this thesis and the recombinant constructs that were created could be used to explore further the role of keratoepithelin in the corneal dystrophies.

The transfected with overexpressing βig-h3 transgene corneal cells can be used as a model to examine their ultrastructure with electron microscopy. The differences between cells that overexpress wild type and mutant genes can be compared as well as the differences from control cells which are not transfected. Especially interesting aspect of this analysis would be investigating the formation or secretion of amyloid and granular aggregates. The availability of the recombinant proteins can also serve as a powerful tool to enhance our understanding on the mechanism of interaction of keratoepithelin with other important corneal proteins, especially those that have been identified to be part of the dystrophic aggregates, e.g. cytokeratin 19, immunoglobulins etc.

The air interface model of organ corneal culture is probably the most efficient model for studying whole corneas ex vivo without compromising the organ integrity (Foreman et al, 1996) where the overall structure and stratification are maintained. Other models of corneal organ culture, where the cornea is submerged in medium, result in loss of epithelial cell layer, epithelial and stromal oedema and keratocyte deterioration. (Richard et al, 1991). This system allows the simultaneous study of all five corneal layers, even when the target is one of them, such as the epithelium. Therefore the interaction between different cell layers is possible and the effects of certain structures (e.g. limbus)

can be observed (e.g. in wound healing studies when cells migrate to the wound from the basal and peripheral areas). Overexpression in the organ culture model can be achieved with the recombinant adenoviruses, thereby creating a cultured model for the study of the corneal dystrophies. The induced changes in the following areas resulting from expression of different mutant constructs could be determined in an attempt to understand the aetiology between different types of dystrophies: cell morphology, epithelial adhesion, extracellular deposits and wound healing.

βig-h3 is induced by TGF-β (Skonier et al 1992), a growth factor which plays an important role in growth and differentiation. TGF-β exerts its effects on wounded or developing tissues by the controlled regulation of a number of genes. It induces the expression and secretion of matrix proteins whereas it has been reported to inhibit the rate of corneal re-epithelialisation (Foreman et al, 1996) and epithelial cell proliferation (Mishima et al, 1992). The temporal expression of βig-h3 mRNA during corneal healing and development (Rawe et al, 1997) especially in the early stages (El-Shabrawi et al, 1998) indicates that keratoepithelin plays a role in the synthesis of new tissue, which it could regulate. The role of βig-h3 during wound healing can also be studied in the cornea by infecting pre- and post wounded corneas with the recombinant adenoviral constructs.

The adenoviruses may "mask" some of the effects of the βig-h3 overexpression due to the effects they impose on the cultured cells, determined from the control virus Rad35. Decrease in the proliferation rate and increase in the apoptosis have been associated with control recombinant adenovirus transfection in some cell types (Teramoto et al, 1999 and 1995). This problem could be avoided by following either of these two non-viral approaches: transfecting the cells with mammalian expression plasmids, in which the wild type and mutant βig-h3 constructs are already cloned or by transducing the recombinant protein in intact cells in culture or tissue by fusing it with the TAT sequence (Guo et al, 2004).

The interaction between cell and extracellular matrix components plays a crucial role in cell proliferation, apoptosis and tumourigenesis. Keratoepithelin, being a component of the extracellular matrix has been investigated regarding its role in human diseases (O'Brien et al, 1996, Gilbert et al, 1998, Schneider et al, 2002). Like its inducer TGF-β, βig-h3 has been implicated with regulation of gene expression in a variety of cell types (see section 1.5.7). It is possible that application of recombinant keratoepithelin causes a change in the gene expression profile of the cultured cells. The identification of possible

genes up- or down-regulated in response to wild type and mutant keratoepithelin could be assessed with microarray analysis.

The experimental procedures carried out during this project offered some valuable information about the difference of the effects of wild type and mutant βig-h3 gene and protein on corneal keratocytes and epithelial cells. These results and recombinant tools can be used to further improve our understanding in both the role of keratoepithelin in corneal dystrophies and the mechanism by which these disorders arise.

MATERIALS

1. PLASMIDS

pΔE1-cI (7.7kb) A combination of two different plasmids: pΔE1sp1A (Microbix) and pcI (Promega). Both plasmids were digested with BamHI and BglII and pCI was inserted into the polycloning restriction enzyme site of pΔE1sp1A. Ampicillin resistant.

Multiple cloning site: NheI
XhoI
EcoRI
MluI
KpnI
XbaI
SalI
AccI
SmaI
BstXI
NotI

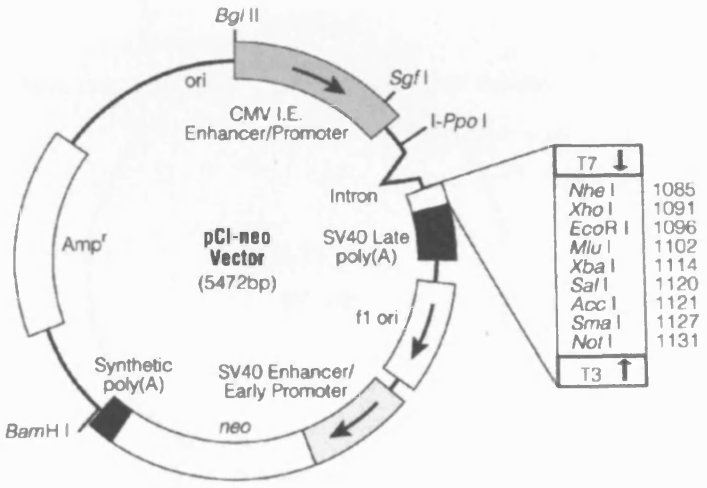

Figure 1: pCI-neo Vector

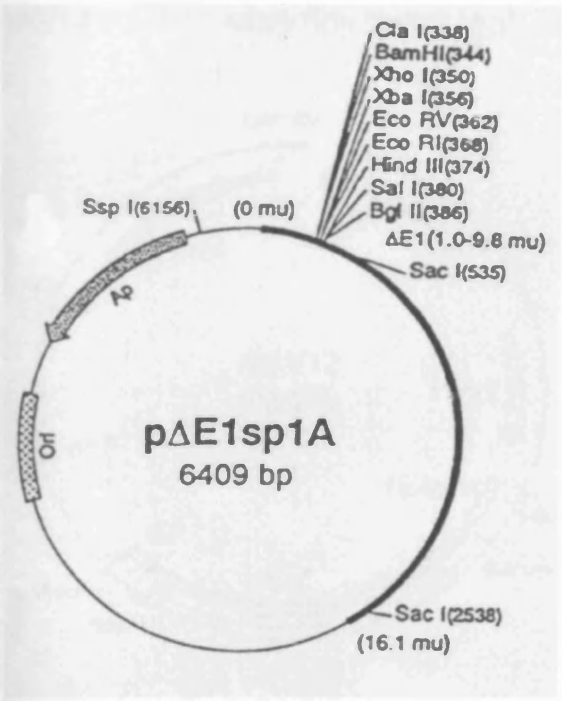

Figure 2: pΔE1sp1A vector

pJM17 (40.07kb) Ampicillin resistant.

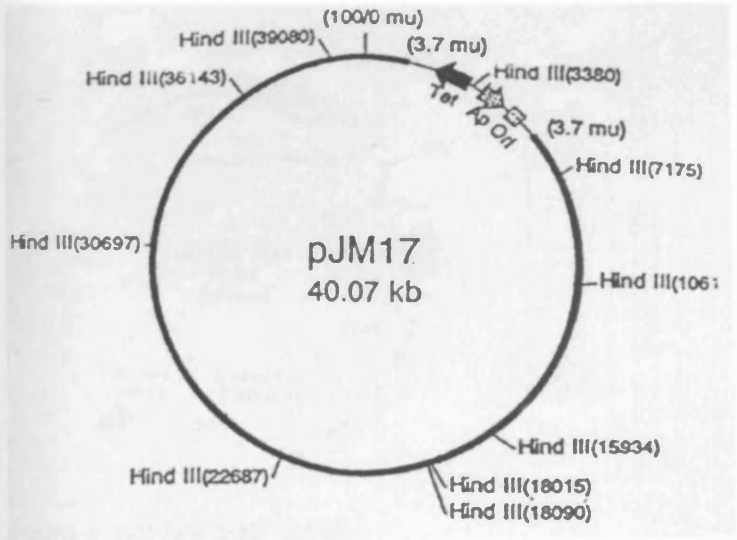

Figure 3: pJM17 vector

pMV12 (13.0kb) Ampicillin resistant

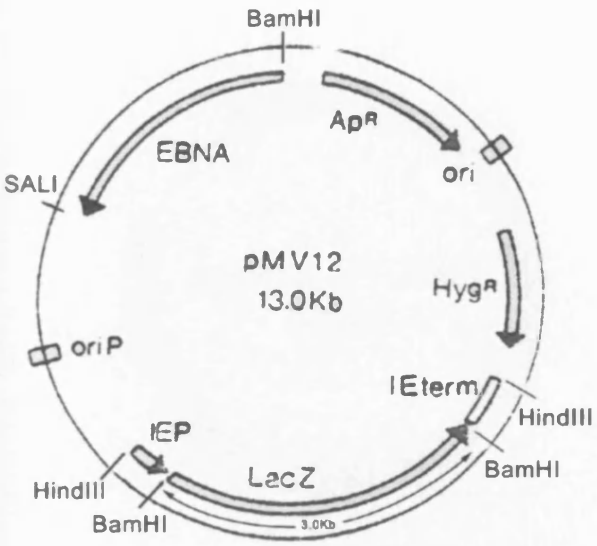

Figure 4: pMV12 vector

pALTER-MAX (5.5kb) Chloramphenicol resistant and /or ampicillin resistant

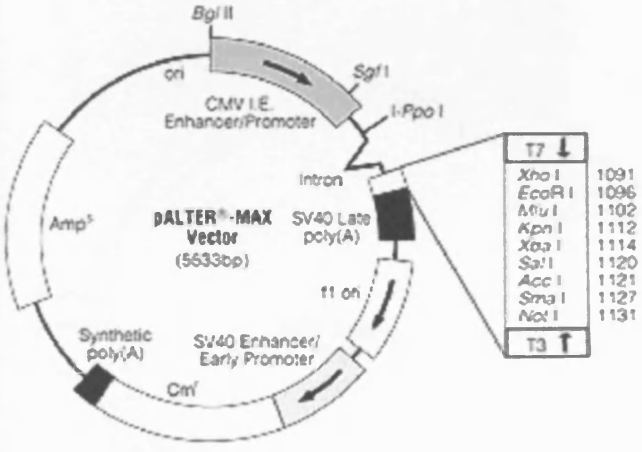

Figure 5: pALTER-MAX vector

pCR®2.1-TOPO (3.9kb) Kanamycin and ampicillin resistant

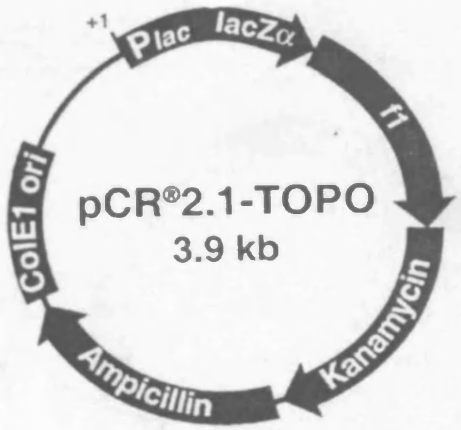

Figure 6: pCR® 2.1-TOPO vector

pET-23c (3.67kb) ampicillin resistant

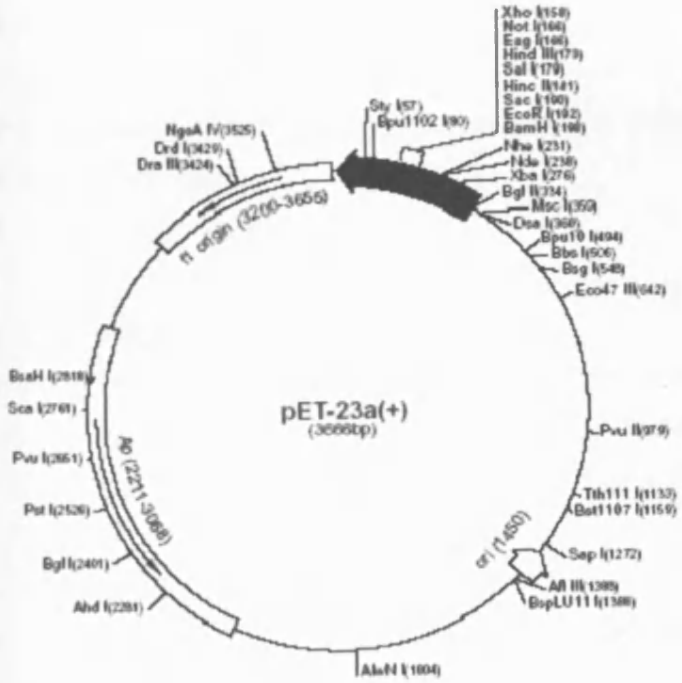

Figure 7: pET-23c vector (Novagen)

pET-16b (5.7kb) amplicillin resistant

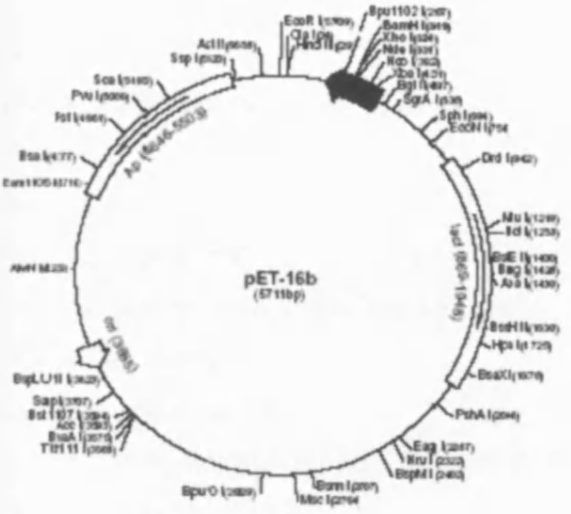

Figure 8: pET16b vector (Novagen)

2. BACTERIAL CELLS

JM109 (Promega)

ES301 mutS (Promega)

DH5α (Molecular Medicine Dept., University of Manchester)

TOPOF' (Invitrogen)

BL21(DE3)pLysS (Novagen)

3. CELL LINES

293 cells (Molecular Medicine Dept., University of Manchester)

HeLa (Molecular Medicine Dept., University of Manchester)

CRL11516 Human corneal epithelial cell line (ATCC)

4. REAGENTS AND CHEMICALS

All reagents used were Molecular Biology/Cell Culture grade purchased from Sigma and AnalaR BDH, unless otherwise stated.

5. NUCLEIC ACIDS

Primers and muagenic oligonucleotides	MWG
DNA ladder 100bp	MBI Fermentas

Gene ruler 1kb	MBI Fermentas
Mass Ruler	FMI Fermentas

6. KITS

AMV Reverse Transcription System	Promega
Premix	Advanced Biotechnologies
MegaMix	Helena Biosciences
Extensor Long PCR	Advanced Biotechnologies
Thermo Sequenance II Dye Terminator	
TOPO TA Cloning	Invitrogen
Cycle Sequencing Kit	Amersham Pharmacia Biotech Inc
Altered Sites Mammalian Mutagenesis System	Promega
QIAGEN Plasmid Mini Kit	Qiagen
QIAGEN Plasmid Maxi Kit	Qiagen
QIAGEN PCR Purification kit	Qiagen
TACS^{TM} Annexin V-FITC detection kit	R&D Systems

7. ENZYMES

AluI	New England Biolabs
CIAP Alkaline Phosphatase	Gibco BRL
HindIII	New England Biolabs
MluI	New England Biolabs
PFU Taq	Stratagene
SpeI	New England Biolabs
T4 DNA ligase	Gibco BRL
XbaI	New England Biolabs
XhoI	New England Biolabs
rLysozyme	Novagen
Benzonase Nuclease	Novagen
RNAse I	Invitrogen

8. PROTEIN EXPRESSION AND ANALYSIS REAGENTS

BugBuster	Novagen
Protease Inhibtor Set III	Calbiochem
Coomassie Brilliant Blue R-250 Stain and Destain	BioRad
Laemmli sample buffer	BioRad

10x Tris/glycine/SDS buffer	BioRad
10x Tris/CAPS cathode buffer	BioRad
Ponceau S	Sigma
Western Blotting Luminol Reagent	Santa Cruz Biotechnology

9. MOLECULAR BIOLOGY SOLUTIONS

Anglian Buffer (10x)

166mM Ammonium sulphate

670mM Tris HCl (pH 8.0)

37mM Magnesium Chloride

1.7mg/m BSA

10x TBE

10.8% Trizma base

5.5% Orthoboric Acid

0.4% 0.5M EDTA

make up to total with H_2O

0.5M EDTA (pH8.0)

186g EDTA

800ml dH_2O

measure pH with 5M NaOH until pH 8.0,

then make up to 1Lt checking pH at 990ml.

1M Tris Hcl pH 8.0

121.4g Tris

800ml H_2O

pH until 8 with HCl and make up to 1Lt

TE buffer

10mM Tris HCL pH 8.0

1mM EDTA pH 8.0

Loading Buffer

5ml 10xTBE

49ml Glycerol

0.1ml 10% (v/v) SDS
Bromophenol Blue
Xylene cyanol

Ethidium Bromide (10mg/ml)
1g EthBr
100ml dH_2O
Stir until dissolved
Store in dark at 4°C

10. BIOCHEMISTRY REAGENTS
4x Sample buffer
3.04g Tris base
8g SDS
40ml glycerol
30ml dH_2O
pH to 6.8 with concentrated HCl
add 20ml β-mercaptoethanol
make up to 100ml with dH_2O dH_2O

10% Resolving gel
(For 2 gels)
4ml H_2O
3.3ml 30% acrylamide mix
2.5ml 1.5M Tris (pH 8.8)
0.1ml 10% SDS
0.1ml 10% ammonium persulfate
4μl TEMED

Stacking gel
(For 2 gels)
2.7ml H_2O
670μl 30% acrylamide mix
500μl 1.0M Tris (pH 6.8)
40μl 10% SDS
40μl ammonium persulfate

4μl TEMED

11. BACTERIAL CULTURE MEDIA

LB broth

10g Tryptone

5g Yeast Extract

5g NaCl

make up to 1L with dH_2O

Autoclave

LB agar

10g Tryptone

5g Yeast Extract

5g NaCl

make up to 1L with dH_2O

Autoclave with 15g Agar

Allow temperature to drop to 45°C before adding antibiotics

Pour to plates, allow to set, cover and store at 4°C.

SOC

2g Tryptone

0.5g Yeast Extract

1ml 1M NaCl

0.25ml 1M KCl

97ml dH_2O

Stir to dissolve and autoclave

Allow to cool to room temperature

Add 1ml 1M $MgCl_2$ 1M $MgSO_4$

1ml 2M glucose

Check pH is 7.0

Filter-sterilise through 0.2μm filter

Store in 20ml aliquots at room temperature

IPTG (0.1M)

1.2g IPTG

dissolve to 50ml dH_2O

Filter-sterilise through a 0.2μm filter

Store in 5ml aliquots at -20°C

X-gal

100mg

dissolve to 2ml with N,N'-dimethylformamide

Store in 0.5ml aliquots in the dark at -20°C

12. Tissue Culture Media

293 medium

500ml Minimum Essential Medium Eagle

50ml Fetal Calf Serum

5ml MEM Non Essential Amino Acids

5ml 2mM L-glutamine

5ml Penicillin Streptomycin

Grow all

500ml DMEM

50ml Horse Serum

25ml Newborn Calf Serum

5ml MEM Non Essential Amino Acids

5ml Sodium pyruvate

5ml 2mM L-Glutamine

RCA medium

500ml DMEM

10ml FCS

5ml MEM Non Essential Amino Acids

5ml Sodium Pyruvate

5ml 2mM L-Glutamine

Maintainance medium

500ml DMEM

50ml FCS

5ml 2mM L-Glutamine

5ml Penicillin-Streptomycin

Freezing medium for 293 cells and HeLa

50% Dulbecco's Modified Eagle's Mediium

10% Dimethyl sulphoxide (DMSO)

40% Fetal Calf Serum

Keratinocyte serum free medium

Keratinocyte serum-free medium (Invitrogen)

5ng/ml human EGF

0.05mg/ml bovine pituitary extract

0.005mg/ml insulin

500ng/ml hydrocortisone

5ml 2mM L-Glutamine

DMEM/F10 medium

100ml DMEM

100ml F-10 medium

10ml FCS

10ml Donor Horse Serum

1ml DMSO

1ml 1mg/ml insulin

20μl 1mg/ml cholera toxin

2ml 2mM L-glutamine

2ml Penicillin-Streptomycin

Caesium Chloride purification Buffers

Buffer A

10mM Tris pH7.5

1mM Magnesium Chloride

135mM Sodium Chloride

Buffer B

Buffer A + 10% glycerol

13 ORGAN CULTURE SOLUTIONS AND MEDIA

All solutions (apart from Betadine) and media were passed trough a 0.2μm filter

20% Betadine

20ml Betadine

80ml sterile PBS

5% Betadine

5ml Betadine

95ml sterile PBS

Antibiotics and Glutamine solution

1g streptomycin sulphate

1g kanamycin sulphate

600mg benzylpenicillin

1.46g L-glutamine

dH_2O to 100ml

Sodium Bicarbonate

7.4g Sodium bibarbonate

in 100ml dH_2O

DMEM 1% agar 1% gelatin

2gr Agar

2gr Gelatin

Mixed with 100ml dH_2O and autoclaved

Then add 20ml 10×DMEM

10ml 7.4% salt solution

2ml antibiotics and glutamine solution

1ml Fungizone

dH_2O to 200ml

DMEM 20% FCS

20ml 10×DMEM

40ml FCS

10ml 7.4% salt solution

2ml Antibiotics and glutamine

1ml Fungizone

127ml dH_2O

MEM with 20% FCS

20ml 10xMEM

40ml FCS

10ml 7.4&% salt solution

2ml Antibiotics & glutamine

1ml fungisone

2ml ddH_2O

Serum-free Trowell's T8

97ml Trowell's T8 medium

2ml Antibiotics and glutamine solution

1ml Fungizone

13. FIXATION AND STAINING SOLUTIONS

4% paraformaldehyde

Dissolve 40g paraformaldehyde in 300ml H_2O

heated at 60-70°C. Add NaOH until solution clears.

Dissolve 15.5g Na_2HPO_4-$2H_2O$ and 34g sucrose in 500ml H_2O.

Filter dissolved paraformaldehyde into ice-cold phosphare buffer.

Adjust pH to 7.4 and make volume up to 1Lt.

Phosphate Buffer

8g NaCl

0.2g KCl

1.44g Na_2HPO_4

0.24g KH_2PO_4

in 800ml H_2O

Adjust pH to 7. 4 with HCl

Add H_2O to 1Lt

Sterilise by autoclaving

X-gal staining solution

42mg Potassium Ferrocyanide

32mg Potassium Ferricyanide

8mg Magnesium Chloride

20mg X-gal in 500μl DMSO

make to 20ml with Phosphate Buffer

REFERENCES

Abraham, N.G.; Da Silva, J.L.; Lavrovsky, Y.; Stoltz, R.A.; Kappas, A.; Dunn, M.W.; Schwartzman, M.L. (1995). "Adenovirus-mediated heme oxygenase-1 gene transfer into rabbit ocular tissues" Invest Ophthalmol Vis Sci 36 (11):2202-2209

Adam, S.A.; Dreyfuss, G. (1987). "Adenovirus proteins associated with mRNA and hnRNA of infected HeLa cells" J Virol 61:3276-3283

Afshari, N. A., Mullally, J. E.; Afshari, M. A.; Steinert, R. F.; Adamis, A. P.; Azar, D. T.; Talamo, J. H.; Dohlman, C. H.; Dryja, T. P. (2001). "Survey of patients with granular, lattice, avellino, and Reis-Bucklers corneal dystrophies for mutations in the BIGH3 and gelsolin genes." Arch Ophthalmol 119(1):16-22.

Aitkenhead, M.; Wang, S. J.; Nakatsu, M. N.; Mestas, J.; Heard, C.; Hughes, C. C (2002). "Identification of endothelial cell genes expressed in an in vitro model of angiogenesis: induction of ESM-1, (beta)ig-h3, and NrCAM." Microvasc Res 63(2):159-71.

Akhtar, S.; Meek, K. M.; Ridgway, A. E.; Bonshek, R. E.; Bron, A. J. (1999). "Deposits and proteoglycan changes in primary and recurrent granular dystrophy of the cornea." Arch Ophthalmol 117(3):310-21.

Akiya, S.; Brown, SI. (1970) "Granular dystrophy of the cornea: characteristic electron microscope lesion" Arch Ophthalmol 84: 179-192

Akiya, S.; Brown, S. I. (1971). "The ultrastructure of Reis-Bucklers' dystrophy." Am. J. Ophthal. 72: 549-554.

Arancibia-Carcamo, C.V.; Oral, H.B.; Haskard, D.O.; Larkin, D.F.P.; George, A.J.T. (1998). "Lipoadenofection-mediated gene delivery to the corneal endothelium." Transplantation 65:62-67

Assouline, M.; Chew, S.J.; Thompson, H.W.; Beuerman, R. (1992). "Effect of growth factors in collagen lattice contraction by human keratocytes." Invest Ophthalmol Vis Sci 33:1742

Bae, J. S.; Lee, S. H.; Kim, J. E.; Choi, J. Y.; Park, R. W.; Yong Park, J.; Park, H. S.; Sohn, Y. S.; Lee, D. S.; Bae Lee, E.; Kim, I. S. (2002). "Betaig-h3 supports keratinocyte adhesion, migration, and proliferation through alpha3beta1 integrin." Biochem Biophys Res Commun 294(5):940-8.

Barry, P.A.; Petroll, W.M.; Andrews, P.M; Cavanagh, H.D.; Jester, J.V. (1995). "The spatial organisation of corneal endothelial cytoskeletal proteins and their relationship to the apical junctional complex." Invest Ophthalmol Vis Sci 36(6):1115-24

Bergelson, B. A.; Fishman, R.F.; Tommaso, C. L. (1997). "Abrupt vessel closure: changing importance, management, and consequences." Am Heart J 134(3):362-81.

Billings, P.C.; Whitbeck, J.C.; Adams, C.S.; Abrams, W.R.; Cohen, A.J.; Engelsberg, B.N.; Howard, P.S.; Rosenbloom, J. (2002). "The transforming growth factor-β-inducible matrix protein βig-h3 interacts with fibronectin" J Biol Chem 277:28003-9

Binder, P.,S.; Rock, M.,E.; Schmidt, K.,C.; Anderson, J.A. (1991). "High-voltage electron microscopy of normal human cornea." Invest Ophthalmol Vis Sci 32:2234

Booth, D. R.; Sunde, M.; Belloti, V.; Robinason, C. V.; Hutchinson, W. L.; Fraser, P. E.; Hawkins P. N.; Robson, C. M.; Radford, S. E.; Blake, C. C.; Pepys, M. B. (1997). "Instability, unfolding and aggregation of human lysozyme variantsunderlying amyloid fibrillogenesis" Nature 385:787-93

Broekhuyse, R.M. (1974). "Tear lactoferrin A bacteriostatic and complexing protein." Invest Ophthalmol 13:550-554

Bron A.J. (1973). "Vortex patterns of the corneal epithelium" Trans Ophthalmol Soc UK 93(0):361-75

Bron, A. J. (2000). "Genetics of the corneal dystrophies: what we have learned in the past twenty-five years." Cornea 19(5):699-711.

Budenz, D.L.; Bennett, J.; Alonso, L.; Maguire, A. (1995). " In vivo gene transfer into murine corneal endothelial and trabecular meshwork cells." Invest Ophthalmol Vis Sci 36 (11):2211-2215

Burgelson, J.M.; Cunningham, J.A.; Droguett, G.; Kurt-Jones, E.A.; Krithivas, A.; Hong, J.S. (1997). "Isolation of a common receptor for coxsackie B viruses and adenoviruses 2 and 5." Science 275:1320-1323

Carson, D. D.; Lagow, E.; Thathiah, A.; Al-Shami, R.; Farach-Carson, M. C.; Vernon, M.; Yuan, L.; Fritz, M. A.; Lessey, B. (2002). "Changes in gene expression during the early to mid-luteal (receptive phase) transition in human endometrium detected by high-density microarray screening." Mol Hum Reprod 8(9):871-9.

Carr, M. D.; Bloemink, M. J.; Dentten, E.; Whelan, A. O.; Gordon, S. V.; Kelly, G.; Frenkiel, T. A.; Hewinson, R. G.; Williamson, R. A. (2003). "Solution structure of the Mycobacterium tuberculosis complex protein MPB70: from tuberculosis pathogenesis to inherited human corneal desease." J Biol Chem 278(44):43736-43.

Carlson, E.C.; Liu, C.Y.; Yang, X.; Greory, M.; Sander, B.; Drazba, J.; Perez, V.L. (2004). "In vivo gene delivery and visualisation of corneal stromal cells using an adenoviral vector and keratocyte-specific promoter" 45(7):2194-200

Carrington, L.M.; Southgate, T.; Saxby, L.A.; Abul-Hassan, K.; Maleniak, T.C.; Castro, M.G., Boulton, M.E. (2000). "Adenovirus-mediated gene transfer to human lens epithelial cells in organ culture." J Cataract Refract Surg 26(6):887-92

Castro, M.G.; Goya, R.G.; Sosa, Y.E.; Rowe, J.; Larregina, A.; Morelli, A.; Lowenstein, P.R. (1997). "Expression of transgenes in normal and neoplastic anterior pituitary cells using recombinant adenoviruses: Long term expression, cell cycle dependency, and effects on hormone secretion." Endocrinology 138 (5):2184-2194

Cayrol, C.; Flemington, E.K. (1995). "Identification of cellular target genes of the Epstein-Barr virus transactivator Zta: activation of transforming growth factor βigh3 (TGF-βigh3) and TGF-β1." J Virol 1995; 69 (7):4207-4212

Chardonnet, Y. and S. Dales (1970). "Early events in the interaction of adenoviruses with HeLa cells. I. Penetration of type 5 and intracellular release of the DNA genome." Virology 40(3):462-77.

Chau, H. M.; Ha, N. T.; Cung, L. X.; Thanh, T. K.; Fujiki, K.; Murakami, A.; Kanai, A. (2003). "H626R and R124C mutations of the TGFBI (BIGH3) gene caused lattice corneal dystrophy in Vietnamese people." Br J Ophthalmol 87(6):686-9.

Chiambaretta, F.; Blanchon, L.; Rabier, B; Kao, W.W.Y.; Liu, J.J.; Dastugue, B.; Rigal, D.; Sapin, V. (2002). "Regulation of corneal keratin-12 gene expression by the human Kruppel-like transcription factor 6" IOVS 43(11):3422-9

Chomczynski, P.; and Sacchi, N. (1987). "Single-step method of RNA isolation by acid guanidium thiocyanate-phenol-chloroform extraction." Anal. Biochem. 162 (1) 156-159

Cintron, C.; Kublin, C.L. (1997). " Regeneration of corneal tissue" Dev Biol; 61(2):346-57

Cenifanto, Y.M.; Kaufman, H.E. (1970). "Secretory immunoglobulin A and herpes keratitis." Infect Immun 2:778

Clout, N. J. and E. Hohenester (2003). "A model of FAS1 domain 4 of the corneal protein beta(ig)-h3 gives a clearer view on corneal dystrophies." Mol Vis 9:440-8.

Clout, N. J.; Tisi, D.; Hohenester, E. (2003). "Novel fold revealed by the structure of a FAS1 domain pair from the insect cell adhesion molecule fasciclin I." Structure (Camb) 11(2):197-203.

Cogan, D.G., Donaldson, D.D., Kuwabara, T., Marshall, D. (1964). "Microcystic dystrophy of the corneal epithelium." Trans Am Ophthalmol Soc 63:213

Cohen, A. K., Rode, H. N., Helleiner, C. W. (1972). "The time of synthesis of satellite DNA in mouse cells (L cells)." Can J Biochem 50(2):229-31.

Dale, S.; Chardonnet, Y. (1973). "Early events in the interaction of adenovirus with HeLa cells. IV association with microtubules and the nuclear pore complex during vectorial movement in the inoculum" 56:456-483

Darby, I. A.; Bisucci, T.; Pittet, B.; Garbin, S.; Gabbiani, G.; Desmouliere, A. (2002). "Skin flap-induced regression of granulation tissue correlates with reduced growth factor and increased metalloproteinase expression." J Pathol 197(1):117-27.

Dales, S.; Chardonnet, Y. (1973). "Early events in the interaction of adenoviruses with HeLa cells. IV. Association with microtubules and the nuclear pore complex during vectorial movement of the inoculum." Virology 56(2):465-83.

Davanger, M.; Evensen, A. (1971). "Role of the pericorneal papillary structure in renewal of corneal epithelium" Nature 229(5286):560-1

De la Chapelle, A. (1992). "Gelsolin-derived familial amyloidosis caused by asparagine or tyrosine substitution for aspartic acid at residue 187." Nature 2:157-160

Devaux, C.; Caillet-Boudin, M. L.; Jacrot, B.; Boulanger, P. (1987). "Crystallization, enzymatic cleavage, and the polarity of the adenovirus type 2 fiber." Virology 161(1): 121-8.

D'Halluin, J.C.; Milleville, M.; Boulanger, P.A.; Martin, G.R. (1978). "Temperature sensitive mutant of adenovirus type 2 blocked in virion assembly: accumulation of light intermediate particles." J Virol 26:344-356

Dieudonne, S. C.; Kerr, J. M.; Xu, T.; Sommer, B.; DeRubeis, A. R.; Kuznetsov, S. A.; Kim, I. S.; Gehron Robey, P.; Young, M. F. (1999). "Differential display of human marrow stromal cells reveals unique mRNA expression patterns in response to dexamethasone." J Cell Biochem 76(2):231-43.

Dighiero, P.; Drunat, S.; Ellies, P.; D'Hermies, F.; Savoldelli, M.; Legeais, J. M.; Renard, G.; Delpech, M.; Grateau, G.; Valleix, S. (2000). "A new mutation (A546T) of the betaig-h3 gene responsible for a French lattice corneal dystrophy type IIIA." Am J Ophthalmol 129(2):248-51.

Dighiero, P.; Valleix, S.; D'Hermies, F.; Drunat, S.; Ellies, P.; Savoldelli, M.; Pouliquen, Y.; Delpech, M.; Legeais, J. M.; Renard, G. (2000). "Clinical, histologic, and ultrastructural features of the corneal dystrophy caused by the R124L mutation of the BIGH3 gene." Ophthalmology 107(7):1353-7.

Dilly, P.N. (1994). "Structre and function of the tear film" Adv Exp Med Biol 350:239-47

Dion, L.D.; Fang, J.; Garver, R.I. Jr. (1996). "Spernatant rescue assay vs. polymerase chain reaction for detection of wild type adenovirus-contaminating recombinant adenovirus stocks." J Virol Meth 56:99-107

Doane, K.J.; Yang, G.; Birk, D.E. (1992). "Corneal cell-matrix interactions: type VI collagen promotes adhesion and spreading of corneal fibroblasts" Expe Cell Res 200(2):490-9

Doi, T.; Ohno, S.; Tanimoto, K.; Honda, K.; Tanaka, N.; Ohno-Nakahara, M.; Yoneno, K.; Suzuki, A.; Nakatani, Y.; Ueki, M.; Tanne, K. (2003). "Mechanical stimuli enhances the expression of RGD-CAP/betaig-h3 in the periodontal ligament." Arch Oral Biol 48(8):573-9.

Dota, A.; Nishida, K.; Honma, Y.; Adachi, W.; Kawasaki, S.; Quantock, A. J.; Kinoshita, S. (1998). "Gelatinous drop-like corneal dystrophy is not one of the beta ig-h3-mutated corneal amyloidoses." Am J Ophthalmol 126(6):832-3.

Dubendorff, J.W. and Studier, F.W. (1991). "Creation of a T7 autogene. Cloning and expression of the gene for bacteriophage T7 RNA polymerase under control of its cognate promoter" J Mol Biol 219:45-59

Duke-Elder, S.; Wybar, K.C. (1960). "The anatomy of the visual system. In: Duke-Elder S, ed. System of ophthalmology." London: Kimpton:92-131

Dunaief, J. L.; Ng, E. W.; Goldberg, M. F. (2001). "Corneal dystrophies of epithelial genesis: the possible therapeutic use of limbal stem cell transplantation." Arch Ophthalmol 119(1):120-2.

Eiberg, H.; Moller, H.U.; Berendt, I.; Mohr, J. (1995). "Assignment of granular corneal dystrophy Groenouw type I locus to within a 2cM interval." Eur J Hum Genet 2:132-138

El-Ashry, M. F.; El-Aziz, M. M.; Larkin, D. F.; Clarke, B.; Cree, I. A.; Hardcastle, A. J.; Bhattacharya, S. S.; Ebenezer, N. D. (2003). "A clinical, histopathological, and genetic study of Avellino corneal dystrophy in British families." Br J Ophthalmol 87(7):839-42.

Elkins T., Hortsch M., Bieber A.J., Snow P.M., Goodman C.S. (1990). "Drosophila fasciclin I is a novel homophilic adhesion molecule that along with fasciclin III can mediate cell sorting." J Cell Biol 110(5):1825-32

Ellies, P.; Bejjani, R. A.; Bourges, J. L.; Boelle, P. Y.; Renard, G.; Dighiero, P. (2003). "Phototherapeutic keratectomy for BIGH3-linked corneal dystrophy recurring after penetrating keratoplasty." Ophthalmology 110(6):1119-25.

Ellies, P.; Renard, G.; Valleix, S.; Boelle, P. Y.; Dighiero, P (2002). "Clinical outcome of eight BIGH3-linked corneal dystrophies." Ophthalmology 109(4):793-7.

El-Shabrawi, Y.; Kubkin, .CL.; Cintron, C. (1998). " mRNA levels of α1(V1) collagen, α1 (XII) collagen, and βig in rabbit cornea during normal development and healing." Invest Ophthalmol Vis Sci 39 (1):36- 44

Endo, S.; Nguyen, T. H.; Fujiki, K.; Hotta, Y.; Nakayasu, K.; Yamaguchi, T.; Ishida, N.; Kanai, A (1999). "Leu518Pro mutation of the beta ig-h3 gene causes lattice corneal dystrophy type I." Am J Ophthalmol 128(1):104-6.

Escribano, J.; Hernando, N.; Ghosh, S.; Crabb, J.; Coca-Prados, M.. (1994). "cDNA from human ocular ciliary epithelium homologous to βig-h3 is preferentially expressed as a extracellular protein in the corneal epithelium." J Cell Physiol 160:511-521

Evans, R.M.; Fraser, N.; Ziff, E.; Weber, J.; Wilson, M.; Darnel, J.E. (1997). "The initiation sites for RNA transcription in AD2 DNA." Cell 12:733-739

Fawcett DW. (1996) "On the occurrence of a fibrous lamina on the inner aspect of the nuclear envelope in certain cells of vertebrates." Am J Anat Jul;119(1):129-45

Ferry, A.P., Benson, W.H.; Weiberg, R.S. (1997). "Combined granular-lattice ("Avellino") corneal dystrophy." Trans Am Ophthalmol Soc 95:61-77

Fehervari, Z.; Rayner, S. A.; Oral, H. B.; George, A. J.; Larkin, D. F. (1997). "Gene transfer to ex vivo stored corneas." Cornea 16(4):459-64.

Felix, C. A.; Kappel, C. C.; Mitsudomi, T.; Nau, M. M.; Tsokos, M.; Crouch, G. D.; Nisen, P. D.; Winick, N. J.; Helman, L. J. (1992). "Frequency and diversity of p53 mutations in childhood rhabdomyosarcoma." Cancer Res 52(8):2243-7.

Fleming, AA.(1922). "One remarkable bacteriolytic element found in tissues and secretions." Proc R Soc Lond [Biol] 93:306

Fogle, J.A., Kenyon, K.R., Stark, W.J., Green, W.R. (1975). "Defective epithelial adhesion in anterior corneal dystrophies" Am J Ophthalmol 79:925-40

Folberg, R.; Alfonso, E.; Croxatto, J.O.; Driezen, N.G.; Panjwani, N.; Laibson, P.R.; Boruchoff, S.A.; Baum, J.; Malbran, E.S.; Fernadez-Meijide, R.(1998). "Cinical atypical granular corneal dystrophy with pathologic features of lattice-like amyloid deposits. A study of the families." Ophthalmology 95:46-51

Ford, L.C.; DeLange, R.J.; Petty, R.W. (1978). "Identification of a non-lysozymal bactericidal factor (beta lysin) in human ters and aqueous humor." Am J Ophthalmol 10:1585

Foreman, D.M.; Pancholi, S.; Jarvis-Evans, J.; McLeod, D.; Boulton, M.E. (1996) "A simple organ culture for assessing the effects of growth factors on corneal re-epithelialization." Exp Eye Res 62:555-564.

Frayer, W. C.; Blodi, F. C. (1959) "The lattice type of familial corneal degeneration: a histopathologic study." Arch. Ophthal. 61: 712-719.

Freshney, R.I. (2000). "Culture of animal cells; a manual of basic technique" New York Willey-Liss, 4th Edition

Fujiki, K.; Nakayasu, K.; (2001). "Corneal dystrophies in Japan." J Hum Genet 46(8):431-5.

Fujiki, K.; Hotta, Y.; Nakayasu, K.; Yokoyama, T.; Takano, T.; Yamaguchi, T.; Kanai, A. (1998). "A new L527R mutation if the βIGH3 gene in patients with lattice corneal dystrophy with deep stromal opacities." Hum Genet 103:286-289

Gao, C.; Negash, S.; Guo, H.T.; Ledee, D.; Wang, H.S.; Zelenka, P. (2002). "CDK5 regulates cell adhesion and migration in corneal epithelial cells" Mol Can Res 1:12-24

Garratt, A.N.; Humpries, N.J. (1995). "Recent insights into ligand binding, activation and signalling by integrin adhesion receptors" Acta Anat (Basel) 154(1):34-45

Genini, M., P. Schwalbe, et al. (1996). "Isolation of genes differentially expressed in human primary myoblasts and embryonal rhabdomyosarcoma." Int J Cancer 66(4):571-7.

George A.J., Arancibia-Carcamo C.V., Awad H.M., Comer R.M., Fehervari Z., King W.J., Kadfachi M., Hudde T., Kerouedan-Lebosse C., Mirza F., Barbaros Oral H.,

Rayner S.A., Tan P.H., Tay E., Larkin D.F. (2000). "Gene delivery to the corneal endothelium" Am J Resp Crit Care Med 162(4 Pt 2):S194-200

Gibson, M. A.; Hatzinikolas, G.; Kumaratilake, J. S.; Sandberg, L. B.; Nicholl, J. K.; Sutherland, G. R.; Cleary, E. G. (1996). "Further characterization of proteins associated with elastic fiber microfibrils including the molecular cloning of MAGP-2 (MP25)." J Biol Chem 271(2):1096-103.

Gibson, M. A.; Kumaratilake, J. S.; Cleary, E. G. (1997). "Immunohistochemical and ultrastructural localization of MP78/70 (betaig-h3) in extracellular matrix of developing and mature bovine tissues." J Histochem Cytochem 45(12):1683-96.

Gilbert, R. E.; Wilkinson-Berka, J. L.; Johnson, D. W.; Cox, A.; Soulis, T.; Wu, L. L.; Kelly, D. J.; Jerums, G.; Pollock, C. A.; Cooper, M. E. (1998). "Renal expression of transforming growth factor-beta inducible gene-h3 (beta ig-h3) in normal and diabetic rats." Kidney Int 54(4):1052-62.

Goldman M.J., Wilson J.M. (1995) "Expression of $\alpha_v\beta_5$ integrin is necessary for efficient adenovirus-mediated gene transfer in the human airway." J Virol 69:5951-5958

Golembieski, W. A. and Rempel, S. A. (2002). "cDNA array analysis of SPARC-modulated changes in glioma gene expression." J Neurooncol 60(3):213-26.

Gregory, C.Y.; Evans, K.; Bhattacharya, S.S. (1995). "Genetic refinement of the chromosome 5q lattice corneal dystrophy to within a 2cM interval." J Med Genet 32:224-226

Grillari, J.; Hohenwarter, O.; Grabherr, R. M.; Katinger, H. (2000). "Subtractive hybridization of mRNA from early passage and senescent endothelial cells." Exp Gerontol 35(2):187-97.

Groenouw, A. (1933). "Knotchenformige Hornhauttrubungen vererbt durch vier Generationen." Klin Monatsbl Augenheilkd 90:577-580

Guo, X.; Hutcheon, A.E.; Zieske, J.D. (2004). "Transduction of functional active TA fusion proteins into cornea" Exp Eye Res 78(5):997-1005

Gupta, S. K. and W. G. Hodge (1999). "A new clinical perspective of corneal dystrophies through molecular genetics." Curr Opin Ophthalmol 10(4):234-41.

Gupta, S. K.; Hodge, W. G.; Damji, K. F.; Guernsey, D. L.; Neumann, P. E. (1998). "Lattice corneal dystrophy type 1 in a Canadian kindred is associated with the Arg124 - -Cys mutation in the kerato-epithelin gene. sgupta@ogh.on.ca." Am J Ophthalmol 125(4):547-9.

Ha, N. T.; Cung le, X.; Chau, H. M.; Thanh, T. K.; Fujiki, K.; Murakami, A.; Kanai, A. (2003). "A novel mutation of the TGFBI gene found in a Vietnamese family with atypical granular corneal dystrophy." Jpn J Ophthalmol 47(3):246-8.

Ha, N. T.; Fujiki, K.; Hotta, Y.; Nakayasu, K.; Kanai, A. (2000). "Q118X mutation of M1S1 gene caused gelatinous drop-like corneal dystrophy: the P501T of BIGH3 gene found in a family with gelatinous drop-like corneal dystrophy." Am J Ophthalmol 130(1):119-20.

Ha, S. W.; Bae, J. S.; Yeo, H. J.; Lee, S. H.; Choi, J. Y.; Sohn, Y. K.; Kim, J. G.; Kim, I. S.; Kim, B. W.2003). "TGF-beta-induced protein betaig-h3 is upregulated by high glucose in vascular smooth muscle cells." J Cell Biochem 88(4):774-82.

Hackworth, L.A.; Faraji-Shadan, F.; Schuschereba, S.T.; Bowman, P.D. (1990)."Serum free culture of porcine and rabbit corneal epithelial cells" Curr Eye Res 9(9):919-23

Hanssen, E.; Reinboth, B.; Gibson, M. A. (2003). "Covalent and non-covalent interactions of betaig-h3 with collagen VI. Beta ig-h3 is covalently attached to the amino-terminal region of collagen VI in tissue microfibrils." J Biol Chem 278(27): 24334-41.

Hashimoto, K.; Noshiro, M.; Ohno, S.; Kawamoto, T.; Satakeda, H.; Akagawa, Y.; Nakashima, K.; Okimura, A.; Ishida, H.; Okamoto, T.; Pan, H.; Shen, M.; Yan, W.;

Kato, Y. (1997). "Characterization of a cartilage-derived 66-kDa protein (RGD-CAP/beta ig-h3) that binds to collagen." Biochim Biophys Acta 1355(3):303-14.

Hasson, T.B.; Soloway, P.D.; Ornelles, D.A.; Doerfler, W.; Shenk, T. (1989). "Adenovirus L1 52- and 55-kilodalton proteins are required for assembly of virions." J Virol 63, 3612-3621

Hedegaard, C. J.; Thogersen, I. B.; Enghild, J. J.; Klintworth, G. K.; Moller-Pedersen, T. (2003). "Transforming growth factor beta induced protein accumulation in granular corneal dystrophy type III (Reis-Bucklers dystrophy). Identification by mass spectrometry in 15 year old two-dimensional protein gels." Mol Vis 9:355-9.

Hellenbroich, Y.; Tzivras, G.; Neppert, B.; Schwinger, E.; Zuhlke, C. (2001). "R124C mutation of the betaIGH3 gene leads to remarkable phenotypic variability in a Greek four-generation family with lattice corneal dystrophy type 1." Ophthalmologica 215(6): 444-7.

Hida, T.; Tsubota, K.; Kigasawa, K. (1987) "Clinical features of a newly recognised type of lattice corneal dystrophy." Am J Ophthalmol 104:241.

Hirano, K.; Klintworth, G.K.; Zhan, Q.; Bennett, K.; Cintron, C. (1997). "βig-h3 is synthesised by cornea epithelium and perhaps endothelium in Fuch's dystrophic corneas." Curr Eye Res 15:965-972

Hoffman, F. (1972). "The surface of epithelial cells of the cornea under the scanning electron microscope" Ophthalmic Res 3:207.

Holland, E. J.; Daya, S. M.; Stone, E. M.; Folberg, R.; Dobler, A. A.; Cameron, J. D.; Doughman, D. J. (1992) "Avellino corneal dystrophy: clinical manifestations and natural history." Ophthalmology 99: 1564-1568, 1992.

Holly, F.J. (1978). "The precorneal tear film." Contact Intraocular Lens Med J 4:134.

Hou, Y. C.; Hu, F. R.; Chen, M. S. (2003). "An autosomal dominant granular corneal dystrophy family associated with R555W mutation in the BIGH3 gene." J Formos Med Assoc 102(2):117-20.

Hudde, T.; Rayner, S. A.; Comer, R. M.; Weber, M.; Isaacs, J. D.; Waldmann, H.; Larkin, D. F.; George, A. J. (1999). "Activated polyamidoamine dendrimers, a non-viral vector for gene transfer to the corneal endothelium." Gene Ther 6(5):939-43.

Hourihan, R. N.; O'Sullivan, G. C.; Morgan, J. G.. (2003). "Transcriptional gene expression profiles of oesophageal adenocarcinoma and normal oesophageal tissues." Anticancer Res 23(1A):161-5.

Hu, Y. C.; Lam, K. Y.; Law, S.; Wong, J.; Srivastava, G. (2001). "Profiling of differentially expressed cancer-related genes in esophageal squamous cell carcinoma (ESCC) using human cancer cDNA arrays: overexpression of oncogene MET correlates with tumor differentiation in ESCC." Clin Cancer Res 7(11):3519-25.

Hutchinson, F. and Stein, J (1977). "Mutagenesis of lambda phage: 5-bromouracil and hydroxylamine." Mol Gen Genet 152(1):29-36.

Inoue, T.; Watanabe, H.; Yamamoto, S.; Maeda, N.; Inoue, Y.; Shimomura, Y.; Tano, Y. (2002). "Recurrence of corneal dystrophy resulting from an R124H Big-h3 mutation after phototherapeutic keratectomy." Cornea 21(6):570-3.

Iwasaki, Y.; Ichikawa, Y.; Igarashi, O.; Aoyagi, J.; Konno, S.; Iguchi, H.; Fujioka, T.; Kawabe, K. (2003). "Plasma TGFbeta1 in ALS patients." Acta Neurol Scand 108(3):221-5

Joo, C. K.; Lee, E. H.; Kim, J. C.; Kim, Y. H.; Lee, J. H.; Kim, J. T.; Chung, K. H.; Kim, J. (1999). "Degeneration and transdifferentiation of human lens epithelial cells in nuclear and anterior polar cataracts." J Cataract Refract Surg 25(5):652-8.

Kaji, T.; Yamada, A.; Miyajima, S.; Yamamoto, C.; Fujiwara, Y.; Wight, T.N.; Kinsella, M.G. (2000). "Cell density-dependent regulation of proteoglycan synthesis by

transforming growth factor-beta (1) in cultured bovine aortic endothelial cells" J Biol Chem 275(2):1463-70

Kaufmann, H. E.; Barron B.A.; McDonald M.B. (1998) " The cornea" Second Edition, Butterworth Heinemann

Kenyon, K.R. (1969) "The synthesis of basement membrane by the corneal epithelium in bullous keratopathy." Invest Ophthalmol 8(2):156-68

Khodadoust; A.A.; Silvestein, A.M.; Kenyon, D.R.; Dowling, J.R. (1968). "Adhesion of regenerating corneal epithelium." The role of basement membrane. Am J Ophthalmol 1968; 65(3);339-48

Kim, H. S.; Yoon, S. K.; Cho, B. J.; Kim, E. K.; Joo, C. K. (2001). "BIGH3 gene mutations and rapid detection in Korean patients with corneal dystrophy." Cornea 20(8):844-9.

Kim, J. E.; Jeong, H. W.; Nam, J. O.; Lee, B. H.; Choi, J. Y.; Park, R. W.; Park, J. Y.; Kim, I. S. (2002). "Identification of motifs in the fasciclin domains of the transforming growth factor-beta-induced matrix protein betaig-h3 that interact with the alphavbeta5 integrin." J Biol Chem 277(48):46159-65.

Kim, J. E.; Kim, E. H.; Han, E. H.; Park, R. W.; Park, I. H.; Jun, S. H.; Kim, J. C.; Young, M. F.; Kim, I. S. (2000). "A TGF-beta-inducible cell adhesion molecule, betaig-h3, is downregulated in melorheostosis and involved in osteogenesis." J Cell Biochem 77(2):169-78.

Kim, J. E.; Kim, S. J.; Jeong, H. W.; Lee, B. H.; Choi, J. Y.; Park, R. W.; Park, J. Y.; Kim, I. S. (2003). "RGD peptides released from beta ig-h3, a TGF-beta-induced cell-adhesive molecule, mediate apoptosis." Oncogene 22(13):2045-53.

Kim, J. E.; Kim, S. J.; Lee, B. H.; Park, R. W.; Kim, K. S.; Kim, I. S. (2000). "Identification of motifs for cell adhesion within the repeated domains of transforming growth factor-beta-induced gene, betaig-h3." J Biol Chem 275(40):30907-15.

Kim, J. E.; Park, R. W.; Choi, J. Y.; Bae, Y. C.; Kim, K. S.; Joo, C. K.; Kim, I. S. (2002). "Molecular properties of wild-type and mutant betaIG-H3 proteins." Invest Ophthalmol Vis Sci 43(3):656-61.

Kim, M. O.; Yun, S. J.; Kim, I. S.; Sohn, S.; Lee, E. H.. (2003). "Transforming growth factor-beta-inducible gene-h3 (beta(ig)-h3) promotes cell adhesion of human astrocytoma cells in vitro: implication of alpha6beta4 integrin." Neurosci Lett 336(2):93-6.

Kitahama, S.; Gibson, M. A.; Hatzinikolas, G.; Hay, S.; Kuliwaba, J. L.; Evdokiou, A.; Atkins, G. J.; Findlay, D. M. (2000). "Expression of fibrillins and other microfibril-associated proteins in human bone and osteoblast-like cells." Bone 27(1):61-7.

Klintworth, G. K. (1999). "Advances in the molecular genetics of corneal dystrophies." Am J Ophthalmol 128(6):747-54.

Klintworth, G. K. (2003). "The molecular genetics of the corneal dystrophies - current status." Front Biosci 8:D687-713.

Klintworth, G. K.; Valnickova, Z.; Enghild, J. J. (1998). "Accumulation of beta ig-h3 gene product in corneas with granular dystrophy." Am J Pathol 152(3):743-8.

Klintworth, G.K.; Enghild, J.; Valnickova, Z. (1994). "Discovery of a novel protein (βig-h3) in normal human cornea". ARVO Abstracts. Invest Ophthalmol Vis Sci; 35: S1938

Kobayashi, A.; Sakurai, M.; Shirao, Y.; Sugiyama, K.; Ohta, T.; Amaya-Ohkura, Y. (2003). "In vivo confocal microscopy and genotyping of a family with Thiel-Behnke (honeycomb) corneal dystrophy." Arch Ophthalmol 121(10):1498-9.

Kocak-Altintas, A. G.; Kocak-Midillioglu, I.; Akarsu, A. N.; Duman, S.. (2001). "BIGH3 gene analysis in the differential diagnosis of corneal dystrophies." Cornea 20(1):64-8.

Konishi, M.; Mashima, Y.; Yamada, M.; Kudoh, J.; Shimizu, N. (1998). "The classic form of granular corneal dystrophy associated with R555W mutation in the BIGH3 gene is rare in Japanese patients." Am J Ophthalmol 126(3):450-2.

Konishi, M.; Yamada, M.; Nakamura, Y.; Mashima, Y. (2000). "Immunohistology of kerato-epithelin in corneal stromal dystrophies associated with R124 mutations of the BIGH3 gene." Curr Eye Res 21(5):891-6.

Konishi, M.; Yamada, M.; Nakamura, Y.; Mashima, Y. (1999). "Varied appearance of cornea of patients with corneal dystrophy associated with R124H mutation in the BIGH3 gene." Cornea 18(4):424-9.

Korvatska, E.; Henry, H.; Mashima, Y.; Yamada, M.; Bachmann, C.; Munier, F. L.; Schorderet, D. F. (2000). "Amyloid and non-amyloid forms of 5q31-linked corneal dystrophy resulting from kerato-epithelin mutations at Arg-124 are associated with abnormal turnover of the protein." J Biol Chem 275(15):11465-9.

Korvatska, E.; Munier, F. L.; Chaubert, P.; Wang, M. X.; Mashima, Y.; Yamada, M.; Uffer, S.; Zografos, L.; Schorderet, D. F. (1999). "On the role of kerato-epithelin in the pathogenesis of 5q31-linked corneal dystrophies." Invest Ophthalmol Vis Sci 40(10):2213-9.

Korvatska, E.; Munier, F. L.; Djemai, A.; Wang, M. X.; Frueh, B.; Chiou, A. G.; Uffer, S.; Ballestrazzi, E.; Braunstein, R. E.; Forster, R. K.; Culbertson, W. W.; Boman, H.; Zografos, L.; Schorderet, D. F. (1998). "Mutation hot spots in 5q31-linked corneal dystrophies." Am J Hum Genet 62(2):320-4.

Korvatska, E.; Munier, F.L.; Zografos, L.; Ahmed, F.; Faggioni, R.; Dovlino-Beuret, A.; Uffer, S.; Persia, G.; Schorderet, D.F. (1996). "Delineation of a 1-cM region in distal 5q containing the locus for corneal dystrophies Groenouw type I and lattice type I and exclusion of the candidate genes SPARC and LOX." Eur J Hum Genet 4:214-218

Kublin, C.L.; Cintron, C. (1996). "βig-h3 is associated with normal development of extracellular matrices in human fetal eyes." Invest Ophthalmol Vis Sci 37:S327

Kuchlle, M.; Cursiefen, C.; Fischer, D.C.; Schlotzer-Schrehardt, U.; Naumann, G.O.H. (1999). " Recurrent macular corneal dystrophy type II 49 years after penetrating keratoplasty." Arch Ophthalmol 117:528-531

Kuchle, M.; Green, W.R.; Volcker, H.E.; Barraquer, J. (1995). "Reevaluation of corneal dystrophies of Bowman's layer and the anterior stroma (Reis-Bucklers and Thiel-Behnke types): a light and electron microscopic study of eight corneas and a review of the literature." Cornea 14 (4):333-354

Kuwabara, T. (1978). "Current concepts in anatomy and histology of the cornea." Contact Intraocular Lens Med J 4:101.

Laibson, P.R.; Krachmer, J.H. (1975). "Familial occurrence of dot (microcystic), map, fingerprint dystrophy of the cornea." Invest Ophthalmol 14(5):397-9.

Lallier, T.; Broner-Fraser, M. (1992). "Alpha 1 beta 1 integrin on neural crest cells recognises some laminin substrata in a Ca(2+)-independent manner" J Cell Biol 119(5):1335-45

Lane, P. H.; Snelling, D. M.; Babushkina-Patz, N.; Langer, W. J.2001). "Sex differences in the renal transforming growth factor-beta 1 system after puberty." Pediatr Nephrol 16(1):61-8.

Landegren, U. (1984). "Measurement of cell numbers by means of the endogenous enzyme hexosaminidaase. Applications to detection of lymphokines and cell surface antigens" J Immunol Meth 67:379-88

Langham, M.E.; Taylor, I.S. (1956). "Factors affecting the hydration of the cornea in the excised eye and the living animal" Br J Ophthalmol 40(6):321-40

Langham, R. G.; Egan, M. K.; Dowling, J. P.; Gilbert, R. E.; Thomson, N. M. (2001). "Transforming growth factor-beta1 and tumor growth factor-beta-inducible gene-H3 in nonrenal transplant cyclosporine nephropathy." Transplantation 72(11):1826-9.

Larkin D.F.P., Oral H.B., Ring C.J.A., Lemoine N.R., George A.J.T. (1996). "Adenovirus-mediated gene delivery to the corneal endothelium." Transplantation 61:363-370

LeBaron, R. G.; Bezverkov, K. I.; Zimber, M. P.; Pavelec, R.; Skonier, J.; Purchio, A. F.. (1995). "Beta IG-H3, a novel secretory protein inducible by transforming growth factor-beta, is present in normal skin and promotes the adhesion and spreading of dermal fibroblasts in vitro." J Invest Dermatol 104(5):844-9.

Lee, E. H. and C. K. Joo (1999). "Role of transforming growth factor-beta in transdifferentiation and fibrosis of lens epithelial cells." Invest Ophthalmol Vis Sci 40(9):2025-32.

Lee, E. H.; Seomun, Y.; Hwang, K. H.; Kim, J. E.; Kim, I. S.; Kim, J. H.; Joo, C. K. (2000). "Overexpression of the transforming growth factor-beta-inducible gene betaig-h3 in anterior polar cataracts." Invest Ophthalmol Vis Sci 41(7):1840-5.

Lee, S. H.; Bae, J. S.; Park, S. H.; Lee, B. H.; Park, R. W.; Choi, J. Y.; Park, J. Y.; Ha, S. W.; Kim, Y. L.; Kwon, T. H.; Kim, I. S. (2003). "Expression of TGF-beta-induced matrix protein betaig-h3 is up-regulated in the diabetic rat kidney and human proximal tubular epithelial cells treated with high glucose." Kidney Int 64(3):1012-21.

Lorenzetti, D.W.; Uotila, M.H.; Parikh, N.; Kaufmann, H.E. (1967). " Central cornea guttata. Incidence in the general population." Am J Ophthalmol 64(6):1155-1158

Lythgoe, J.N. (1976). "The arrangement of collagen fibrils in the iridescent cornea of the scorpion fish Taurulus (Cottus) Bubalis, and the transparency of vertebrate corneal stroma" J Physiol 262(1):1-13

Mahy, B.W.J. (1991). "Virology: A practical approach." IRL Press, Oxford. Chapter 9:193-205.

Martin, S.J.; Reutelingsperger, C.P.; McGahon, A.J.; Rader, J.A.; van Schie, R.C.; LaFace, D.M.; Green, D.R. (1995). "Early distribution of plasma membrane phosphatidylserine is a general feature of apoptosis regardless of the initiating stimulus: inhibition by overexpression of Bcl-2 and Ab1 J Exp Med 182(5):5191-200

Martin, W.; Brown, C.; Zhang, Y.J., Wu, R. (1991). "Growth and differentiation of primary tracheal epithelial cells in culture: regulation by extracellular calcium" J Cell Physiol 147(1):138-48

Maier, A. and Mayne, R. (1987). "Distribution of connective tissue proteins in chick muscle spindles as revealed by monoclonal antibodies: a unique distribution of brachionectin/tenscin." Am J Anat 180:226-236

Malecaze, F.; Couderc, B.; De Neuville, S.; Serres, B.; Mallet, J.; Douin-Echinard, V.; Manenti, S.; Revah, F.; Darbon, J.M. (1999). "Adenovirus-mediated suicide gene transduction: Feasibility in lens epithelium and in prevention of posterior capsule opacifiction in rabbits." Human Gene Therapy 10:2365-2372

Mashima, Y.; Imamura, Y.; Konishi, M.; Nagasawa, A.; Yamada, M.; Oguchi, Y.; Kudoh, J.; Shimizu, N. (1997). "Homogeneity of kerato-epithelin codon 124 mutations in Japanese patients with either of two types of corneal stromal dystrophy." Am J Hum Genet 61(6):1448-50.

Mashima, Y.; Nakamura, Y.; Noda, K.; Konishi, M.; Yamada, M.; Kudoh, J.; Shimizu, N. (1999). "A novel mutation at codon 124 (R124L) in the BIGH3 gene is associated with a superficial variant of granular corneal dystrophy." Arch Ophthalmol 117(1):90-3.

Mashima, Y.; Yamamoto, S.; Inoue, Y.; Yamada, M.; Konishi, M.; Watanabe, H.; Maeda, N.; Shimomura, Y.; Kinoshita, S. (2000). "Association of autosomal dominantly inherited corneal dystrophies with BIGH3 gene mutations in Japan." Am J Ophthalmol 130(4):516-7.

Maurice, D.M. (1984) "The corneal and sclera. p. 1. In Davson H (ed): The eye. Vol 1B. Vegetative physiology and biochemistry." 3rd Edition. Academic Press, Orlando, FL

Maurice, D.M.(1957) "The structure and transparency of the cornea." J Physiol 136(2):263-86

Melleman, I. (1992). "The importance of being acidic: the role of acidification in intracellular membrane traffic." J Exp Biol 39-45

Meretoja, J. (1969). "Familial systemic paramyloidosis with lattice dystrophy of the cornea, progressive cranial neuropathy, skin changes and various internal symptoms." Ann Clin Res 1:314-324

Mishima, H.; Nakamura, M.; Murakami, J.; Nishida, T.; Otori, T. (1992). "Transforming growth factor-β modulates effects of epithelial cells." Curr Eye Res 11:691-696

Maniatis, T.; Fritsch, E.F.; Sambrook, J. (1984) " Molecular Cloning: A laboratory manual" Cold Spring Harbour Laboratory

Mathew, B.; Brownstein, S.; Bao, W.; Klintworth, G. K.; Singh, D. (2003). "Unusual superficial variant of granular corneal dystrophy with amyloid deposition." Arch Ophthalmol 121(2):269-71.

Meitinger, T. (1997). "Widening the view." Nat Genet 15(3):224-5.

Mizejewski, G.J. (1999). "Role of integrins in cancer:survey of expression patterns" Proc Soc Exp Biol Med 222(2):124-38

Moczar, M.; Moczar, E. (1973). "Macromolecular composition of the extracellular matrix of the bovine corneal stroma during embryonic and postnatal development" Exp Eye Res 17(1):5-17

Morand, S.; Buchillier, V.; Maurer, F.; Bonny, C.; Arsenijevic, Y.; Munier, F. L.; Schorderet, D. F. (2003). "Induction of Apoptosis in Human Corneal and HeLa Cells by Mutated BIGH3." Invest Ophthalmol Vis Sci 44(7):2973-9.

Mull, D.J.; Peters, J.H.; Nichols, R.L. (1970). "Immunoglobulins, secretory component, and transferrin in the eye secretions of infants in regions with and without endemic trachoma." Infect Immun 2:489

Munier, F. L.; Frueh, B. E.; Othenin-Girard, P.; Uffer, S.; Cousin, P.; Wang, M. X.; Heon, E.; Black, G. C.; Blasi, M. A.; Balestrazzi, E.; Lorenz, B.; Escoto, R.; Barraquer, R.; Hoeltzenbein, M.; Gloor, B.; Fossarello, M.; Singh, A. D.; Arsenijevic, Y.; Zografos, L.; Schorderet, D. F. (2002). "BIGH3 mutation spectrum in corneal dystrophies." Invest Ophthalmol Vis Sci 43(4):949-54.

Munier, F. L.; Korvatska, E.; Djemai, A.; Le Paslier, D.; Zografos, L.; Pescia, G.; Schorderet, D. F. (1997). "Kerato-epithelin mutations in four 5q31-linked corneal dystrophies." Nat Genet 15(3):247-51.

Muthiah, P.; Stuhlsatz, H.W.; Greiling, H. (1974). "Composition of corenal proteoglycans. Density gradient centrifugation and chromatographic studies" Hoppe Seylers Z Physiol Chem 355 (8):924-34

Nam, J. O.; Kim, J. E.; Jeong, H. W.; Lee, S. J.; Lee, B. H.; Choi, J. Y.; Park, R. W.; Park, J. Y.; Kim, I. (2003). "Identification of the alphavbeta3 integrin-interacting motif of betaig-h3 and its anti-angiogenic effect." J Biol Chem 278(28):25902-9.

Newsome, D.A.; Foidart, J.M.; Hassell, J.R. (1981). "Detection of specific collagen types in normal and keratoconus corneas." Invest Ophthalmol Vis Sci 20:738

Nicolaides, N et al. (1981). "Meibomian gland studies: Comparison of steer and human lipids." Invest Ophthalmol Vis Sci 20:522

Nichols, B.A.; Chiappino, M.L.; Dawson. C.R. (1985). "Demonstration of the mucous layer of the tear film by electron microscopy." Invest Ophthalmol Vis Sci 26:464-473

O'Brien, E. R.; Bennett, K. L.; Garvin, M. R.; Zderic, T. W.; Hinohara, T.; Simpson, J. B.; Kimura, T.; Nobuyoshi, M.; Mizgala, H.; Purchio, A.; Schwartz, S. M. (1996). "Beta ig-h3, a transforming growth factor-beta-inducible gene, is overexpressed in atherosclerotic and restenotic human vascular lesions." Arterioscler Thromb Vasc Biol 16(4):576-84.

Ohno, S.T.; Noshiro, M.; Makihira S.; Kawamoto, T.; Shen, M.; Yan, W.; Kawashima-Ohya, Y.; Fujimoto, K.; Tanne, K.; Kato, Y. (1999) "RGD-CAP βig-h3 enhances the spreading of chondrocytes and fibroblasts via integrin $\alpha_1\beta_1$." Biochim Biophys Acta 1451(1):196-205

Ohno, S.; Doi, T.; Fujimoto, K.; Ijuin, C.; Tanaka, N.; Tanimoto, K.; Honda, K.; Nakahara, M.; Kato, Y.; Tanne, K. (2002). "RGD-CAP (betaig-h3) exerts a negative regulatory function on mineralization in the human periodontal ligament." J Dent Res 81(12):822-5.

Ohno, S.; Doi, T.; Tsutsumi, S.; Okada, Y.; Yoneno, K.; Kato, Y.; Tanne, K. (2002). "RGD-CAP ((beta)ig-h3) is expressed in precartilage condensation and in prehypertrophic chondrocytes during cartilage development." Biochim Biophys Acta 1572(1):114-22.

Okada, M.; Yamamoto, S.; Inoue, Y.; Watanabe, H.; Maeda, N.; Shimomura, Y.; Ishii, Y.; Tano, Y. (1998). "Severe corneal dystrophy phenotype caused by homozygous R124H keratoepithelin mutations." Invest Ophthalmol Vis Sci 39(10):1947-53.

Okada, M.; Yamamoto, S.; Tsujikawa, M.; Watanabe, H.; Inoue, Y.; Maeda, N.; Shimomura, Y.; Nishida, K.; Quantock, A. J.; Kinoshita, S.; Tano, Y. (1998). "Two distinct kerato-epithelin mutations in Reis-Bucklers corneal dystrophy." Am J Ophthalmol 126(4):535-42.

Okada, M.; Yamamoto, S.; Watanabe, H.; Inoue, Y.; Tsujikawa, M.; Maeda, N.; Shimomura, Y.; Nishida, K.; Kinoshita, S.; Tano, Y.1998). "Granular corneal dystrophy with homozygous mutations in the kerato-epithelin gene." Am J Ophthalmol 126(2):169-76.

Okada, M.; Yamamoto, S.; Watanabe, H.; Shimomura, Y.; Tano, Y. (2000). "Granular corneal dystrophy with homozygous mutations in the kerato-epithelin gene." Am J Ophthalmol 129(3):411-2.

Oral, H.B.; Larkin, D.F.P.; Fehervani, Z.; Byrnes, A.P.; Rankin, A.M.; Haskard, D.O.; Wood, M.J.A.; Dallman, M.J.; George, A.J.T. (1998). "Ex vivo adenovirus-mediated gene transfer and immunodulatory protein production in human cornea." Gene Therapy 4:639-647

Oshima, Y.; Sakamoto, T.; Yamanaka, I.; Nishi, T.; Ishibashi, T.; Inomata, H. (1998). "Targeted gene transfer to corneal endothelium in vivo by electric pulse." Gene Therapy 5:1347-1354

Lowenstein, P.R; Enquist, L.W. (1996) "Protocols for Gene Transfer in Neuroscience: Towards Gene Therapy of Neurological Disorders" John Wiley and Sons Chapter 7:81-92.

Pang, C. P.; Lam, D. S. (2002). "Differential occurrence of mutations causative of eye diseases in the Chinese population." Hum Mutat 19(3):189-208.

Park S.W., Bae J.S., Kim K.S., Park S.H., Lee B.H., Choi J.Y., Park J.Y., Ha S.W., Kim Y.L., Kwon T.H., Kim I.S., Park R.W. (2004). "Beta ig-he promotes renal proximal tubular epithelial cell adhesion, migration and proliferation through the interaction with $\alpha_3\beta_1$ integrin" Exp Mol Med 36(3):211-9

Park, S.; Ahn, H. C.; Kim, J. E.; Kim, I. S.; Lee, B. J. (2002). "Letter to the Editor: Backbone (1)H, (15)N, and (13)C resonance assignments of the repeated domain of human betaig-h3 protein." J Biomol NMR 24(4):367-8.

Paufique, L.; Bonnet, M. (1966). "La dystrophie corneenne heredo-familiale de Reis-Bucklers." Ann. Oculist. 199: 14-37.

Paul, L. C. (2001). "Beta(ig) H-3: why should we know about this molecule?" Transplantation 72(11):1725-6.

Perutz, M.F. (1997). "Mutations make enzymes polymerise" Nature 385:773-5

Perveen, R.; Hart-Holden, N.;, Dixon, M.J.; Wiszniewski, W.; Fryer, A.E.; Brunner, H.G.; Pinkners, A.J.; van Beersum, S.E.; Black, G.C. (1999). "Refined genetic and physical localization of the Wagner disease (WGN1) locus and the genes CRTL1 and CSPG2 to a 2- to 2.5-cM region of chromosome 5q14.3." Genomics *15*, 57 (2):219-226

Rawe, I. M.; Zhan, Q.; Burrows, R.; Bennett, K.; Cintron, C. (1997). "Beta-ig. Molecular cloning and in situ hybridization in corneal tissues." Invest Ophthalmol Vis Sci 38(5):893-900.

Rayner, S.A.; Gallop, J.L.; George, A.J.T.; Larkin, D.F.P. (1998). "Distribution of integrins $\alpha_v\beta_5$, $\alpha_v\beta_3$ and α_v in normal human cornea: possible implications in clinical and therapeutic adenoviral infection." Eye. 12 (2):273-7

Reinstein, D.Z.; Silverman, R.H.; Rondeau, M;J.; Coleman, D.J. (1994). "Epithelial and corneal thickness measurements by high-frequency ultrasound digital signal processing." Ophthalmology 101(1):140-6.

Rice, N. S. C.; Ashton, N.; Jay, B.; Blach, R. K. (1968). "Reis-Bucklers' dystrophy: a clinico-pathological study." Brit. J. Ophthal. 52: 577-603.

Richard, N.R.; Anderson, J.A.; Weiss, J.L.; Binder, P.S. (1991). "Air/liquid corneal organ culture: a light microscopic study." Curr Eye Res 10:739-749

Ridgway, A. E.; Akhtar, S.; Munier, F. L.; Schorderet, D. F.; Stewart, H.; Perveen, R.; Bonshek, R. E.; Odenthal, M. T.; Dixon, M.; Barraquer, R.; Escoto, R.; Black, G. C. (2000). "Ultrastructural and molecular analysis of Bowman's layer corneal dystrophies: an epithelial origin?" Invest Ophthalmol Vis Sci 41(11):3286-92.

Rittig, M.; Lutjen-Drecoll, E.; Rauterberg, J.; Jander, R.; Mollenhauer, J. (1990). "Type VI collagen in the human iris and ciliary body." Cell Tissue Res 259:305-312

Rodrigues, M.M.; Streeten, B.W.; Krachmer, J.M. (1983). "Microfibrillar protein and phospholipid in granular cornea dystrophy." Arch Ophthalmol 101:802

Rozzo, C.; Fossarello, M.; Galleri, G.; Sole, G.; Serru, A.; Orzalesi, N.; Serra, A.; Pirastu, M. (1998). "A common beta ig-h3 gene mutation (delta f540) in a large cohort of Sardinian Reis Bucklers corneal dystrophy patients. Mutations in brief no. 180. Online." Hum Mutat 12(3):215-6.

Ruoslahti, E. Proteoglycans in cell regulation. J Biol Chem 1989; 264, 13369-13372

Russo, L. M.; Brammar, G. C.; Jerums, G.; Comper, W. D.; Osicka, T. M. (2003). "The effect of ramipril on albumin excretion in diabetes and hypertension: the role of increased lysosomal activity and decreased transforming growth factor-beta expression." J Hypertens 21(2):419-28.

Russo, L. M.; Osicka, T. M.; Brammar, G. C.; Candido, R.; Jerums, G.; Comper, W. D. (2003). "Renal processing of albumin in diabetes and hypertension in rats: possible role of TGF-beta1." Am J Nephrol 23(2):61-70.

Sakimoto, T.; Kanno, H.; Shoji, J.; Kashima, Y.; Nakagawa, S.; Miwa, S.; Sawa, M. (2003). "A novel nonsense mutation with a compound heterozygous mutation in TGFBI gene in lattice corneal dystrophy type I." Jpn J Ophthalmol 47(1):13-7.

Santo, R.M.; Yamaguchi, T.; Kanai, A.; Okisaka, S.; Nakajima, A. (1995). "Clinical and histopathologic features of corneal dystrophies in Japan." Opthalmology 102(4):557-67

Sasaki, H.; Kobayashi, Y.; Nakashima, Y.; Moriyama, S.; Yukiue, H.; Kaji, M.; Kiriyama, M.; Fukai, I.; Yamakawa, Y.; Fujii, Y.2002). "Beta IGH3, a TGF-beta inducible gene, is overexpressed in lung cancer." Jpn J Clin Oncol 32(3):85-9.

Sasaki, H.; Roberts, J.; Lykins, D.; Fujii, Y.; Auclair, D.; Chen, L. B. (2002). "Novel chemiluminescence assay for serum periostin levels in women with preeclampsia and in normotensive pregnant women." Am J Obstet Gynecol 186(1):103-8.

Sakamoto, T.; Oshima, Y.; Nakagawa, K.; Ishibashi, T.; Inomata, H.; Sueishi, K. (1999). "Target gene transfer of tissue plasminogen activator to cornea by electric pulse inhibits intracameral fibrin formation and cornea cloudiness." Human Gene Therapy 10:2551-2557

Saiki, R.; Gelfand, D.; Stoffel, S. (1988). "Primer-directed enzymatic amplification of DNA with a thermostable polymerase." Science 239:487-91

Schenker, T. and B. Trueb (1998). "Down-regulated proteins of mesenchymal tumor cells." Exp Cell Res 239(1):161-8.

Schneider, D.; Kleeff, J.; Berberat, P. O.; Zhu, Z.; Korc, M.; Friess, H.; Buchler, M. W. (2002). "Induction and expression of betaig-h3 in pancreatic cancer cells." Biochim Biophys Acta 1588(1):1-6.

Schorderet, D. F.; Menasche, M.; Morand, S.; Bonnel, S.; Buchillier, V.; Marchant, D.; Auderset, K.; Bonny, C.; Abitbol, M.; Munier, F. L. (2000). "Genomic characterization and embryonic expression of the mouse Bigh3 (Tgfbi) gene." Biochem Biophys Res Commun 274(2):267-74.

Schmitt-Bernard, C. F.; Chavanieu, A.; Derancourt, J.; Arnaud, B.; Demaille, J. G.; Calas, B.; Argiles, A. (2000). "In vitro creation of amyloid fibrils from native and Arg124Cys mutated betaIGH3((110-131)) peptides, and its relevance for lattice corneal amyloid dystrophy type I." Biochem Biophys Res Commun 273(2):649-53.

Schmitt-Bernard, C. F.; Chavanieu, A.; Herrada, G.; Subra, G.; Arnaud, B.; Demaille, J. G.; Calas, B.; Argiles, A. (2002). "BIGH3 (TGFBI) Arg124 mutations influence the amyloid conversion of related peptides in vitro." Eur J Biochem 269(21):5149-56.

Schmitt-Bernard, C. F.; Guittard, C.; Arnaud, B.; Demaille, J.; Argiles, A.; Claustres, M.; Tuffery-Giraud, S. (2000). "BIGH3 exon 14 mutations lead to intermediate type I/IIIA of lattice corneal dystrophies." Invest Ophthalmol Vis Sci 41(6):1302-8.

Schmitt-Bernard, C. F.; Schneider, C.; Argiles, A. (2002). "Clinical, histopathologic, and ultrastructural characteristics of BIGH3(TGFBI) amyloid corneal dystrophies are supportive of the existence of a new type of LCD: the LCDi." Cornea 21(5):463-8.

Schwarz, W. (1953). "Electron-microscopical studies in differentiation of corneal and scleral fibrils in man" Z Zelforsch Mikrosk Anat 38(1):78-86

Seabra, M.C., Ho Y.K., Anant J.S. (1995). "Deficient geranylgeranylation of Ram/Rab27 in choroideremia." J Biol Chem 270:24420-24427

Seitz, B.; Moreira, L.; Baktanian, E.; Sanchez D.; Gray, B.; Grodon, EM.; Anderson, W.F.; McDonnell, P.J. (1998). "Retroviral vector-mediated gene transfer into keratocytes in vitro and in vivo." Am J Ophthalmol 126 (5):630-639

Shapiro, M.S.; Friend, J.; Thoft, R.A. (1981). "Corneal re-epithelialisation from the conjunctiva" Invest Ophthalmol Vis Sci 21(1):135-42

Shaw, A.R.; Ziff, E.B. (1980). "Transcripts from the adenovirus 2 major late promoter yield a single early family of 3'coterminal mRNAs and five latefamilies." Cell 22:905-916

Shen, Y. and Shenk, T. E. (1995). "Viruses and apoptosis." Curr Opin Genet Dev 5(1):105-11.

Shering, A.F.; Bain, D.; Stewart, K.; Epstein A.L.; Castro, M.G.; Wilkinson, G.W.G.; Lowenstein, P.R. (1997) "Cell type-specific expression in brain cell cultures from a short human cytomegalovirus major immediate early promoter depends on whether it is inserted into herpesvirus or adenovirus vectors." J Gen Virol 78:445-459

Shrewing, L.; Collins, L.; Lightman, S.L.; Hart, S.; Gustafsson, K.; Fabre, J.W. (1997). "A nonviral vector system for efficient gene transfer to corneal endothelial cells via membrane integrins." Transplantation 64:763-769

Siddiqui, N. and Afshari, N.A. (2002). "The changing face of the genetics of corneal dystrophies." Curr Opin Ophthalmol 13(4):199-203.

Skonier, J.; Bennett, K.; Rothwell, V.; Kosowski, S.; Plowman, G.; Wallace, P.; Edelhoff, S.; Disteche, C.; Neubauer, M.; Marquard, H.; Rodgers, J.; Purchio, A.F. (1994). "βig-h3: A transforming growth factor-β-responsive gene encoding a secreted protein that inhibits cell attachment in vitro and suppresses the growth of CHO cells in nude mice." DNA Cell Biol 13 (6):571-584

Skonier, J.; Neubauer, M.; Madisen, L.; Bennett, K.; Plowman, G.D.; Purcio, A.F. (1992) "cDNA cloning and sequence analysis of βig-h3, a novel gene induced in a human adenocarcinoma cell line after treatment with transforming growth factor-β." DNA Cell Biol 11:511-522

Small, K.W.; Mullen, L.; Barletta, J.; Graham, K.; Glasgow, B.; Stern, G.; Yee, R. (1996). "Mapping of Reis-Bucklers' corneal dystrophy to chromosome 5q. Am J Ophthalmol 121:384-390

Snead, D. R. and Mathews, B.N. (2002). "Differences in amyloid deposition in primary and recurrent corneal lattice dystrophy type 1." Cornea 21(3):308-11.

Sperling. S.; Jacobsen, S.R. (1980). "The surface coat on human corneal endothelium." Acta Ophthalmol (Copenh) 58:96

Srivastava, O. P. and Srivastava K. (1999). "cAMP-dependent phosphorylation of betaig-h3 protein in human corneal endothelial cells." Curr Eye Res 19(4):348-57.

Stewart, H.; Black, G. C.; Donnai, D.; Bonshek, R. E.; McCarthy, J.; Morgan, S.; Dixon, M. J.; Ridgway, A. A. (1999). "A mutation within exon 14 of the TGFBI (BIGH3) gene on

chromosome 5q31 causes an asymmetric, late-onset form of lattice corneal dystrophy." Ophthalmology 106(5):964-70.

Stewart, H. S.; Ridgway, A. E.; Dixon, M. J.; Bonshek, R.; Parveen, R.; Black, G. (1999). "Heterogeneity in granular corneal dystrophy: identification of three causative mutations in the TGFBI (BIGH3) gene-lessons for corneal amyloidogenesis." Hum Mutat 14(2):126-32.

Stock, E. L.; Feder, R. S.; O'Grady, R. B.; Sugar, J.; Roth, S. I. (1991). "Lattice corneal dystrophy type IIIA. Clinical and histopathologic correlations." Arch Ophthalmol 109(3):354-8.

Stone, E. M.; Mathers, W. D.; Rosenwasser, G. O.; Holland, E. J.; Folberg, R.; Krachmer, J. H.; Nichols, B. E.; Gorevic, P. D.; Taylor, C. M.; Streb, L. M.; et al. (1994). "Three autosomal dominant corneal dystrophies map to chromosome 5q." Nat Genet 6(1):47-51.

Streeten, B. W.; Qi, Y.; Klintworth, G. K.; Eagle, R. C., Jr.; Strauss, J. A.; Bennett, K. (1999). "Immunolocalization of beta ig-h3 protein in 5q31-linked corneal dystrophies and normal corneas." Arch Ophthalmol 117(1):67-75.

Stuart, P.M.; Usui, N.; Randhawa, R.S.; Laycock, L.A.; Fleming, T.P.; Pepose, J.S. (1997). "Differential effects of HSV-1 and HCMV infection on adhesion molecule expression on human corneal keratocytes" Curr Eye Res 16(5):496-502

Studier, F.W.; Moffatt, B.W. (1986). "Use of bacteriophage T7 RNA polymerase to direct selective high-level expression of cloned genes" J Mol Biol 219:37-44

Sun, T.T. and Vidrich, A. (1981). "Keratin filaments of corneal epithelial cells." Vision Res 21(1):55-63

Swallow, D.M.; Edwards, Y. (1997). "Protein Dysfunction in human genetic disease." βios Scientific Publisher

Smolin G.; Thoft R.A. (1994). "The cornea" Third Edition, Little, Brown and Company

Tas, F.; Yavuz, E.; Aydiner, A.; Saip, P.; Disci, R.; Iplikci, A.; Topuz, E. (2000). "Angiogenesis and p53 protein expression in breast cancer: prognostic roles and interrelationships." Am J Clin Oncol 23(6):546-53.

Teramoto, S.; Johnson, L.G.; Huang, W.; Leigh, M.W.; Boucher, R.C. (1995). "Effect of adenoviral vector infection on cell proliferation in cultured primary human airway epithelial cells" Hum Gene Ther 6(8):1045-53

Teramoto, S.; Matsue, T.; Matsui, H.; Ohga, E.; Ishii, T.; Ouchi, Y. (1999) "Recombinant E1-deleted adenovirus vector induces apoptosis in two lung cancer cell lines" Eur Respir J 13(5):1125-32

Tihanyi, K.; Bourbonniere, M.; Houde, A.; Rancourt, C.; Weber, J.M. (1993). "Isolation and properties of adenovirus type 2 proteinase." J Biol Chem 268:1780-1785

Tonjum, A.M. (1974) "Permeability of horseradish peroxidase in the rabbit corneal epithelium." Acta Ophthalmol (Copenh) 52(5):650-658

Tseng, S.C. (1989) "Concept and application of limbal stem cells" Eye 3(2):141-57

Tsubota, K.; Inoue, H.; Ando, K.; Ono, M.; Yoshino, K.; Saito, I. (1998) "Adenovirus-mediated gene transfer to the ocular surface epithelium." Exp Eye Res 67:531-538

Tsujikawa, M.; Shimomura, Y.;, Okada, M.; Yamamoto, S.; Tano, Y.; Kurahashi, H. (1998). " Novel polymorphisms in the βig-h3 gene." J Hum Genet 43:214-215

Tsujikawa, K.; Tsujikawa, M.; Yamamoto, S.; Fujikado, T.; Tano, Y. (2002). "Allelic homogeneity due to a founder mutation in Japanese patients with lattice corneal dystrophy type IIIA." Am J Med Genet 113(1):20-2.

Tsujimoto, H.; Nishizuka, S.; Redpath, J. L.; Stanbridge, E. J. (1999). "Differential gene expression in tumorigenic and nontumorigenic HeLa x normal human fibroblast hybrid cells." Mol Carcinog 26(4):298-304.

Vinogradova, V.L.; Basova, N.N. (1979). "Micromethod of carrying out the passive hemagglutination reaction for detecting antibodies to influenza A2 virus in tears and aqueous humor." Lab Delo 6:338

Vaughan-Thomas, A., Young, R.D., Philips A.C., Duance, V.C. (2001). "Characterization of Type XI collagen-glycosamoniglycan interactions" J Biol Chem 276(7):5303-5309

Villaverde, A.; Cario, M.M. (2003). "Protein aggregation in recombinant bacteria: biological role of inclusion bodies" Biotechnol Lett 25:1385-95

Wang, M.; Munier, F.; Araki-Saski, K.; Schorderet, D. (2002). "TGFBI gene transcript is transforming growth factor-beta1-responsive and cell density-dependent in a human corneal epithelial cell line." Ophthalmic Genet 23(4):237-45.

Warren, J. F.; Abbott, R. L.; Yoon, M. K.; Crawford, J. B.; Spencer, W. H.; Margolis, T. P. (2003). "A new mutation (Leu569Arg) within exon 13 of the TGFBI (BIGH3) gene causes lattice corneal dystrophy type I." Am J Ophthalmol 136(5):872-8.

Watanabe, H.; Hashida, Y.; Tsujikawa, K.; Tsujikawa, M.; Maeda, N.; Inoue, Y.; Yamamoto, S.; Tano, Y.2001). "Two patterns of opacity in corneal dystrophy caused by the homozygous BIG-H3 R124H mutation." Am J Ophthalmol 132(2):211-6.

Weidle, E.G. (1989). "[Differential diagnosis of corneal dystrophies of the Groenouw I, Reis-Buckler and Thiel-Behnke type]." Fortschr Ophthalmol 86 (4), 265-71

Weidle, EG. (1999). "[Honeycomb-shaped corneal dystrophy of Thiel and Behnke. Reclassification and distinction from reis-Bucklers' corneal dystrophy]." Klin Monatsbl Augenheilkd 214(3):125-35

Wickham T.J.; Mathras P.; Chesrech D.A.; Nomerow G.R. (1993). "Integrins alpha v beta 3 and alpha v beta 5 promote adenovirus internalisation but not virus attachment." Cell 73:309-319

Williams, J.L.; Garcia, J.; Harrich, D.;, Pearson L, Wu F, Gaynor R. Lymphoid specific gene expression of the adenovirus early region 3 promoter is mediated by NK-κB binding motifs. EMBO J 1990; 9:4435-4442

Wolf, J. (1968) "The secretory activity and the cuticle of the corneal endothelium." Doc Ophthalmol 25:150

Yamamoto, S.; Okada, M.; Tsujikawa, M.; Shimomura. Y.; Nishida, K.; Inoue, Y.; Watanabe, H.; Maeda, N.; Kkurahashi, H.; Kinoshita, S.; Nakamura, Y.; Tano, Y.; (1998) "A kerato-epithelin (βig-h3) mutation in lattice corneal dystrophy type IIIA." Am J Hum Genet 1998; 62:719-722

Yamamoto, S.; Okada, M.; Tsujikawa, M.; Morimura, H.; Maeda, N.; Watanabe, H.; Inoue, Y.; Shimomura, Y.; Kinoshita, S.; Tano, Y. (2000). "The spectrum of beta ig-h3 gene mutations in Japanese patients with corneal dystrophy." Cornea 19(3 Suppl):S21-3.

Yancopoulos, G.D.; Davies, S.; Gale, N.W.; Rudge, J.S.; Wiegand, S.J.; Holash, J. (2000). "Vascular-specific growth factors and blood vessel formation" Nature 407(6801):242-8

Yee, R.W.; Sullivan, L.S.; Lai, H.T.; Stock, E.L.; Lu, Y.; Khan, M.N.; Blanton, S.H.; Daiger, S.P. (1997). "Linkage mapping of Thiel-Behnke corneal dystrophy (CDB2) to chromosome 10q23-q24" Genomics 46:152-4

Yoshida, S.; Kumano, Y.; Yoshida, A.; Hisatomi, T.; Matsui, H.; Nishida, T.; Ishibashi, T.; Matsui, T. (2002). "An analysis of BIGH3 mutations in patients with corneal dystrophies in the Kyushu district of Japan." Jpn J Ophthalmol 46(4):469-71.

Yoshida, S.; Kumano, Y.; Yoshida, A.; Numa, S.; Yabe, N.; Hisatomi, T.; Nishida, T.; Ishibashi, T.; Matsui, T. (2002). "Two brothers with gelatinous drop-like dystrophy at different stages of the disease: role of mutational analysis." Am J Ophthalmol 133(6):830-2.

Yun, S. J.; Kim, M. O.; Kim, S. O.; Park, J.; Kwon, Y. K.; Kim, I. S.; Lee, E. H. (2002). "Induction of TGF-beta-inducible gene-h3 (betaig-h3) by TGF-beta1 in astrocytes: implications for astrocyte response to brain injury." Brain Res Mol Brain Res 107(1):57-64.

Zhao, G.; Wang, C.; Sun, W.; Zhang, W.; Li, Y.; Sheng, H.; Liang, T. (2002). "Expression of betaig-h3 in keratoconus and normal cornea." Chin Med J (Engl) 115(9): 1401-4.

Zhao, Y. L.; Piao, C. Q.; Hei, T. K. (2002). "Downregulation of Betaig-h3 gene is causally linked to tumorigenic phenotype in asbestos treated immortalized human bronchial epithelial cells." Oncogene 21(49):7471-7.

Zhao, Y. L.; Piao, C. Q.; Hei, T. K. (2003). "Tumor suppressor function of Betaig-h3 gene in radiation carcinogenesis." Adv Space Res 31(6):1575-82.

Zhao, Y. L.; Piao, C. Q.; Wu, L. J.; Suzuki, M.; Hei, T. K. (2000). "Differentially expressed genes in asbestos-induced tumorigenic human bronchial epithelial cells: implication for mechanism." Carcinogenesis 21(11):2005-10.

Zhang, Z.; Vuori, K.; Reed, J.C.; Ruoslahti, E. (1995). "The alpha5 beta 1 integrin supports survival of cells on fibronectin and up-regulates Bsl-2 expression" Proc Natl Acad Sci USA 92(13):6161-5

Zhu, D.; Kim, Y.; Steffes, M.W.; Groppoli, T.J.; Butkowski R.J.; Mauer, S.M. (1994). "Application of electron microscopic immunocytochemistry to the human kidney: distribution of type IV and type VI collagen in normal human kidney." J Histochem Cytochem 42:577-584

Zinn, K.; McAllister, L.; Goodman, C.S. (1988). "Sequence analysis and neuronal expression of fasciclin I in grasshopper and Drosophila." Cell 20, 53(4):577-87

Zorn-Kruppa, M.; Tykhonova, S.; Belge, G.; Diehl, H.A.; Engelke, M. (2004). "Comparison of human corneal cultures for cytotoxicity testing" ALTEX 21(3):129-34